Vapour-liquid-liquid equilibria measurements for the dehydration of low molecular weight alcohols via heterogeneous azeotropic distillation

by

Leanne Brits

Thesis presented in partial fulfilment
of the requirements for the Degree

of

MASTER OF ENGINEERING
(CHEMICAL ENGINEERING)

in the Faculty of Engineering
at Stellenbosch University

Supervisor
Dr CE Schwarz

Co-Supervisor
Prof AJ Burger

March 2015

Declaration

By submitting this thesis electronically, I declare that the entirety of the work contained therein is my own, original work, that I am the sole author thereof (save to the extent explicitly otherwise stated), that reproduction and publication thereof by Stellenbosch University will not infringe any third party rights and that I have not previously in its entirety or in part submitted it for obtaining any qualification.

23 February 2015

ABSTRACT

The operation and optimisation of a distillation train directly effects the total energy consumption of a typical processing plant. With this in mind, the efficient separation of low molecular weight alcohol azeotropes, using heterogeneous azeotropic distillation, is of great economic and environmental importance.

Heterogeneous azeotropic distillation involves the addition of an extraneous component, known as an entrainer, to the mixture to facilitate separation. Benzene has long been replaced as the entrainer of choice, due to its carcinogenic nature, and research into finding a more suitable entrainer has commenced. To determine if an entrainer is suitable for a particular separation, detailed phase behaviour information of the ternary alcohol/entrainer/water system is required; vapour-liquid (VLE), vapour-liquid-liquid (VLLE) equilibria data and the composition of all azeotropes present. This is complicated by the fact that thermodynamic models (like the nonrandom two-liquid (NRTL), universal functional (UNIFAC) and universal quasichemical (UNIQUAC) activity coefficient models) often fail to predict the phase equilibria of ternary systems. The lack of available experimental phase equilibria data, and the inability of thermodynamic models to predict phase equilibria data, has fueled the need for the experimental determination of accurate, repeatable isobaric VLE, VLLE and azeotropic data. With this in mind, this research is focused on **the experimental determination of VLE, VLLE and azeotropic data for three low molecular weight alcohol/entrainer/water systems at 101.3 kPa.**

Following an extensive literature study on azeotropes, applicable separation techniques and available VLE and VLLE data in literature, the **ethanol/2-butanone/water**, **n-propanol/2-butanone/water** and **iso-propanol/2-butanone/water systems** were chosen for experimental investigation. The experimental determination was carried out in a Gillespie type still, equipped with an ultrasonic homogenizer. The temperature and pressure accuracies of the equipment were found to be 0.03°C and 2mbar respectively. The chosen experimental methodology was verified, and its repeatability tested, through the measurement of isobaric VLE and VLLE data of ethanol/isooctane, ethanol/n-butanol/water and n-propanol/isooctane/water systems at 101.3 kPa and subsequent comparison of the measured data with literature data. The compositional error reported, taking into account experimental and analysis effects, is ±0.014 mole fraction. All experimentally determined data sets, verification and new data, were tested for thermodynamic consistency by using the Wisniak modification of the Herrington test, the L/W consistency test, as well as the McDermott-Ellis consistency test, and found to be consistent. The Othmer-Tobias correlation was used to ensure the measured LLE data followed a steady trend, with all R-values larger than 0.910.

For all three of the new systems chosen, the absence of ternary heterogeneous azeotropes was noted. The presence of a ternary homogeneous azeotrope was found for both the ethanol/2-butanone/water and iso-propanol/2-butanone/water systems. No ternary azeotropes are present for the n-propanol/2-butanone/water system.

Suitable entrainers were compared to 2-butanone (MEK) by plotting measured data and literature information of five similar alcohol/entrainer/water systems on a ternary phase diagram. It was found that MEK could not be considered as a suitable entrainer for *heterogeneous* azeotropic distillation of ethanol, n-propanol and IPA. This is due to the absence of a ternary heterogeneous azeotrope for the aforementioned alcohol/MEK/water systems.

Finally, the ability of thermodynamic models (NRTL, UNIFAC and UNIQUAC) to predict experimental data was determined both visually and through descriptive statistics. This entailed the inspection of ternary phase diagrams and the calculation and evaluation of average absolute deviation (AAD) and and average absolute relative deviation (AARD%) values. The measured data were modelled in Aspen Plus®. It was found that none of the models could predict the ternary systems with acceptable accuracy and the data were regressed. In general, the regressed parameters for the NRTL, UNIFAC and UNIQAC models improved the model predictions when compared to the built-in Aspen parameters. The UNIFAC model predicted the ethanol/MEK/water and n-propanol/MEK/water systems most accurately while none of the models could predict the IPA/MEK/water systems with acceptable accuracy.

OPSOMMING

Die ontwerp en optimering van 'n distillasietrein het ‘n duidelike effek op die totale energieverbruik van ‘n tipiese prosesaanleg. Met dit in gedagte, is ‘n meer doeltreffende skeiding van lae molekulêre massa alkohol aseotrope, met behulp van heterogene aseotropiese distillasie, voordelig vir die ekonomie en die omgewing.

Heterogene aseotropiese distillasie behels die toevoeging van 'n eksterne komponent, wat bekend staan as 'n skeidingsagent, om uiteindelik die skeiding te fasiliteer deur die komponente se dampdrukke te verander. Benseen was in die verlede ‘n gewilde skeidingsagent, maar dit is a.g.v. sy karsenogeniese eienskappe nie meer aanvaarbaar om te gebruik nie. Nuwe navorsing in hierdie veld fokus dus onder andere op die identifisering van meer geskikte skeidingsagente. Om te bepaal of 'n skeidingsagent geskik is, word indiepte fasegedrag inligting benodig, i.e. damp-vloeistof en damp-vloeistof-vloeistof ewewigsdata en die samestelling van alle aseotrope teenwoordig. Ongelukkig kan termodinamiese modelle dikwels nie die fasegedrag van ternêre stelsels voorspel nie. Dit, sowel as die beperkte beskikbaarheid van eksperimentele ewewigsdata in die literatuur, het dus hierdie navorsing aangevuur. Die projek het gefokus op **die experimentele bepaling van damp-vloeistof en damp-vloeistof-vloeistof ewewigsdata en aseotropiese data vir drie alkohol/skeidingsagent/water-stelsels by 101.3 kPa.**

Na ‘n indiepte literatuurstudie van aseotrope, gepaste skeidingstegnieke en beskikbare damp-vloeistof en damp-vloeistof-vloeistof ewewigsdata, is 2-butanone (MEK) gekies as ‘n moontlike skeidingsagent en die **etanol/MEK/water-**, **n-propanol/MEK/water-** en **iso-propanol/MEK/water-**stelsels gekies vir eksperimentele ondersoek. Die data is met ‘n dinamiese Gillespie eenheid gemeet, toegerus met ‘n ultrasoniese homogeniseerder om vloeistof-vloeistof skeiding te voorkom. Die akkuraatheidsbande van temperatuur- en druk meetinstrumente was 0,03°C en 2 mbar, onderskeidelik. Die eksperimentele metode en die herhaalbaarheid van metings is bevesting, deur die isobariese damp-vloeistof en damp-vloeistof-vloeistof ewewigsdata van etanol/iso-oktaan, etanol/n-butanol/water en n-propanol/iso-oktaan/water te vergelyk met onafhanklike stelle ooreenstemmende data uit die literatuur. Die gesamentlike eksperimentele en analitiese fout wat gemaak kon word tydens bepaling van molfraksie samestellings was ±0.014 molfraksie. Alle gemete eksperimentele data is getoets vir termodinamiese samehang deur middel van beide die L/W en McDermott-Ellis konsekwentheidstoetse. Die Othmer-Tobias korrelasie is gebruik om seker te maak dat die gemete LLE data ‘n konstante tendens volg, met alle R-waardes groter as 0.910.

Vir al drie van die nuwe stelsels wat gekies is, was 'n drieledige *heterogene* aseotroop afwesig. Die teenwoordigheid van drieledige *homogene* aseotrope is egter waargeneem vir die etanol/MEK/water- en IPA/MEK/water-stelsels. Geen drieledige aseotrope is vir die n-propanol/MEK/water-sisteem gevind nie.

Alle gemete data, asook literatuur inligting van vyf soortgelyke alkohol/skeidingsagent/water sisteme, is op 'n drieledige fase diagram voorgestel om die skeidingsagente met mekaar te vergelyk. Hiervolgens word dit getoon dat MEK nie as 'n gepaste skeidingsagent vir *heterogene* aseotropiese distillase beskou kan word nie a.g.v. die afwesigheid van 'n drieledige heterogene aseotroop in die voorgenoemde alkohol/MEK/waterstelsels.

Die vermoë van die termodinamiese modelle (NRTL, UNIFAC en UNIQUAC) om die eksperimentele data te voorspel is visueel (per grafiek) sowel as deur beskrywende statistiek bepaal. Dit behels die inspeksie van drieledige fasediagrame en die berekening en evaluasie van die gemiddelde absolute afwyking en gemiddelde absolute relatiewe afwykingswaardes. Hierdie teoretiese data is met Aspen Plus® bepaal. Nie een van die modelle kon die drieledige stelsels se fasegedrag met aanvaarbare akkuraatheid voorspel nie. Die parameters vir die NRTL-,UNIFAC- en UNIQUAC-modelle kan verbeter word deur middel van regressie, in vergelyking met die ingeboude Aspen parameters. Dit is bevind dat die UNIFAC model die etanol/MEK/water- en n-propanol/MEK/water-stelsel die beste kan voorspel. Nie een van die bogenoemde modelle kon egter die fasegedrag van die IPA/MEK/water-stelsel voorspel nie.

ACKNOWLEDGEMENTS

This research has been financially supported by Sasol Technology (Pty) Ltd. Opinions expressed and conclusions arrived at are those of the author and are not necessarily attributed to the sponsors. I would like to acknowledge Aspen Plus, a registered trademark of Aspen Technology, Inc.

I would also like to personally thank the following people for their guidance and contribution to the completion of this work:

- Dr C.E. Schwarz for giving me the opportunity to do a Masters in Engineering and working with you, and seeing the potential in me. Cara, thank you for the countless meetings and chats over the past two years, you have been a true rock.
- Prof. A.J. Burger for all the guidance and input, your insight into all that is Chemical Engineering has been invaluable.
- Mrs. H. Botha and Mrs. L. Simmers, for your assistance with the analytical side of my research work. Two smiling faces always willing to take time out of their busy schedule to help me out.
- My colleagues in the Postgrad Office for making this Chemist feel so welcome. All the quick coffee-dates and catch-up sessions to keep me motivated.
- My parents, Paul and Sanet Brits, for your continuous support and love. Pappa, always being there to make light of things and Mamma, for never letting me lose focus on what's important.
- Stuart Campbell, you are my best friend and the nicest person I know. Without you this would not have been possible. Thank you for keeping me motivated and positive.

To the Lord, who has walked this path with me from the very beginning. I give all glory to You.

TABLE OF CONTENTS

ABBREVIATIONS

Abbreviation	Description
AARD %	Average absolute relative deviation percentage
B_i	Bottoms product of column i
D_i	Distillate of column i
DEGEE	Diethyleneglycol monoethyl ether
DIPE	Diisopropyl ether
DNPE	Di-propyl ether
EtOH	Ethanol
F	Feed
GC	Gas chromatography
IPA	Isopropanol
LLE	Liquid-liquid equilibrium
MEK	Methyl ethyl ketone
MSDS	Material safety data sheet
MTBE	Methyl tert-butyl ether
NRTL	Non-random Two Liquid
RCM	Residue curve maps
UNIFAC	Universal Functional Activity Coefficient
UNIQUAC	Universal Quasichemical Theory
VLLE	Vapour-liquid-liquid equilibrium

NOMENCLATURE

Symbol	Description	Units
A	Helmholtz energy	[J]
a	Activity	
B_i	Antoine's Constant	
C_i	Antoine's Constant	
D	Parameter in L/W consistency test	
F	Degrees of freedom	
$\widehat{f}_i$	Fugacity of component *i*	[Pa]
f_0	Arbitrary reference fugacity	[Pa]
G	Gibbs energy	[J.mol^{-1}]
G^E	Excess Gibbs energy	[J.mol^{-1}]
G^{id}	Gibbs energy of an ideal solution	[J.mol^{-1}]
H	Enthalpy	[J]
H^E	Heat of mixing	[J]
L_i	Parameter in L/W consistency test	[K]
M_W	Molecular mass	[g.mol^{-1}]
N	Number of species	
N_T	Total number of experimental runs	
n	Number of moles	[mol]
P	Total system pressure	[Pa]
P_i^{sat}	Vapour pressure of component *i*	[Pa]
Poy_i	Poynting correction for pressure	
q_i	Surface area parameter of UNIQUAC model	
R	Ideal gas constant	[J.mol^{-1}.K^{-1}]
S	Entropy	[J.K^{-1}]
s_i	Molar entropy	[J.K^{-1}.mol^{-1}]
T	Temperature	[K]
T^{bub}	Mixture bubble temperature	[K]
T^{vap}	Boiling temperature	[K]
U	Internal energy	[J]
u_{ij}	Interaction energy	[J.mol^{-1}]

Symbol	Description	Units
V	Volume	[m^3]
v_i	Molar volume for component *i*	[$m^3.mol^{-1}$]
V^E	Volume of mixing	[m^3]
W_i	Parameter in L/W consistency test	[$K.mol^{-1}$]
x_i	Mole fraction of component *i* in the liquid phase	
y_i	Mole fraction of component *i* in the vapour phase	
α	Parameter of NRTL model	[Pa.K]
α	The degree of enrichment (the ease of separation)	
ζ	Volume parameter of UNIQUAC model	
Θ	Surface area fraction group of UNIFAC model	
Γ_k	Residual contribution	
γ_i	Activity coefficient of component *i*	[$J.mol^{-1}$]
θ_i	Area fraction parameter of UNIQUAC model	
μ	Chemical Potential	[$J.mol^{-1}$]
ξ	Nonlinear time scale	
π	Number of phases	
τ	Parameter of NRTL model	[Pa.K]
ϕ	Fugacity coefficient	
Φ	Segment or volume fraction parameter of UNIQUAC model	

TABLES

TABLE OF FIGURES

1 INTRODUCTION

The design of a chemical process, and the resulting processing plant, involves a hierarchy of intricate and ingenious activities with the focus placed on the recovery, separation and purification of products and by-products. The requirement of pure chemical compounds in industrial and pharmaceutical applications has prompted the research and development of new separation techniques. The innovative design of these techniques has a large effect on the overall capital and operating costs of processing plants. Heterogeneous azeotropic distillation of low molecular weight alcohols, to be used as alternative fuel sources, is considered one of these pioneering separation techniques.

1.1 Motivation and industrial relevance

Distillation is currently the most widely used separation technique, providing an advantageous trade-off between purity and throughput. The design, implementation and optimisation of a distillation train have a critical effect on the economics of an entire process. This is due to the fact that distillation accounts for more than half of the total energy consumption of a typical chemical plant (Julka et al., 2009). Simple distillation relies on compositional differences of the coexisting vapour and liquid phases at equilibrium. As a result of this, not all chemical mixtures of interest are acquiescent to distillation; for example, it is difficult to distil close-boiling mixtures and impossible to distil azeotropic mixtures (Doherty & Knapp, 2000).

In today's economic and environmental climate, the use of hydrocarbon-based fuels is being scaled back and the necessity of renewable energy sources, like bio-fuels, has arisen. The benefits of bio-fuels include a net reduction of carbon emissions, resulting in an immediate improvement in local air quality, fiscal development and energy security (Santoch et al., 2010). Biodiesel, bioethanol and biobutanol are important examples of bio-fuels. Considered to be the most promising, bioethanol has a high energy value and is currently employed as a gasoline-additive to enhance combustibility and octane number (Singh & Prasad, 2011). This means that most diesel powered vehicles accommodate bio-fuel blends and the substitution of fossil fuels with bio-fuels can occur with relative ease. Ethanol and gasoline blending is beneficial when the water content is less than 0.5% (v/v). In cases where the water content is higher than this, separation occurs within the gasoline-mixture leading to an upper gasoline-rich phase and a lower ethanol/water phase which collects dirt and sediment (Kumar et al., 2010). An ethanol/water solution forms a minimum-boiling azeotrope with a composition of 89.4 mol% ethanol and 10.6 mol% water at a temperature and pressure of 78.2 °C and 101.3 kPa respectively (Gmehling et al., 1994).

Since azeotropic mixtures cannot be separated using simple distillation, several separation techniques have been proposed/employed. These include: membrane processes, adsorption processes, chemical dehydration processes and azeotropic distillation processes (Santosh et al., 2010). Azeotropic distillation processes can be divided into three sub-sets: homogeneous azeotropic distillation, heterogeneous azeotropic distillation and extractive distillation. All of these three methods involve the addition of an extraneous component, referred to as an entrainer, which facilitates separation by altering the relative volatilities of the components in the azeotropic. Heterogeneous azeotropic distillation utilises the resulting liquid-liquid immiscibilities and minimum boiling azeotropes to overcome the effect of the alcohol/water azeotrope (Doherty & Knapp, 2004). In 1902, the first successful application of heterogeneous azeotropic distillation was implemented using benzene as an entrainer for the dehydration of ethanol (Young, 1902). Due to the harmful and carcinogenetic nature of benzene, the focus of current research has shifted to finding an appropriate entrainer to replace benzene for the dehydration of low molecular weight alcohols.

1.2 Phase Equilibria and Thermodynamic Models

Entrainer selection is a critical step in the design of heterogeneous azeotropic distillation processes, as the choice of entrainer determines the separation sequence and, consequently, the overall economics of the process (Julka et al., 2009). Method development relies on accurate phase behaviour information, vapour-liquid equilibrium (VLE) and vapour-liquid-liquid equilibrium (VLLE) data for the particular alcohol/entrainer/water system of interest (Hoffman, 1964). Thermodynamic models (NRTL, UNIFAC and UNIQUAC) have been developed which model multi-component phase equilibrium data from binary data. However, the determination of accurate VLE and VLLE data is of critical importance as thermodynamic models often fail in predicting accurate phase behaviour (Seader & Henley, 1998).

This research project will focus on the experimental determination of VLE and VLLE data for several alcohol/entrainer/water systems and the comparison of the resulting data with predictions modelled by the thermodynamic models listed above. This project aspires to investigate a suitable entrainer, without the health effects associated with benzene, for the dehydration of low molecular weight alcohols.

1.3 Project Aim and Objectives

The aim of this research project is the measurement and evaluation of accurate, repeatable isobaric VLE and VLLE data for three alcohol/entrainer/water systems (ethanol, n-propanol and iso-propanol) at 101.3 kPa. This data can then be used to methodically assess and compare the performance of the selected entrainer for the dehydration of low-molecular weight alcohol, with entrainers currently used in industry. This data will also be used to evaluate the ability of thermodynamic models to interpolate and, to a limited extent, extrapolate phase behaviour.

The research was performed while targeting the following objectives:

1. To perform an extensive literature study focussing on azeotropes, heterogeneous azeotropic distillation of low-molecular weight alcohol/water azeotropes and entrainer selection methodology.
2. To select a possible entrainer for the dehydration of low-molecular weight alcohols.
3. To verify experimental procedure and equipment for the determination of VLE and VLLE data at 101.3 kPa.
4. To measure VLLE data of three ternary alcohol/entrainer/water systems:
    - Ethanol/entrainer/water
    - n-Propanol/entrainer/water
    - iso-Propanol/entrainer/water
5. To compare entrainers for the dehydration of ethanol, n-propanol and iso-propanol using ternary phase diagrams and heterogeneous azeotropic distillation principles.
6. To assess the ability of thermodynamic model predictions (NRTL, UNIFAC and UNIQUAC) to successfully model phase equilibria data by comparison with experimentally obtained data.

As can be deduced from the above project aim and objectives, the scope of this project is limited to the determination of VLLE data for three ternary systems and will not focus extensively on thermodynamic modelling.

1.4 Thesis Overview

Figure 1-1 provides a schematic overview of the layout of this thesis. A comprehensive literature study on azeotropy, alcohol/water azeotropes, methods of separating azeotropic mixtures and phase equilibrium diagrams is presented in Chapter 2. This chapter also includes the motivation behind the use of heterogeneous azeotropic distillation. In Chapter 3, the fundamentals of isobaric low-pressure phase equilibrium (LLE, VLE and VLLE) are discussed. In addition to this, the criteria for equilibrium, the phase rule, chemical potential, fugacity and activity are defined. Furthermore, Chapter 3 deals with the thermodynamic models and thermodynamic consistency testing methods used in this thesis. The purpose, problems and methods of measuring VLLE are discussed in Chapter 4. Chapter 5 presents the available alcohol/entrainer/water VLLE data, potential entrainers and the three systems to be measured for the Masters study. Chapter 6 details the materials, methods and apparatus used. The verification and novel data obtained for this thesis presented in Chapter 7. Chapter 7 also includes thermodynamic modelling and data regression. Finally, all conclusions and recommendations are summarized in Chapter 8.

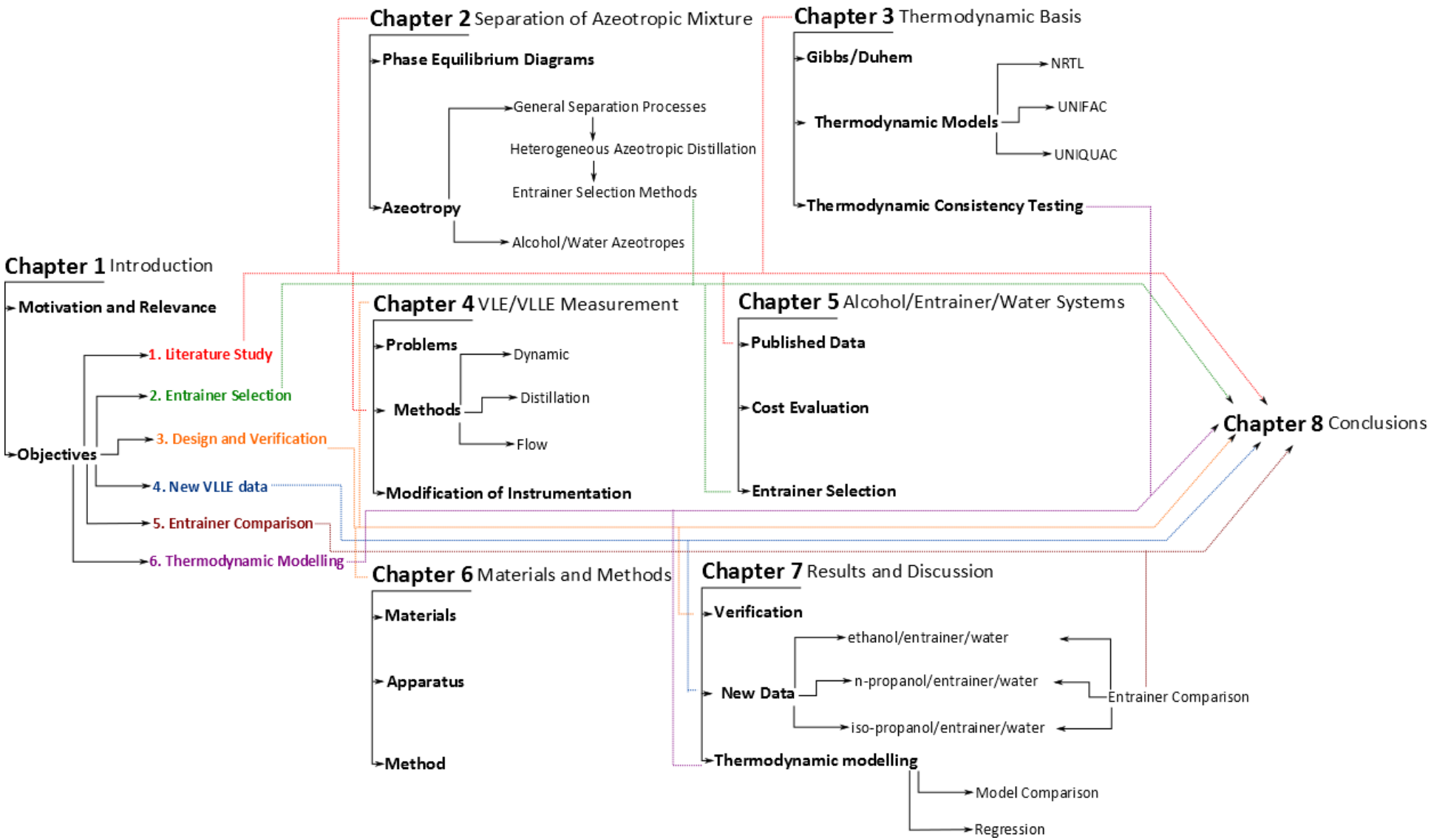

Figure 1-1: ***Schematic of thesis layout.***

2 SEPARATION OF AZEOTROPIC MIXTURES

When considering a particular process as a feasible separation technique to separate an azeotropic mixture, it is of great importance that the nature of the mixture in question is known (Doherty & Knapp, 2000). As a result, a critical examination of available literature on the nature of azeotropic mixtures, azeotropes in industry and separation techniques applied to separate alcohol/water azeotropes is discussed in the following chapter. As mentioned in the previous introductory chapter, separation of azeotropic mixtures is impossible via ordinary distillation. Through the addition of an ancillary separating agent, the separation of azeotropic mixtures can be achieved. Possible techniques for identifying suitable separating agents are also discussed.

2.1 Azeotropy

An azeotropic mixture can be defined as a mixture, at equilibrium, that retains the same composition in the vapour state as the coexisting liquid state at a certain pressure (Doherty & Knapp, 2000). The word azeotrope is derived from the Greek words α (no), ζέειν (boil) and τρόπος (turning); meaning "no change when boiled" (Luyben, 2010). Examples of azeotropic mixtures are numerous and widespread (Horsley, 1973, Gmehling et al. 1994). In the growing biofuel industries, the occurrence of azeotropes, which form between water and low-molecular weight alcohols, is commonplace (Luyben, 2010).

An azeotrope, present in a binary mixture, can be classified either as a minimum-boiling azeotrope or a maximum-boiling azeotrope; approximately 90% of all azeotropes fall under the former category (Rousseau & Fair, 1987). Azeotropic behaviour occurs when molecules in a chemical mixture have dissimilar structures and elemental features (Hoffman, 1964). Interactions between components in the mixture on a molecular level lead to either positive or negative deviations from Raoult's law (Equation 2.1). Conversely, ideal mixtures obey Raoult's law and the components will generally have similar physiochemical properties (Gmehling, 1946, Doherty & Knapp, 2000).

With maximum-boiling azeotropes, the molecules demonstrate attractive intermolecular forces leading to negative deviations from Raoult's law ($\gamma_i < 1$). Examples of binary mixtures that display this type of azeotropic behaviour (Figure 2-1a and 2-1b) include the acetone/water system and the nitric acid/water system (Luyben, 2010). The attractive forces lead to an overall decrease in effective vapour pressure of the components and an overall increase in boiling point; the boiling temperature is higher than that of the pure components (Rousseau & Fair, 1987).

In minimum-boiling azeotropic systems, like that of ethanol/water, the presence of dissimilar functional groups (the non-polar CH_3-CH_2-group in ethanol and the polar OH-group in water), leads to repulsive forces between the components in the mixture. This phenomenon, illustrated in Figure 2-1c and 2-1d, leads to an overall increase in effective vapour pressures of the components; the overall boiling temperature of the system is lower than that of the pure components (Luyben, 2010). In cases where the repulsive forces are extreme, like that of the n-butanol/water system, the mixture forms what is known as a heterogeneous minimum-boiling binary azeotrope and a region exists where there is two liquid phases. The composition, in this case, of the vapour phase is identical to the two separate liquid phases. The above examples of alcohol/water azeotropic systems demonstrate positive deviations from Raoult's law ($\gamma_i > 1$) (Doherty & Knapp, 2000).

Heterogeneous binary azeotropes can be separated without the use of a separating agent. Through the exploitation of the liquid-liquid phase separation, a decanter can be used to produce high-purity products by feeding the two resulting liquid phases to two separate columns (Luyben, 2010).

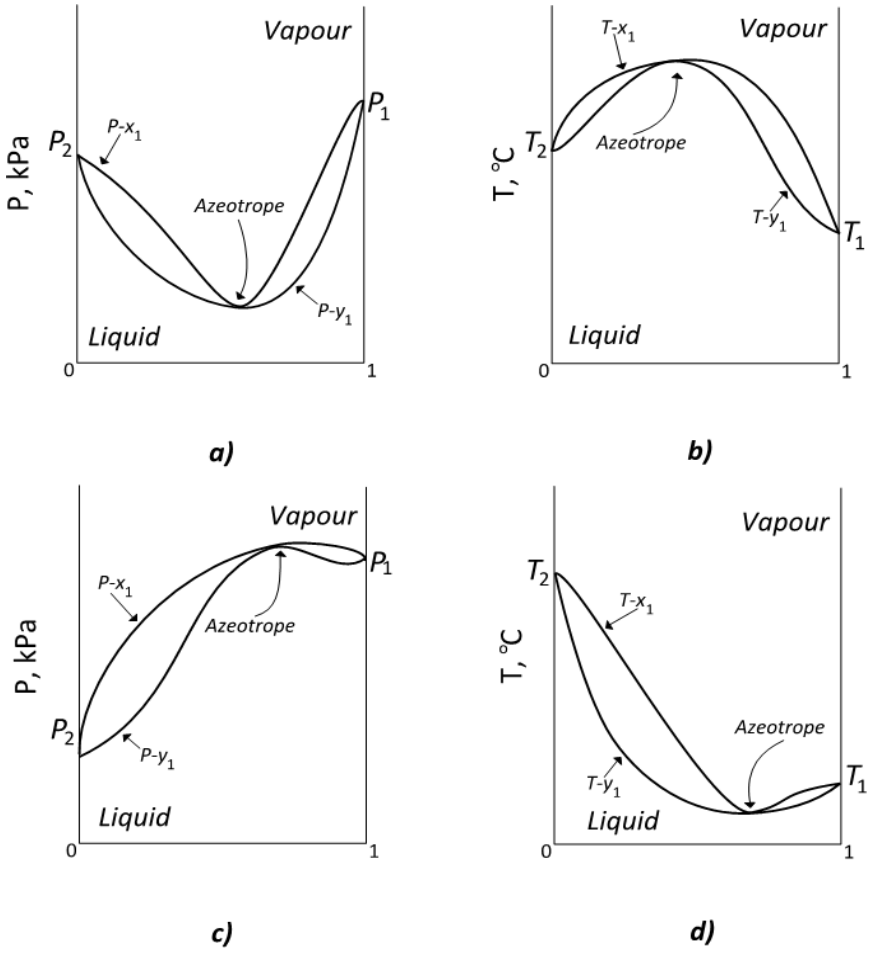

Figure 2-1: ***P-x-y and T-x-y phase diagrams where the x-axis is the composition, in mole fraction, of one the components in the binary mixture; (a) P-x-y diagram of a binary, maximum-boiling azeotrope; (b) T-x-y diagram of a binary, maximum-boiling azeotrope; (c) P-x-y diagram of a binary, minimum-boiling azeotrope; (d) T-x-y diagram of a binary, minimum-boiling azeotrope. According to Doherty and Knapp (2000).***

2.1.1 Phase Equilibrium

The following section deals with the phase equilibrium behaviour of an *i*-component azeotropic mixture. In otherwords a mixture with the number *i* chemical components. Several of the concepts and equations used in this section will tie directly into the work discussed in Chapter 3 (Thermodynamic Basis), but will be highlighted here as it lays a foundation for this research project.

2.1.1.1 Vapour-liquid Equilibrium

By definition, every component *i* in a c-component azeotropic mixture, at equilibrium, will have vapour and liquid phase fugacities equal to each other:

$$\hat{f}_i^{\,v} = \hat{f}_i^{\,l} \qquad [2.1]$$

Where,

$\hat{f}_i^{\,v}$ = the fugacity of component *i* in the vapour phase

$\hat{f}_i^{\,l}$ = the fugacity of component *i* in the liquid phase

and *i* = 1, 2….*c*

Using the equation of state method, the vapour fugacity can be represented in the following way, based on deviation from the ideal gas state:

$$\hat{f}_i^{\,v} = \hat{\varphi}_i^{\,v}\, y_i P \qquad [2.2]$$

Where,

$\hat{\varphi}_i^{\,v}$ = the vapour phase fugacity coefficient of component *i*

y_i = mole fraction of component *i* in the vapour phase

P = the total system pressure

The ideal liquid phase fugacity can be represented as:

$$\hat{f}_i^{\,l} = \hat{\varphi}_i^{\,l} x_i P \qquad [2.3]$$

Where,

x_i = mole fraction of component *i* in the liquid phase

Alternatively, the fugacity of the component *i* in the liquid phase can be obtained by consuderting the deviation from an ideal solution by incorporation of the liquid activity coefficient of component *i* in the liquid phase:

$$\hat{f}_i^{\,l} = x_i \gamma_i f_i^l \qquad [2.4]$$

Where,

γ_i= liquid activity coefficient

and

$$f_i^l = \varphi_i^{sat} P_i^{sat} \, exp\left(\frac{1}{RT} \int_{P_i^{sat}}^{P} V_i^l \, dP\right) \qquad [2.5]$$

Where,

φ_i^{sat}= the fugacity coefficient of pure component *i* at the system temperature and vapour pressure, as calculated from the vapour phase equation of state

P_i^{sat}= liquid vapour pressure of component *i*

The $exp\left(\frac{1}{RT}\int_{P_i^{sat}}^{P} V_i^l \, dP\right)$ term is known as the Poynting correlation.

When dealing with phase equilibria at low pressure (pressures lower than 1 bar),

$$\varphi_i^{sat} = 1 \qquad [2.6]$$

$$\hat{\varphi}_i^{\,v} = 1 \qquad [2.7]$$

$$exp\left(\frac{1}{RT} \int_{P_i^{sat}}^{P} V_i^l \, dP\right) = 1 \qquad [2.8]$$

Therefore Raoult's law is modified to the following, at low pressures:

$$y_i P = x_i \gamma_i P_i^{sat} \qquad [2.9]$$

Accordingly, Equation 2.9 is known as the Modified Raoult Law.

At equilibrium:

$$\widehat{\varphi_i^v} y_i = \widehat{\varphi_i^l} x_i \quad [2.10]$$

The activity coefficient, denoted by the symbol γ_i, can be defined as the measure of the component *i's* liquid-phase non-ideality in an azeotropic mixture of *c*-components.

Where γ_i = 1 is considered to be ideal, the above equation simplifies to the Modified Raoult's law:

$$y_i P \approx x_i P_i^{sat} \quad [2.11]$$

Deviations in non-ideal mixtures can be either positive ($\gamma_i > 1$) or negative ($\gamma_i < 1$), depending on the interactions between the molecules found in the mixture. It must also be said that the value of the activity coefficient is dependent upon both temperature and composition.

At the azeotropic points on the phase diagrams, see Figure 2-1, the vapour and liquid phases have the same molar composition:

$$y_i = x_i \quad [2.12]$$

By restricting the system to a binary mixture, the following relationship is identified for a homogeneous binary azeotrope:

$$\frac{\gamma_2}{\gamma_1} = \frac{P_1^{sat}}{P_2^{sat}} \quad [2.13]$$

Equation 2.13 demonstrates that only small deviations from Raoult's law are necessary for an azeotrope to exist. It also illustrates that the larger the difference in boiling points of the two compounds, the greater the non-ideality and therefore the less likely it will be that an azeotrope will be present. In other words, only compounds with small differences in vapour pressures can form azeotropes; the larger the difference becomes, the less likely it is that the azeotrope will form. In *Perry's Chemical Engineer's Handbook (*1997) the authors stated that, in general, compounds with boiling points further than approximately 30°C will not form an azeotrope. As with most heuristic statements, exceptions to this rule exist; the hydrogen chloride/water system forms a maximum boiling azeotrope and their boiling points differ by a 185°C (Doherty & Knapp, 2000).

An empirical study (Martin, 1984) showed that a binary mixture forms a minimum-boiling azeotrope when the ratio of the pure component vapour pressures is less than the infinite dilution activity coefficient of the less volatile component:

$$\gamma_2^{\infty} > \frac{P_1^{sat}}{P_2^{sat}} \qquad [2.14]$$

When comparing partially miscible mixtures with completely miscible mixtures, partially miscible mixtures are more non-ideal and, resultantly, more likely to form azeotropes (Hoffman, 1964, Luyben, 2010). Characteristically, these azeotropes are heterogeneous azeotropes where two or more liquid phases are in equilibrium with a vapour phase (Doherty & Knapp, 2000).

Figure 2-2 is a schematic of isobaric binary phase diagrams illustrating the difference between homogeneous- and heterogeneous-azeotropes. As can be seen from Figure 2-2a, when the liquid composition (x_1) is equal to x_1^{AZ}, the vapour composition, y_1, is also equal to x_1^{AZ}. Homogeneous azeotropes occur when the immiscibility exists over a limited range and the azeotrope falls outside of the two-liquid (L-L) phase region. The mixture boils at constant temperature and composition, and there are two distinct phases (vapour and liquid phases). Of course, cases exist where no L-L region occurs (Figure 2-1d).

A heterogeneous azeotrope exists where the overall liquid composition x_1^0 is equal to the vapour composition, y_1 (Figure 2-2b). The mixture boils at constant temperature and composition; however, at that point, there are three distinct phases (vapour and two liquid phases).

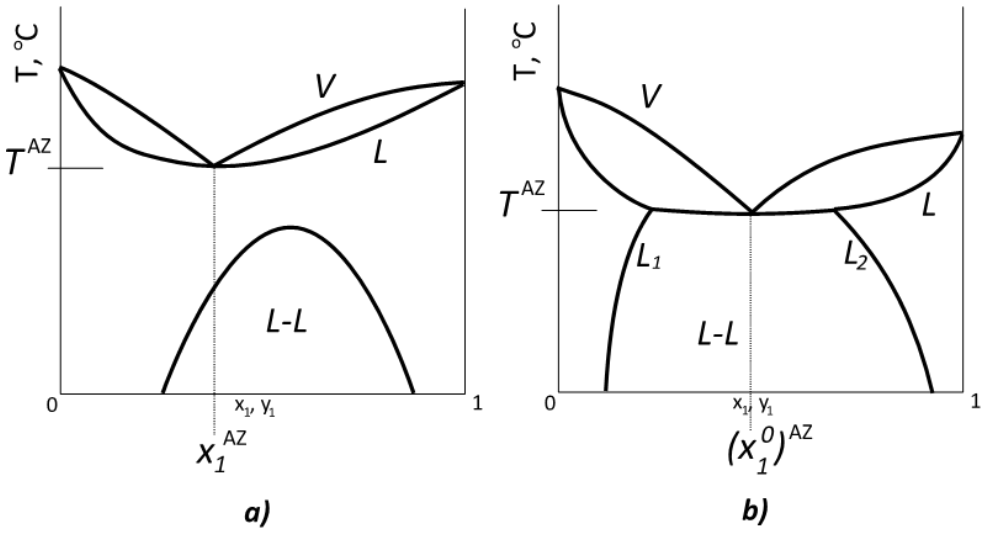

Figure 2-2: ***Schematic isobaric phase diagrams for binary azeotropic mixtures; a) Homogeneous azeotrope; b) Heterogeneous azeotrope. According to Gomis et al. (2000).***

It can be inferred that only minimum boiling heterogeneous azeotropes exist due to the fact that positive deviations from Raoult's law are necessary for liquid phase immiscibility.

2.1.1.2 Liquid-liquid Equilibrium

The following relationship pertains to the liquid-liquid equilibrium:

$$x_i^{L1}\gamma_i^{L1} = x_i^{L2}\gamma_i^{L2} \quad [2.15]$$

Where,

x_i^{L1} = mole fraction of component *i* in the liquid phase 1

γ_i^{L1} = the activity coefficient of component *i* in the liquid phase 1

x_i^{L2} = mole fraction of component *i* in the liquid phase 2

γ_i^{L2} = the activity coefficient of component *i* in the liquid phase 2

Possible methods of finding the activity coefficient (γ_i) using thermodynamic models is discussed in Chapter 3.

2.1.2 Separation by distillation

The relative volatility of most mixtures is a function of temperature, pressure and composition (Doherty & Knapp, 2000). When a liquid mixture is partially evaporated, also known as simple distillation, separation can occur when the vapour and liquid phases have different compositions. The vapour phase steadily becomes enriched with the more volatile components while the liquid phase is enriched with the more non-volatile components (Rousseau & Fair, 1987). The degree of enrichment (the ease of separation), also known as the relative volatility, can be defined as:

$$\alpha_{ij} = \frac{y_i x_j}{x_i y_j} = \frac{\gamma_i {P_i}^{sat}}{\gamma_j {P_j}^{sat}} \quad [2.16]$$

The larger the value of α_{ij} the easier it is to separate the two components in question. Mixtures that are ideal, non-ideal, close-boiling and so on, which have relative volatilities close to unity, will be difficult to separate using simple distillation. For a *c*-component homogeneous azeotrope (in other words binary, ternary, quaternary, et cetera) it is known that $y_i = x_i$ (Equation 2.8). Therefore, at the azeotropic point, $\alpha_{ij} = 1$ for all components and no enrichment takes place. Consequently, homogeneous azeotropes cannot be separated using ordinary distillation.

Doherty & Knapp (2000) stated that alternative separation techniques should generally be used when α_{ij} is less than 1.15. The aforementioned alternative separation techniques are discussed in Section 2.4.

2.2 Alcohol/Water Azeotropes

Azeotropes are rarely encountered in petroleum industries due to the similar physiochemical behaviour of the hydrocarbon components. In chemical and bio-fuel industries, however, a myriad of azeotropes occur between low molecular weight alcohols and other components (Luyben, 2010). Although methanol and ethanol are widely used as fuel-additives, the propanol-isomers show great promise due to their higher energy densities and comparatively low affinity for water (Veloo et al., 2010). This project focuses on ethanol/water, n-propanol/water and iso-propanol/water azeotropes formed at 101.3 kPa:

- Ethanol and water forms an azeotrope with a composition of 89.5 mole % ethanol and 10.5 mole % water at 78.12 °C (Gmehling et al. 1994).
- iso-Propanol and water forms an azeotrope with a composition of 67.28 mole % iso-Propanol and 32.72 mole % water at 87.72 °C (Gmehling et al. 1994).
- n-Propanol and water forms an azeotrope with a composition of 43.17 mole % n-Propanol and 56.83 mole % water at 87.59°C (Gmehling et al. 1994).

2.2.1 Ethanol

Ethanol (CH_3CH_2OH) is a low molecular weight alcohol with unique properties; this has led to its use in a variety of organic synthesis pathways, in beverages, as an antifreeze agent and as an excellent alternative fuel source (Logsdon, 2000). The legal requirement of oxygenates in gasoline (Clean Air Act, 1990) has fuelled the growth of ethanol production and purification (Fernandez & Keller, 2000). Ethanol has widely replaced methyl tert-butyl ether (MTBE) as an oxygenate due to MTBE's associated environmental risk (Henley et al., 2014). More than 95% of U.S. gasoline contains ethanol (Adair & Wilson, 2009).

Ethanol is industrially produced by the direct or indirect hydration of ethylene, a by-product of several industrial processes (Logsdon, 2000). The direct hydration of ethylene involves the sulphuric acid catalysed vapour-phase hydration of ethylene (Cotelle, 1861). The indirect method is a three-step reaction also known as the esterification-hydrolysis process (Muller & Miller, 1957). However, the fermentation of carbohydrates (starch, sugar and/or cellulose) accounts for approximately 70% of global ethanol production (Davenport et al., 2002). Fermentation is the anaerobic conversion of energy-rich materials containing sugars, or compounds which are capable of being converted into sugar (starches), to ethanol, carbon dioxide and/or organic acids by micro-organisms (Junker, 2004). Ethanol can directly be converted from sugars whereas starches must first be hydrolysed to fermentable sugars (Logsdon, 2004). On account of water being present in the above mentioned

industrial processes, an alternative separation technique is required to produce anhydrous ethanol (Haelssig et al., 2011).

2.2.2 n-Propanol

n-Propanol ($CH_3CH_2CH_2OH$), also known as n-propyl alcohol, has physiochemical properties similar to low molecular weight primary alcohols like ethanol. n-Propanol is used as a solvent in flexographic printers and as a chemical intermediate in several important industrial processes (Unruh & Pearson, 2000). n-Propanol has a high octane number and has anti-knock properties (Biofuels, 2010).

n-Propanol is synthesised by a two-step reaction: hydroformylation of ethylene followed by the hydrogenation of propanal. It is also produced as a product of Fishcer-Tropsch chemistry. Sasol, in South Africa, is one of only six n-propanol producers in the world (Unruh & Pearson, 2000).

2.2.3 iso-Propanol

Isopropanol ($(CH_3)_2CHOH$), also known as IPA, is a clear, colourless liquid and is classified as a first generation biofuel (Biofuels 2010). Like most low molecular weight alcohols, IPA has a low order of toxicity. IPA is known as a "gas dryer"; it has a high octane number and is currently employed as a fuel oxygenate. The addition of IPA to fuel prevents water freezing in gas lines in colder climates. It is also used as a solvent and/or chemical intermediate in various pharmaceutical and industrial applications (Logsdon & Loke, 2000).

Both propanol-isomers can be produced using fermentation processes. However, the largest producers of propanol are petrochemical industries (Veloo et al., 2010). IPA can be synthesised by the indirect or direct hydration of propylene or by the hydrogenation of acetone (Logsdon & Loke, 2000). IPA has a tendency to associate and form azeotropes with a number of compounds, including water, a number of hydrocarbons, other low molecular weight alcohols, ketones and ethers (Gmehling et al., 1994). The importance of alternative separation techniques, in lieu of simple distillation, is evident.

2.2.4 Discussion

South Africa has a large number of chemical, pharmaceutical and petrochemical industries that produce aqueous, low molecular weight alcohol mixtures as products and/or by-products. The Fischer-Tropsch process is a key component of gas to liquid technology, and is used extensively by Sasol and PetroSA. This process is made up of a series of catalysed chemical reactions which lead to the conversion of carbon monoxide and hydrogen into liquid hydrocarbons and other important organic compounds. Anderson (1984) considered water, primary alcohols and/or α-olefins to be principal primary products of the Fischer-Tropsch synthesis process. As a result, the conceptual

design and the subsequent implementation of separation techniques, like heterogeneous azeotropic distillation, are of obvious importance.

2.3 Azeotropic Phase Equilibrium Diagrams

The critical study and analysis of the structural properties of VLE and VLLE diagrams is required to appreciate the unique behaviour of azeotropic mixtures. Furthermore, the investigation of VLE and VLLE diagrams is considered to be the starting point for the prediction of feasible separation techniques (Westerberg and Wahnschafft, 1996). The following section looks at the various phase diagrams that can be constructed for several non-ideal mixtures.

2.3.1 Vapour-liquid Equilibrium Diagrams

Graphical representation of vapour-liquid equilibrium (VLE) aids the identification of the thermodynamic state of a mixture as well as the composition of the phases present at a certain condition. These VLE diagrams are generally constructed at constant pressure (a *T*-x diagram) or constant temperature (a *P*-x diagram) (see Figure 2-1). Graphical representation of a *c*-component VLE is limited by the number of components in the mixture. In a *c*-component mixture, the composition space needs to be (c-1)-dimensional. Consequently, binary mixtures composition space is one-dimensional, for ternary mixtures the composition space is two-dimensional, and so on (Seader & Henley, 1998).

The graphical VLE representation of binary mixtures is illustrated in Figure 2-3. The left hand column in Figure 2-3 presents a combined graph of boiling and condensation temperatures and the right-hand column illustrates the equilibrium phase mapping. Figure 2-3a represents the behaviour of a zeotropic mixture; a mixture where there are no azeotropes present.

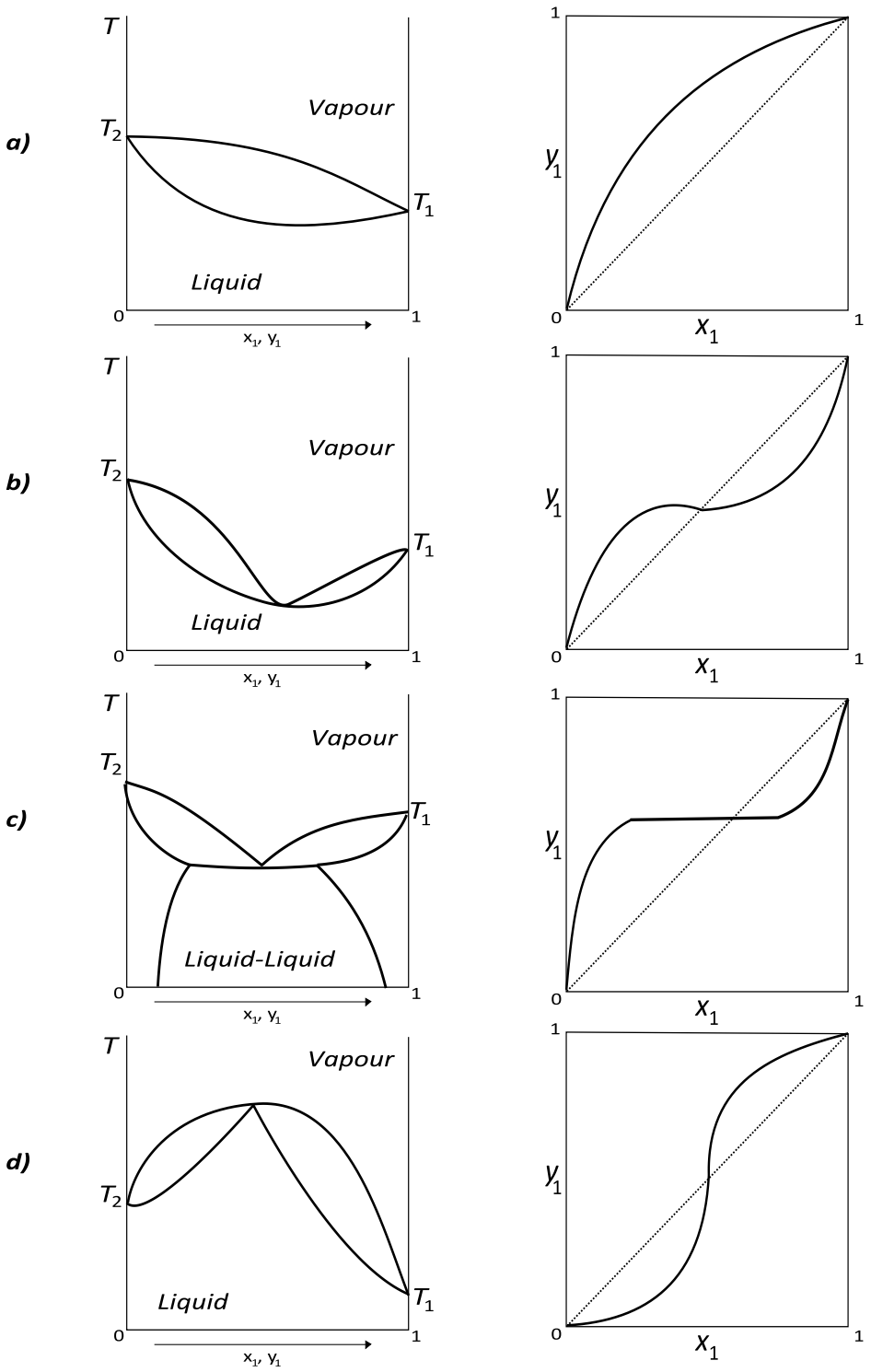

Figure 2-3: ***Graphical representations of the VLE for the most common types of binary mixtures at constant pressure: a) zeotropic; b) minimum-boiling homoazeotrope; c) minimum-boiling heteroazeotrope; d) maximum-boiling azeotrope. According to Koretsky (2004).***

2.3.2 Liquid-liquid Equilibrium Diagrams

As mentioned in Section 2.1.1.1, considerable (positive) deviations from Raoult's law results in the formation of two, partially miscible or immiscible, liquid phases (Doherty & Knapp, 2000). Figure 2-4, graphically represents this liquid-liquid equilibrium (LLE) phenomenon.

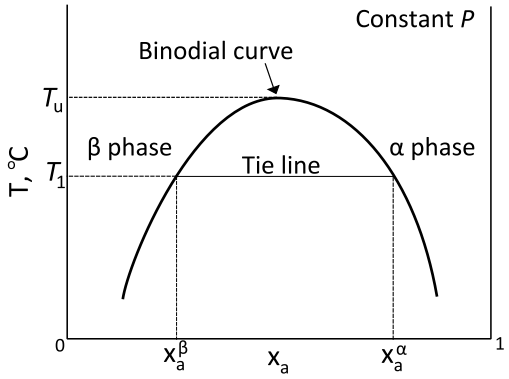

Figure 2-4: ***Binary liquid-liquid phase equilibrium diagram. According to Koretsky (2004).***

Figure 2-4 illustrates the existence of an bimodal curve (also known as the coexistence curve). This curve denotes the condition with which two distinct phases may exist. From this binodal curve, the line that separates the single-liquid region from the liquid-liquid region, tie-lines can be drawn to determine the compositions of the two liquid phases. The temperature, T_u, denotes the upper consulate temperature, above which the mixture no longer separates into two liquid phases. Like ternary VLE diagrams, ternary LLE diagrams can be represented by an equilateral or rectangular triangle (Figure 2-5).

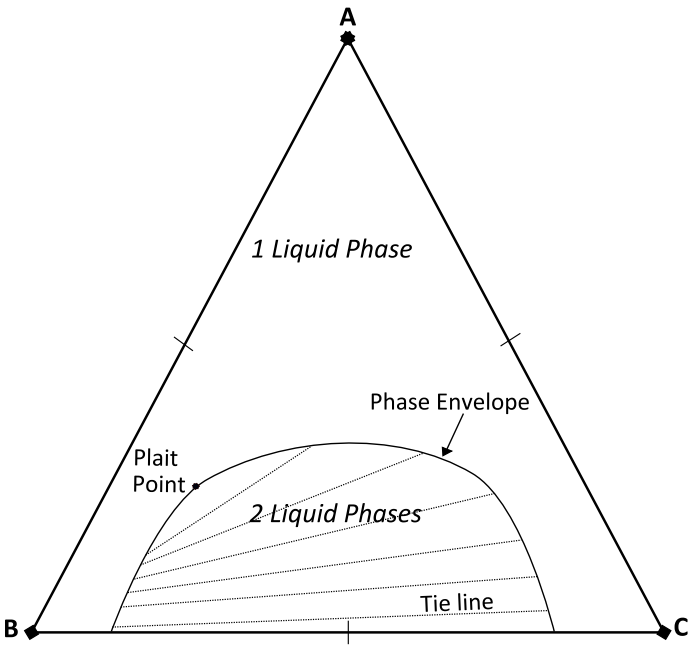

Figure 2-5: ***Ternary liquid-liquid phase equilibrium diagram of a system with three components: A,B and C. Redrawn and adapted from Seader and Henley (2006).***

2.3.3 Vapour-liquid-liquid Equilibrium Diagrams

Understanding the properties of ternary heterogeneous vapour-liquid-liquid equilibrium (VLLE) phase diagrams is vital to the ultimate comprehension of azeotropic distillation. Figure 2-6 shows the schematic representation of a homogeneous and heterogeneous ternary VLLE on a *T-x-y* prism. The grey-area where the LLE and VLE surfaces meet is called the heterogeneous liquid boiling surface (Figure 2-6b).

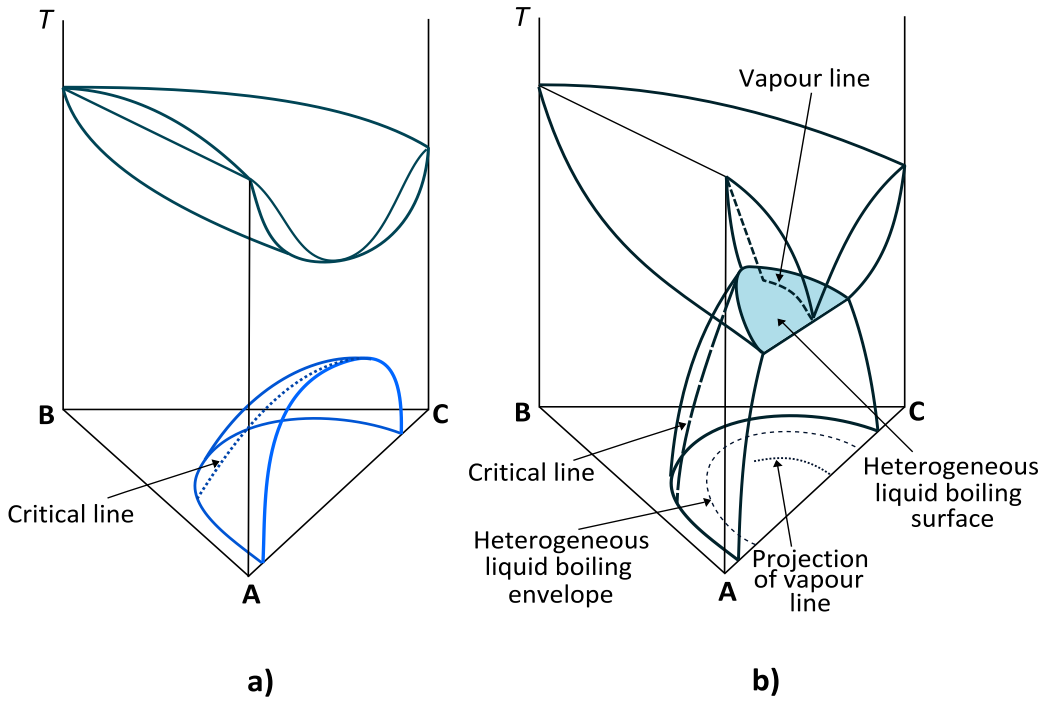

Figure 2-6: ***Schematic isobaric phase diagrams for ternary azeotropic mixtures. a) Homogeneous liquid phase at all boiling points; b) heterogeneous liquid phase for some boiling points. According to Doherty & Knapp (2000).***

It is arduous to interpret these types of prisms; therefore other representations are commonly used to illustrate VLLE. Projection of the compositional space onto the base of the triangle is a convenient way of representing VLLE. The resulting graphical representation must not be confused with an isothermal liquid-liquid binodal curve (discussed in Section 2.3.2). Each projected vapour and liquid line varies with temperature; in other words, each line crossing the boiling envelope represents a different boiling temperature (Figure 2-7). Each number (1-6) corresponds to a different set of samples taken from the vapour, organic liquid phase and inorganic liquid phase.

In this particular diagram, Figure 2-7, a ternary heterogeneous azeotrope exists where the vapour phase line lies on the tie-line connecting the two liquid phases (at the 5th set of samples taken). In agreement with mass balance rules, at this azeotropic point, the vapour phase composition will be equal to the overall liquid phase composition.

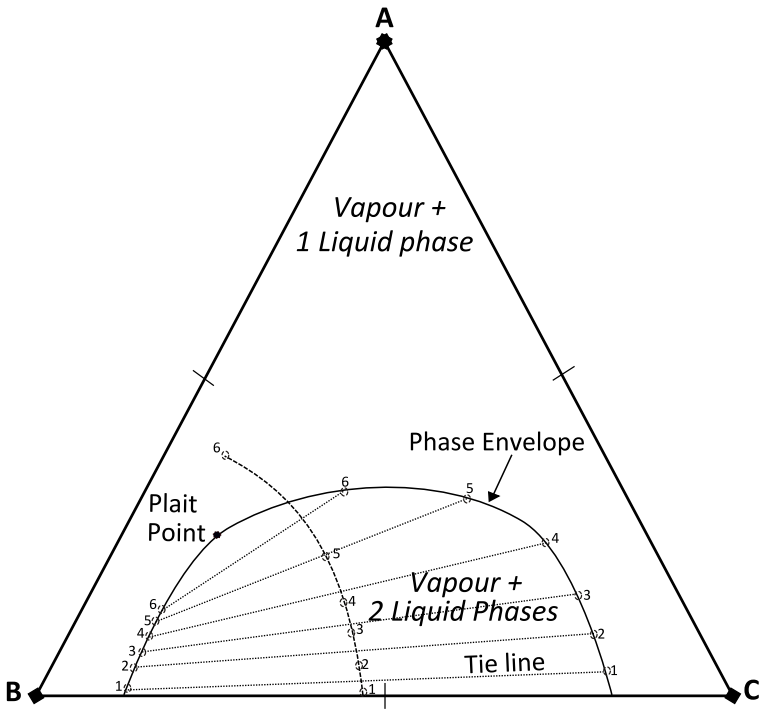

Figure 2-7: ***Ternary vapour-liquid-liquid phase equilibrium diagram. According to Seader and Henley (2006).***

2.3.4 Residue Curves

Residue curve maps (RCM) are a useful separation synthesis tool as they assist the practicing engineer in visualising VLLE issues that may affect the consequential modelling and application of an appropriate separation technique (Julka et al., 2009). RCM forms an important element in entrainer feasibility determination methodology (De Villiers et al., 2002). It is another form for graphically representing VLE and VLLE of a multi-component mixture.

With simple distillation, the vapour phase is continuously removed causing the liquid phase composition to change constantly (enriched with the less volatile species) until a pure species remains. Simple RCMs represent the liquid composition profiles, in mole or mass fractions, of a simple distillation column operating at infinite reflux. These composition trajectories move from the lightest component in the mixture to the heaviest.

Therefore, a residue curve can be described as the change in composition of a mixture during continuous evaporation at the condition of vapour-liquid equilibrium. RCMs are generated using simulation software, like Aspen Plus® (Julka et al., 2009). A simple distillation process can be described by:

$$\frac{dx_i}{d\xi} = x_i - y_i \qquad [2.17]$$

Where ξ is a nonlinear time scale related to the fraction of liquid remaining in the column at any point in time. Doherty & Perkins (1978) discuss a detailed mathematical treatment of this nonlinear time scale.

Residue curves can only originate, deflect from or terminate at the azeotropes or pure components in the mixture. The composition space is made up of pure-component vertices that run from the lightest component to the heaviest. These points are known as nodes and are classified as unstable nodes (the points at which curves originate), stable nodes (where curves terminate) and saddles (from which residue curves deflect) (Julka, Chiplunkar & O'Young, 2009:47). These nodes and saddles correspond to Equation 2.17, equating to zero.

Figure 2-8 represents the simplest residue curve map possible for a ternary, non-azeotropic mixture. The arrows follow the direction of decreasing boiling temperature. Using this RCM as an example, along with the directions of the residue curves, the light component is an unstable node; the intermediate component represents a saddle point; and the heavy component is a stable node (Doherty & Knapp, 2000).

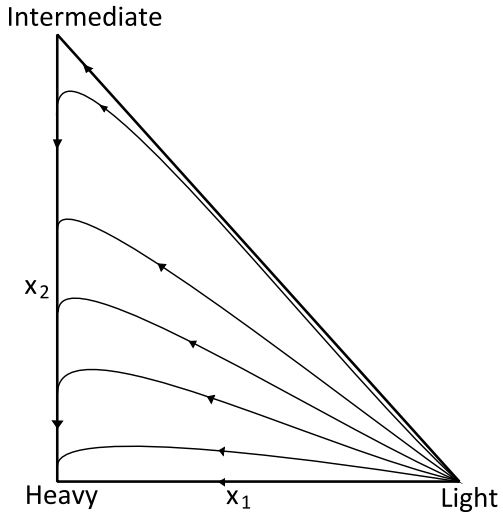

Figure 2-8: ***Residue curve map for a ternary nonazeotropic mixture. According to Doherty & Knapp (2000).***

RCMs for ternary mixtures containing one or more azeotropes are possible. Figure 2-9 represents one of the six possible RCMs for ternary mixtures containing a single azeotrope. When ordering the components from low to high, with regard to their respective boiling points, the sequence of D→C→A or B is obtained (where "C "represents a minimum-boiling azeotrope).

The residue curve, C-D represents a simple distillation boundary, or separatrices, and restricts the efficacy of simple distillation (Doherty & Knapp, 2000). Although azeotropic mixtures cannot be separated through simple distillation, RCMs prove to be extremely useful. RCMs can be used to test the consistency of experimental azeotropic data (Foucher et al., 1991).

However, simple distillation residue curve maps cannot graphically represent a system with more than four components (Doherty & Knapp, 2000).

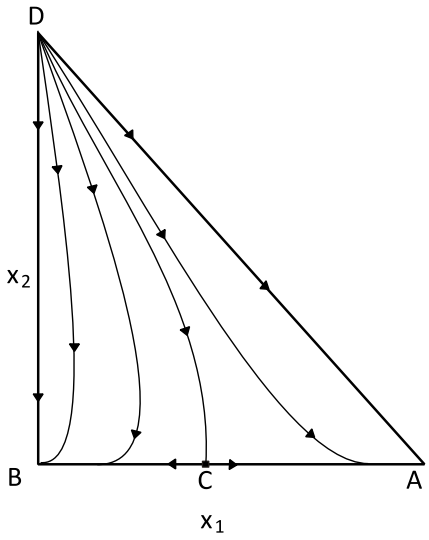

Figure 2-9: ***Residue curve map for a ternary mixture with a distillation boundary running from pure component D to the binary azeotrope C. According to Doherty & Knapp (2000).***

Figure 2-10 represents a typical RCM for ethanol/benzene/water system, generated using Aspen Plus®, at 101.3 kPa. The number of curves have been limited to seven to avoid complexity. This illustrates the presence of the ternary azeotrope as well as the distillation boundaries present.

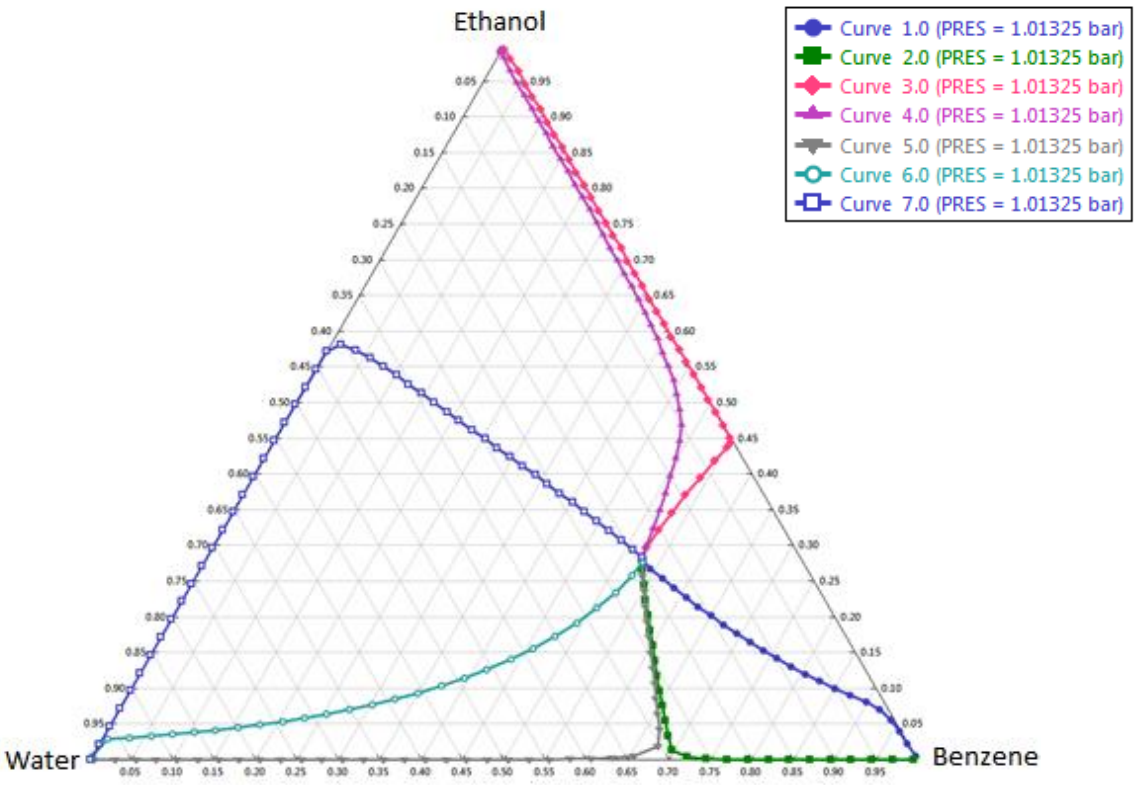

Figure 2-10: ***Residue curve map for ethanol/benzene/water system at 101.3 kPa. Modelled in Aspen Plus® using NRTL.***

2.4 Separation of water/alcohol azeotropes

The design and optimisation of separation processes in chemical process industries, such as chemical and biofuel industries, is of vital importance (Barnicki, Hoyme & Siirola, 2000). The process finally chosen and implemented does not only relate to the purity of the final product obtained, but also to the cost and energy consumption of the entire plant. In extreme cases, approximately half of the total energy usage and a third of the capital costs of a chemical plant have been known to contribute to sustaining and running the distillation columns involved (Gunawan & Chien, 2008).

There are various techniques applied in industry for separating mixtures that form one or more homoazeotropes. Principle distillation-based techniques are discussed in the following section and are considered to be the oldest and most frequently used (Doherty & Knapp, 2000). These distillation methods include:

- Pressure-swing distillation, wherein some azeotropes can be circumvented using two or more columns operated at different pressures.
- Distillation in the presence of ionic salts that alter the relative volatilities of the components.
- Reactive distillation, where the separating agent reacts with a particular component in the mixture.
- Extractive or homogeneous azeotropic distillation, where a completely miscible liquid separating agent (known as a solvent or extractive agent) is added to alter the relative volatilities.
- Heterogeneous azeotropic distillation, where an agent known as the entrainer, forms one or more azeotropes and causes immiscibility.

Alternative separation techniques, known as hybrid distillation systems, have been successfully implemented. These include membrane separation techniques, used in conjunction with distillation (Doherty & Knapp, 2000). The following discussion is limited to the separation of homogeneous azeotropic mixtures; however multiple phases and heterogeneous azeotropic mixtures may result from the separation technique applied. The discussion will be centred on the separation of anhydrous ethanol from a water-ethanol binary mixture.

2.4.1 Membrane-distillation hybrids

There are several membrane-hybrid separation techniques that have been used in industry to produce anhydrous ethanol, including reverse osmosis, vapour permeation and pervaporation. In the late 1980s, Sander and Soukup (1988) published a paper on the complete design and operation of a pervaporation plant for the dehydration of ethanol. These types of processes rely on mass

transfer operations and are considered to be highly selective and energy efficient. Membrane-distillation hybrids, however, are difficult to design and low overall system capacity and inordinate start-up costs are some of the disadvantages associated with this type of separation technique (Haelssig, Tremblay & Thibault, 2012:492; Sander & Soukup, 1988:463).

Figure 2-11 illustrates the mechanism with which membrane distillation functions. The membrane acts as the separating agent by preferentially absorbing and allowing one of the azeotrope-forming components to pass through the semi-permeable barrier into the permeate. The mixture that remains behind, enriched with the other azeotrope-forming components, is called the retentate (Seader & Henley, 1998).

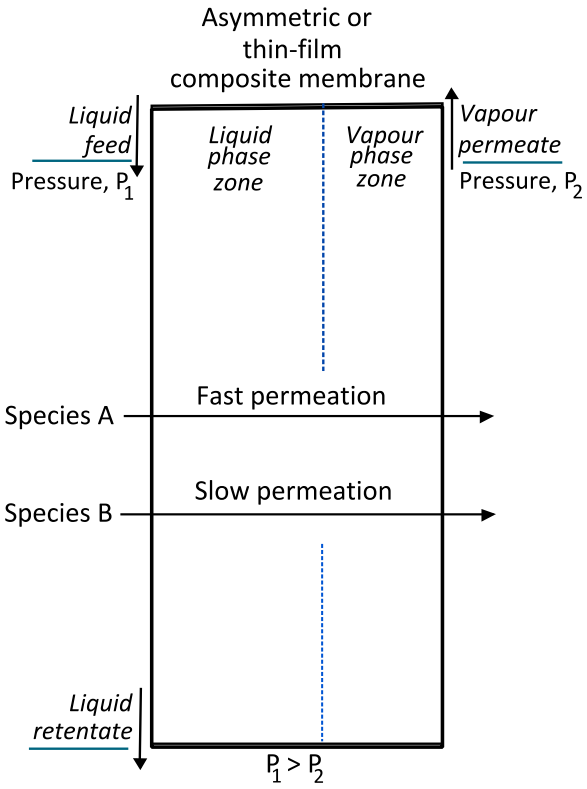

Figure 2-11: ***Schematic illustration of the mechanism upon which membrane distillation functions. According to Seader & Henley (1998).***

Pervaporation has been used extensively as a dehydration method and consists of a distillation column and a pervaporation unit (Haelssig, Tremblay & Thibault, 2012:492). The distillation column acts as a pre-concentrator for the membrane (Figure 2-12). Industrial applications of pervaporation include the dehydration of low molecular weight alcohols and ketones as well as the separation of organic-organic azeotropes and isomers (Seader & Henley, 1998). The separation of the water-ethanol azeotrope is achieved through the use of a hydrophilic laminated membrane (Figure 2-11). Water can permeate through the membrane, leaving behind a mixture of increasing concentrations of ethanol (Haelssig, Tremblay & Thibault, 2012:492). The feed to the membrane is generally in the form of a liquid mixture (in this case, an ethanol-water azeotrope) at a pressure, P1. The membrane

selectively allows species A (water) to permeate through the membrane. However, species B (ethanol) frequently has finite permeability. A pressure, P2, often a vacuum, is used as an alternative to a sweep fluid. This causes the permeate to vaporise.

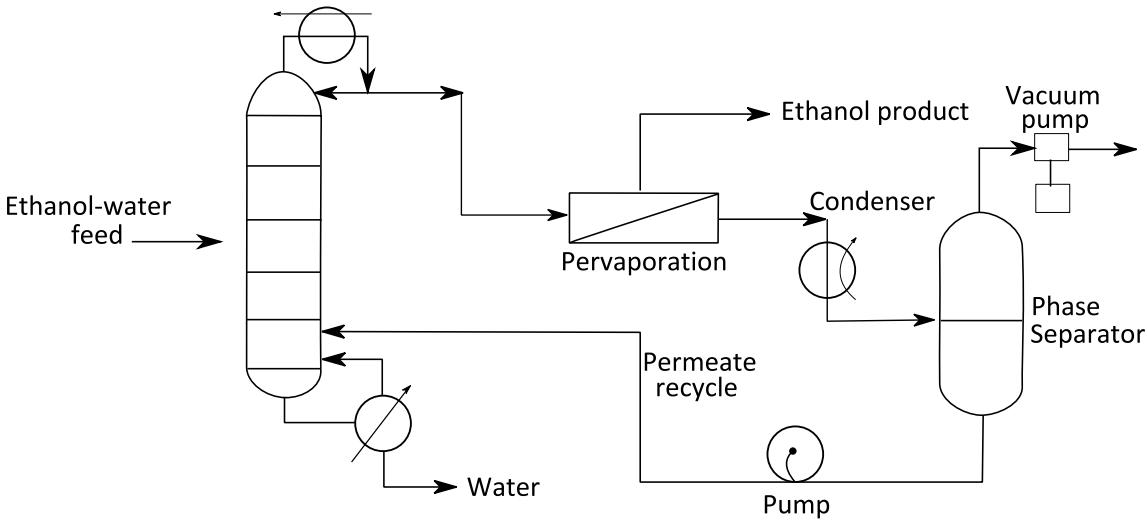

Figure 2-12: ***Pervaporation separation scheme; Hybrid process for removal of water from ethanol. According to Ho & Sirkar (1992).***

Naturally, the separation does not depend on vapour-liquid equilibrium and vapour-liquid-liquid equilibrium information (Sander & Soukup, 1988:463).

2.4.2 Pressure-Swing distillation

As discussed in Section 2.1, azeotropes are temperature- and pressure-sensitive. When the azeotropic compositional change is appreciable over a tolerable pressure range, pressure-swing distillation techniques can be used to separate both minimum- and maximum-boiling azeotropes. This involves a two-column distillation sequence, where the distillation columns are operated at different pressures (Figure 2-13) (Ognisty, 1995:40).

The feed, *F*, is mixed with the recycle-stream from the second column to form the feed, F_1, for the first column. The first column operates at P_1 and the second column operates at a different pressure, P_2. The pure component *A* is removed as the bottom product, B_1 in the set-up illustrated in Figure 2.13b. The distillate, D_1, pressure is changed and fed into the succeeding column and the pure component, *B*, is recovered as the bottom product, B_2. The larger the shift in azeotropic composition, the smaller the required recycle flow rate will be. As a result, the required column diameters will be smaller in addition to a more economical the distillation sequence.

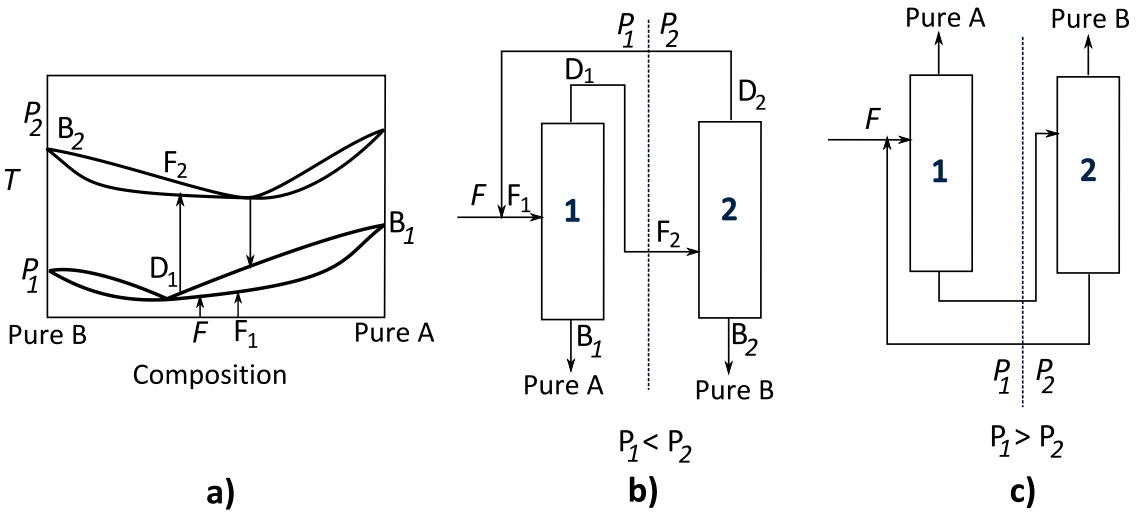

Figure 2-13: ***Pressure-swing distillation; a) T-y-x curves at pressures P_1 and P_2 for a minimum-boiling azeotrope; b) Distillation sequence for a minimum-boiling azeotrope; c) Distillation sequence for a maximum-boiling azeotrope. According to Ognisty (1995).***

Successful applications of this distillation method can be found in published literature; however, its application is limited to the pressure-sensitivity of azeotropic mixtures (Knapp & Doherty, 1992:346).

The cost advantage of this type of method is clear: because the columns are operated at different pressures, they are readily thermally integrated. However, thermal integration affects the ability to control the distillation sequence. Therefore, there is an overall compromise between controllability and the economic advantages associated with pressure-swing distillation methods. (Knapp & Doherty, 1992:346).

When considering pressure-swing distillation as an appropriate separation process for the water/ethanol azeotrope, Knapp and Doherty (1992) estimated the total energy consumption to be 7 500 kJ/kg ethanol, operating at a high pressure of 10 atm. This is due to the fact that the ethanol/water azeotrope is notoriously pressure insensitive (Seader & Henley, 1999).

Pressure-swing distillation is considered to be the most expensive distillation method, when compared to extractive distillation and heterogeneous azeotropic distillation, for separating the water/ethanol azeotrope (Knapp & Doherty, 1992:346).

2.4.3 Salt-Effect Distillation

Salt-effect distillation, also known as salt extractive distillation or salt rectification, is a form of extractive distillation (discussed in Section 2.4.5.3). Rather than using a high boiling liquid as a separating agent, as is the case with extractive distillation, salt-effect distillation makes use of a completely miscible, non-volatile salt or a combination of salts (Seader & Henley, 1998).

The salt-based separating agent is added, as a solid or a melt, directly into the column by dissolving it into the refluxing liquid and can be found in appreciable amounts on all trays throughout the column (Furter, 1993). The separating agent acts by altering the relative volatility of the mixture (Doherty & Knapp, 2000).

Owing to the fact that the salt-based separating agent is non-volatile, purification steps of the resulting distillate are not required as the salt will never enter the distillate overhead vapour.

Therefore, no scrubbing section is required above the feed entry point to strip the separating agent from the overhead, pure product (Luyben, 2010). Recycling the separating agent is relatively straight-forward: the ionic salt(s) exit the column at the bottom with the other non-volatile components where a recovery step, generally a drying process, produces the salt(s) that can be fed directly back into the column (Furter, 1993:1). This translates into lower energy requirements, in comparison to recovery via distillation, and an economical separation process (Luyben, 2010).

When comparing extractive distillation and salt-effect distillation, the use of salt as separating agent leads to higher production capacity and lower energy consumption; this is a direct result of the effects the ionic salts have on the liquid components (Seader & Henley, 1999; Lei, Li & Chen, 2003:121).

Salt-effect distillation is not widely implemented in industry as transportation of the ionic salt through a system is problematic, with erosion being a major concern (Furter, 1993).

2.4.4 Reactive Distillation

In both academic and industrial sectors, interest in reactive distillation has grown considerably over the past few years. In comparison to other distillation methods, the use of reactive distillation as a separating process generally leads to shifting reaction equilibrium and economical energy usage (Wu, Lee, Tsai, Huang & Chien, 2013).

For illustrative purposes, assume a reactive entrainer, E, is added to a binary azeotropic mixture of A and B components. Where component A is the lower-boiling component and component B is the higher-boiling component. If E and B were to react, selectively, to produce a product C (a higher-boiling compound than A which does not form an azeotrope with A), pure A can be obtained as a distillate at the top of the column. The remaining B and E, as well as C, can then be removed from the same column as the bottoms and fed to a second column where the compounds B and E can be retrieved. The reaction product, C, is then broken up by the reverse-reaction to B and E and separated using a third column. Pure compound B can then be obtained. The entrainer, E, can then simply be recycled back to the first column (Guo, Chin & Lee, 2004:3758; Wu et al., 2013).

This may seem like a simple distillation process but a few conditions, according to Seader and Henley (1998), must hold true:

- The chemical reactions must occur in the liquid phase or at the interface between a solid catalyst and a liquid.
- The reaction temperatures and pressures must be feasible for the distillation process.
- The reaction must be driven by equilibrium, in other words the product formed should be distilled off immediately to cause a shift in equilibrium that drives the reaction near to completion.

For the dehydration of low molecular weight alcohols to obtain fuel-grade components, this is not necessarily a feasible separation technique as it requires chemical reactions taking place (Guo, Chin & Lee, 2004:3758). Commercial application of reactive distillation includes the esterification of acetic acid with ethanol to produce ethyl acetate and water (Seader & Henley, 1998). However, no industrial application of reactive distillation to produce anhydrous ethanol has been documented.

2.4.5 Entrainer-addition methods

Through the addition of an extraneous liquid component to an azeotropic mixture, one can achieve significant physiochemical changes to the mixture's resulting VLE behaviour. This extraneous liquid component is known as an *entrainer*. Depending on the role and properties of the entrainer, entrainer-addition based distillation methods can be classified into three sub-categories:

- Homogeneous azeotropic distillation: the entrainer is completely miscible in the original azeotropic mixture and the distillation is carried out in a single-feed column (Section 2.4.5.1).
- Heterogeneous azeotropic distillation: the entrainer forms a heteroazeotrope with one or more of the components in the original azeotropic mixture and a decanter system is required in the distillation process (Section 2.4.5.2).
- Extractive distillation: the entrainer is a liquid with a higher boiling-point than the original mixture components and the distillation is carried out using a two-feed column (Section 2.4.5.3).

When an entrainer-addition method is used to obtain a desired separation objective, the design of an economic recovery system for the entrainer is of paramount importance.

2.4.5.1 Homogeneous azeotropic distillation

A general definition of homogeneous azeotropic distillation is the distillation of a mixture containing one or more azeotropes without exploiting any liquid-phase immiscibilities.

Subsequently, the addition of the entrainer to the azeotropic mixture may or may not form an additional azeotrope. This type of classification also applies to the distillation of non-azeotropic mixtures, to which an entrainer is added to explicitly lead to the formation of an azeotrope in order to aid the distillation of one or more of the components within the mixture (Doherty & Perkins, 1978:281).

Homogeneous azeotropic distillation also encompasses the distillation of azeotropic mixtures, where the desired separation can be achieved without the addition of a separating agent (Seader & Henley, 1999).

As mentioned, the separation is achieved without exploiting any liquid-liquid immiscibilities in the mixture and requires the use of two or more columns; at least one column is employed to cause the azeotrope rupture and another for entrainer recovery (Luyben, 2010). Seader and Henley (1999) listed several conditions, compiled from other published literature, that an entrainer must satisfy for homogeneous azeotropic distillation to be feasible and achievable. These conditions are based on the rule that if two components, A and B, are to be separated using an entrainer, E, the subsequent distillation boundary cannot be connected to the A-B azeotrope. Additionally, either A or B must be a saddle.

There are 125 different possible residue curve maps that represent all ternary mixtures (Doherty & Knapp, 2000). There are a total of five groups of A/B/E azeotropic systems which satisfy the above-mentioned conditions.

Seven of the most favourable RCMs are illustrated in Figure 2-14, for the distillation of a binary minimum-boiling azeotrope. Doherty and Knapp (2000) stated that if an A/B/E azeotropic system does not yield one of these seven RCMs, it is unlikely homogeneous azeotropic distillation will be a suitable separation process.

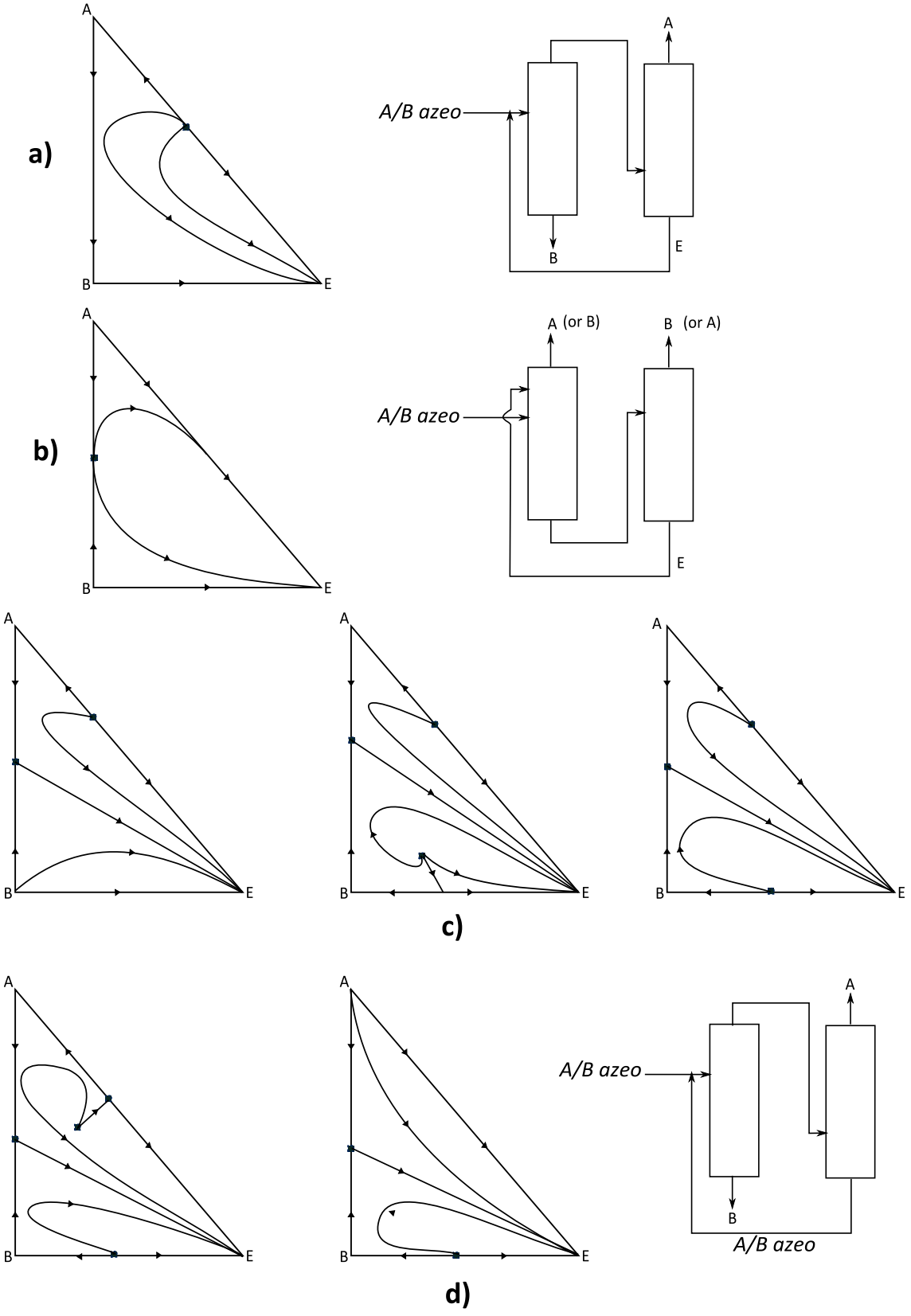

Figure 2-14: ***Seven of the most favourable RCMs and corresponding column sequences for homogeneous azeotropic distillation of a minimum-boiling binary azeotrope, where the symbol ■ represents an azeotrope; a) Where the entrainer is intermediate boiling and no new azeotropes are introduced; b) Extractive distillation with a heavy solvent that does not introduce new azeotropes; c) Where the entrainer is intermediate boiling and introduces a maximum-boiling azeotrope; d) the same column configuration as case c), but the separating is lower boiling. According to Doherty & Knapp (2000).***

Even though this may not appear to be a costly separation technique, it is rare that an entrainer that allows for separation into pure components using only homogeneous azeotropic distillation can be found.

However, homogeneous azeotropic distillation is a technique generally applied, in industry, in sequence with other separation techniques (Shulgin et al., 2001:2742).

2.4.5.2 Heterogeneous azeotropic distillation

Due to the restrictive nature of homogeneous azeotropic distillation, heterogeneous azeotropic distillation is often the solution to separation problems in industry (Urdaneta et al., 2002:3849).

When liquid-liquid immiscibility is exploited to achieve the separation objective, along with the addition of an entrainer to the azeotropic mixture, the separation is classified as heterogeneous azeotropic distillation. The separating agent, or entrainer, is added to the azeotropic mixture to form additional minimum-boiling azeotropes, whether it be binary and/or ternary heterogeneous azeotropes. Heterogeneous azeotropic distillation is used to separate close-boiling binary mixtures and minimum-boiling binary azeotropes, as in the ethanol/water system, by making specific use of a distillate decanter; to pass the distillation boundary by liquid-liquid phase splitting. Due to the boundary crossing, the distillation objective of separating two components that do not lie in the same distillation region can be achieved (Haelssig et al., 2001:714).

In general, the bottoms' composition is close to one of the pure components; the overhead vapour from the column is close to the composition of the heterogeneous azeotrope and, when condensed, forms two liquid phases in the decanter. The liquid-phase containing the bulk of the entrainer will be fed back to the column and, if necessary, the "pure" liquid-phase may be fed to an additional column for further separation and purification (Luyben, 2010).

The first successful application of heterogeneous azeotropic distillation was the dehydration of ethanol using benzene as an entrainer (Luyben, 2010). It is the main focus of this research project as it is a "perfect" example of the advantages of heterogeneous azeotropic distillation: high throughput and purity. However, the environmental concerns associated with this method has led to the need to find an entrainer without the associated health risks.

Figure 2-15 shows the general column sequence used for separating a binary A/B heterogeneous azeotropic mixture. Note the decanter, used to separate the A-rich phase from the B-rich phase.

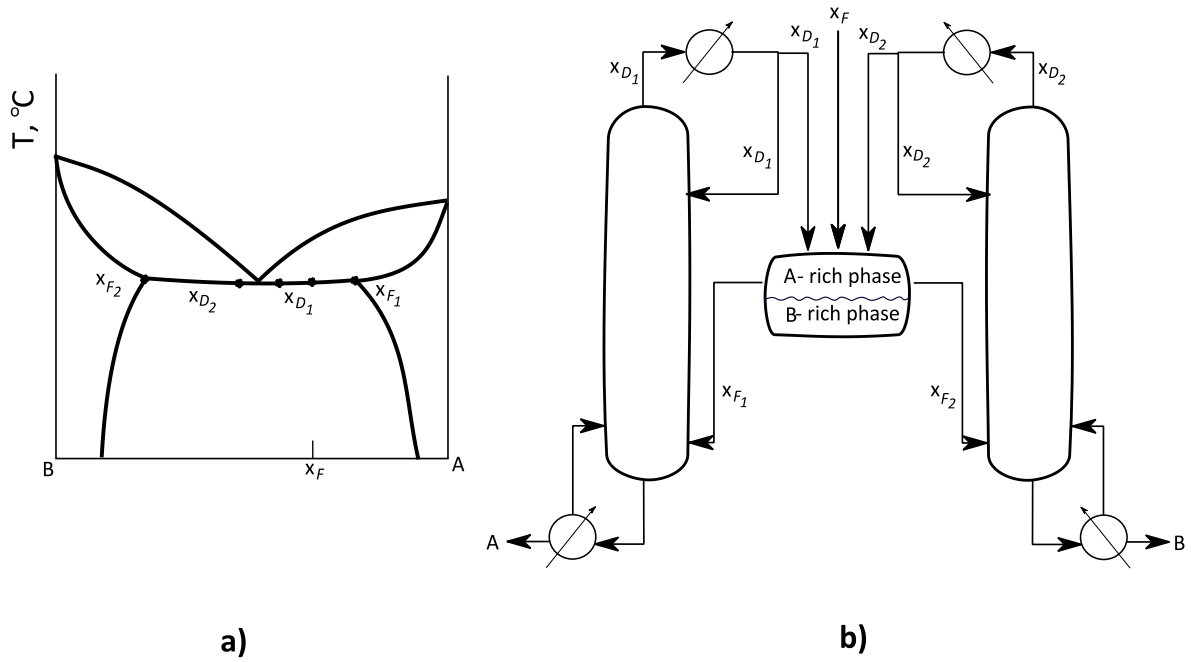

Figure 2-15: ***Column sequence for separating a binary heterogeneous azeotropic mixture; a) phase diagram; b) column sequence. According to Doherty & Knapp (2000).***

Taking ethanol/benzene/water as an example, the entrainer, benzene, has limited miscibility with one of the components (in this case water due to the hydrophobic/hydrophilic interactions). The addition of benzene leads to the formation of two minimum-boiling binary azeotropes; one homogeneous and the other heterogeneous (see Figure 2-16). There are three distinct distillation regions, formed by the presence of the distillation boundaries illustrated by the thick black lines. As can be seen from Figure 2-16, the pure ethanol and water components lie in different regions (Moussa & Jiménez, 2006:4304).

A typical separation sequence consists of two distillation columns (an azeotropic distillation column and a recovery column) and, like with the separation of a binary mixture, a decanter (Figure 2-17). A typical feed, F, consisting of 0.5 mol fraction ethanol and 0.5 mol fraction water is fed to the first azeotropic distillation column. Benzene is added to the azeotropic column from a mixer. The distillate from this column, D_1, has a composition of the ternary heterogeneous azeotrope. The bottoms, B_1, is relatively pure ethanol. In the decanter, the two liquid phases (L_1 and L_2) are separated due to their differences in densities. L_1, the organic liquid phase is fed back into the azeotropic distillation column where L_2, the aqueous phase is fed into the recovery column. Benzene is recovered as the distillate, D_2, and water is obtained as the bottoms product, B_2. Utilising this set-up, water can be separated from ethanol using benzene as entrainer. Unfortunately, the range of feasible entrainers is once again limited for low molecular weight alcohol/water systems.

For this particular research project, the focus is placed on finding suitable entrainers for the dehydration of low molecular weight alcohols using heterogeneous azeotropic distillation, with

the emphasis placed on the determination of VLE and VLLE data to aid the design of an appropriate separation sequence.

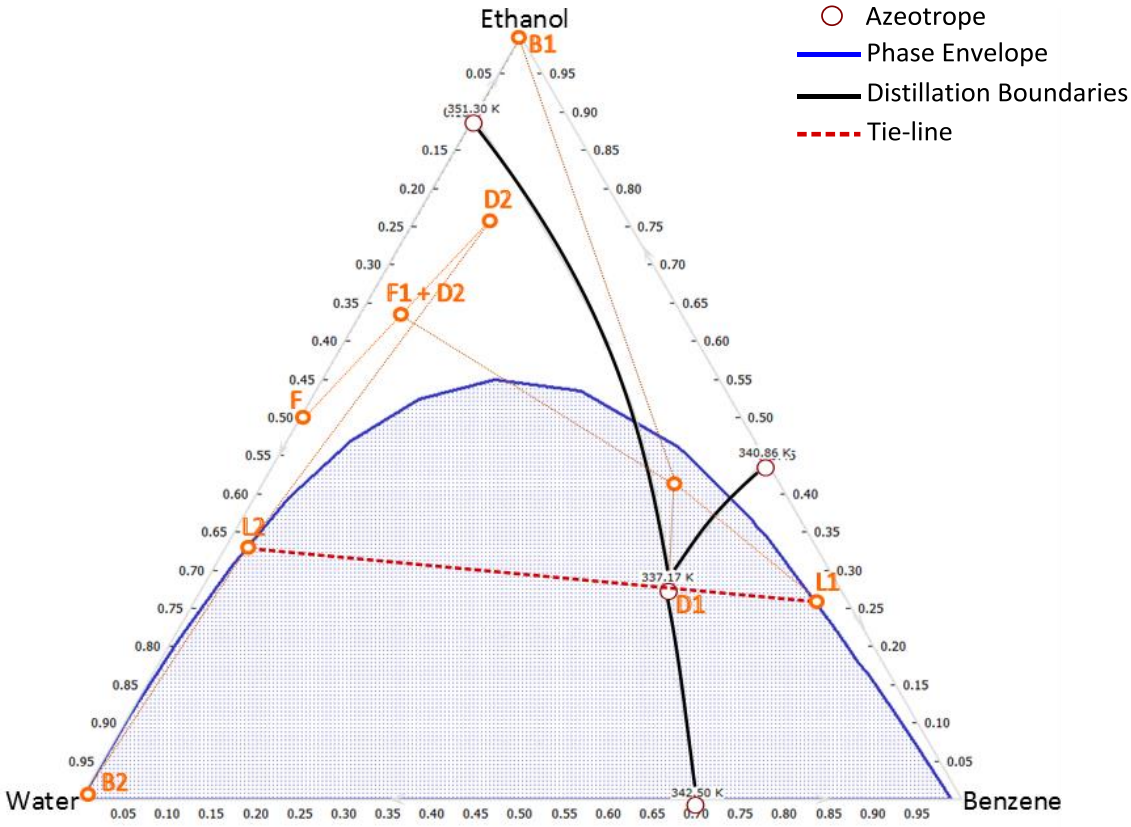

Figure 2-16: ***Distillation curve for the ethanol/benzene/water system at 101.3 kPa. Modelled in Aspen Plus® using NRTL.***

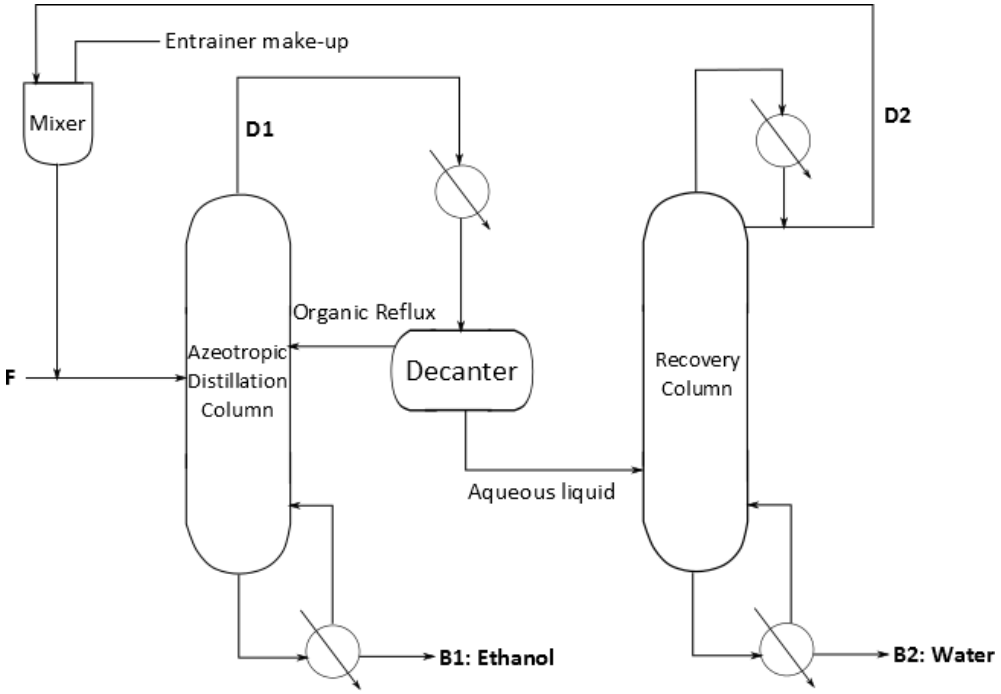

Figure 2-17: ***Column sequence for separating a ternary heterogeneous azeotropic mixture; ethanol/benzene/water at 101.3 kPa. According to Doherty & Knapp (2000).***

2.4.5.3 Extractive distillation

Extractive distillation is widely used in chemical and petrochemical industries to separate azeotropes, close-boiling and other mixtures that have key components with low relative volatilities over an appreciable range of concentrations (Seader & Henley, 1999). Extractive distillation is generally used to achieve the desired separation objective when the resulting phase diagram, of the mixture to be separated, has a severely "pinched" region over a limited composition range, known as a tangent pinch (Knapp & Doherty, 1992: 346). Extractive distillation can be defined as distillation in the presence of a miscible, higher-boiling liquid separating agent (also known as a solvent) which does not form azeotropes with the other components in the mixture once added (Benedict & Rubin, 1945:353). Extractive distillation can be subdivided into three categories: the separation of minimum-boiling azeotropic mixtures, the separation of maximum-boiling azeotropic mixtures and the separation of non-azeotropic mixtures. The solvent is specifically chosen to interact differentially with the components of the mixture by altering their relative volatilities. These newly introduced interactions exist predominately in the liquid-phase (Wang et al., 2013:627; Knapp & Doherty, 1992:346).

When the feed is a minimum-boiling azeotropic mixture, the solvent is added to the tray above the feed stage and can be found in appreciable concentrations throughout the column. A binary minimum-boiling azeotropic mixture, that can be separated into its pure components using extractive distillation, has a residue curve map and column sequence similar to that shown in Figure 2-14b.

Little of the solvent is lost to the overhead vapour due to its volatility. In the first, extractive, column the component with the higher volatility in the presence of the solvent is distilled overhead as a relatively pure distillate, A (or B). The other component leaves the column with the solvent and is subsequently separated using a second, solvent recovery, column. The product that leaves the top of the column is a relatively pure distillate, B (or A), and the solvent is recycled back to the first column (Lei, Li & Chen, 2003:121; Doherty & Knapp, 1999). The extractive distillation of ethanol from water using ethylene glycol is an important example of this type of distillation (Doherty & Malone, 2001).

Alternatively, if the feed is a maximum-boiling azeotropic mixture, the solvent enters the column *with* the feed. However, the number of maximum-boiling azeotropic systems is far fewer than minimum-boiling azeotropic systems; the successful applications of extractive distillation to the separation of maximum-boiling azeotropes are also scarcer.

Finding a higher-boiling solvent that does not result in a distillation boundary (i.e. the resulting distillation boundary is extremely curved) is exceptionally difficult (Doherty & Knapp, 2000). See Figure 2-18 for the resulting RCM suitable for for separating a maximum-boiling azeotropic mixture.

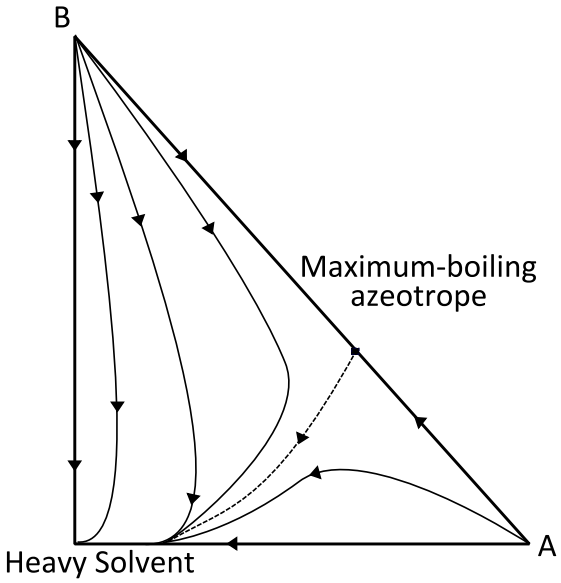

Figure 2-18: ***Residue curve map for separating a maximum boiling azeotrope using a high boiling solvent; where the symbol ■ represents an azeotrope and (----) represents a distillation boundary. According to Doherty & Knapp (2000).***

The extractive distillation of non-azeotropic mixtures is far more common. The petrochemical industry utilises extractive distillation to separate and/or purify close-boiling mixtures. The distillation sequence is identical to that used to separate minimum-boiling azeotropic mixtures (Figure 2.14c).

Extractive distillation, on the other hand, behaves in an unpredictable way at high reflux ratios; increasing the reflux ratio may decrease product purity. As the reflux ratio increases, the number of stages required for separation decreases until it reaches a minimum where an increase in reflux ratio, from that point onwards, will lead to an increase in stages required for separation (Lei, Li & Chen, 2003:121). Another disadvantage of extractive distillation is the fact that only one of the components can be extracted from the top of the first column. This component need not be the pure component with the lowest volatility mixture. For example, when extractive distillation is used to dehydrate ethanol using gasoline as extractive solvent, the lower boiling ethanol leaves in the bottom stream with the solvent. A way to identify which compound will leave the column with the solvent is to construct a pseudo-binary y-x phase diagram, see Figure 2-19.

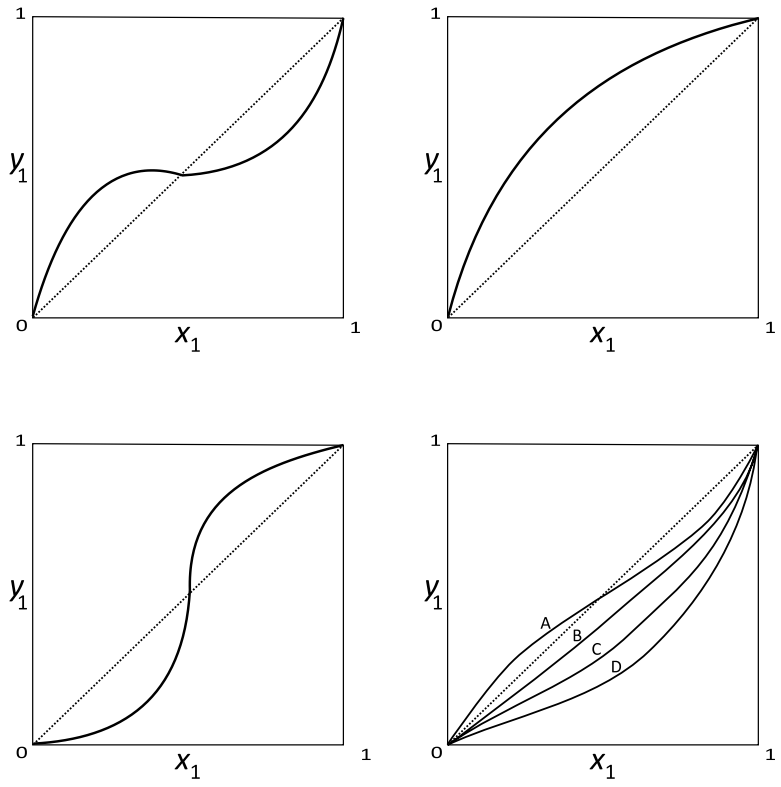

Figure 2-19: ***Pseudo-binary (solvent-free) y-x phase diagrams; a) No solvent present; b) and c) sufficient solvent present to eliminate pseudo-azeotrope; d) experimental VLE data for benzene-cyclohexane using aniline: A, B, C and D represent 0, 30, 50 and 90 mol% aniline. According to Kolbe, Gmehling & Onken (1979).***

2.5 Summary

Most mixtures containing organic components, like low molecular weight alcohols, form non-ideal systems. In extreme non-ideal systems, azeotropes are likely to form. If the homogeneous azeotrope formed in a binary mixture (ethanol-water, n-propanol-water and iso-propanol-water) is not pressure sensitive, membrane-distillation hybrids or distillation methods are used to effectively separate the mixture into its pure components. Distillation-based methods are used in 90% of all cases in industry due to its potential for high feed concentration, throughput and purity (Ghehling et al. 1994). The design, operation and control of distillation techniques are well-known and widely publicised, in contrast to separation techniques, such as membrane-distillation hybrids (Smith, 1995).

Distillation, however, results in large energy costs and additional complexities introduced by the presence of an entrainer. Industrial applications of membrane-based separation techniques are limited due to the fact that membranes are expensive and can only tolerate restricted feed volumes. Therefore entrainer-addition methods will solely be considered in this work for their distinct economic advantage, robust and flexible equipment, and tolerance for a variety of feed concentrations.

The experimental generation and subsequent analysis of ternary VL(L) diagrams is an important and efficient tool to for the design and application of entrainer-addition based distillation processes. For this work, three different entrainer-addition methods were discussed:

- *Homogeneous azeotropic distillation* is limited due to the fact that only a few resulting ternary system (alcohol/water/azeotrope) can be separated using this separation technique.
- *Heterogeneous azeotropic distillation* several VL(L)E diagram structures, with one or more heterogeneous azeotropes, can be separated using a simple distillation column in combination with a decanter.
- *Extractive distillation* is an advantageous separation technique, with a broad range of feasible entrainers, however, it is extremely energy intensive.

Due to the restrictive nature of extractive distillation and homogeneous azeotropic distillation, heterogeneous azeotropic distillation is generally the separation technique utilized in industry. With the combination of high throughput and purity, low operation costs and ease of thermal integration, heterogeneous azeotropic distillation is the technique of choice. The focus of this research project is to find a suitable entrainer, which can be added to an alcohol/water mixture, making heterogeneous azeotropic distillation possible.

Consequently, this work will focus on the dehydration of low molecular weight alcohols using heterogeneous azeotropic distillation.

3 THERMODYNAMIC BASIS

As discussed in Chapter 2, the thermodynamic depiction of vapour-liquid and vapour-liquid-liquid equilibrium data is a useful tool in predicting a feasible operating space in which any distillation process can take place. In the absence of experimental data, sound thermodynamic principles are required to predict VLE and VLLE data. This chapter gives an in-depth account of the thermodynamic basis used to predict VLE and VLLE data. The selected activity coefficient models, NRTL, UNIQUAC and UNIFAC, are discussed in the following sections as well as the thermodynamic consistency testing methods used in this work.

3.1 Thermodynamic Background

Given a system consisting of π phases and *m* species, the criterion for phase equilibrium is:

$$T^{(1)} = T^{(2)} = \cdots = T^{(\pi)} \quad [3.1]$$

$$P^{(1)} = P^{(2)} = \cdots = P^{(\pi)} \quad [3.2]$$

$$\mu_1{}^{(1)} = \mu_1{}^{(2)} = \cdots = \mu_1{}^{(\pi)} \quad [3.3]$$

$$\mu_2{}^{(1)} = \mu_2{}^{(2)} = \cdots = \mu_2{}^{(\pi)}$$

$$\vdots \qquad \vdots \qquad \vdots \quad [3.4]$$

$$\mu_m{}^{(1)} = \mu_m{}^{(2)} = \cdots = \mu_m{}^{(\pi)}$$

Where μ_i is the intensive, chemical potential governing mass transfer and the phase is denoted by the parenthesis and the species denoted by the subscript (Smith et al., 2005).

An absolute value for chemical potential, μ_i, cannot be determined experimentally. However, changes in the chemical potential can be calculated when accompanied with arbitrary changes in the independent variables (temperature, pressure and composition). Relating temperature and pressure, the chemical potential for a pure substance can be written as (Smith et al., 2005):

$$d\mu_i = -s_i dT + v_i dP \quad [3.5]$$

Where s_i is the molar entropy and v_i the molar volume.

The degrees of freedom, *F,* for a particular mixture at equilibrium is:

$$F = N + 2 - \pi \quad [3.6]$$

Where *N* is the number of chemical species and π is the number of phases present. This is an indication of the number of intensive variables that must be specified to fix all remaining variables.

3.1.1 Fundamental Property Relations

From the three fundamental thermodynamic properties (enthalpy, *H*, Helmholtz energy, *A,* and Gibbs energy, *G,)* (3.7-3.9), the definitions of four fundamental property relations (3.10-3.13) can be defined (Smith et al., 2005):

$$H \equiv U + PV \quad [3.7]$$

$$A \equiv U - TS \quad [3.8]$$

$$G \equiv H - TS \quad [3.9]$$

$$dU = TdS - PdV \quad [3.10]$$

$$dH = TdS + VdP \quad [3.11]$$

$$dA = -PdV - SdT \quad [3.12]$$

$$dG = VdP - SdT \quad [3.13]$$

In terms of extensive thermodynamic potential, the following four criteria exist for equilibrium in a closed system (Prausnitz, Lichtenthaler & de Azevedo, 1999):

$$dU_{S,V} = 0 \quad [3.14]$$

$$dH_{S,P} = 0 \quad [3.15]$$

$$dA_{T,V} = 0 \quad [3.16]$$

$$dG_{T,P} = 0 \quad [3.17]$$

The Gibbs free energy of an *m*-component mixture is a function of temperature, pressure and mole number of each species and can be written as (Smith et al., 2005):

$$dG = \left(\frac{\partial G}{\partial T}\right)_{P,n_i} dT + \left(\frac{\partial G}{\partial P}\right)_{T,n_i} dP + \sum_{i=1}^{m} \left(\frac{\partial G}{\partial n_i}\right)_{T,P,n_{j\neq i}} dn_i$$

$$= -SdT + VdP + \sum_{i=1}^{m} \bar{G}_i^{\,E} dn_i \qquad [3.18]$$

Where,

$$d\mu_i = -s_i dT + v_i dP \qquad [3.19]$$

This relation (3.18) is known as the Gibbs/Duhem equation and describes the relationship between changes in chemical potential (3.5) of the components in the mixture (Smith et al., 2005).

3.1.2 Chemical Potential and Fugacity

As mentioned, chemical potential does not have an immediate equivalent in the physical world. Therefore an auxiliary function is given by the idea of fugacity (Prausnitz, Lichtenthaler & de Azevedo 1999):

$$\mu_i = \mu_i^0 + RT \ln \frac{f}{f_0} \qquad [3.20]$$

With the arbitrary reference values of μ_i^0 and f_0, if one is chosen independently, the other is fixed. The ratio $\frac{f}{f_0}$ is known as the *activity* (a_i) and at equilibrium:

$$\hat{f}_i^{\,v} = \hat{f}_i^{\,l} \qquad [3.21]$$

$$\hat{\varphi}_i^{\,v} y_i = \hat{\varphi}_i^{\,l} x_i \qquad [3.22]$$

As discussed in Section 2.1.1, the modified Raoult's law, at low pressures (P < 1 bar) is:

$$y_i P = x_i \gamma_i P_i^{sat} \qquad [3.23]$$

3.1.3 Excess Property Relations

Where a residual property is the difference between an ideal and real gas property, an excess property is defined as the difference between the partial molar property of a component in a real mixture and the same component in an ideal mixture at the same temperature, pressure and composition.

For example, the excess Gibbs energy is defined as (Smith et al., 2005):

$$G^E \equiv H^E - TS^E = G - G^{id} \quad [3.24]$$

It can be proven that the excess Gibbs energy property relation becomes (Smith et al., 2005):

$$d\left(\frac{nG^E}{RT}\right) = \frac{nV^E}{RT}dP - \frac{nH^E}{RT^2}dT + \sum_i \frac{\bar{G}_i^E}{RT}dn_i \quad [3.25]$$

3.1.4 Activity, activity coefficients and the Gibbs/Duhem equation

It has been shown that the activity coefficient is a partial property with respect to $\frac{nG^E}{RT}$ (Smith et al., 2005). The activity of a substance can be considered to be an indication of how "active" a substance is relative to its standard state. This is due to the fact that activity is a measure of the difference between the substance's chemical potential (f_i) at the state of interest and that at its standard state (f_i^0) (Stanley, 1999):

$$a_i(T,P,x)) = \frac{f_i(T,P,x)}{f_i(T,P^0,x^0)} \quad [3.26]$$

Where P^0 and x^0 are arbitrary, specified pressure- and composition-values.

When dealing with non-ideal mixtures, where the activity does not equal the molar composition, the activity coefficient (γ_i) is used to describe the departure from non-ideality:

$$\gamma_i \equiv \frac{a_i}{x_i} = \frac{f_i}{x_i f_i^0} \quad [3.27]$$

By using the Gibbs/Duhem equation (3.18) for a multi-component system, and the definition of activity coefficient, it has been proven that (Smith et al., 2005):

$$d\left(\frac{nG^E}{RT}\right) = \frac{nV^E}{RT}dP - \frac{nH^E}{RT^2}dP + \sum_i x_i \ln \gamma_i \quad [3.28]$$

And, from the above:

$$\ln \gamma_i = \left[\frac{\partial\left(\frac{nG^E}{RT}\right)}{\partial n_i}\right]_{P,T,n_j} \quad [3.29]$$

$$\frac{G^E}{RT} = \sum_i x_i \ln \gamma_i \quad [3.30]$$

3.2 Excess Gibbs Energy Models

In the above sections, it was proven that phase equilibria can be described by excess Gibbs energy, used in conjunction with the modified Raoult's law to calculate activity coefficients. There are several thermodynamic models that model $\frac{nG^E}{RT}$ using predetermined parameters. The following discussion will be limited to the NRTL, UNIQUAC and UNIFAC models. This is due to their known ability to predict and correlatively predict phase equilibria of polar mixtures. All parameter values discussed can be obtained from literature, estimated, or found as built-in parameters in Aspen Plus®.

3.2.1 NRTL (Non-random Two Liquid) Equation

Developed by Renon and Prausnitz (1968), the NRTL equation is an extension of the Wilson's derivation. Experimental data for a large number of binary systems is required. The NRTL equation contains three types of parameters (α_{ji}, τ_{ji}, τ_{ij}) and is valid for multi-components VLE, LLE and VLLE:

$$\frac{G^E}{RT} = \sum_i x_i \frac{\sum_i x_i \tau_{ji} G_{ji}}{\sum_k x_k G_{ki}} = x_i x_j \left(\frac{\tau_{ji} G_{ji}}{x_i + x_j G_{ji}} + \frac{\tau_{ij} G_{ij}}{x_j + x_i G_{ij}}\right) \quad [3.31]$$

Where:

$$G_{ji} = exp\left(-\alpha_{ji}\tau_{ji}\right) \quad [3.32]$$

And,

$$\tau_{ij} = a_{ij} + \frac{b_{ij}}{T} + e_{ij} \ln T + f_{ij} T \quad [3.33]$$

The parameter in G_{ji}, expressed as α_{ji}, is tendency of species *i* and *j* to be distributed in a non-random manner.

From Equation 3.29 and 3.31 it can be proven that:

$$\ln \gamma_i = x_j^2 \left[\tau_{ji} \left(\frac{G_{ji}}{x_i + x_j G_{ji}} \right)^2 + \frac{\tau_{ij} G_{ij}}{\left(x_j + x_i G_{ij} \right)^2} \right] \quad [3.34]$$

For both equations, $\ln \gamma_i$, can be obtained by interchanging the subscript *i* with *j*. These equations have been derived for an *i* and *j* component mixture.

3.2.2 UNIQUAC (UNIVERSAL QuasiChemical Theory) Equation

The UNIQUAC (universal quasichemical) model, developed by Abrams and Prausnitz (1975), is based on statistical mechanical theory and allows both size and energy differences between the components in a mixture to result in local compositions (Stanley, 1999):

$$\frac{G^E}{RT} = \frac{G^E_{combinatorial}}{RT} + \frac{G^E_{residual}}{RT} \quad [3.35]$$

The first term accounts for molecular size and shape differences, and the second term accounts largely for energy differences:

$$\frac{G^E_{combinatorial}}{RT} = \sum_i x_i \ln \frac{\phi_i}{x_i} + \frac{z}{2} \sum_i x_i q_i \ln \frac{\theta_i}{\phi_i} \quad [3.36]$$

$$\frac{G^E_{residual}}{RT} = -\sum q_i x_i \ln \left(\sum \theta_j \tau_{ji} \right) \quad [3.37]$$

Where,

q_i= surface area parameter for species *i*

θ_i= area fraction of species *i* = $x_i q_i / \sum x_j q_j$

ϕ_i= segment or volume fraction of species *i*

and

$$\ln \tau_{ij} = \frac{\left(u_{ij} - u_{jj} \right)}{RT} \quad [3.38]$$

The average interaction energy, u_{ij}, is the species *i*-species *j* interaction and z is the average coordination number. Combining the above equations yields the following UNIQUAC expression for activity coefficients (Stanley, 1999):

$$\ln \gamma_i = \ln \gamma_i(combinatorial) + \ln \gamma_i(residual) \quad [3.39]$$

$$\ln \gamma_i(combinatorial) = \ln \frac{\phi_i}{x_i} + \frac{z}{2} q_i \ln \frac{\theta_i}{\phi_i} + l_i - \frac{\phi_i}{x_i} \sum_j x_j l_j \quad [3.40]$$

$$\ln \gamma_i(residual) = q_i \left[1 - \ln \left(\sum_j \theta_j \tau_{ji} \right) - \sum_j \frac{\theta_j \tau_{ij}}{\sum_k \theta_k \tau_{kj}} \right] \quad [3.41]$$

Where

$$l_i = (r_i - q_i) z/2 - (r_i - 1) \quad [3.42]$$

3.2.3 UNIFAC (Universal Functional Activity Coefficient) Equation

The UNIFAC (UNIQUAC Functional-group Activity Coefficient) model is based on the UNIQUAC model. This model has been studied extensively and appears in several works (Fredenslund, 1989, Kojima & Tochigi, 1979). The combinatorial term (first term) is evaluated by means of the same method as the UNIQUAC model. The residual term is evaluated by a group contribution method. The residual contribution to the logarithm of the activity coefficient of group k in the mixture, $\ln \Gamma_k$, is computed from:

$$\ln \Gamma_k = Q_k \left[1 - \ln \left(\sum_m \Theta_m \Psi_{mk} \right) - \sum_m \frac{\Theta_m \Psi_{km}}{\sum_n \Theta_n \Psi_{nm}} \right] \quad [3.43]$$

Where,

Θ_m = surface area fraction of group *m* = $X_m Q_m / \sum_n X_n Q_n$

X_m= mole fraction of group *m* in the mixture

and

$$\Psi_{mn} = exp \left[\frac{-(u_{mn} - u_{nn})}{kT} \right] = \exp \left[\frac{-a_{mn}}{T} \right] \quad [3.44]$$

Where, u_{mn} is a measure of the interaction energy between groups *m* and *n*. The residual part of the activity coefficient of species *i* is computed from:

$$\ln \gamma_i(residual) = \sum_k v_k^{(i)} \left[\ln \Gamma_k - \ln \Gamma_k^{(i)}\right] \quad [3.45]$$

Where $v_k^{(i)}$ is the number of *k* groups present in species *i*, $\Gamma_k^{(i)}$ is the residual contribution to the activity coefficient of group *k* in a pure fluid of species *i* molecules (Sum & Sandier, 1999).

3.3 Thermodynamic Consistency Testing

For equilibria phase data to be considered accurate for design and modelling purposes, the reliability and consistency of the data needs to be established. The thermodynamic consistency of the experimentally determined data is tested in order to determine their conformance to physical phenomena, in particular, the Gibbs/Duhem equation (see Equation 3.18). If the data-set satisfies the physical criteria of well-formulated consistency tests, in principle, the data is considered accurate (Sandler, 2006). An alternative to Equation 3.27, for a multi-component mixture:

$$\sum x_i d \ln \gamma_i = \frac{H^E}{RT^2} dT - \frac{V^E}{RT} dP \quad [3.46]$$

Where H^E and V^E are the heat and volume of mixing respectively. The Gibbs/Duhem equation enforces a coupling between the partial properties of the components in a mixture and is the basis of most thermodynamic consistency tests (Wisniak, 1993). At constant temperature and pressure, for a binary mixture, Equation 3.46 simplifies to:

$$x_1 \frac{d \ln \gamma_1}{dx_1} + x_2 \frac{d \ln \gamma_2}{dx_1} = 0 \quad [3.47]$$

Veracious data satisfy the Gibbs/Duhem relation; adequate data obeys this relation within reasonable limits (Wisniak et al., 1996). This means that consistency tests will not give a unique, concluding answer concerning the quality of the data. Nonetheless, when treated with rigour and reasonable assumptions, consistency tests provide valuable information on empirical data.

3.3.1 L/W Wisniak Consistency Test

In the case of constant temperature and pressure, the Gibbs/Duhem equation establishes a simple relationship between the plots of $\ln(\gamma_2/\gamma_1)$ vs. x_1. This relationship is used to test the thermodynamic consistency of each experimental point, also known as a "point-to-point test" (Wisniak, 1994).

Owing to the fact that empirical data is rarely measured at constant temperature and pressure, the following expressions are important:

- Isothermal: $$\int_0^1 \ln\frac{\gamma_1}{\gamma_2} dx_1 = -\int_{P_2}^{P_1} \frac{V^E}{RT} dP \quad [3.48]$$
- Isobaric: $$\int_0^1 \ln\frac{\gamma_1}{\gamma_2} dx_1 = -\int_{T_2}^{T_1} \frac{H^E}{RT} dT \quad [3.49]$$

In the isothermal case, the volume of mixing can be neglected and the thermodynamic consistency test can be performed according to the Redlich-Kister method (Redlich and Kister, 1949).

In contrast, for the isobaric case, the heat of mixing cannot be neglected. Wisniak (1993) proposed a set of equations that relate the excess Gibbs free energy of a mixture with its boiling point at equilibrium:

$$\frac{G^E}{RT} = \sum_i x_i \ln \gamma_i \quad [3.50]$$

Where,

$$\gamma_i = \frac{y_i P}{x_i P_i^{sat}} \quad [3.51]$$

The Clausius-Clapeyron equation is employed:

$$\ln\frac{P}{P_i^{sat}} = \frac{\Delta H_i^{sat}\left(T_i^{sat} - T\right)}{RT_i^{sat}T} = \frac{\Delta S_i^{sat}\left(T_i^{sat} - T\right)}{RT} \quad [3.52]$$

Where,

P_i^{sat} = vapour pressure of component i

T_i^{sat} = boiling temperature of component i

and the enthalpy and entropy terms are in terms of vaporisation.

$$G^E = \sum_i x_i \Delta S_i^{sat} \left(T_i^{sat} - T\right) + RT \sum_i x_i \ln \frac{y_i}{x_i} \quad [3.53]$$

Wisniak (1993) defined the following terms:

$$\Delta S = \sum_i x_i \Delta S_i^{sat} \quad [3.54]$$

$$w = \sum_i x_i \ln \frac{y_i}{x_i} \quad [3.55]$$

Leading to the expression for the bubble point of the mixture:

$$T^{bub} = \sum_i \frac{T_i^{sat} x_i \Delta S_i^{sat}}{\Delta S} - \frac{G^E}{\Delta S} + \frac{RTw}{\Delta S} \quad [3.56]$$

Rearranging this equation (Wisniak, 1993):

$$L_i = \sum_i \frac{T_i^{sat} x_i \Delta S_i^{sat}}{\Delta S} - T^{bub} = \frac{G^E}{\Delta S} - \frac{RTw}{\Delta S} = W_i \quad [3.57]$$

The left-hand side, *L*-values, will be positive except for the case where an azeotrope is present. The sign of G^E, calculated by Equation 3.57, will be positive or negative, depending of the system exhibits positive or negative deviations from ideality. The sign of W_i will be consistent with that of the left-hand side. Integrating over the entire compositional range:

$$L = \int_0^1 L_i \, dx_i = \int_0^1 W_i dx_i = W \quad [3.58]$$

Wisniak (1993) proposed that equality of *L* and *W*, serves as a test for thermodynamic consistency of experimental data:

$$D = 100 \frac{|L - W|}{L + W} \quad [3.59]$$

Wisniak (1993) proposed a maximum value for *D* of *3* to *5* to indicate thermodynamic consistency.

3.3.2 McDermott-Ellis Consistency Test

McDermott and Ellis (1965) derived a multicomponent consistency test from the Gibbs/Duhem equation. As a result of this, this test can be used in conjunction with the L/W consistency test to determine the reliability of empirically determined vapour-liquid equilibrium data.

Aptly known as the McDermott-Ellis consistency test, it is derived by integrating Equation 3.46 over all considered points using the trapezium rule (McDermott & Ellis, 1965):

$$0 = \sum_{i=1}^{N} (x_{ia} + x_{ib})(\ln \gamma_{ib} - \ln \gamma_{ia}) \qquad [3.59]$$

Here, the summation is over all components for every two consecutive experimental points, taken in pairs of *a* and *b* (McDermott & Ellis, 1965). In order to identify inconsistent data as they appear, this consistency test was chosen and applied on a point-to-point basis. Consequently, each consecutive pair of data points were independently considered (Sandler, 2006).

As mentioned previously, perfect data would strictly adhere to the above equation, but leniency needs to be introduced for experimentally determined VLE data. This leniency was introduced by the criteria used for determining whether data are consistent or inconsistent. McDermott and Ellis (1965) stated that a maximum deviation be allowed relating to the cube of the difference of mole fraction in the liquid phase at the two points. An exemplar maximum deviation in Equation 3.59 of 0.01 was allowed for accuracies in composition of ±0.001 (McDermott & Ellis, 1964). This maximum deviation was later redefined by Wisniak and Tamir (1977):

$$D_{max} = \sum_{i=1}^{N} (x_{ia} + x_{ib}) \left(\frac{1}{x_{ia}} + \frac{1}{y_{ia}} + \frac{1}{x_{ib}} + \frac{1}{y_{ib}} \right) \Delta x$$

$$+ 2 \sum_{i=1}^{N} |\ln \gamma_{ib} - \ln \gamma_{ia}| \Delta x + \sum_{i=1}^{N} (x_{ia} + x_{ib}) \frac{\Delta P}{P} \qquad [3.60]$$

$$+ \sum_{i=1}^{N} (x_{ia} + x_{ib}) \beta_i \left(\frac{1}{|t_a + \delta_i|^2} + \frac{1}{|t_a + \delta_i|^2} \right) \Delta t$$

Where all of the Δ-terms are the accuracies of the mole fractions; pressure and temperature of the experimental data set are being tested. The β_i- and δ_i-term are the B_i and C_i Antoine constants of the component in question, respectively (Sandler, 2006).

3.3.3 LLE Consistency Testing

After extensive research, it was concluded that no consistency tests, derived from the Gibbs/Duhem relation, exist for empirically determined liquid-liquid equilibrium data. Looking back at the previous sections, it can be seen that tests derived from the Gibbs/Duhem relation are based on the evaluation, for a single phase, of activity coefficients or excess Gibbs energy calculated by means of activity coefficients (Herrington, 1947). When dealing with vapour-liquid equilibrium, activity coefficients (γ_i) are easily calculated. In contrast, liquid-liquid equilibrium relations, applied to two liquid phases (α and β), allow solely for ratios of activity coefficients to be considered:

$$(\gamma_i x_i)^{\alpha} = (\gamma_i x_i)^{\beta} \qquad [3.61]$$

Correlations to evaluate LLE data have been proposed by both Hand (1930), and Othmer and Tobias (1942) (Verhoeye, 1970). These types of correlations are considered to be a useful tool for the evaluation of LLE data (Treybal, 1963). The correlations assume the following expressions in logarithmic form (Carniti et al., 1978):

- Hand (1930): $$\log\frac{x_{32}}{x_{22}} = k_H \log\frac{x_{31}}{x_{31}} + c_H \qquad [3.62]$$
- Othmer-Tobias (1942): $$\log\frac{1-x_{22}}{x_{22}} = k_{OT} \log\frac{1-x_{11}}{x_{11}} + c_{OT} \qquad [3.63]$$

Where x_{ji} is the weight fraction of the component *i* in the *j*-rich liquid phase and k_H, c_H, k_{OT} and c_{OT} are constants. Treybal (1963) confirmed that x_{ji} can be interchanged for molar fraction if using the Hand correlation (Equation 3.62). However, an analogous demonstration is not possible for the Othmer-Tobias correlation.

Carniti et al. (1978) performed a critical analysis of the sensitivity as well as random errors associated with each method and found the Hand correlation to be highly insensitive. Although the Othmer-Tobias correlation also demonstrated insensitivity, it is considered to be a superior test for LLE data in comparison to the Hand correlation (Carniti et al. 1978). LLE data can be analysed by plotting ($\log\frac{1-x_{22}}{x_{22}}$) vs. ($\log\frac{1-x_{11}}{x_{11}}$) and testing for a good linear correlation coefficient by applying a least-square regression (*R*-value). Carniti et al. (1978) reported a value of *R*=0.990 as the lowest limit for a good linear correlation coefficient.

The experimentally determined LLE data will be tested using this correlation method and deemed accurate for *R*-values larger than 0.990.

3.3.4 VLLE Consistency Testing

No consistency test could be found in literature that applies, explicitly, to experimentally determined vapour-liquid-liquid equilibrium data. VLE consistency tests (like the L/W consistency test and the McDermott-Ellis test) are applied to VLLE data in order to decide their consistency. The validity of these tests when applied to VLLE data, however, is speculative and the reliability and accuracy of VLLE data is ascertained by rigorous verification of the phase equilibrium equipment.

Mass balances performed on all samples' analyses are also a good indication of the reliability of the data. As discussed in Section 2.3.3, according to mass balance rules, the overall liquid sample's composition will lie on the tie line between the organic and aqueous liquid phase. A sample calculation can be found in Appendix D.

3.3.5 Summary of Thermodynamic Consistency

Substantial empiricism and arbitrariness surround the analysis and application of consistency tests. This may bring into question their functionality as a gauge of equilibrium data accuracy. On the other hand, thermodynamic consistency testing provides a means of testing phase equilibria data. The application of consistency tests requires reasonable assumptions and thermodynamic models, approached with rigour and an ultimate thorough examination of the data and results of the test (Wisniak et al., 1997). In order to show that any set of experimental data is justly representative of a system, equipment verification and the analysis of mass balances are required. This combinatory, meticulous approach is applied for all data sets generated for this research work. Results of the thermodynamic consistency tests can be found in Appendix F.

4 METHODS OF LOW-PRESSURE VLE AND VLLE MEASUREMENT

Despite the availability of powerful modelling software, which is only as powerful as the thermodynamic models employed, the rising demand for experimental (vapour-liquid-liquid) equilibrium data can be seen (Gomis et al., 2010). All phase equilibria (VLE, LLE and VLLE) data are thus vital in the modelling, design and optimization of separation processes (Wyczesany, 2014).

In comparison to existing VLE data, the acquisition of multicomponent VLLE data is challenging. Table 4-1 lists the isobaric VLLE data available from literature. A total of 61 ternary systems have been studied and published over 88 years, of which 50 systems are measured at atmospheric pressures. This lack of VLLE data is justified by the difficulty with which it is determined experimentally. Equipment that is commercially available is designed for the determination of VLE data; in other words, the equipment is designed to measure equilibria involving a homogeneous liquid. Two approaches have been published that circumvent this problem: using VLE equipment to measure VLLE data and the modification of VLE equipment to measure VLLE data. These issues will be discussed in detail in the following sections.

The incentive for generating isobaric multicomponent vapour-liquid-liquid equilibrium data is the fact that heterogeneous azeotropic distillation columns operate at an approximately constant, low-pressure. The appropriate simulation and subsequent application of such an azeotropic distillation column requires knowledge of the size and shape of the isobaric heterogeneous region as well as the gradient of the liquid-liquid tie-lines. These features are obtained from accurate VLLE data and influence the entire distillation sequence: affecting the composition of the condensed vapour that exits the top of the distillation, which alters the composition of the two liquids separated in the decanter (Gomis et al., 2005, Gomis et al., 2007).

Table 4-1 : ***Source of published experimental multicomponent VLLE isobaric data. Adapted from Pienaar et al. (2012) with additional info added.***

System	Reference	Date	Method	P/kPa	No. data points
(Water + ethanol + benzene)	Barbaudy	1927	Distillation	101.3	6
(Water + allylic alcohol + trichloroethylene)	Hands and Norman	1945	Distillation	101.3	6
(Water + allylic alcohol + carbon tetrachloride)	Hands and Norman	1945	Distillation	101.3	6
(Water + acetone + chloroform)	Reinders and De Minjer	1947	Distillation	101.3	22
(Water + acetonitrile + acrylonitrile)	Blackford and York	1965	Distillation	101.3	6
(Water + cyclohexanone oxime + nitrocyclohexane)	Lutugina and Soboleva	1967	Dynamic Othmer	101.3	11
(Water + acetonitrile + acrylonitrile)	Volpicelli	1968	Distillation	101.3	5
(Water + 2-propanol + cyclohexane)	Verheoye	1968	Distillation	101.3	6
(Water + acetic acid + p-xylene)	Murogova et al.	1971	Dynamic Othmer	Atmospheric	13
(Water + methanol + ethyl acetate)	Van Zandijcke and Verhoeye	1974	Dynamic Othmer	101.3	6
(Water + ethanol + ethyl acetate)	Van Zandijcke and Verhoeye	1974	Dynamic Gillespie	101.3	4
	Lee et al.	1996	Dynamic Othmer	Atmospheric	11
	Gomis et al.	2000	Dynamic Gillespie	101.3	5
(Water + methanol + n-butanol)	Newsman and Vahdat	1977	Flow	99.2	10
(Water + ethanol + n-butanol)	Newsman and Vahdat	1977	Flow	102.2	7
(Water + n-propanol + n-butanol)	Newsman and Vahdat	1977	Flow	99.7	13
(Hexane + benzene + tetramethylene sulfone)	Rawat et al.	1980	Dynamic Othmer	101.3	5
(Water + 2-propanol + 1-butanol)	Aicher et al.	1995	Dynamic Gillespie	Atmospheric	16
(Water + ethanol + 1-butanol)	Gomis et al.	2000	Dynamic Gillespie	101.3	4
	Iwakabe and Kosogue	2001	Dynamic Gillespie	101.3	4
(Water + 2-propanone + 2-butanone)	Gomis et al.	2000	Dynamic Gillespie	101.3	6
(Water + ethanol + diethyl ether)	Gomis et al.	2000	Dynamic Gillespie	101.3	7
(Water + 1-butanol + n-butyl acetate)	Gomis et al.	2000	Dynamic Gillespie	101.3	8
(Ethanol + 2-butanol + water)	Iwakabe and Kosogue	2001	Dynamic Gillespie	101.3	12
(Water + 1-propanol + 1-pentanol)	Asensie et al.	2002	Dynamic Gillespie	101.3	7
(Water + n-propanol + cyclohexane)	Lee and Shen	2003	Dynamic Othmer	101.3	23
(Water + ethanol + isooctane)	Font et al.	2003	Dynamic Gillespie	101.3	10
(Water + isopropanol + isooctane)	Font et al.	2004	Dynamic Gillespie	101.3	8
(Water + ethanol + cyclohexane)	Gomis et al.	2005	Dynamic Gillespie	101.3	11
(Water + ethanol + heptane)	Gomis et al.	2006	Dynamic Gillespie	101.3	14
(Water + ethanol + hexane)	Gomis et al.	2007	Dynamic Gillespie	101.3	21

System	Reference	Date	Method	P/kPa	No. data points
(Water + ethanol + n-butyl acetate)	Younis et al.	2007	Dynamic Othmer	101.3	9
	Younis et al.	2007	Dynamic Othmer	80.0	7
	Younis et al.	2007	Dynamic Othmer	48.0	7
(Water + acetone + methyl ethyl ketone)	Younis et al.	2007	Dynamic Othmer	101.3	8
(Water + acetone + n-butyl acetate)	Younis et al.	2007	Dynamic Othmer	101.3	11
	Younis et al.	2007	Dynamic Othmer	80.0	6
	Younis et al.	2007	Dynamic Othmer	48.0	6
(Water + ethanol + acetone + n-butyl acetate)	Younis et al.	2007	Dynamic Othmer	101.3	35
	Younis et al.	2007	Dynamic Othmer	80.0	30
	Younis et al.	2007	Dynamic Othmer	48.0	29
(Water + ethanol + toluene)	Gomis et al.	2008	Dynamic Othmer	101.3	8
(Diisopropyl ether + isopropyl alcohol + water)	Lladosa et al.	2008	Dynamic Gillespie	100.0	12
(Di-n-propyl ether + n-propyl alcohol + water)	Lladosa et al.	2008	Dynamic Gillespie	100.0	11
(Water + acetic acid + methyl acetate + p-xylene)	Lee and Lin	2008	Dynamic Othmer	101.3	25
(Water + ethanol + p-xylene)	Gomis et al.	2009	Dynamic Gillespie	101.3	11
(Water + cyclohexane + isooctane)	Penquenín et al.	2010	Dynamic Gillespie	101.3	4
(Water + ethanol + cyclohexane +isooctane)	Lladosa et al.	2011	Dynamic Gillespie	101.3	51
(Water + 2-butanol + 2-butanone)	Lladosa et al.	2011	Dynamic Gillespie	101.3	12
(Water + 4-methyl-2-pentanone + 2-butanol)	Lladosa et al.	2011	Dynamic Gillespie	101.3	14
(Water + hexane + toluene)	Penquenín et al.	2011	Dynamic Gillespie	101.3	4
(Water + ethanol + hexane + toluene)	Penquenín et al.	2011	Dynamic Gillespie	101.3	25
(Water + heptane + cyclohexane)	Penquenín et al.	2011	Dynamic Gillespie	101.3	4
(Water + ethanol + cyclohexane + heptane)	Penquenín et al.	2011	Dynamic Gillespie	101.3	35
(Water + n-butanol + n-hexane)	Gomis et al.	2012	Dynamic Gillespie	101.3	11
(Water + isoprenyl acetate + acetic acid)	Wang et al.	2013	Dynamic Gillespie	101.3	14
(Water + acetic acid + cyclohexane)	Lui et al.	2013	Dynamic Gillespie	101.3	14
(Water + ethanol + diisopropyl ether)	Pienaar et al.	2013	Dynamic Gillespie	101.3	21
(Water + n-propanol + diisopropyl ether)	Pienaar et al.	2013	Dynamic Gillespie	101.3	18
(Water + n-propanol + isooctane)	Pienaar et al.	2013	Dynamic Gillespie	101.3	17
(Water + 2-butanol + *p*-xylene)	Gomis et al.	2014	Dynamic Gillespie	101.3	19
(Water + n-butanol + 2,3-butaediol)	Wu et al.	2015	Dynamic Othmer	101.3	11

When comparing experimental VLLE data with generated data, it can be seen that the models fail at accurately modelling the heterogeneous region. Both the size and shape of the calculated heterogeneous region does not agree with the size and shape of the experimentally determined data. In some cases, the homogeneous points are portrayed as heterogeneous (Gomis et al., 2005, Gomis et al., 2007).

The direct empirical determination of VLLE data involves the separation of samples into two liquid phases and one vapour phase which are in true equilibrium with each other. The concentration of these three phases is determined analytically using a combination of gas chromatography (GC) analysis and Karl-Fischer analysis. Presently, there is no commercially available instrumentation that is capable of measuring three separate phases in equilibrium (Gomis et al., 2000). Ultimately, researchers must use modified instruments, usually used in the determination of VLE, due to the problems encountered with measuring VLLE with VLE instruments. These problems and modifications are discussed in the following sections.

4.1 Problems with Measuring VLLE

Before discussing the possible methods and modified instruments used in the determination of isobaric VLLE data, the problems encountered with the experimental determination of systems with miscibility gaps are discussed. As mentioned in Section 2.2, all of the alcohol/water systems (C_3-alcohols and lower) of interest, are fully miscible with water and exhibit this type of miscibility gap once an appropriate entrainer is added. Butanol and other longer-chain alcohols exhibit two liquid phases when mixed with water.

Consider the general shape of a temperature composition diagram of a binary system with partial immiscibility:

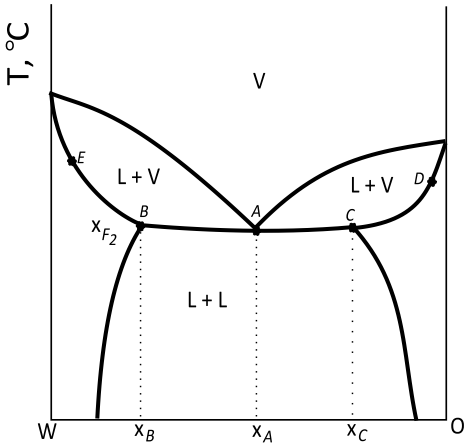

Figure 4-1 : ***Temperature composition diagram of a binary partially miscible system. According to Gomis, Ruiz and Asensi (2000).***

According to the phase rule, for a binary system, when the three phases (two liquid phases and a vapour phase) are in equilibrium, there is only one degree of freedom. By specifying the pressure at 101.3 kPa, there is a single temperature, T_a, and a single set of compositions. At this condition, as can be seen from figure 4.1, the points *B* and *C* represent the two liquid compositions and *A* represents the vapour composition. Any mixture in the boiling flask of the still with a composition between *B* and *C* will give the bubble point T_a (Gomis et al., 2000). Owing to the fact that this concentration range is wide, one would expect a steady temperature to be easily reached. Nevertheless, experimental observations indicated that it is impossible to obtain equilibrium for binary systems of limited miscibility. Temperature fluctuations of more than 10°C occur when using a dynamic instrument (Gomis et al. 2000). It was observed that, without an appropriate modification to the VLE instrument, a sudden decrease in temperature occurs, coinciding with a sudden evaporation in the boiling flask. The resulting vapour pushes a large amount of liquid through the Cottrell pump (see Figure 4-4). Gomis et al. (2000) attempted to explain this oscillation of temperature and vapour return by means of a binary system water (W)-organic solvent (O) example. At any given moment, there are two liquid phases in the boiling flask with compositions x_B and x_C at the temperature T_A. Slight heating of the boiling flask leads to the formation of a vapour of composition x_A. This vapour composition is richer in water in comparison to the liquid organic phase. As a result, the water content of the upper organic layer decreases, shifting from *C* to *D*. Consequently, the composition of the upper organic liquid phase changes and causes an increase in bubble temperature. This displacement leads to a transfer of water from the lower aqueous layer to the upper organic liquid layer.

Similar effects occur in the aqueous phase, leading to the displacement of composition from point *B* towards *E*. If the mass transfer rate between the phases is large enough, these changes in composition and temperature will be negligible. However, from visual analysis of the interface between the two liquid phases, it can be deduced that a limited mass transfer is possible between the phases. For the alcohol/entrainer/water systems studied in this research project, the difference in densities between the organic and aqueous liquid phases leads to a very clear liquid interface. Gomis et al. (2000) stated that, for this reason, the water transfer rate is small in comparison to the quantity of water removed by the vapour phase. In conclusion, without modification of equipment, large oscillations in temperature and phase concentrations can be expected.

Gomis et al. (2000) considered flow discontinuity of the phases as a second effect leading to instability in the still, owing to the fact that the stirrer in the mixing chamber does not possess the capacity to maintain a stable dispersion of the two liquid phases. The liquid passing preferentially to the boiling flask is usually the heavier aqueous phase (Gomis et al., 2000).

As a result, the organic phase accumulates in the mixing chamber and will eventually flow down to the boiling flask, producing a sudden evaporation. If this problem isn't rectified by mechanical or magnetic agitation, the liquid returning from the mixing chamber will largely contain one phase and VLLE data cannot be determined (Gomis et al., 2000).

4.2 Isobaric VLLE Measurement Methods

Several reviews of experimental equipment and procedures are published in literature for both high- and low-pressure VLE measurement; the latter deals with high-pressure vapour-liquid equilibrium measurement. Hala et al. (1967) used five groups to classify VLE measurement techniques: the distillation method, the circulation or dynamic methods, the static method, dew/bubble point method and the flow method. Similarly, Raal and Mühlbauer (1998) classified VLE measurement techniques into five groups. Gomis et al. (2010) established that *distillation*, *dynamic* and the *flow* methods have been used to determine VLLE data.

As can be deduced from Table 4-1, the oldest method is that of distillation and is seldom used. Nonetheless, it is a cornerstone to VLLE measurement (being the first method used to determine VLLE data) and will be discussed in the following section. The static method and dew-point and/or bubble-point method are useful in determining isothermal VLE data but not isobaric data, and are therefore not applicable to this research (Gomis et al., 2000).

4.2.1 Distillation Method

The distillation method involves the distillation of a large quantity of liquid mixture of known composition, with the small portion of distillate being analysed in order to determine the composition of the vapour in equilibrium with the liquid in the boiling flask (Gomis et al., 2010). The assumption made is that, due to the size of the original liquid mixture, the composition of the liquid phase remains virtually unchanged.

The last known use of the distillation method for VLLE measurement was in 1968. Both Verhoeye (1968) and Volpicelli (1968) used an Othmer-type still, modified by a three-way stopcock; making the transition from a still based on the circulation principle to one based on the distillation method. Another modification applied to transform distillation VLE instruments into VLLE measuring instruments is the agitation of the boiling flask (Gomis et al. 2000). Volpicelli (1968) heated the vapour return line whenever fractioning of the condensed vapour occurred. Although these modifications to the distillation methodology form part of the basis of VLLE measurement, all exhibit the inability to attain true thermodynamic equilibrium (Hala et al. 1967).

Figure 4-2 is a schematic of the modified Othmer design used in the determination of VLLE data by Verhoeye (1968) and Volpicelli (1968).

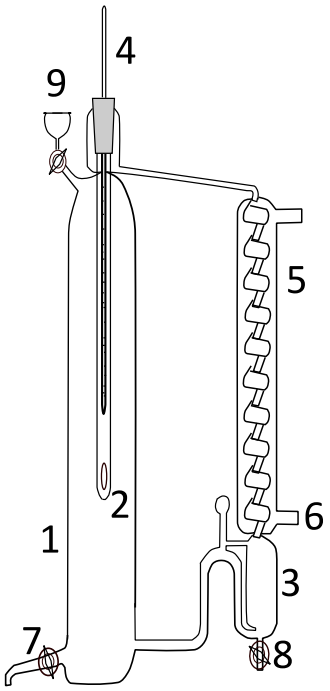

Figure 4-2: ***Original modified Othmer dynamic VLE still: 1. Boiling chamber; 2. Vapour tube; 3. Condensate receiver; 4. Thermometer; 5. Condenser; 6. Drop counter; 7. Liquid sampling point; 8. Vapour sampling point; 9. Load point. Figure redrawn and adapted from Raal and Mühlbauer (1998).***

4.2.2 Dynamic Method

Stills which are based on the dynamic method, with either circulation of only the vapour phase (dynamic Othmer) or circulation of both the liquid and vapour phases (dynamic Gillespie), account for a large fraction of published VLE and VLLE data. Figure 4-3 illustrates the basic functioning of a dynamic-based apparatus, according to Gomis et al. (2000).

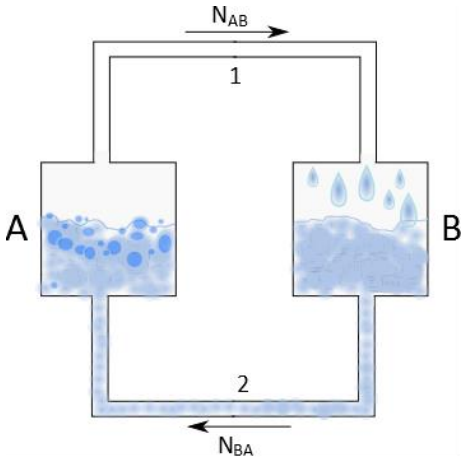

Figure 4-3: ***Circulation in the dynamic equilibrium apparatus. Figure redrawn and adapted from Gomis et al. (2010).***

The liquid feed in distillation flask A is heated and the resulting vapour passed to flask B via a conduit (1). In flask B, it is condensed and, once full, returned to distillation flask A via a second conduit (2) (Gomis et al., 2010). This process continues until a steady state is reached; the compositions in both flasks remains unchanged with passing time. Therefore, the mass flow from the distillation flask A equals that from the condensate (Gomis et al., 2010).

Dynamic equilibrium stills can be subdivided into two groups: dynamic Othmer apparatus and dynamic Gillespie apparatus (Raal and Mühlbauer, 1998).

4.2.2.1 Dynamic Othmer

Like the modification made by Verhoeye (1968) and Volpicelli (1968), the experimental apparatus of Othmer has been modified to conform to dynamic methodology; the vapour sample generated by boiling the liquid is led through a condenser and the condensate is returned to the boiling flask. By doing so, the vapour phase is recirculated. The liquid sample is taken directly from the boiling chamber, as seen in Figure 4-2.

Several problems surround the structure of the Othmer still which, in turn, raises concerns about the reliability and accuracy of measured data (Raal and Mühlbauer, 1998). For one, the method of temperature measurement is undesirable seeing as only the vapour phase temperature is investigated. In order to determine accurate temperature, the temperature probe must be in contact with both phases (Raal and Mühlbauer, 1998).

Furthermore, the large boiling chamber may result in the partial condensation of the vapour phase on the chamber walls. This will lead to a change in composition and true equilibrium would not be measured. Fitting a vacuum jacket to the experimental set-up would compensate for this condensation. However, this solution could lead to superheating of the wall and flashing of the liquid phase (Raal and Mühlbauer, 1998).

Until the publication by Gomis et al. (2008), the publication of VLLE data, measured with a dynamic Othmer still, had slowly diminished and ceased. The circulation of a single phase is inadequate for the generation of accurate VLLE data (Gomis et al. 2010).

4.2.2.2 Dynamic Gillespie

The Gillespie apparatus is considered to be a more suitable design when comparted to the experimental apparatus of Othmer. It is considered to be the superior experimental set-up for measuring isobaric VLLE data due to the circulation of both liquid and vapour phases, which is accomplished with a Cottrell pump (Raal and Mühlbauer, 1998).

The Cottrell pump was developed by Frederick Cottrell (1919) and consists of a simple tube, entraining a column of liquid with slugs of vapour. By doing this, it brings both the liquid and vapour phases into contact with the thermometer, providing an accurate equilibrium temperature measurement. A schematic of the original dynamic Gillespie VLE still can be seen in Figure 4-4. The feed mixture is boiled in the boiling chamber (1). The Cottrell pump (2) pulls a mixture of liquid and vapour into the disengagement chamber (4).

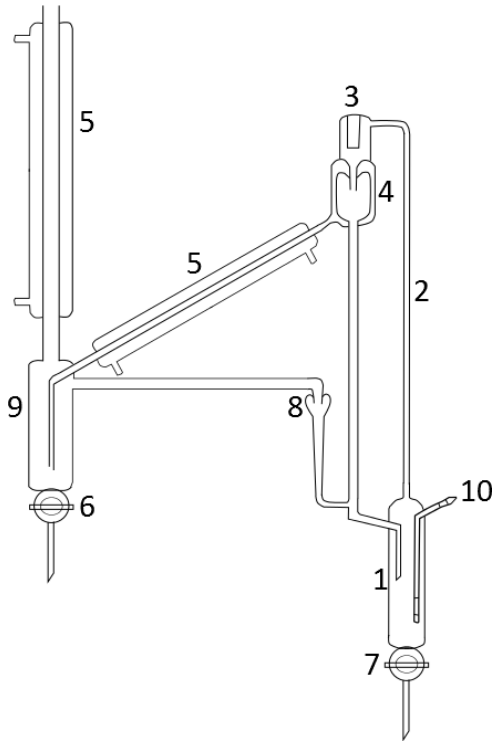

Figure 4-4: ***Gillespie dynamic VLE still: 1. Boiling flask; 2. Cottrell tube; 3. Thermometer well; 4. Vapour-liquid separating chamber; 5. vapour condensers; 6. Condensate sample cock; 7. Liquid sample cock; 8. Droplet counter; 9. Condensate receiver; 10. Internal heater. Figure redrawn and adapted from Raal and Mühlbauer (1998).***

This initial Gillespie design has been modified by several authors to circumvent certain flaws of this experimental set-up (Van Zandijcke and Verhoeye, 1974, Gomis et al., 2000). An example of a modification made to the original Gillespie design is the addition of a sampling port following the disengagement chamber (4) (also known as the vapour-liquid separation chamber). This allows for uninterrupted operation during sampling. If the liquid were to be sampled from the boiling chamber; that is, from valve (7), it would not be a representative sample (Malanowski, 1982, Raal & Mühlbauer, 1998). Another modification, made by subsequent researchers, is the insulation of the separation chamber to prevent partial condensation of the equilibrium vapour phase within the disengagement chamber (Raal & Mühlbauer, 1998).

Another potential flaw of the initial Gillespie design, considered by Raal and Mühlbauer (1998), is the use of a simple Cottrell tube. It was thought to be an unsatisfactory device for the rapid attainment of equilibrium. Through the use of a spiralled Cottrell tube, mass transfer may be improved; along with a significant increase in interfacial areas and contact times (Gomis et al., 2010).

Gomis et al. (2000) modified the Gillespie unit by incorporating an ultrasonic homogenizer in the distillation flask in order to emulsify the two liquid phases. This modification will be discussed in further detail in section 4.5.

4.2.3 Flow Method

The flow method is unique in the fact that the equilibrium chamber is fed continuously by one, or two, steady-state feed stream(s). The feed stream in question is of constant composition and may contain a liquid, vapour, or a combination of the two (Gomis et al., 2010). The flow method is solely applicable to systems in which the time needed to attain phase equilibrium is relatively small (Dohrn et al., 2010). The still is made up of three units: feed vessel, boiler and equilibrium chamber (Newshan & Vahdat, 1977).

This method was initially developed to overcome difficulties encountered with the dynamic method in obtaining equilibrium data for systems that produce heterogeneous liquid mixtures as the feed stream may consist of a heterogeneous liquid (Gomis et al., 2010). The only authors to use this method in measuring VLLE data were Newshan and Vahdat (1977). Reasoning behind the lack of VLLE data measured using this method could be attributed to the complexity of the equipment and the sheer bulk of chemicals required to measure equilibrium data (Gomis et al., 2010).

4.3 Preferred Equipment and Methodology

Gomis et al. (2010) concluded, from a comprehensive study on the available methods for determining VLLE data, that equipment based on the dynamic method is (at present) best-suited for isobaric VLE and VLLE data measurement.

Modifications made to commercially available equipment based on the Gillespie principle have proven to be superior, when compared with dynamic equipment based on the Othmer principle. This is due to the fact that dynamic Othmer equipment only recirculates the vapour phase, whereas dynamic Gillespie equipment recirculates both liquid and vapour phases (Gomis et al., 2010). Therefore, this will be the equipment used for this research project.

As discussed in section 4.1, there are certain problems that are encountered when measuring isobaric VLLE. These problems can be overcome by increasing the extent to which the phases in the boiling flask are mixed (by mechanical stirring or by means of an ultrasonic homogeniser) or by modifying the equipment such that the two liquid phases, resulting from the splitting of the heterogeneous mixtures, remain separated between the outlet of the Cottrell pump and the boiling flask, through which it must return to the Cottrell pump (Gomis et al., 2000, 2010).

For this research project, modifications were made to the commercially available Gillespie set-up to avoid these problems. These modifications are discussed in the following section.

4.3.1 Modification to Instrument

In order to obtain accurate, repeatable VLLE data from a commercially available instrument, modifications were made; it was fitted with an ultrasonic homogeniser. Gomis et al. (2000) has shown that the application of ultrasound, as a modification to dynamic instruments used for the determination of VLE data, is a useful way to obtain equipment for the determination of isobaric VLLE data (Gomis et al., 2000). The attached ultrasonic homogeniser is used to overcome the mass transfer issues faced when measuring VLLE data. Taking this into account, the commercially available set-up was modified accordingly.

The partly miscible liquid phases are emulsified by the subsequent exposure to ultrasonic sound. In systems with two liquid phases, like the low-molecular weight alcohol/water systems being studied, the sonic power results in a phenomenon known as cavitation. Cavitation, in this particular case, is the ultrasonic-induced formation, growth and collapse of gas-vapour filled bubbles in a liquid (Figure 4-5). The liquid phases are subjected to ultrasonic sound, which leads to extremely high acoustic pressures and causes pressure fluctuations within the liquid (Ashokkumar & Mason, 2007). This results in thorough mixing and, as a result, evades the problems discussed in section 4.1.

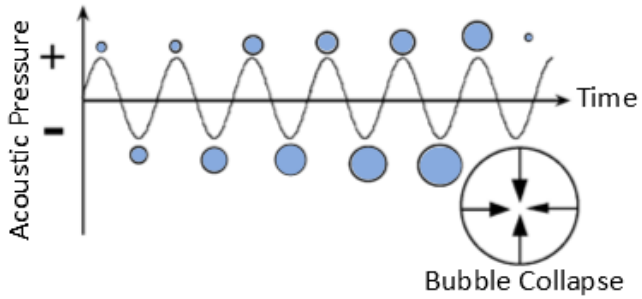

Figure 4-5: ***Schematic representation of cavitation. According to Ashokkumar & Mason (2007).***

The ideal location and positioning of the ultrasonic homogenizer (UH), in the dynamic instrument, have been investigated (see Figure 4-6) (Gomis et al. 2000). Both the mixing chamber (5) and the

boiling flask (2) were considered as locations for the homogenizer. The latter was deemed to be ideal, due to the energy contribution of the homogenizer to the liquid in the mixing chamber (5) at its bubble temperature. It was found that the extra energy led to ebullition and the resulting bubbles obstructed the circulation of the liquid phases through the back flow tube (4) (Gomis et al., 2000). When the ultrasonic homogenizer is positioned in the boiling flask (2), the energy contribution of the homogenizer is added to the energy delivered by the electrical immersion heater (1) without generating secondary effects (Gomis et al., 2000).

Preferably, the homogenizer should be placed parallel to the boiling flask; this positioning would lead to global agitation and maximum achievable mass transfer rate. However, this position is occupied by the immersion heater and therefore the homogenizer was positioned as close as possible to the flask and heater (approximately 30°, as illustrated in Figure 4-6).

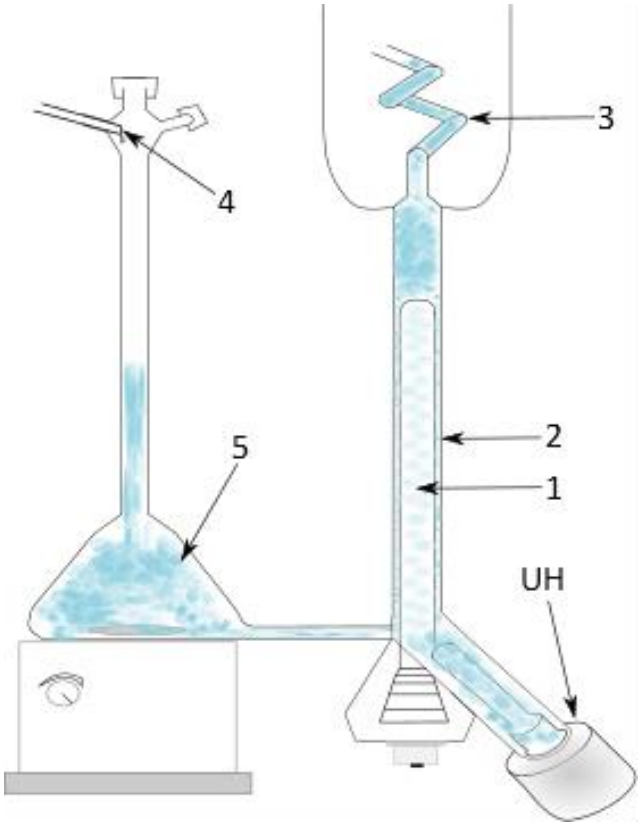

Figure 4-6: ***Optimum location and positioning of ultrasonic homogenizer: 1) immersion heater, 2) boiling flask, 3) Cottrell pump, 4) back flow tube, 5) mixing chamber and UH) ultrasonic homogenizer. Addapted from Pienaar et al. (2012).***

Although Gomis et al. (2000) have tested this modification thoroughly, extensive verification of the modified instrumentation was performed (see section 8.1) in order to confidently report accurate VLLE data.

5 EVALUATION OF ALCOHOL/WATER/ENTRAINER SYSTEMS

5.1 Literature study and evaluation of suitable entrainers

As mentioned in Section 2.5, the undertaking of entrainer selection should be approached using thermodynamic and physical insights; this involves the exploration of intermolecular forces and VLE and VLLE diagrams available in literature (Simmrock et al., 1993). Entrainers are generally selected based on the knowledge and understanding of a same or similar process (Julka et al., 2009).

5.1.1 Available literature data of suitable entrainers

Using the accumulated available literature data from Table 4-1, a condensed list of potential entrainers for the dehydration of low molecular weight alcohols can be seen in Table 5-1. Given the systematic methodology of entrainer selection, as discussed in section 2.5, this list is merely a guideline for the selection of systems for experimental measurement of new VLLE data. Consequently, it can be assumed that there are other substances, not listed in Table 5-1, that can facilitate alcohol/water azeotropic heterogeneous distillation but these are the only substances of which isobaric VLLE data is available.

Table 5-1: Source of published experimental multicomponent VLLE isobaric data. Adapted from Pienaar et al. (2012) with additional info added.

Entrainer	Aqueous Alcohol	Measurement Method	Quantity		Pressure (kPa)	Reference
Benzene	Ethanol	Distillation	6 VLLE		101.3	(Barbaudy, 1926)
Cyclohexane	Ethanol	Dynamic Gillespie	11 VLLE	27 VLE	101.3	(Gomis *et al.*, 2005)
	n-Propanol	Dynamic Othmer	23 VLLE	31 VLE	101.3	(Lee and Shen, 2003)
	iso-Propanol	Distillation	6 VLLE	40 VLE	101.3	(Verhoeye, 1968)
Hexane	Ethanol	Dynamic Gillespie	21 VLLE	49 VLE	101.3	(Gomis *et al.*, 2007)
	n-Butanol	Dynamic Gillespie	13 VLLE	42 VLE	101.3	(Gomis *et al.*, 2012)
Heptane	Ethanol	Dynamic Gillespie	14 VLLE	30 VLE	101.3	(Gomis *et al.*, 2006)
Isooctane	Ethanol	Dynamic Gillespie	10 VLLE	17 VLE	101.3	(Font *et al.*, 2003)
	n-Propanol	Dynamic Gillespie	17 VLLE	17 VLE	101.3	(Pienaar *et al.*, 2013)
	iso-Propanol	Dynamic Gillespie	8 VLLE	22 VLE	101.3	(Font *et al.*, 2004)
DIPE	Ethanol	Dynamic Gillespie	21 VLLE	17 VLE	101.3	(Pienaar *et al.*, 2013)
	n-Propanol	Dynamic Gillespie	18 VLLE	17 VLE	101.3	(Pienaar *et al.*, 2013)
	iso-Propanol	Dynamic Gillespie	12 VLLE		100	(Lladosa *et al.*, 2008)
DNPE	n-Propanol	Dynamic Gillespie	11 VLLE		100	(Lladosa *et al.*, 2008)
2-Butanone	2-Butanol	Dynamic Gillespie	12 VLLE		101.3	(Lladosa *et al.*, 2011)

5.1.2 Evaluation of suitable entrainers

This section looks at the prospective suitable entrainers in detail: the cost and properties of said entrainer, as well as the ternary diagrams in which these entrainers are compared for ethanol, n-propanol and iso-propanol. Comprehensive MSDS forms for each of these substances can be found in Appendix A.

5.1.2.1 Benzene

Benzene is an aromatic hydrocarbon with a formula of C_6H_6. It is a colourless, volatile liquid with a sweet odour (McMurray, 1996). Exposure to benzene may occur either occupationally or domestically as a result of the omnipresent use of benzene-containing petroleum products, solvents and other chemicals such as detergents, plastics and pesticides (IARC, 1987; WHO, 2007). Benzene is a naturally occurring compound in crude petroleum (Batchelder, 1970). This means that the processing of petroleum products, coking of coal and the production of aromatic compounds (used in other consumer products) will ultimately lead to human exposure. Exposure occurs mostly through inhalation due to the volatility of benzene (WHO, 2007). Human exposure has been associated with a range of acute and long term health effects and diseases, including cancer and aplastic anaemia (IARC, 2009). Short term exposure effects include dizziness, headaches, tremors, confusion, and/or unconsciousness (IARC, 1987).

The commercial use of benzene as entrainer for the dehydration of ethanol is widely published and was first established in the 1900s (Young, 1902; Black, 1980; Ryan and Doherty, 1989; Luyben, 2012). However, due to aforementioned health effects for humans associated with exposure to benzene, alternative entrainers have become necessary (Gomis, 2007).

5.1.2.2 Cyclohexane

Cyclohexane is a cyclic hydrocarbon with a formula of C_6H_{12}. Like benzene, it is a colourless liquid with a sweet, chloroform-like odour and can be found in crude petroleum (McMurray, 1996, EPA 1994). Cyclohexane is mainly used by chemical companies that manufacture adipic acid and caprolactam (McMurray, 1996). These chemicals are subsequently used to make nylon (EPA, 1994). Cyclohexane exposure, when compared to benzene, is far less hazardous due to its rapid breakdown and removal in exhaled air and urine (WHO, 2000). However, when exposed to a large amount of cyclohexane in a short period of time, adverse side effects can be noticed; the break-down of the human nervous system has been observed, causing tremors and convulsions (EPA 1994).

Gomis et al. (2005) reported that, due to the carcinogenic nature of benzene, cyclohexane has become one of the most utilized entrainers to separate ethanol and water and is currently in use in

numerous plants around the world. The reported uncertainties in temperature and pressure measurements were 0.006°C and 0.1 kPa respectively. Gomis et al. (2005) estimated the accuracy of the mole fraction measurements at ±0.005 for the water in the liquid organic phase and cyclohexane in the aqueous phase and approximately ±0.002 for all of the other compounds. The experimentally determined data points were tested using thermodynamic principles by the point-to-point L/W Wisniak consistency test. All the values were reported to fall between 0.98 and 1.00 and were consequently considered to be thermodynamically consistent. Gomis et al. (2005) also compared the experimentally obtained VLLE data with VLLE data modelled using UNIFAC and NRTL. As discussed in sections 3.8 - 3.10, a similar approach will be applied in this work.

Cyclohexane has also been suggested as entrainer for the dehydration of n-propanol (Challis, 1954). A dynamic Othmer unit was used in the experimental determination of 23 isobaric VLLE data points of the n-propanol/cyclohexane/water system at 101.3 kPa by Lee and Shen (2003). Temperature and pressure uncertainties were reported as 0.1 K and 1 mmHg, respectively. The authors designed the Othmer-type equilibrium cell in a manner that allowed avoidance of liquid entrainment and heat loss through the vapour path wall. This was achieved through the insulation of the vapour path wall with a vacuum jacket and an additional jacket with silicon oil (Lee & Shen, 2003). No mention was made of any levels of accuracy for the reported mole fraction values but the experimentally determined data was compared with UNIQUAC and NRTL predictions.

Binary parameters were determined for the NRTL and UNIQUAC models from the experimental data of the ethanol/cyclohexane/water system. Lee and Shen (2003) concluded that the UNIQUAC model is not suitable for this particular system and that the NRTL predictions were satisfactory (with the worst AARD% value reported as 10.69%).

5.1.2.3 Hexane

Hexane is a colourless volatile liquid that is insoluble in water, highly flammable and can easily be deprotonated. Typical laboratory uses of hexanes include as a solvent in the extraction of oily substances from soil and water for analysis and in the preparation of organolithiums (McMurray, 1996). Its solvent properties are further applied in the extraction of edible oils from seeds and vegetable crops (EPA, 1999). The use of n-hexane in pharmaceuticals is currently being phased out due to its long term toxicity in humans. Exposure to this liquid leads to the formation of the toxic hexane-2,5-dione metabolite (Soriano et al. 1996). Acute exposure of humans to high levels of n-hexane causes mild central nervous system effects (dizziness, giddiness, slight nausea and headaches). Chronic exposure to n-hexane in air is associated with polyneuropathy in humans (numbness, muscular weakness, loss of vision, headache and fatigue) (EPA, 1999). Due to the lack of

data regarding carcinogenicity in humans, n-hexane has been placed in Group D by the EPA. Group D encompasses chemicals that are considered to be unclassifiable to human carcinogenicity (EPA, 1999).

Gomis et al. (2013) reported that the requirement for more advantageous biofuel sources, like n-butanol, is surpassing that of the more frequently used ethanol. A total of 13 isobaric VLLE and 42 isobaric VLLE data points were accumulated using a Dynamic Gillespie unit modified by Gomis et al. (2005). The pressure in the still was kept at 101.3 kPa throughout the entire experimental procedure, measured and controlled within an accuracy of 0.1 kPa (Gomis et al, 2013). The reported uncertainties in temperature measurements were given as 0.006 K; the authors listed the percent uncertainty (uncertainty x 100/measurand) as 2%. The experimentally determined data points were tested using thermodynamic principles by the point-to-point L/W Wisniak consistency test. All the values were reported to be between 0.96 and 1.00. The experimentally determined VLLE and VLE data was then compared to a thermodynamic model (UNIFAC) and UNIQUAC and NRTL simulated results.

5.1.2.4 Heptane

n-Heptane is a straight-chain alkane with a molecular formula of C_7H_{16}. At atmospheric conditions, it is a colourless liquid with a mild gasoline-like odour. Exposure to heptane occurs through inhalation, ingestion or absorption when in contact with skin and eyes. Prolonged exposure may cause skin irritation, nausea, loss of appetite and dizziness (CDC, 1969). Heptane is generally used in laboratories due to its non-polar solvent nature; however, it is also commercially used in paints and other substances generally used outdoors (McMurray, 1996). The use of heptane as entrainer for the dehydration of low-molecular weight alcohols is advantageous, given that it is a common component in gasoline (Gomis et al., 2007). Heptane occupies the zero point of the octane rating scale (McMurray, 1996).

5.1.2.5 Isooctane

Isooctane (2,2,4-trimethylpentane) is a hydrocarbon which is one of the eighteen octane-isomers, with a formula of $(CH_3)_3CCH_2CH(CH_3)_2$. It is a highly volatile liquid and, when inhaled or brought into contact with skin and eyes, causes irritation and a burning sensation (MSDS form). Isooctane is the standard 100 point on the octane rating scale and is an essential component in gasoline, increasing the knock resistance of the particular fuel (Machado et al., 2013).

Clairns and Furzer (1990) carried out a theoretical study, using the UNIFAC group contribution method, to determine the potential of isooctane as entrainer for the dehydration of ethanol. In the

same year, these authors published an experimental study on the separation of ethanol and water by the addition of commercial-grade isooctane containing 11 other chemical components (Clairns and Furzer, 1990). Font et al. (2003) were the first to measure 10 isobaric VLLE and 17 isobaric VLE data points at 101.3 kPa for the ethanol/isooctane/water system, using pure isooctane. The same modified Gillespie unit, described by Gomis et al. (2000), was used for the experimental work.

Pienaar et al. (2013) published 17 isobaric VLLE and 17 isobaric VLE data points for the n-propanol/isooctane/water system at 101.3 kPa. This is the same commercial all-glass dynamic recirculating still, modified by coupling an ultrasonic homogenizer to the boiling flask, as discussed in section 6.2, that will be used for this research project. The accuracy of the reported data was estimated to be 0.02 times the mole fraction. The maximum uncertainty of the reported for temperature and pressure measurement was estimated at 0.12 K and 0.50 kPa respectively. The thermodynamic consistency of the data was established by applying the Wisniak modification of the Herrington area test (Wisniak 1994), L/W Wisniak consistency test and the McDermott-Ellis consistency test. The Othmer Tobias correlation (Othmer & Tobias, 1942) was used to ensure the measured LLE data followed a steady trend.

5.1.2.6 DIPE

DIPE (diisopropylether) is a colourless liquid with a molecular formula of $C_6H_{14}O$. As is typical with ethers, DIPE forms explosive peroxides when exposed to oxygen for long periods of time. In the laboratory, DIPE functions as a solvent to extract polar compounds from aqueous solutions. It is also commonly used as an antiknocking agent in gasoline (Chamorro et al. 2001).

5.1.2.7 2-Butanone

2-Butanone, the only ketone-type entrainer that will be considered, has a molecular formula of $CH_3C(O)CH_2CH_3$ and is commonly referred to as MEK (methyl ethyl ketone). It is a colourless liquid with a sweet odour (similar to acetone) and is widely used as an industrial solvent (Turner & McCreery, 1981). MEK is extracted by fractionation from streams resulting from the liquid-phase oxidation of heavy naptha and the Fischer-Tropsch reaction (Ashford's Dictionary of Industrial Chemicals, 2011). Berckmuller et al. (1994) demonstrated that MEK can be used as a fuel tracer. This means that it can be used to quantify fuel concentration due to its positive dependence between relative fluorescence and temperature. An important criterion for an effective fuel tracer is that it burns in a similar fashion to the fuel (Serinyel et al., 2010).

Lladosa et al. (2011) measured a total of 12 isobaric VLLE data points for the 2-butanol/MEK/water system at 101.3 kPa. The instrumentation used was the same as described by the authors in a

previous publication, discussed above (Lladosa et al. 2008). The thermodynamic consistency of the experimental ternary VLLE data was tested using the point-to-point L/W Wisniak consistency test, with all the values ranging between 0.92 and 1.10. The results were evaluated through the application of thermodynamic models (NRTL, UNIQUAC and the UNIFAC). Lladosa et al. (2011) also used the Wisniak-Tamir modification of the McDermott-Ellis consistency test. The data was considered to be thermodynamically consistent with all calculated D values lower than D_{max}.

5.1.3 Cost evaluation of suitable entrainers

Bulk chemical prices of the suitable entrainers can be found in Table 5-2. The values have been obtained from ICIS, considered to be the world's largest petrochemical market provider. The current exchange rate used for these calculations, obtained from www.xe.com, is:

$$1.00\ USD = 11.00\ ZAR \qquad [5.1]$$

The *Chemical Engineering*'s Plant Cost Index (CEPCI) was used to determine the cost of the chemicals at the end of the year 2014 (Marshall, 2014):

$$Cost\ in\ year\ A = Cost\ in\ year\ B\ \frac{Cost\ index\ in\ year\ A}{Cost\ index\ in\ year\ B} \qquad [5.2]$$

Table 5-2 : ***Bulk chemical prices of suitable entrainers***

Chemical	Cost (ZAR/tonne)
Benzene	15,451.00
Cyclohexane	15,862.00
Hexane	11,588.00
Heptane	7,050.00
Isooctane	15,565.00
DIPE	23,577.00
MEK	8,053.00

5.2 Entrainer Selection

When selecting an entrainer, it is imperative that the separation sequence is considered as a whole; entrainer regeneration is vital. When comparing an entrainer that leads to the formation of a new homogeneous azeotrope with an entrainer that leads to the formation of a heterogeneous azeotrope, the latter is preferred (Laroche, Andersen & Morari, 1992:38). Finding a candidate entrainer for the heterogeneous azeotropic distillation of an alcohol/water azeotropic system involves the use of comprehensive thermodynamic and physical principles. The determination and analysis of vapour-liquid-liquid equilibria (VLLE) data of the systems in question are, therefore, of paramount importance (Julka et al. 2009).

From this, a feasible distillation-based sequence can be designed for the particular mixture. Entrainers are chosen using prior knowledge, or experience, of a similar entrainer-component with a similar azeotropic system. Of course, the economic and environmental impact of the subsequent use of the chosen entrainer needs to be considered. The nature of azeotropes complicates the optimization of a separation sequence and one cannot rely solely on the modelling of equilibrium data (Doherty & Knapp, 2000).

Through the use of RCM technology, cost-effective solutions to a separation objective can be found. However, there are certain drawbacks of this type of entrainer selection method. Along with significant prior expertise in the correct analysis RCM technology, a good physical-property model and azeotropic database is required (Julka et al. 2009).

Several methodologies for finding the most feasible entrainer for a system are published in literature, with some focusing on the use of UNIFAC group contributions for screening entrainers, and others the use of hydrogen-bonding tendencies (Brignole et al., 1986). Typical entrainers used for the dehydration of low molecular weight alcohols (ethanol, n-propanol and iso-propanol) are discussed in Section 5.1.

Considering the lack of available VLE and VLLE data on MEK systems, the fact that it does not have the same carcinogenic properties as benzene, and the fact that MEK would not affect an engine if residue were to remain behind, MEK was chosen as the component to be studied in this project. It is inexpensive and readily available and could easily be integrated into separation sequences. **In summary, the following three systems were chosen for this experimental study:**

- **Ethanol/MEK/Water**
- **n-Propanol/MEK/Water**
- **iso-Propanol/MEK/Water**

5.3 Available binary phase information

MEK and benzene forms a homogeneous minimum azeotrope with 0.450 mole fraction MEK at 78.30°C, where MEK and water forms a homogeneous minimum azeotrope with 0.670 mole fraction MEK at 73.50°C (Tanaka, 1985).

The tables below (Table 5-3 and 5-4) lists some of the available binary VLE data for MEK/alcohol and water/alcohol systems. This study was executed with the aim of identifying azeotropic behaviour; therefore this table is only a condensed list of available binary phase data. This information will be used in the Results and Discussion chapter to compare azeotropic compositions.

Table 5-3: ***Compilation of binary, azeotropic data for 2-butanone/alcohol systems compiled from a variety of references.***

Entrainer	Alcohol	Ideality	Isobaric/ Isothermal	Pressure/ Temperature	y_i (mole fraction)	References
2-Butanone	‡Ethanol	Azeotrope	Isobaric	101.32 kPa	0.5714	(Lecat, 1947)
		Azeotrope	Isothermal	55°C	0.4140	(Nagata *et al*, 1976)
		Azeotrope	Isobaric	93.33 kPa	0.5050	(Marinichev & Vasileva, 1976)
		Azeotrope	Isothermal	25°C	0.2610	(Ohta *et al*, 1981)
		Azeotrope	Isobaric	101.32 kPa	0.4500	(Tanaka, 1985)
		Azeotrope	Isobaric	101.32 kPa	0.5050	(Wen & Tu, 2007)
		Azeotrope	Isobaric	20 kPa	0.688	(Martinez *et al*, 2008)
		Azeotrope	Isobaric	101.32 kPa	0.483	(Martinez *et al*, 2008)
	n-Propanol	Ideal	Isobaric	101.32 kPa		(Lecat, 1947)
		Ideal	Isobaric	101.32 kPa		(Kalnitskaya & Komarova, 1977)
		Ideal	Isobaric	20 kPa		(Martinez *et al*, 2008)
		Ideal	Isobaric	101.32 kPa		(Martinez *et al*, 2008)
	‡iso-Propanol	Azeotrope	Isobaric	101.32 kPa	0.6650	(Nagata *et al*, 1963)
		Azeotrope	Isobaric	101.32 kPa	0.7900	(Nagata *et al*, 1976)
		Azeotrope	Isobaric	20 kPa	0.750	(Martinez *et al*, 2008)
		Azeotrope	Isobaric	101.32 kPa	0.605	(Martinez *et al*, 2008)

‡ An abbreviated list of literature data

Table 5-4: ***Compilation of binary, azeotropic data for water/alcohol systems systems compiled from a variety of references.***

H_2O	Alcohol	Ideality	Isobaric/ Isothermal	Pressure/ Temperature	y_i (mole fraction)	References
Water	‡Ethanol	Azeotrope	Isothermal	50°C	0.9439	(Wilson *et al*, 1979)
		Azeotrope	Isobaric	101.32 kPa	0.8940	(Tanaka, 1985)
		Azeotrope	Isobaric	40 kPa	0.9200	(Connemann *et al*, 1990)
		Azeotrope	Isobaric	101.33 kPa	0.8970	(Zemp & Francesconi, 1992)
		Azeotrope	Isobaric	101.32 kPa	0.8930	(Kurihara *et al*, 1993)
		Azeotrope	Isobaric	100 kPa	0.893	(Orchillés *et al*, 2010)
		Azeotrope	Isobaric	101.32 kPa	0.901	(Kamihama *et al*, 2012)
		Azeotrope	Isobaric	101.32 kPa	0.912	(Lai *et al*, 2014)
	‡n-Propanol	Azeotrope	Isobaric	101.32 kPa	0.4317	(Young & Fortey, 1902)
		Azeotrope	Isobaric	101.32 kPa	0.4330	(Tochigi *et al*, 1985)
		Azeotrope	Isobaric	101.32 kPa	0.4320	(Tanaka, 1985)
		Azeotrope	Isothermal	40°C	0.3950	(Zielkiewicz & Konitz, 1991)
	‡iso-Propanol	Azeotrope	Isobaric	101.32 kPa	0.6835	(Langdon & Keyes, 1942)
		Azeotrope	Isobaric	101.32 kPa	0.6840	(Tochigi *et al*, 1985)
		Azeotrope	Isothermal	80°C	0.6764	(Wu *et al*, 1988)
		Azeotrope	Isobaric	101.32 kPa	0.6700	(Rajendran *et al*, 1991)

‡ An abbreviated list of literature data

6 MATERIALS & METHODS

6.1 Apparatus

An all-glass dynamic recirculating still used to experimentally determine VLE and VLLE data is presented graphically in Figure 6-1. This commercially available still (VLE 100 D) is manufactured in Germany by Pilodist and is widely referenced in literature in which VLE data is obtained. The still was modified by Pilodist by coupling an ultrasonic homogenizer (17), manufactured by Braun Labsonic P, to the boiling flask of the still. This ensures thorough mixing of the liquid and vapour phases as well as the emulsification of the two liquid phases when a heterogeneous mixture occurs at equilibrium. All silicone seals and o-rings had to be replaced with Viton-based products in order to withstand the solvent effects of the chemicals used as well as the high temperatures reached during experimental runs. The maximum operating temperature of the still has been determined to be 250°C, with equilibrium temperatures measured by a Pt-100 probe connected to a digital Hart Scientific thermometer. This thermometer has an accuracy of 0.03°C at 0°C, according to the original certificate of calibration. The system is controlled by a Pilodist M101 control system and a VLE software package.

6.1.1 Unit Description

With reference to the Figure 6-1, evaporation of the starting liquid mixture in the mixing chamber (1.1) ensues via the electrical immersion heater (10) which is concentrically installed into the flow heater (1.3). The heated vapour-liquid mixture then passes through an extended, spiralling contact line known as the Cottrell pump (1.2). Subsequently, the phases pass over the thermometer (7), which is used to measure the bubble point. In the separation chamber, the gas and liquid phases are split, condensed and consequently returned to the mixing chamber (1.1) via the receiving lines. Within the mixing chamber (1.1), the returned mixture is mechanically stirred using a magnetic stirrer (3) before being returned to the immersion heater (10). Considering the flammable and explosive nature of the components used, the unit is installed in an extraction cabinet.

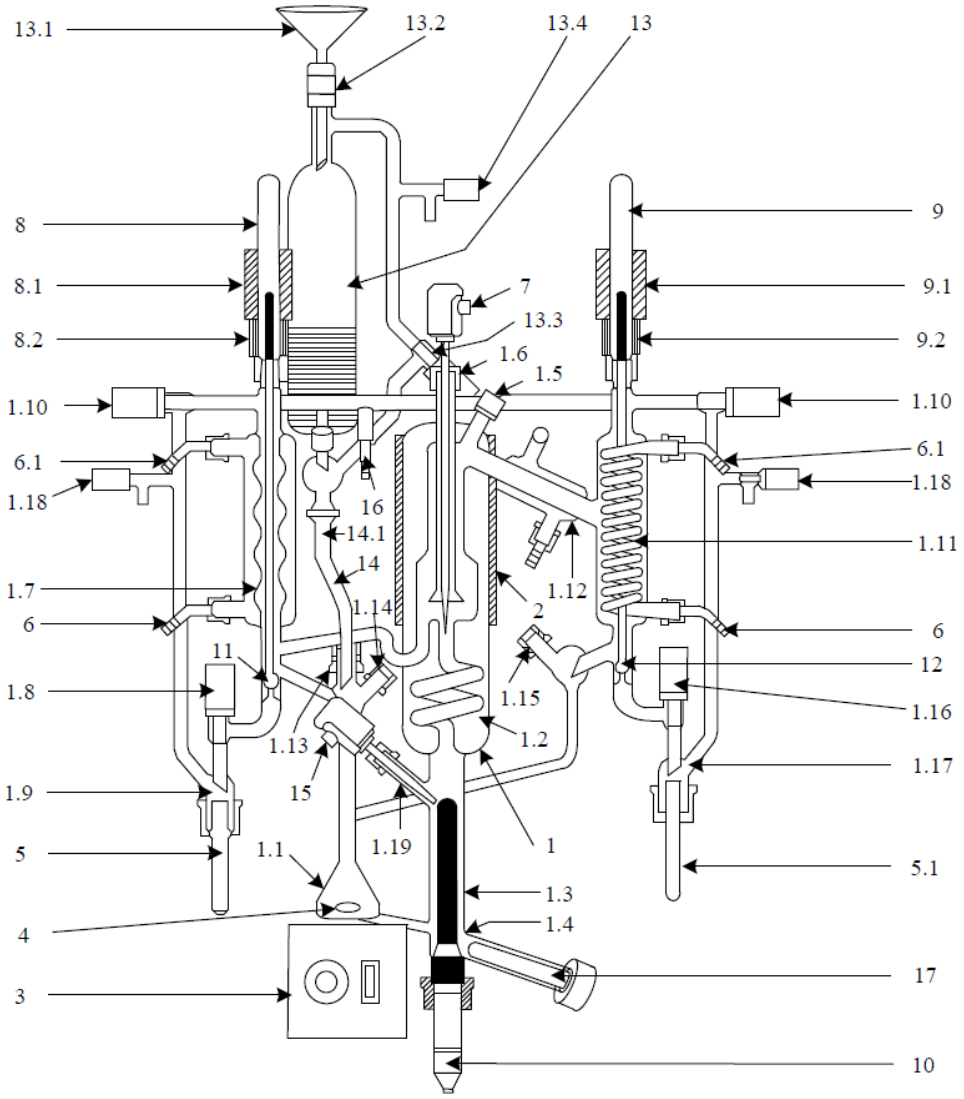

Figure 6-1: ***Schematic representation of the Pilodist dynamic recirculating still used for VLE and VLLE measurements. 1) Glass body of still, 1.1) Mixing chamber, 1.2) Cottrell pump, 1.3) Flow heater, 1.4) Discharge valve, 1.5) Sampling nozzle for vapour phase, 1.6) Temperature probe nozzle, 1.7) Cooler for liquid phase, 1.8) Stop valve, 1.9) Sampling nozzle for liquid phase, 1.10) Stop valve, 1.11) Condenser, 1.12) Condenser 1.13) Filler nozzle, 1.14) Sampling nozzle for the liquid phase, 1.15) Sampling nozzle for the vapour phase, 1.16) Stop valve, 1.17) Sampling nozzle for the vapour phase, 1.18) Aeration valves 1.19) Temperature probe nozzle, 2) Compensation heating jacket, 3) Magnetic stirrer, 4) Stirring magnet, 5) Glass receiver tubes, 6) Hose connection olive with screw cap, 7) Temperature sensor, 8-9) Valve caps, 10) Immersion heater rod, 11) Valve rod for the liquid phase, 12) Valve rod for the vapour phase, 13) Feed Burette, 14) Inlet line, 15) Temperture sensor, 16) Glass connecting olive for vacuum or positive pressure and 17) Ultrasonic homogenizer probe. Figure reprinted with permission (Pienaar, 2011)***

6.2 Experimental Procedure

This section includes a general discussion of general experimental procedure used to obtain VLE and VLLE data. All numerical references used in this section relate back to Figure 6-1. For a detailed version, see Appendix I.

6.2.1 Initial Procedure

Before the commencement of a new experimental set of data, the still is washed with acetone to prevent contamination of the still with impurities. The tap to allow cooling water through condensers (1.11 & 1.12) and the liquid cooler (1.7) should be opened and checked for constant flow. The operating pressure conditions are selected (atmospheric, vacuum or overpressure) and maintained. The burette must be filled with approximately 110ml of starting mixture via the filler nozzle (13.1). The stop valves (1.10) must now be opened in order to ensure that the entire apparatus maintains equal pressure during the course of the experimental run. The software is programmed to achieve suitable system temperatures and pressures to vaporise the starting mixture, causing vapour and liquid return.

6.2.2 Experimental Runs

In approximately 5 minutes, liquid return should begin. If liquid return does not occur, the power must be increased by 2% and monitored for a further 5 minutes before being re-adjusted. Under the appropriate power settings (depending on ambient temperature and boiling temperature of the starting mixture), vapour return should be evident in 20 minutes, with a sudden increase in the recorded bubble temperature. During this period of time, the pressure will fluctuate and will require monitoring and adjustment until a stable pressure of 101.3 kPa is reached. Once this has been achieved, the ultrasonic homogeniser can be switched on to ensure thorough mixing of the liquid and vapour phases. Owing to the concave nature of the sample wells (11 & 12), periodic flushing is required. This entails opening the stop valves (1.8 & 1.16) as well as the solenoid valves (9) by using the Pilodist remote control, allowing the congregated liquid to wash away into the receiver vials (5 & 5.1). This process ensures that the final vapour and liquid samples will not be contaminated. The collected liquid should be drained from the vials and the valves closed again. Equilibrium is achieved within in the still after approximately 60 minutes, indicated by a steady registered vapour temperature and a steady liquid return as well as a droplet return rate of approximately 30 drops per minute on the vapour side. Samples are now taken according to the procedure detailed in the following section.

6.2.3 Sampling

6.2.3.1 Vapour phase

Using a gas-tight syringe, containing a known amount of standard, a sample is taken directly from the gaseous phase in the separation chamber at the sampling nozzle (1.5). The addition of the standard compound prevents phase separation effects that occur as a result of temperature change.

For this experimental work, approximately 0.2 ml of Acetonitrile was used as standard, as it is completely miscible with water and the chemicals used. The resulting mixture is then placed in a 2 ml vial for further analysis.

6.2.3.2 Liquid phases

For the sampling of the aqueous and organic liquid phases, a sample is taken according to the flushing procedure discussed above. The liquid return can either flow back into the mixing chamber (1.1) or be deviated by using the solenoid valves (9). Approximately 4 ml of the dispersed liquid phases is obtained in the receiving vial (5). Fitted with a silicone rubber cover, the sampling vial is then placed in a water bath, with a temperature equal to the boiling point of the mixture, for two hours. After this period of time, using a gas-tight syringe (containing a known amount of Acetonitrile), a sample of each one of the distinctive liquid phases is taken and placed in 2 ml sample vials.

A sample of the overall liquid phase (global heterogeneous mixture) is also taken off using the same gas-tight syringe method through the sampling nozzle (1.14). When taking the overall liquid phase sample, approximately 0.4 ml of Acetonitrile is added to guarantee a homogeneous mixture.

6.2.4 Draining and Washing

When a satisfactory number of experimental runs have been executed for a particular binary or ternary mixture, the still must be drained and washed. This aids the removal of any non-volatile components from the still and avoids contamination of the feed mixture for the subsequent experimental run.

6.3 Analysis

Sample analysis was performed using both capillary gas chromatography and Karl Fischer titration, owing to the fact that the column-detector combination used could not quantify the amount of water within the samples. A complete explanation and sample calculation can be seen in Appendix D.

6.4 Materials

All chemicals used, including their purities and suppliers, are listed in the table below. Distilled water with a conductivity of 2 µS/cm was used for the experimental work. The cause of the impurities, as listed by the suppliers, was investigated through the use of GC as well as Karl Fischer Titration. No impurities were identified on the resultant chromatograms and the prominent impurity was

identified as water through titration. The water content of the alcohols was determined, using Karl Fischer titration, and can be found reported in Table 6-2.

Table 6-1 : ***Chemicals used in experimental and analysis work***

Component	Molecular Weight	CAS number	Assay	Supplier	Product number
Methanol	32.04	67-56-1	≥99.9%	Sigma Aldrich	34860
Acetone	58.08	67-64-1	≥99.8%	Sigma Aldrich	34850
Acetonitrile	41.05	75-05-8	≥99.8%	Sigma Aldrich	271004
Ethanol	46.07	64-17-5	≥99.8%	Sigma Aldrich	676829
n-Propanol	60.10	71-23-8	≥99.5%	Sigma Aldrich	82090
Isopropanol	60.10	67-63-0	≥99.5%	Sigma Aldrich	278475
n-Butanol	74.12	71-36-3	≥99.9%	Sigma Aldrich	537993
2-Butanone	72.11	78-93-3	≥99.7%	Sigma Aldrich	34861
Isooctane	114.23	540-84-1	≥99.0%	Sigma Aldrich	34862
2-Pentanol	88.15	6032-29-7	≥98.0%	Sigma Aldrich	P8017
2-Ethyl-1-Hexanol	130.23	104-76-7	≥99.6%	Sigma Aldrich	538051

Technical grade nitrogen, supplied by Afrox, was used for overpressure control in the phase equilibrium still, with ultra-high purity helium and technical grade air, also supplied by Afrox, used for gas chromatography.

Further reagents for the Karl Fischer titrations include HYDRANAL®-Methanol dry and HYDRANAL®-Composite 5, supplied by Sigma Aldrich. HYDRANAL®-Composite 5 is the world's most frequently used pyridine-free Karl Fischer reagent for one-component titration. It contains all the reactants, i.e. iodine, sulfur dioxide and imidazole, dissolved in diethyleneglycol monoethyl ether (DEGEE).

Table 6-2 : Measured water content of alcohols used in experimental work

Component	Water content/ mass %
Ethanol	0.01302
n-Propanol	0.04978
Isopropanol	0.05021
n-Butanol	0.00698

6.5 Accuracy, Uncertainty and Error analysis

The error associated with the reported molar compositions, mainly arises from experimental and analysis effects. This section considers all possible sources of error, in order to report an accurate maximum error in the presented raw data.

The pressure in the still was 101.3 kPa, measured and controlled with an accuracy of 0.1 kPa. The pressure gauge was calibrated and, according to its certificate of calibration, has a quoted accuracy of 0.1%. However, pressure measurement and control is independent of the VLE software, and was achieved manually. The maximum pressure deviations in pressure associated with this manual control was ±2 mbar.

The temperature probes were also recalibrated before the commencement of experimental work, with the vapour temperature probe found to have developed a constant drift of 0.1 °C since the previous calibration. Copies of the original certificates of calibration, provided by institutions that are SANSA accredited, can be found in Appendix B.

Guidelines for the evaluation and expression of uncertainty, provided by the National Institute of Standards and Technology (NIST), were followed. The method B was chosen as the uncertainty determination method. A short discussion can be found in Appendix L.

6.5.1 Experimental Effects

As an experimental output, the equilibrium compositions are associated with experimental inputs. There are two user-controlled inputs; heater power and pressure. Therefore, error in reported equilibrium compositions is associated with these inputs. During an experimental run, as described in section 6.3.3, the heater power does not vary and its impact on compositional error is treated as insignificant. The installed pressure regulating unit (Wika UT-10 unit) has a quoted accuracy of 0.1% of its full scale output (1.6bar abs): maximum 1.6mbar error. The certificate of calibration can be found in Appendix B. For analysis purposes, the pressure effects on composition were tested using the NRTL thermodynamic model for the ethanol/2-butanone/water system. Due to the fact that the vapour phase composition is more sensitive to pressure changes, in comparison to the liquid phase compositions, as well as the fact that, in the coming sections, it was seen that this model does not adequately predict the liquid-liquid region, the study on the possible deviation was limited to the vapour phase.

The compositions were determined through NRTL calculations at 101.1 kPa, 101.3 kPa and 101.5 kPa. The obtained compositions can be seen in Table 6-3.

Table 6-3: ***Tabulated results for pressure deviation error analysis.***

Pressure (kPa)	Water (mol fraction)	MEK (mol fraction)	Ethanol (mol fraction)
101.1	0.34791	0.638717	0.013376
101.3	0.34803	0.638595	0.013376
101.5	0.34815	0.638478	0.013376
Maximum absolute deviation:	**0.00122**		

The compositional deviations associated with the worst-case pressure fluctuations (an estimated ±2 mbar) can be seen plotted on a ternary phase diagram in Figure 6-2. Figure 6-2 shows the experimental data as well as the predicted phase compositions at the three different pressures, modelled using the NRTL model. It can be seen, from this figure and the data obtained, that the fluctuations in pressure would not affect the accuracy of the data presented, when taking the spread in data points into account.

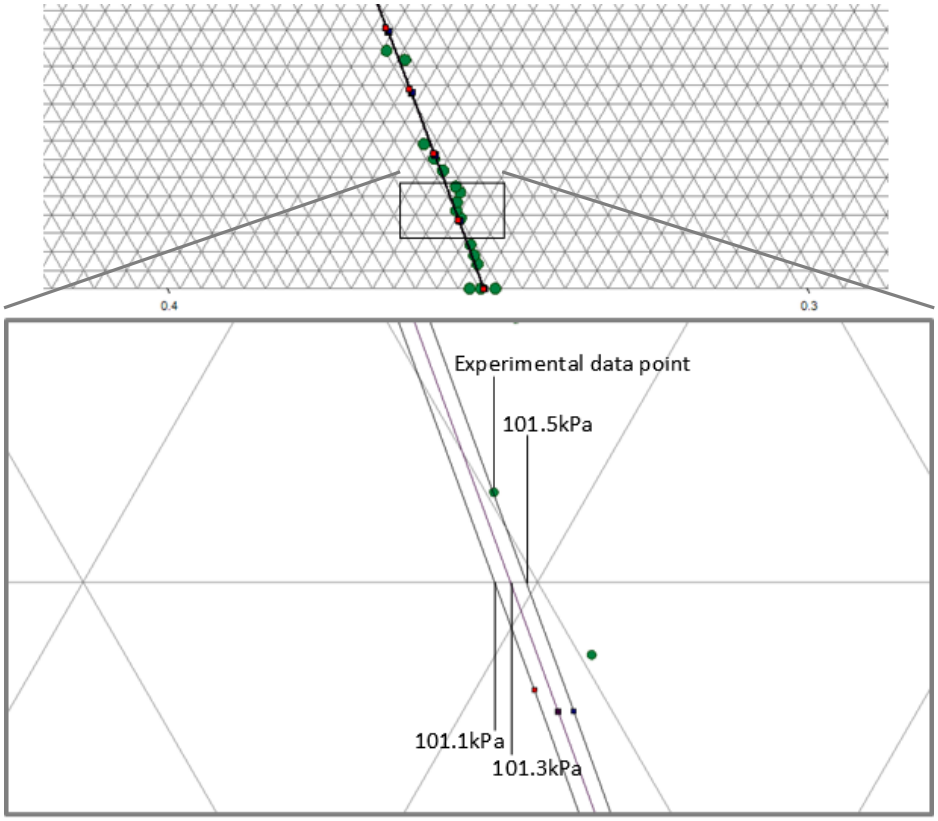

Figure 6-2: ***Error effects of pressure deviations on associated equilibrium composition measurement, modelled using NRTL.***

From these compositions (see Table 6-3), it was seen that pressure fluctuations of ± 2mbar will not significantly influence the compositional accuracy (±0.0012 mole fraction) (see Table 6-3).

6.5.2 Analysis Effects

Along with the errors introduced by experimentation, the preparation and analysis of samples are other sources of error. It is therefore of vital importance to test the reproducibility of GC- and KF-data for each system studied for this research. Detailed calibration results can be found in Appendix C.

For each system, three samples of known composition were compared and analyzed using GC. Deviations in the predictions for each system were determined and a maximum deviation quantified (±0.0138 mole fraction).

A total of 38 samples with varying water content were prepared using distilled water and HYDRANAL®-Methanol dry (≤0.01% Water). The samples were titrated (twice) using the Karl Fisher titration method to determine the average associated error. It was found that for samples with less than 0.005 wt% water could not be analyzed. The maximum deviation was found to be ±0.023 %. This computes to approximately ±0.001 mole fraction deviation and consequently considered negligible. This shows that the error associated with analysis effects are restricted to GC-analysis, for this research project, as the Karl Fisher titration method is extremely sensitive to samples containing more than 0.005 wt% water. This is indeed the case with all the samples considered as the new systems measured are all water-containing.

The full results of the analysis error are provided in Appendix C, including the response factors of the detectors with respect to the internal standard.

6.5.3 Summary

The equilibrium temperatures are measured by a Pt-100 probe connected to a digital Hart Scientific thermometer. This thermometer has an accuracy of 0.03 at 273 K, 0.05 at 323 K and 0.10 at 473 K, according to the original certificate of calibration. The still never reached a temperature above 350 K during the experimental runs performed. As mentioned, the installed pressure regulating unit (Wika UT-10 unit) has a quoted accuracy of 0.1% of its full scale output (1.6bar abs): maximum 1.6mbar error. The heating power can be measured and controlled by a Pilodist M101 control system and a VLE software package where the pressure was controlled manually.

The heater power does not vary substantialy and its impact on compositional error is treated as insignificant. Error introduced by pressure fluctuations during experimental runs and error

introduced due to sample analysis are additive (±0.0139 mole fraction). To be able to confidently report new experimental data, the error used in the marker size and thermodynamic testing is rounded up to ±0.014 mole fraction.

7 RESULTS AND DISCUSSIONS

With the experimental apparatus and approach outlined in the previous chapter, the results of this experimental study will now be addressed. This chapter details the verification of the experimental methodology and finally the generated VLLE data for each of the three systems listed in section 5.2. A detailed set of experimental data can be found in Appendix E.

7.1 Verification

In order to confidently authenticate the accuracy and repeatability of all new data generated by the equipment, the equipment had to be verified. The equipment and methodology was verified against systems with two or more independent sets of agreeing data. Consequently, the isobaric VLE for the binary ethanol/isooctane system and the VLLE for the ternary ethanol/n-butanol/water at 101.3 kPa was selected for verification. The system of n-propanol/isoooctane/water, solely measured and published by our research group, was chosen to test the repeatability of the experimental set-up.

The reasoning behind the selection of a system including water is obvious and successfully complicates the sampling method in order to verify the entire experimental procedure.

7.1.1 Ethanol/Isooctane system

The ethanol/isooctane system was compared with four independent, published sets of data. The results and comparison of the equilibrium measurements and published data can be seen in Figure 7-1 and Figure 7-2.

Visually, the experimental data compares well with both the thermodynamic model and the reference data. There are some deviation and overall scatter in the measured data points. This could be due to the fact that the data was not obtained during one experimental operation: starting with pure ethanol and adding isooctane after each set of sampels is taken. The ethanol/isooctane VLE data was generated starting with a still containing pure ethanol as well as starting with a still containing pure isooctane. The data was also measured over several months where several problems (detailed in Appendix M) were addressed and rectified. When considering the compositional error associated with this work (±0.014 mole fraction), the deviation is accounted for. Due to the lack of reference data in the region of low ethanol concentration, the experimental data was compared to data generated by dew-point calculations (see Figure 7-3). Again, the experimental data compared satisfactory against calculated data.

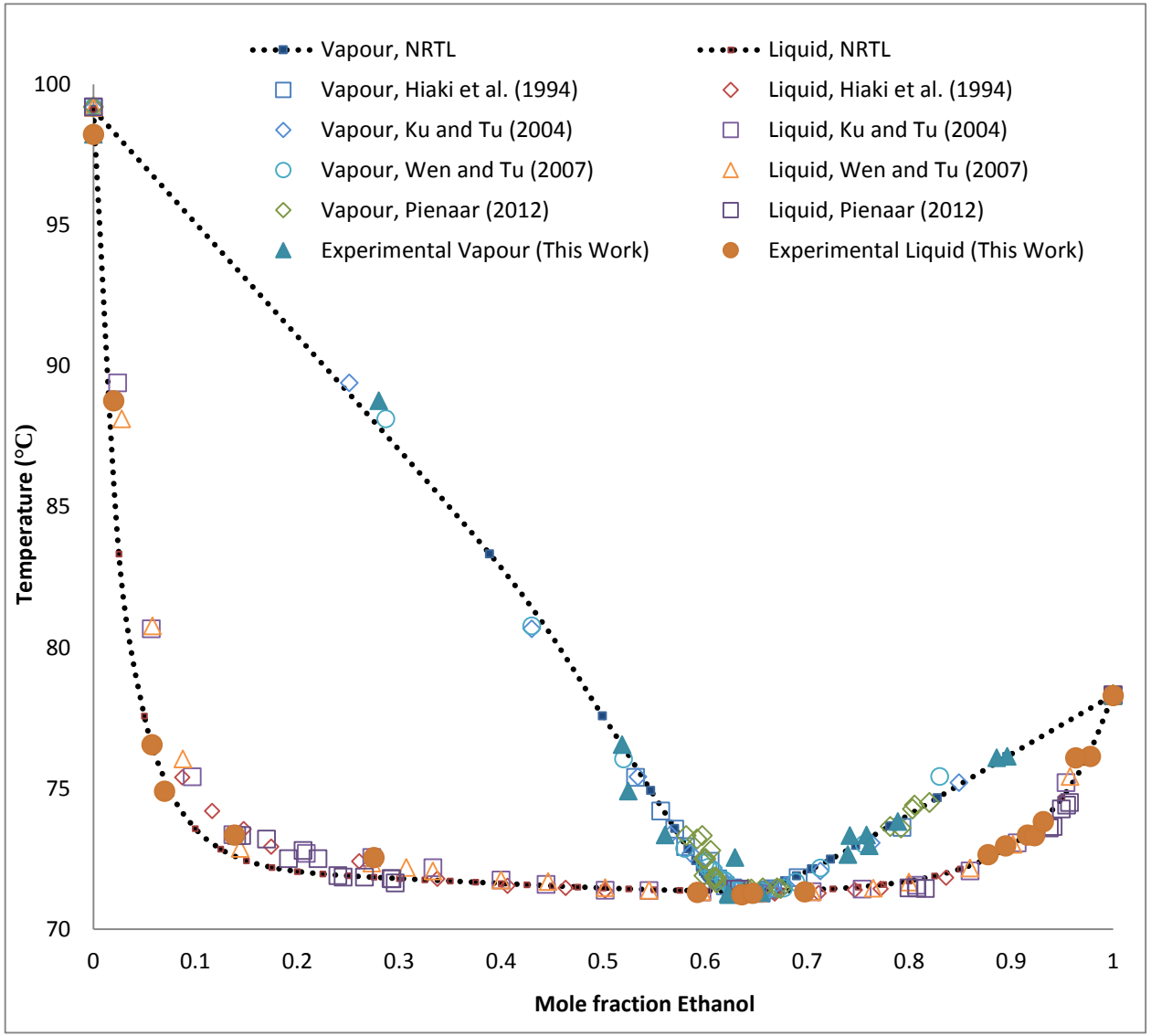

Figure 7-1: ***T-x-y phase diagram of measured Ethanol/Isooctane VLE data at 101.325 kPa, compared to data published by Haiki et al. (1994), Ku and Tu (2005) and Pienaar et al. (2012) and to the NRTL thermodynamic model.***

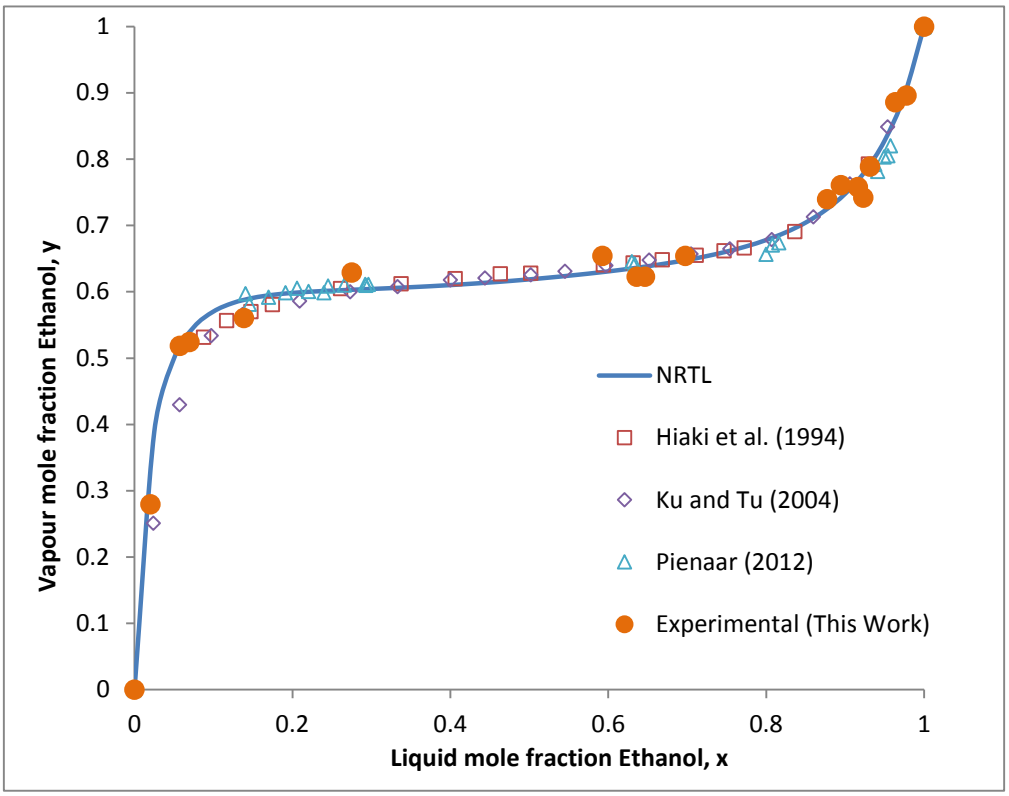

Figure 7-2: ***Binary T-x-y phase diagram of measured Ethanol/Isooctane VLE data at 101.325 kPa, compared to data published by Haiki et al. (1994), Ku and Tu (2005) and Pienaar et al. (2012) and to the NRTL thermodynamic model.***

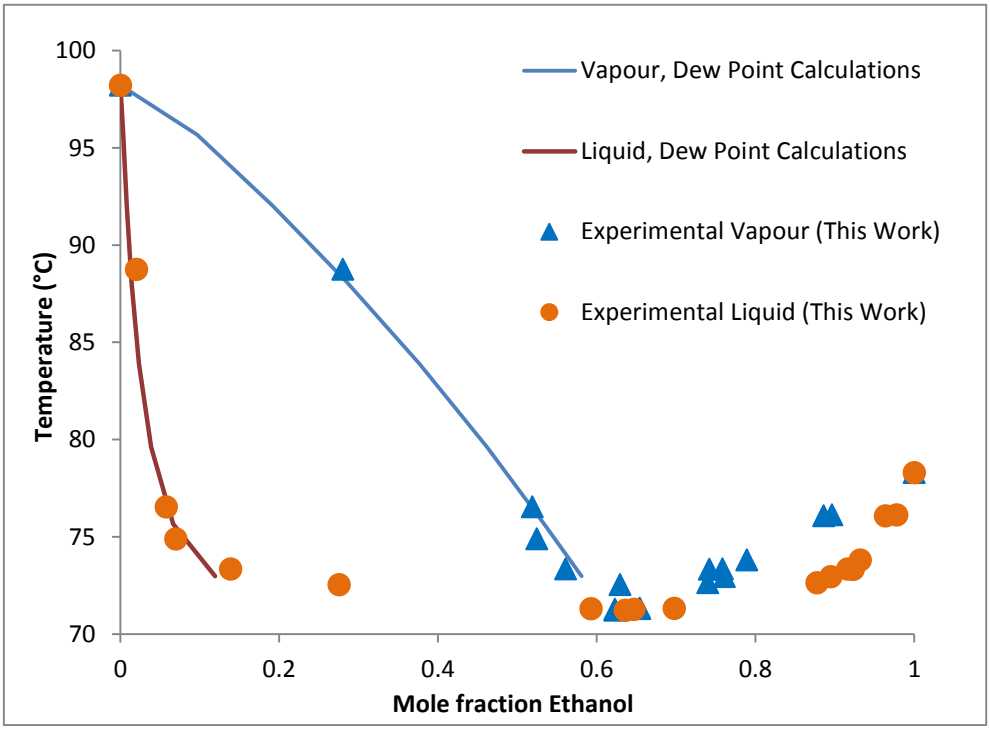

Figure 7-3: ***Binary T-x-y phase diagram of measured Ethanol/Isooctane VLE data at 101.325 kPa, compared to calculated data.***

The binary, minimum-boiling azeotrope composition, determined experimentally, compared well to published values (Table 7-1).

Table 7-1: Minimum-boiling azeotrope composition comparison.

Reference	Temperature (°C)	x_ethanol	y_ethanol
This work	71.28	0.623	0.647
Hiaki et al.	71.29	0.632	0.644
Ku and Tu	71.29	0.652	0.648
Wen and Tu	71.29	0.652	0.648
Pienaar et al.	71.42	0.630	0.645

Finally, the generated data's thermodynamic consistency was tested using the L/W Consistency Test and the McDermott-Ellis Consistency Test. The experimental VLE data passed both tests. It passed the point-to-point L/W Wisniak consistency test with all the values ranging between 0.92 and 1.10. The data was considered to be thermodynamically consisted with all calculated D value lower than D_{max}. Details and results of all thermodynamic consistency testing can be found in Appendix F.

7.1.2 Ethanol/n-Butanol/Water

The ethanol/n-butanol/water system was chosen due to the fact that three independent sets of published data are available for this ternary system, which are all in agreement. Newsham and Vahdat (1977) measured this system using the flow method, Gomis et al. (2000) with an all glass dynamic recirculating still and Pienaar et al. (2012) measured the experimental data with the still used in this experimental study.

On the resulting ternary diagram (Figure 7-4) the experimentally determined data and the published data are not compared to thermodynamic models (NRTL, UNIFAC or UNIQUAC). This is due to the fact that none of these models manage to accurately predict the equilibrium phase compositions.

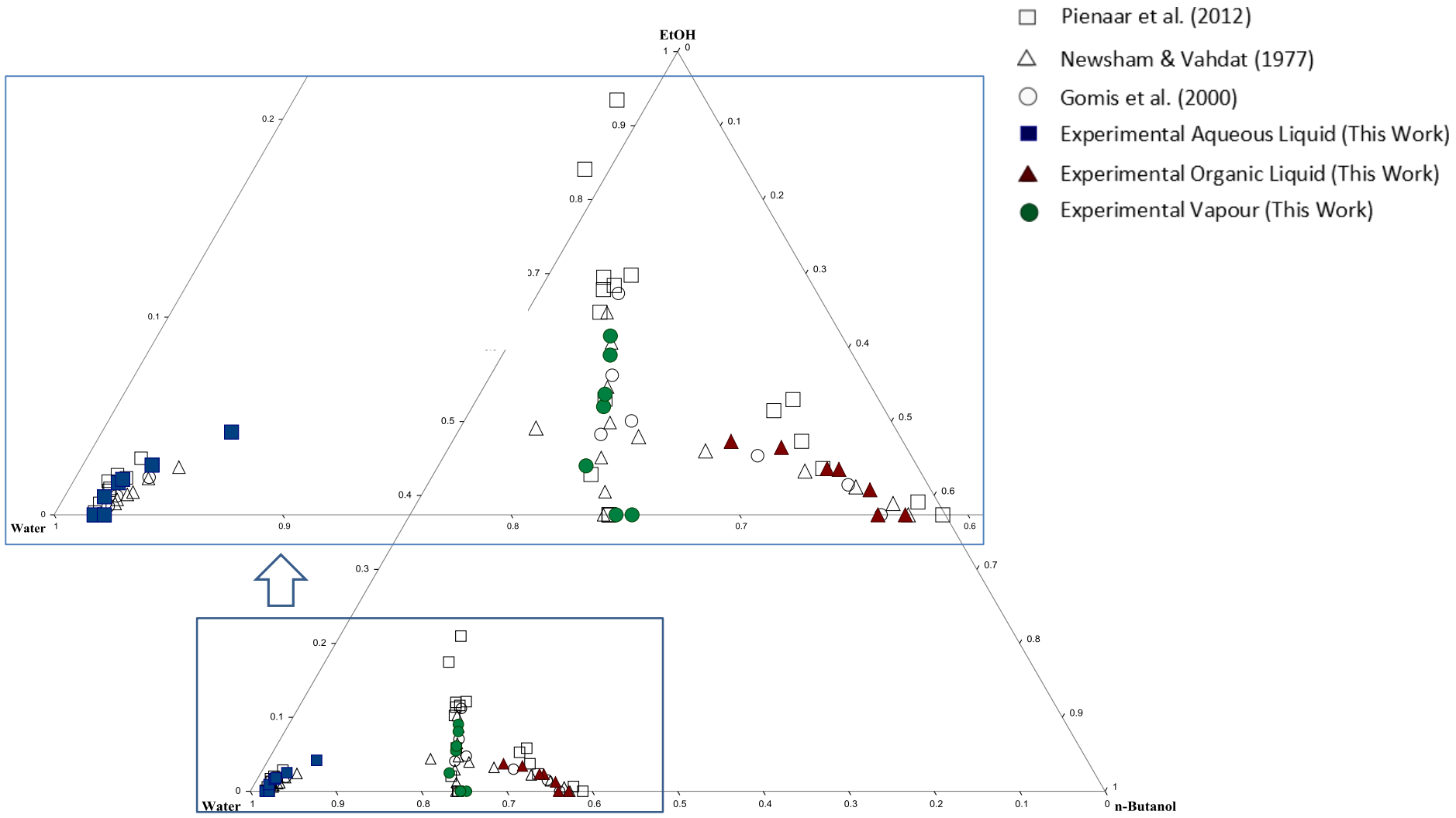

Figure 7-4: T*ernary phase diagram of measured Ethanol/n-Butanol/Water VLLE data at 101.3 kPa, compared with data published by Newsham and Vahdat (1977), Gomis et al. (2000) and Pienaar et al. (2013).*

From the ethanol/n-butanol/water ternary diagram (Figure 7-4) it can be seen that the liquid phases (aqueous and organic) correlate well with published data. However there are some discrepancies between the experimental vapour phase data and published vapour phase data. These deviations and scatter could possibly be ascribed to the dissimilar sampling and analytical methods used between the research groups. Newham and Vahdat (1977) sampled directly from the still and added an appropriate solvent to avoid demixing. The composition of the phases was “estimated” using a Perkin Elmer model 900 gas chromatograph. Gomis et al. (2000) constructed a vapour circulation line to connect a chromatograph directly to the vapour-liquid separation chamber. The tube walls were superheated with resistance tape controlled by a potentiometer so that the vapour becomes unsaturated and condensation is avoided.

However, by taking into account the experimental deviations associated with each of these, agreeing, sets of data, the vapour phase compositions correlate well with the sets of published data. With this, and the fact that the liquid-phase compositions show excellent correlation, the experimental set-up and procedure was verified and deemed accurate and repeatable.

The generated data’s thermodynamic consistency was tested using the L/W Consistency Test (all values ranging between 0.91 and 1.00) and the McDermott-Ellis Consistency Test (all calculated D values lower than D_{max}). Details and results of all thermodynamic consistency testing can be found in Appendix F.

7.1.3 Repeatability analysis - n-Propanol/Isooctane/Water

In order to determine the repeatability of VLLE measurements, of a water-containing system, the n-propanol/isooctane/water ternary system was studied. For this particular system, Pienaar et al. (2012) has published a data-set. Repeatability analysis was accomplished by adding a water/isooctane mixture of known composition to the still (sample a1). After which n-Propanol was added to the still and another data point determined (sample a2). The still was then washed as described in Section 6.3.6 and the process repeated (sample b1 and b2). Results of this analysis can be found tabulated in Table 7-2.

Table 7-2: ***Results for repeatability analysis for n-propanol/isooctane/water at 101.3 kPa.***

Temperature (K)	Organic			Aqueous			Overall			Run
	x_{water}	$x_{isooctane}$	$x_{propanol}$	x_{water}	$x_{isooctane}$	$x_{propanol}$	y_{water}	$y_{isooctane}$	$y_{propanol}$	
352.31	0.0114	0.9886	0.0000	0.9988	0.0012	0.0000	0.4710	0.5290	0.0000	Pienaar
352.35	0.0121	0.9879	0.0000	0.9995	0.0005	0.0000	0.4716	0.5284	0.0000	a1
352.00	0.0112	0.9868	0.0020	0.9992	0.0005	0.0003	0.4719	0.5269	0.0013	a2
352.26	0.0105	0.9895	0.0000	0.9982	0.0018	0.0000	0.4691	0.5309	0.0000	b1
351.89	0.0086	0.9892	0.0023	0.9983	0.0014	0.0004	0.4703	0.5285	0.0012	b2

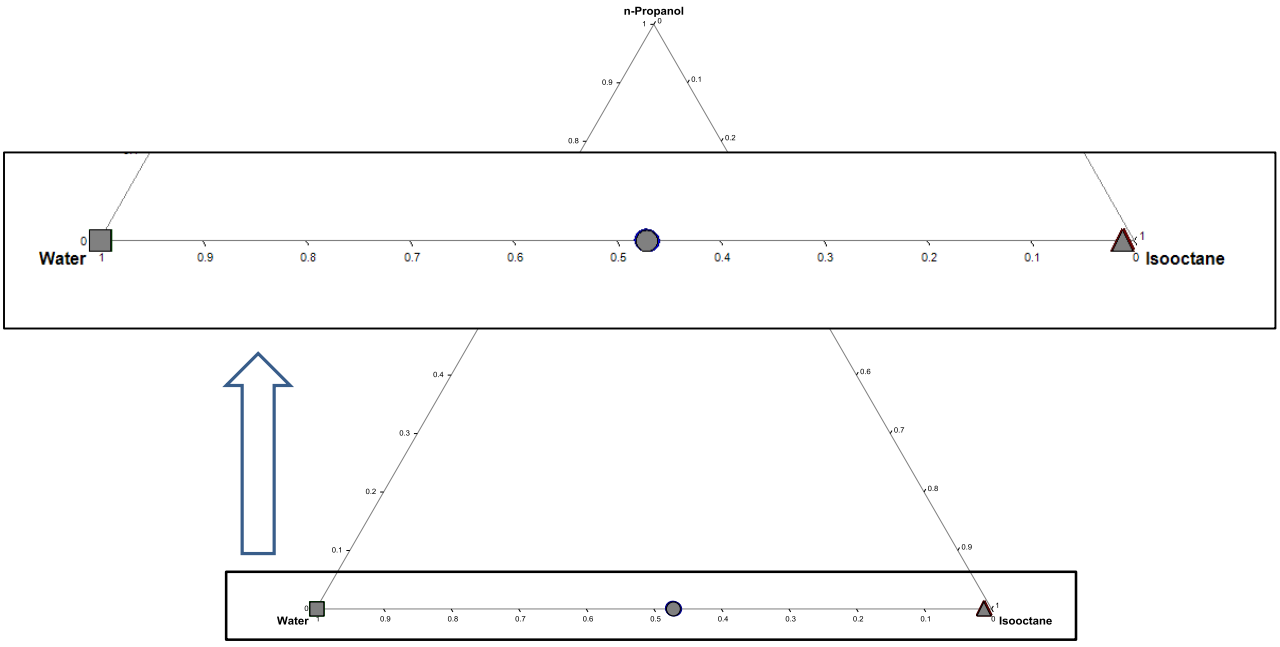

Figure 7-5: ***Ternary phase diagram for n-propanol/isooctane/water at 101.3 kPa.***

When plotting all the resulting data points (including the literature data) on a ternary diagram (Figure 7-5), it is difficult if not impossible, to differentiate between the points. When taking a closer look at the three areas (aqueous region, organic region and overall liquid region), by decreasing the area being studied, a better sense of repeatability is obtained (see Figure 7-6).

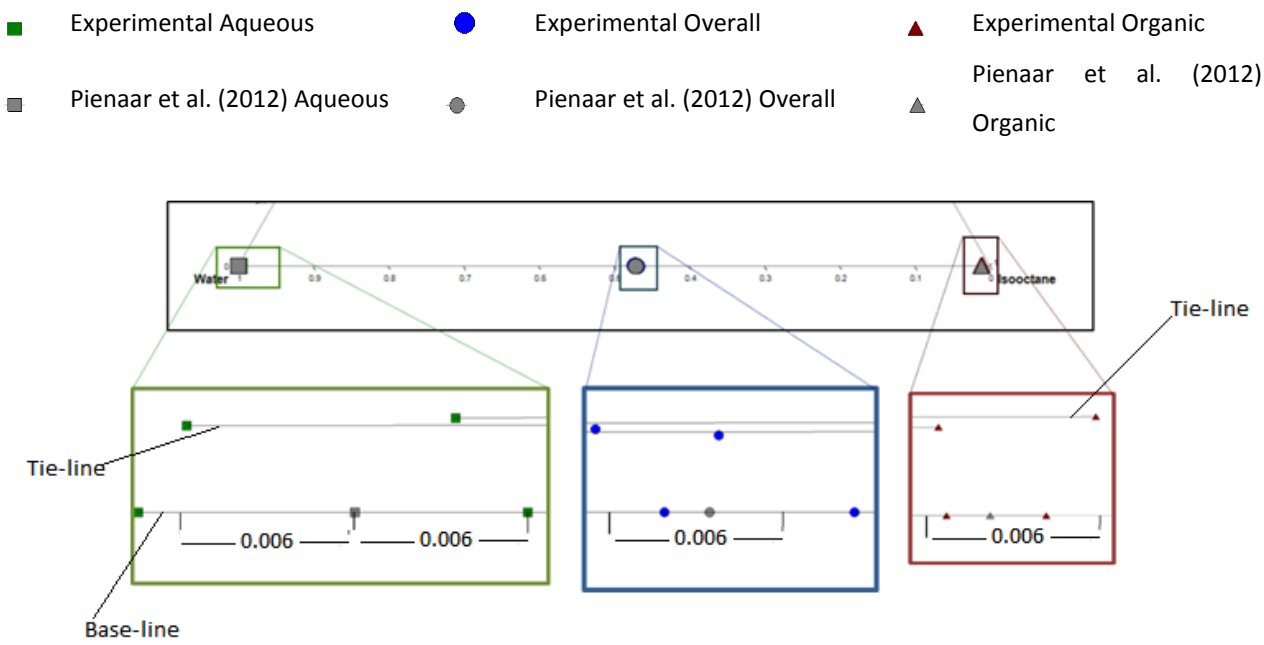

Figure 7-6: ***Illustration of accuracy and repeatability using the n-propanol/isooctane/water system at 101.3 kPa.***

Figure 7-6 illustrates sections of the ternary phase diagram of n-propanol/isooctane/water (Figure 7-5) enlarged. From this it can be seen that there is small deviation from one experimental run to the next, the largest deviation found to be 0.0006 mole fraction. If the marker-size had to reflect the compositional error (±0.014 mole fraction), as it does in Figure 7-5, this deviation becomes negligible. In the following section, pertaining new phase equilibria data, this method of including the error into the size of the markers will be used.

For equilibrium data to be considered accurate and true, mass balance rules are applied (Section 2.33). If the overall liquid data points lie on the tie-lines connecting the aqueous- and organic-liquid phases, the data can be regarded as accurate. In figure 7-6 it can be seen that this is indeed the case, as the overall liquid compositions lie on the tie-lines connecting the aqueous and organic liquid compositions. This form of verification was applied to all new data measured for this experimental study.

7.1.4 Verification Summary

The experimental apparatus and approach was verified using two binary (one VLE and one VLLE) and one ternary system (VLLE only). VLE data was measured for the binary ethanol/isooctane system and VLLE for ethanol/n-butanol water at 101.3 kPa. The generated data was compared to three or more independent sets of agreeing data and found to be accurate and repeatable. The experimental methodology was further tested by measuring the repeatability of experimental runs. This was achieved by studying the n-propanol/isooctane/water system at low isooctane concentrations. All deviations from published data were accounted for by including the compositional error associated with this work (±0.014 mole fraction). The generated data, for verification purposes, were tested for thermodynamic consistency using the L/W Consistency Test and the McDermott-Ellis Consistency Test. The error in composition was included into the marker size of all ternary phase diagrams.

7.2 New Phase Equilibria Data

The following section looks at the new experimental data measured, VLLE data for three water containing systems:

- Ethanol/MEK/water
- n-Propanol/MEK/water
- iso-Propanol/MEK/water

7.2.1 Ethanol/MEK/Water VLLE data

The measured VLLE data for the system ethanol/MEK/water can be found plotted in Figure 7-7. The detailed phase equilibrium data can be found tabulated in Appendix E and the results of the L-W consistency test as well as the McDermott-Ellis consistency test can be found in Appendix F. The maximum value of D for the L/W Consistency Test was 0.92. The data passed the McDermott-Ellis Consistency test owing to the fact that all values of D were lower than their respective D_{max} values. Liquid phase regularity was checked using the Othmer-Tobias correlation. The graphical results of the Othmer-Tobias correlation can be seen in Appendix G. Accordingly, the data-set was deemed thermodynamic consistent.

As discussed in Section 3.5, homogeneous binary azeotropes exist between all of the components; ethanol/water, ethanol/MEK and MEK/water. The range in composition of the MEK/water homogeneous binary azeotrope was obtained from the listed, literature values in Table 5-3. This was plotted as a range in Figure 7-7, as well as Figure 7-9 and Figure 7-10. This was done to illustrate the accuracy of the experimentally obtained composition for the MEK/water azeotrope for this work. For the ethanol/MEK/water system, it can be seen that the binary azeotrope composition obtained experimentally falls within the range reported by several literature sources.

It can also be seen that the vapour phase lies outside the liquid-liquid heterogeneous region. This means that it is impossible for a heterogeneous ternary azeotrope to exist for this system. However, by studying the ethanol/MEK/water system's RCM, modelled using Aspen Plus® and the NRTL thermodynamic model, it is suggested that a homogeneous ternary azeotrope exists with a composition of 52.34 mol% MEK, 24.89 mol% water and 22.77 mol% ethanol at a temperature and pressure of 73.2 °C and 101.3 kPa respectively.

It was interesting to notice from the experimentally determined VLLE ternary diagram (Figure 7-7), that the vapour phase seems to tend towards the water-ethanol azeotrope's composition.

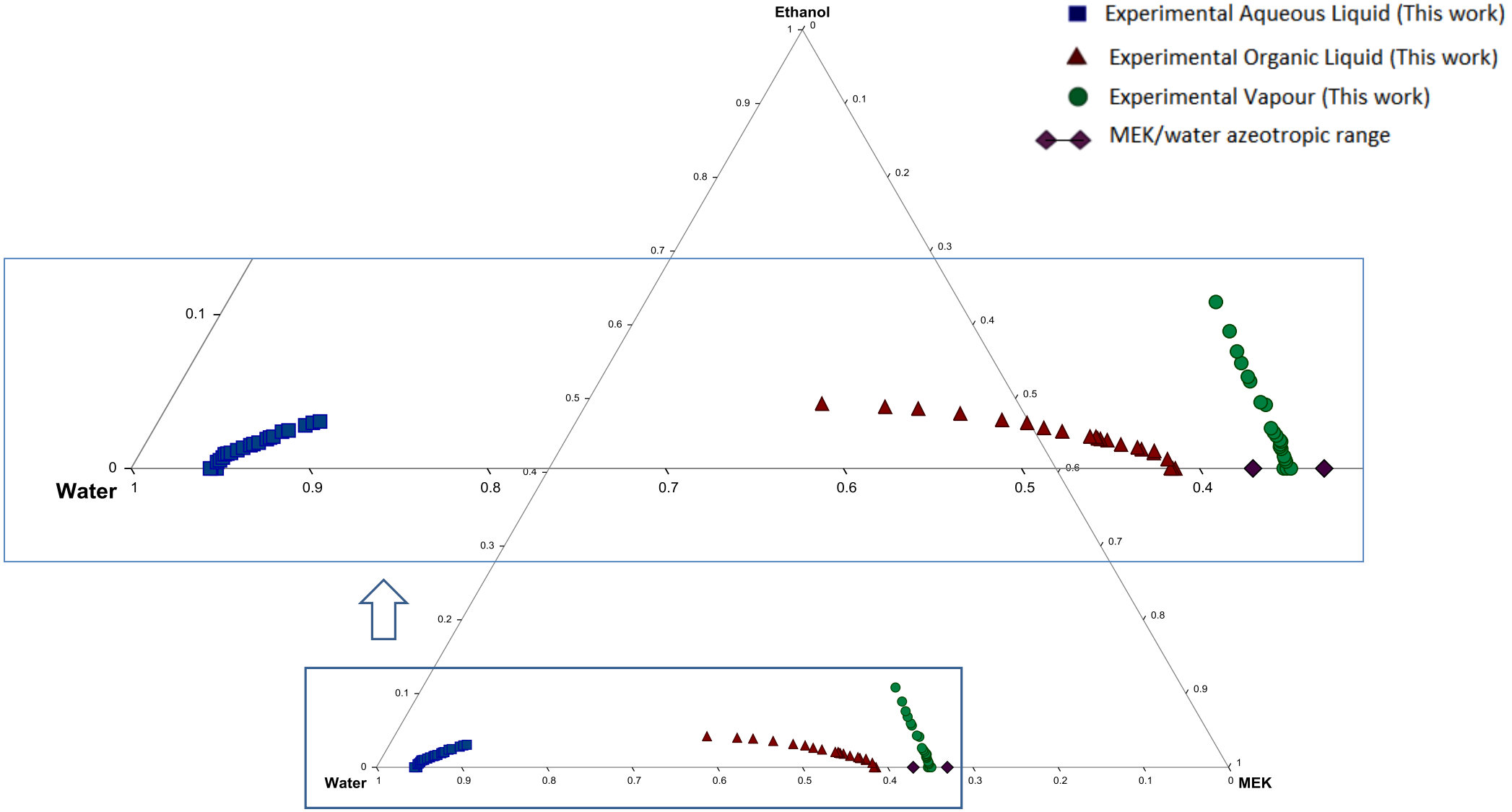

Figure 7-7: ***Ternary phase diagram of measured Ethanol/MEK/Water VLLE data at 101.325 kPa.***

On the grounds that these ternary diagrams take months to measure, a closer look was taken at the experimental data points of the ethanol/MEK/water system to ensure that the system remained unchanged from experimental-run to experimental-run. The aqueous phase was chosen to illustrate this and the data points grouped by day of measurement (Figure 7-8). The compositional change from day to day follows the expected trend and the deviations are considered to be slight and negligible. This further confirmed the accuracy of the newly determined and presented VLLE phase data.

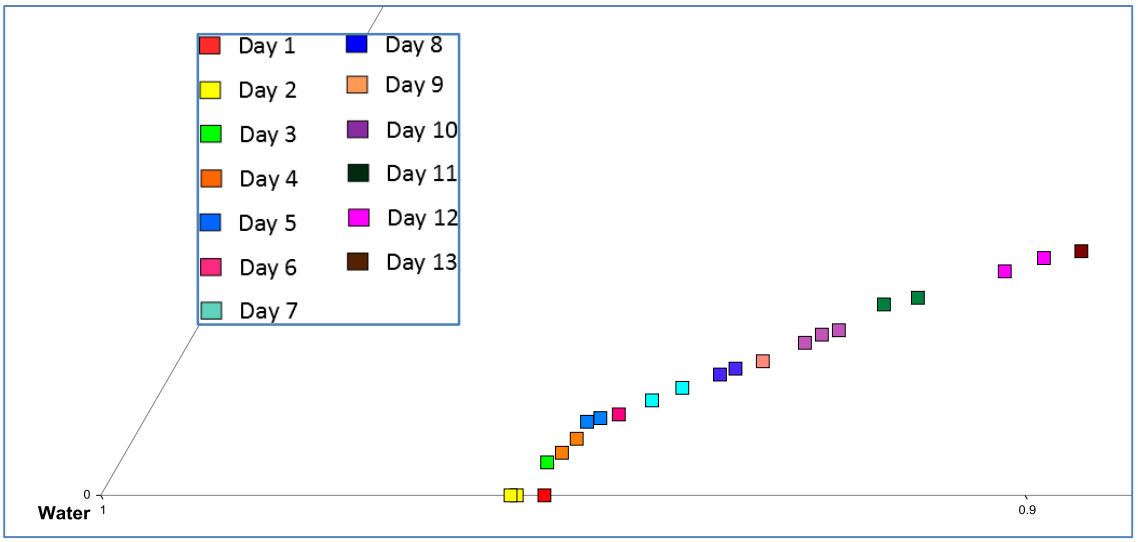

Figure 7-8: ***Illustration of the effect of time on equilibrium still feed for the Ethanol/MEK/Water at 101.3 kPa.***

7.2.2 n-Propanol/MEK/Water VLLE data

The VLLE data generated for the n-propanol/MEK/water system is plotted in Figure 7-9 and the data can be found tabulated in Appendix E. The data is considered thermodynamically consistent by passing both the L/W consistency test as well as the McDermott-Ellis consistency test. The results of the thermodynamic consistency tests and the Othmer-Tobias correlation can be found tabulated in Appendix F and Appendix G respectively.

As can be seen from Figure 7-9, that there is no binary azeotrope that exists between MEK and n-propanol. This is confirmed by published literature (Table 7-4).

This is an interesting observation when considering the small structural change from ethanol to n-propanol. Like with the ethanol/2-butanone/water system no ternary heterogeneous azeotrope exists for the n-Propanol/MEK/Water system. The vapour phase compositions lie outside of the heterogeneous liquid region. The measured binary homogeneous MEK/water azeotrope falls within the range of reported literature compositions (see Figure 7-9).

The vapour phase, like with the ethanol/MEK/water vapour equilibrium phase compositions, tends towards the corresponding binary homogeneous azeotrope (n-propanol/water azeotrope). It is also assumed, from thermodynamic modelling, that a ternary homogeneous azeotrope does not exist outside of the heterogeneous liquid region. In other words, the only azeotropes found for this ternary system is the homogeneous binary n-propanol/water azeotrope and the homogeneous binary water/MEK azeotrope.

It can be seen from Figure 7-9, that the experimentally determined VLLE data follows a steady trend and the liquid-liquid region is slightly larger than that seen for the ethanol/MEK/water system.

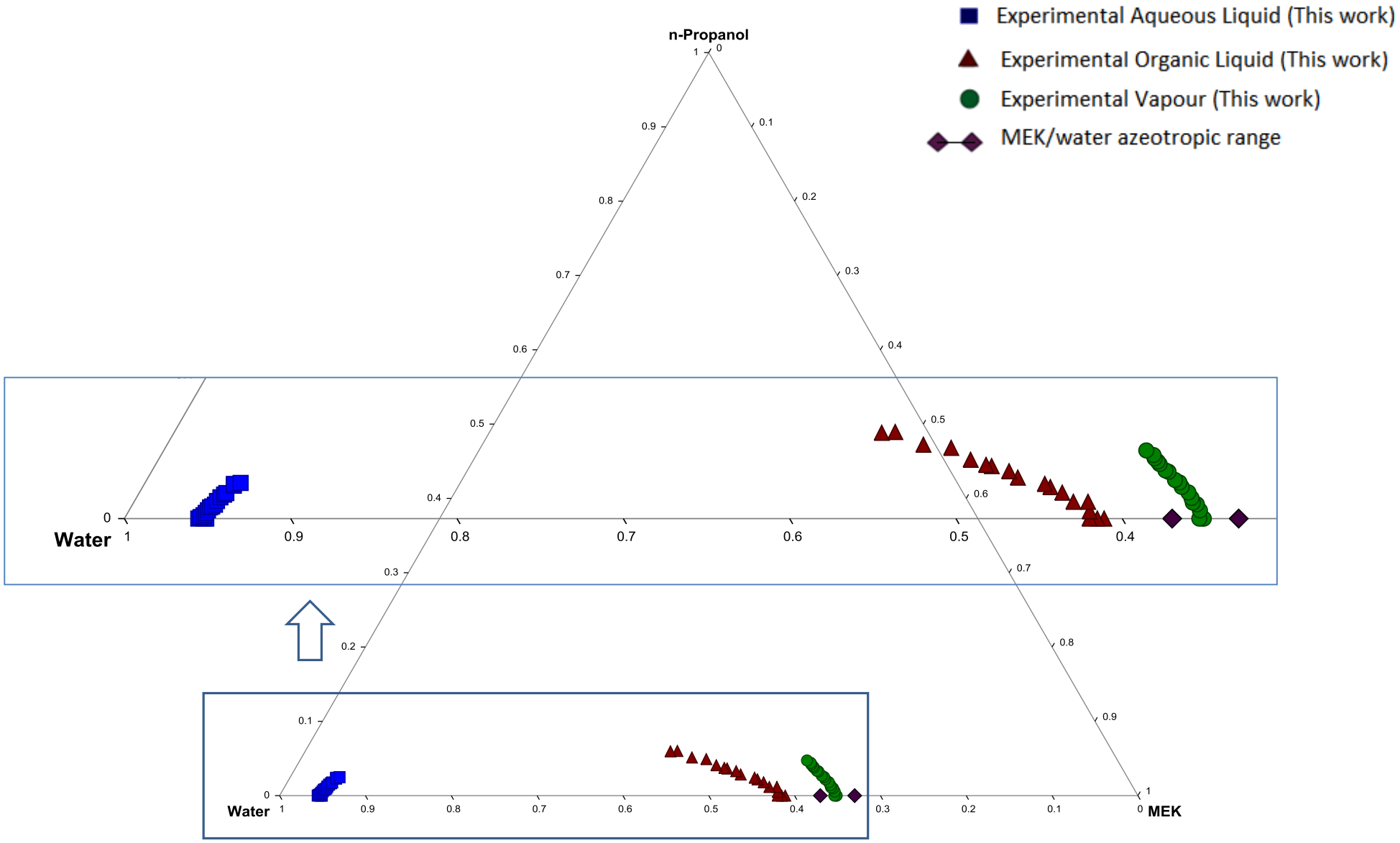

Figure 7-9: ***Ternary phase diagram of measured n-Propanol/MEK/Water VLLE data at 101.325 kPa.***

7.2.3 IPA/MEK/Water VLLE data

In Figure 7-10 the experimental VLLE data measured for the IPA/MEK/Water system is presented graphically. Detailed phase equilibrium data is tabulated in Appendix E. The generated data's thermodynamic consistency was tested using the L/W Consistency Test and the McDermott-Ellis Consistency Test. The data passed the point-to-point L/W Wisniak consistency test with all the values ranging between 0.93 and 1.00. The data was considered to be thermodynamically consisted with all calculated D value lower than D_{max}. Details and results of all thermodynamic consistency testing can be found in Appendix F.

As with the previous systems (ethanol/MEK/water and n-propanol/MEK/water), the liquid phase data was checked using the Othmer-Tobias correlations (results illustrated in Appendix G).

The liquid-liquid region for the IPA/MEK/water system is the largest in comparison to the ethanol/MEK/water and n-propanol/MEK/water systems. Again, the absence of a ternary heterogeneous azeotrope is noted and through thermodynamic model predictions the presence of a ternary homogeneous azeotrope was noted.

7.2.4 Azeotrope Comparison

This section compares the azeotropic compositions measured with that published from several research groups as well as with azeotropes found through thermodynamic modelling (NRTL, UNIFAC and UNIQUAC models). A comprehensive list of azeotropic literature data can be found tabulated in Table 5-3. Built-in Aspen Plus® parameters were used to determine the binary azeotropic compositions. The built-in parameters can be found listed in Appendix H.

As can be seen from Table 7-2, thermodynamic models predict a homogeneous ternary azeotrope for the ethanol/MEK/water system at 101.3 kPa within a range of 72.92 - 73.07°C. The temperature measured at the last equilibrium composition within the liquid-liquid heterogeneous region was 72.50°C. This would suggest that the homogeneous ternary azeotrope could have been found with further experimentation and by moving into the VLE-region. However, considering the scope of this research project and the time-scale associated with each data point determination (approximately two-three days), the experimental determination of the ternary homogeneous azeotrope for the ethanol/MEK/water and IPA/MEK/water systems were left for future work.

Although there is some deviation between the reported homogeneous binary water/MEK azeotrope compositions, when including the associated experimental and analytical error (±0.014 mole fraction), this deviation becomes negligible.

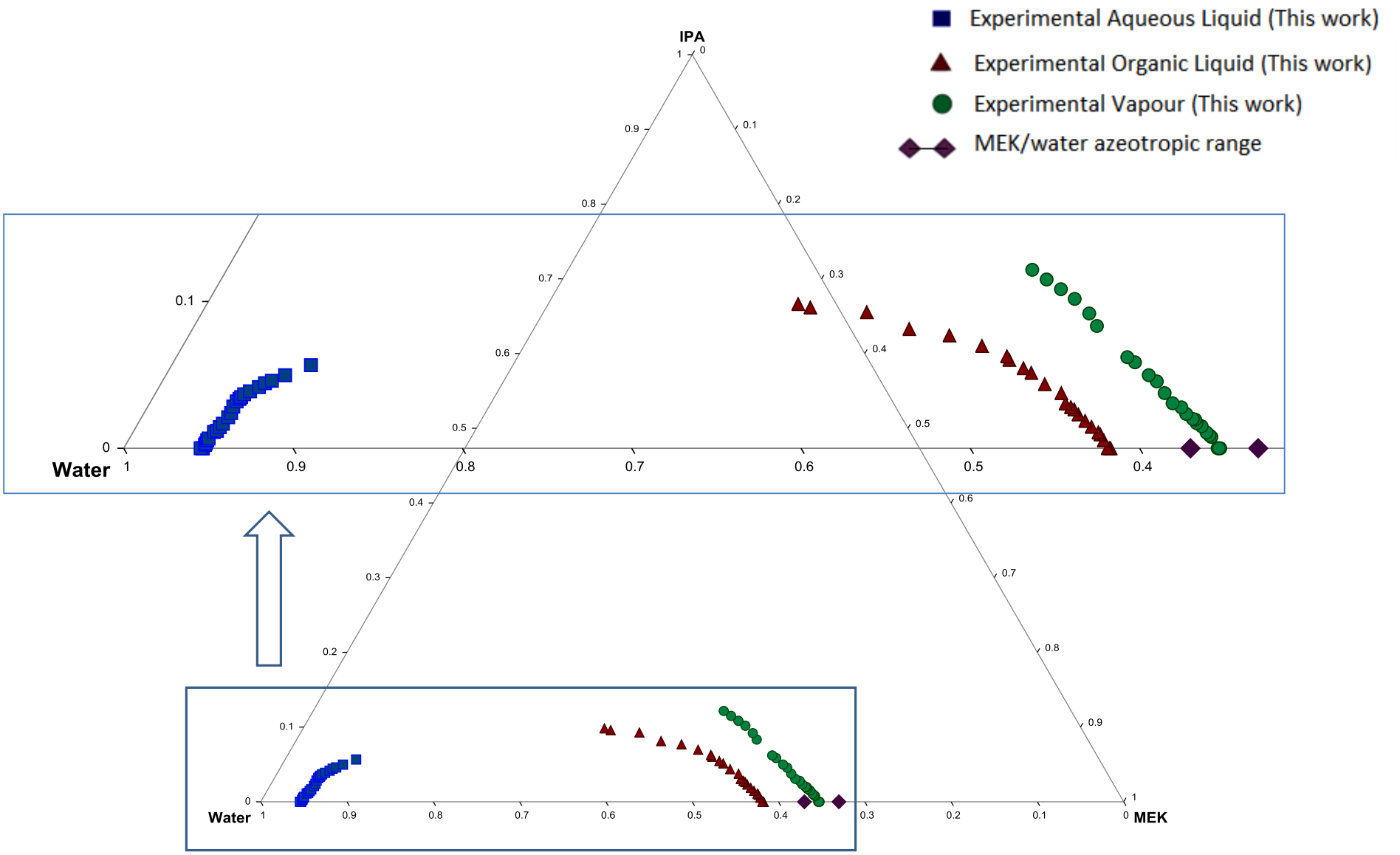

Figure 7-10: ***Ternary phase diagram of measured IPA/MEK/Water VLLE data at 101.325 kPa.***

Table 7-3: ***Comparison of experimentally determined azeotropic compositions with compositions from literature and thermodynamic models for the ethanol/MEK/water system at 101.3 kPa.***

Azeotrope:	**Classification:**	**Temperature (°C):**	**y_{Water}**	**y_{MEK}**	**y_{EthOH}**	**Reference/Model:**
Homogeneous	Unstable Node	73.04	0.2489	0.5234	0.2277	NRTL
Homogeneous	Unstable Node	72.92	0.1385	0.5306	0.3310	UNIFAC
Homogeneous	Unstable Node	73.07	0.2633	0.5420	0.1947	UNIQUAC
Homogeneous	Binary	78.1	0.1070	-	0.8930	Zemp et al. (1992)
Homogeneous	Binary	78.18	0.088	-	0.912	Lai et al. (2014)
Homogeneous	**Binary**	**78.15**	**0.1050**	**-**	**0.8950**	**This work**
Homogeneous	Saddle	78.15	0.1048	-	0.8952	NRTL
Homogeneous	Saddle	78.04	0.1067	-	0.8933	UNIFAC
Homogeneous	Saddle	78.16	0.1001	-	0.8999	UNIQUAC
Homogeneous	Binary	74.31	-	0.5050	0.4950	Wen & Tu (2007)
Homogeneous	Binary	74.31	-	0.4830	0.5170	Martinez et al. (2008)
Homogeneous	Saddle	74.19	-	0.4998	0.5002	NRTL
Homogeneous	Saddle	73.33	-	0.4943	0.5057	UNIFAC
Homogeneous	Saddle	74.19	-	0.4997	0.6098	UNIQUAC
Homogeneous	Binary	73.50	0.3300	0.6700	-	Tanaka (1985)
Homogeneous	**Binary**	**73.50**	**0.3527**	**0.6473**	**-**	**This work**
		73.64	**0.3510**	**0.6490**	**-**	**This work**
		73.55	**0.3487**	**0.6513**	**-**	**This work**
Heterogeneous	Saddle	73.68	0.3505	0.6495	-	NRTL
Homogeneous	Saddle	73.64	0.3076	0.6924	-	UNIFAC
Heterogeneous	Saddle	73.47	0.3466	0.6534	-	UNIQUAC

Table 7-4: ***Comparison of experimentally determined azeotropic compositions with compositions from literature and thermodynamic models for the n-propanol/MEK/water system at 101.3 kPa.***

Azeotrope:	**Classification:**	**Temperature (°C):**	y_{Water}	y_{MEK}	$Y_{n\text{-}Propanol}$	**Reference/Model:**
Homogeneous	Binary	87.72	0.5684	-	0.4316	Gmehling et al. (1994)
Homogeneous	Saddle	87.67	0.5972	-	0.4028	NRTL
Homogeneous	Saddle	88.16	0.5774	-	0.4226	UNIFAC
Homogeneous	Saddle	87.70	0.5931	-	0.4069	UNIQUAC
Homogeneous	Binary	73.50	0.3300	0.6700	-	Tanaka (1985)
Homogeneous	**Binary**	**73.60**	**0.3518**	**0.6482**	**-**	**This work**
		73.62	**0.3510**	**0.6490**	**-**	**This work**
		73.59	**0.3537**	**0.6463**	**-**	**This work**
Homogeneous	Saddle	73.65	0.3644	0.6356	-	NRTL
Homogeneous	Saddle	73.64	0.3076	0.6924	-	UNIFAC
Homogeneous	Saddle	73.47	0.3649	0.6351	-	UNIQUAC

As mentioned in section 7.2.2, no azeotrope exists between MEK and n-propanol. This is reflected, along with experimentally determined azeotropic compositions and literature azeotropic compositions, in Table 7-3.

It is known that only small deviations from Raoult's law are necessary for an azeotrope to exist and that the larger the difference in boiling points, of the two compounds, the more non-ideal and consequently less likely that an azeotrope will be present. Considering the boiling points of ethanol (78.37°C), n-propanol (97.22°C), iso-propanol (82.5°C) and MEK (79.64°C) the reason for the absence of the n-propanol/MEK azeotrope can be deduced.

Table 7-4 lists the experimentally determined azeotropic compositions, literature values as well as modelled data using thermodynamic models (NRTL, UNIFAC and UNIQUAC) for the IPA/MEK/water system. All three of the mentioned thermodynamic models predict the existence of a homogeneous ternary azeotrope within the temperature range of 73.37-73.63°C. In other words, the ternary azeotrope lies outside of the liquid-liquid phase region. However, the thermodynamic models fail to accurately predict the binary water/IPA azeotrope. While a homogeneous ternary azeotrope in all likelihood does exist, the composition and temperature predicted by the thermodynamic models are questionable due to their inaccurate prediction of the IPA/water azeotrope. As mentioned, further experimentation is beyond the scope of this work but is required to determine the exact composition and temperature location of the azeotrope.

As with the ethanol/MEK/water system, both the n-propanol/MEK/water and iso-propanol/MEK/water systems' experimentally determined water-MEK azeotropic compositions correlate well, with only slight deviations which are accommodated for by the inclusion of the associated error (±0.014 mole fraction).

Table 7-5: ***Comparison of experimentally determined azeotropic compositions with compositions from literature and thermodynamic models for the IPA/MEK/water system at 101.3 kPa.***

Azeotrope:	**Classification:**	**Temperature (°C):**	**y_{Water}**	**y_{MEK}**	**Y_{IPA}**	**Reference/Model:**
Homogeneous	Unstable Node	73.64	0.3036	0.6863	0.0101	NRTL
Homogeneous	Unstable Node	73.52	0.3338	0.5838	0.0824	UNIFAC
Heterogeneous	Unstable Node	73.37	0.3431	0.5992	0.0576	UNIQUAC
Homogeneous	Binary	87.59	0.5650	-	0.4350	Gmehling et al. (1994)
Homogeneous	Saddle	80.01	0.3064	-	0.6936	NRTL
Homogeneous	Saddle	80.18	0.3272	-	0.6728	UNIFAC
Homogeneous	Binary	79.57	0.3528	-	0.6472	UNIQUAC
Homogeneous	Binary	77.45	-	0.6650	0.3350	del Mar Olaya et al. (1964)
Homogeneous	Binary	77.50	-	0.6050	0.3950	Martinez et al. (2008)
Homogeneous	Saddle	75.98	-	0.6025	0.3975	NRTL
Homogeneous	Saddle	76.56	-	0.6324	0.3676	UNIFAC
Homogeneous	Saddle	76.50	-	0.6274	0.3726	UNIQUAC
Homogeneous	Binary	73.50	0.3300	0.6700	-	Tanaka (1985)
Homogeneous	**Binary**	**73.53**	**0.3524**	**0.6476**	**-**	**This work**
		73.60	**0.3539**	**0.6461**	**-**	**This work**
		73.55	**0.3531**	**0.6469**	**-**	**This work**
Homogeneous	Saddle	73.64	0.3076	0.6924	-	NRTL
Homogeneous	Saddle	73.65	0.3644	0.6356	-	UNIFAC
Heterogeneous	Saddle	73.47	0.3466	0.6534	-	UNIQUAC

The successful determination of the composition of the binary homogeneous azeotrope of the water/MEK azeotrope for each of the three systems, was used in the determination of alternative parameters for the NRTL, UNIQUAC and UNIFAC models to aid their ability in predicting ternary phase behaviour. This will, however, be discussed in the coming thermodynamic modelling section.

7.2.5 Entrainer Comparison

For comparative purposes, the data measured in this work is compared with the five entrainers considered in Section 5.1.2: cyclohexane, hexane, heptane, isooctane and DIPE. Benzene has been omitted due to its carcinogenic nature and disuse in industry.

The data discussed in the mentioned section has been plotted in Figures 7-11 to 7-13. As can be seen from these figures, the absence of a ternary heterogeneous azeotrope limits the use of heterogeneous azeotropic distillation as a separation technique. The figures also include the liquid-liquid tie-line on which the ternary heterogeneous azeotrope can be found, where applicable.

Due to the fact that the distillate from a heterogeneous distillation column has a composition close to that of the ternary heterogeneous azeotrope (if present), the aqueous phase composition of that point can be directly related to the amount of water removed from the decanter. In other words, the higher the water content of the aqueous phase at the heterogeneous azeotropic point, the more efficient the separation process becomes.

In Figure 7-10 and Figure 7-11, it can be seen that cyclohexane should be the entrainer of choice for the dehydration of ethanol due to its large water content. Figure 7-12 suggests that isooctane is a suitable entrainer for the dehydration of n-propanol and IPA.

Unfortunately, none of the alcohol/MEK/water systems exhibit a ternary heterogeneous azeotrope and MEK is therefore not considered to be a suitable entrainer for the dehydration of C_2- and C_3-alcohols using heterogeneous azeotropic distillation. However, NRTL, UNIFAC and UNIQUAC all predict a ternary homogeneous azeotrope for the systems ethanol/MEK/water and IPA/MEK/water. These two alcohols could therefore possibly be dehydrated using homogeneous azeotropic distillation and MEK as entrainer.

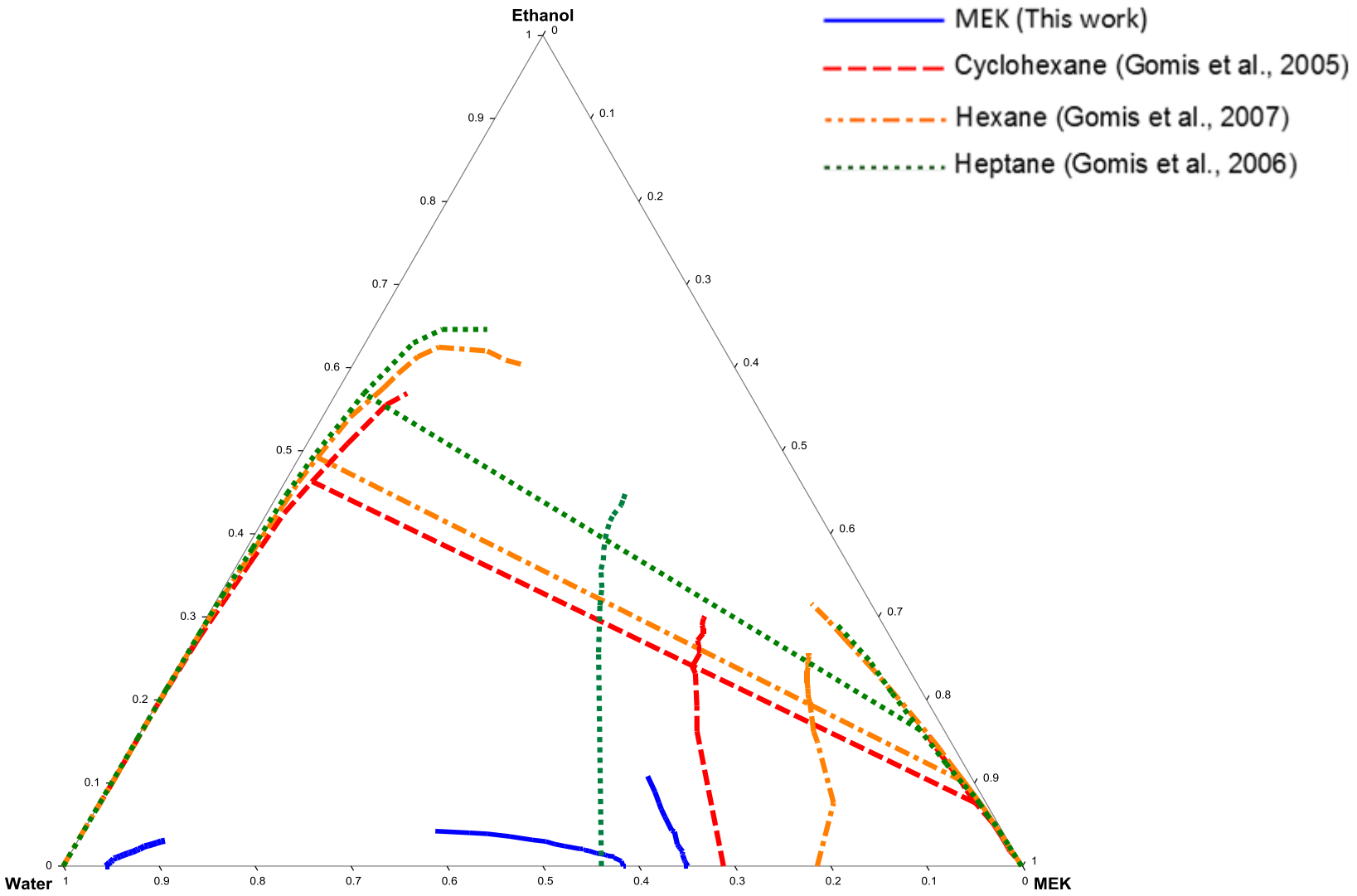

Figure 7-11: ***Entrainer comparison for Ethanol dehydration using heterogeneous azeotropic distillation at 101.3 kPa.***

The erratic lines are indicative of experimental data being plotted and not thermodynamic models. Lines were used to illustrate the size and shape of the phase behaviour.

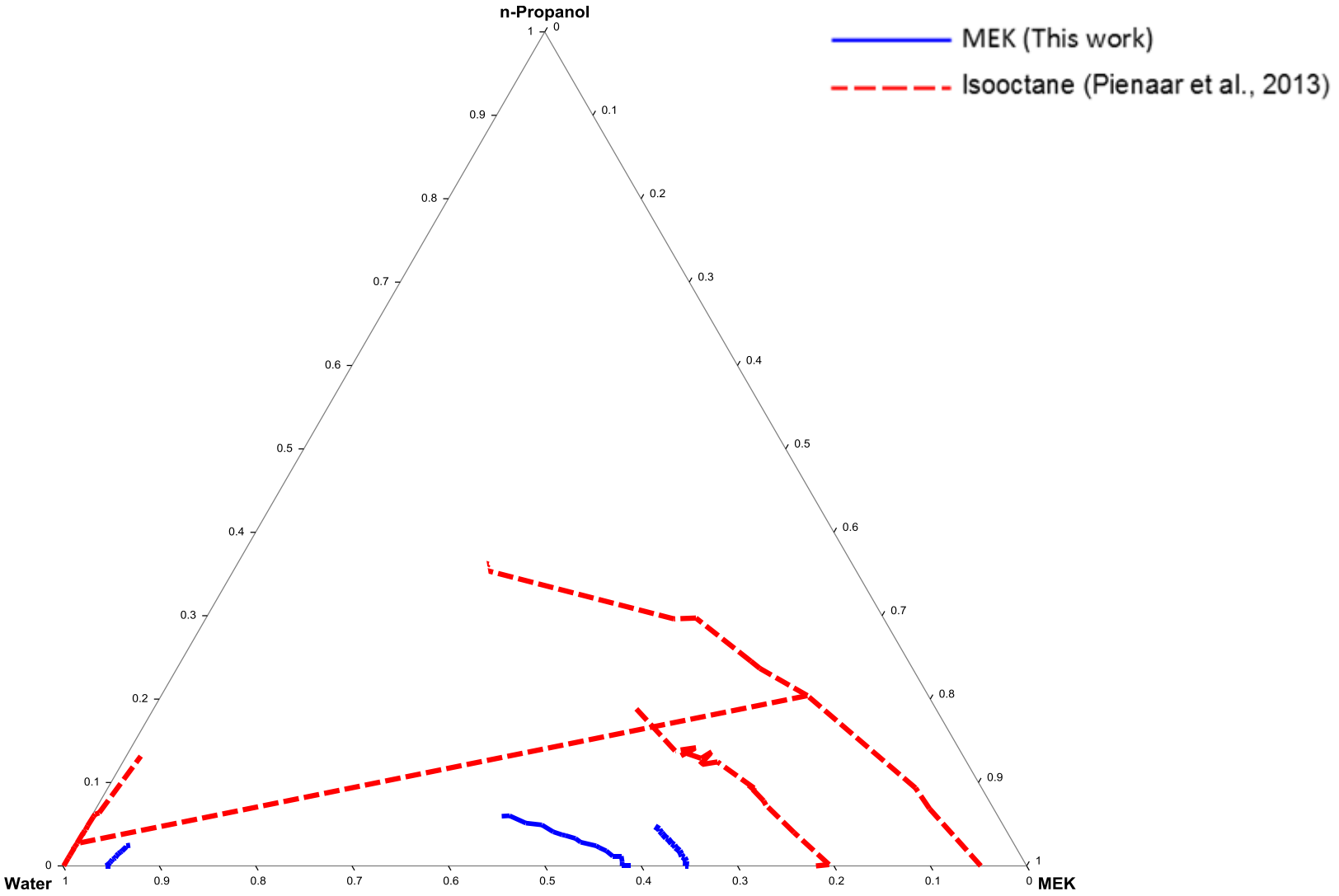

Figure 7-12: ***Entrainer comparison for n-Propanol dehydration using heterogeneous azeotropic distillation at 101.3 kPa.***

The erratic lines are indicative of experimental data being plotted and not thermodynamic models. Lines were used to illustrate the size and shape of the phase behaviour.

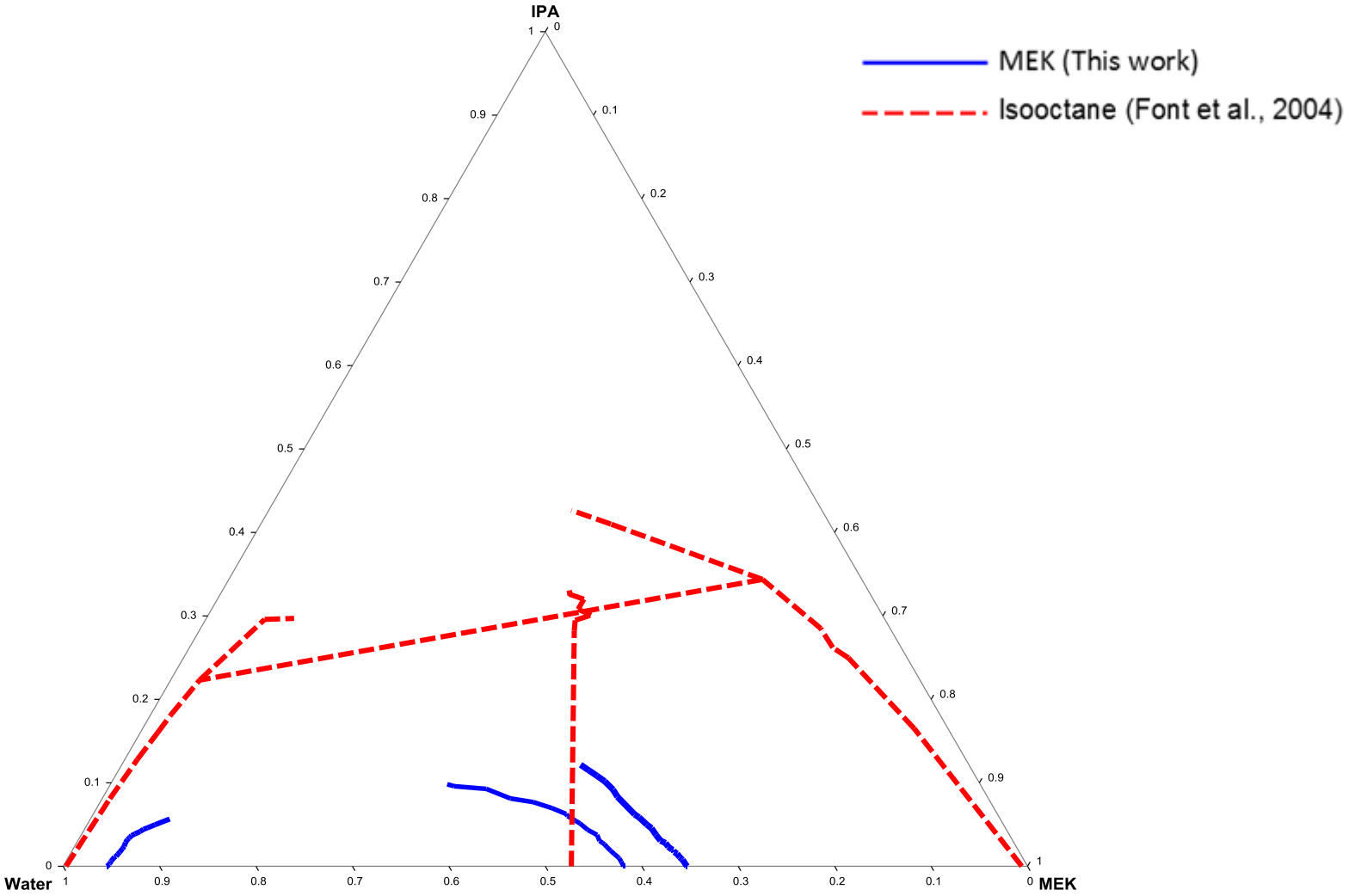

Figure 7-13: ***Entrainer comparison for IPA dehydration using heterogeneous azeotropic distillation at 101.3 kPa.***

The erratic lines are indicative of experimental data being plotted and not thermodynamic models. Lines were used to illustrate the size and shape of the phase behaviour.

7.2.6 Results Summary

For the three systems for which new phase equilibrium data were measured (ethanol/MEK/water, n-propanol/MEK/water and IPA/MEK/water), the detailed data can be found tabulated in Appendix E and the results of the L/W consistency test as well as the McDermott-Ellis consistency test can be found in Appendix F. The graphical results of the Othmer-Tobias correlations can be seen in Appendix G. The vapour phase compositions, for each of the three systems, were outside the liquid-liquid phase envelope and the absence of heterogeneous azeotropes was established. The possibility of a ternary homogeneous azeotrope was noted for the ethanol/MEK/water and IPA/MEK/water system and the prospect of ethanol and IPA dehydration using MEK as entrainer for homogeneous azeotropic distillation was established.

7.3 Thermodynamic Modelling

One of the aims of this research work is to compare experimental phase equilibria data with data simulated using thermodynamic models. The thermodynamic models NRTL, UNIFAC and UNIQUAC were chosen for their known ability to model polar, non-electrolytic phase equilibria data at low pressures. Data simulation was achieved through the use of Aspen Plus® using the built-in default Aspen Plus® parameters. The built-in parameters are tabulated in Appendix H.

Comparison between experimental data and simulated data is accomplished by plotting the data sets onto a ternary diagram as well as the calculation of the average absolute deviation (AAD) values and the average absolute relative deviation (AARD%) values. These values statistically quantify the ability of the models to model the experimental data:

$$AAD = \frac{1}{N_T}\sum_{i=1}^{N_T}\left|x_{i,calculated} - x_{i,measured}\right| \qquad [7.1]$$

$$AARD\% = \frac{100}{N_T}\sum_{i=1}^{N_T}\left|\frac{x_{i,calculated} - x_{i,measured}}{x_{i,measured}}\right| \qquad [7.1]$$

Where N_T is the total number of experimental runs performed. Example calculations can be found can be seen in Appendix J. Detailed tables of AAD and AARD% values can be found in Appendix K.

The AAD and AARD% values are also calculated and tabulated for all binary azeotropes measured and reported in the following sections.

7.3.1 Ethanol/MEK/Water

The ternary phase diagram comparing experimental data and simulated data can be seen in Figure 7-16. Firstly, considering the azeotropes of the ethanol/MEK/water system at 101.3 kPa (see Table 7-6) the thermodynamic models predict a ternary homogeneous azeotrope (not found with experimental data and can therefore not be compared) and three, homogeneous binary azeotropes.

Table 7-6: ***Comparison of experimental azeotropes with model predictions for the ethanol/MEK/water system.***

Source	Temperature (°C)	AAD	AARD%	y_{Water}	y_{MEK}	y_{EthOH}	AAD	AARD%
This work	**78.15**			**0.105**	**-**	**0.895**		
NRTL	78.15	0.000	0.19	0.105	-	0.895	0.000	0.213
UNIFAC	78.04	0.110	1.62	0.107	-	0.893	0.003	1.809
UNIQUAC	78.16	0.010	4.67	0.100	-	0.900	0.010	5.214
This work	**73.50**			**0.353**	**0.647**	**-**		
This work	**73.64**			**0.351**	**0.649**	**-**		
This work	**73.55**			**0.349**	**0.651**	**-**		
NRTL	73.68	0.117	0.43	0.351	0.650	-	0.003	0.65
UNIFAC	73.64	0.077	12.31	0.308	0.692	-	0.086	18.97
UNIQUAC	73.47	0.093	1.19	0.347	0.653	-	0.008	1.84

From the AAD and AARD% values it can be seen that the UNIFAC model gives the worst prediction for the water/MEK azeotrope (0.086 and 18.97%) and the NRTL model the best correlative prediction for both the water/ethanol (0.000 and 0.213%) and water/MEK azeotrope (0.003 and 0.659%). Overall, it can be deduced, from the relatively low AAD and AARD% values that the thermodynamic models (NRTL, UNIQUAC and UNIFAC to a lesser extent) predict the binary azeotropes present in the ethanol/water/MEK system well.

In order to compare the capability of the models' ability to predict the overall phase behaviour, both visual (Figure 7-16) and statistical methods (AAD and AARD% values) were used. Figure 7-14 shows the AAD values and Figure 7-15 the AARD% values calculated for the ethanol/MEK/water system. From Figure 7-14, it can be seen that the UNIFAC model best predicts the phase envelope but fails to predict the vapour phase compositions. This fact is reflected in the the AAD and AARD% values; with the the lowest AARD% values (1.24% and 2.50% for organic and aqueous compositions, respectively) and the highest AARD% value (13.62%) calculated for vapour phase compositions. Owing to the fact that the NRTL model best fits the experimental vapour phase compositions, deduced from visual and statistical inspection, the model was subsequently used for error analysis in Section 6.4.

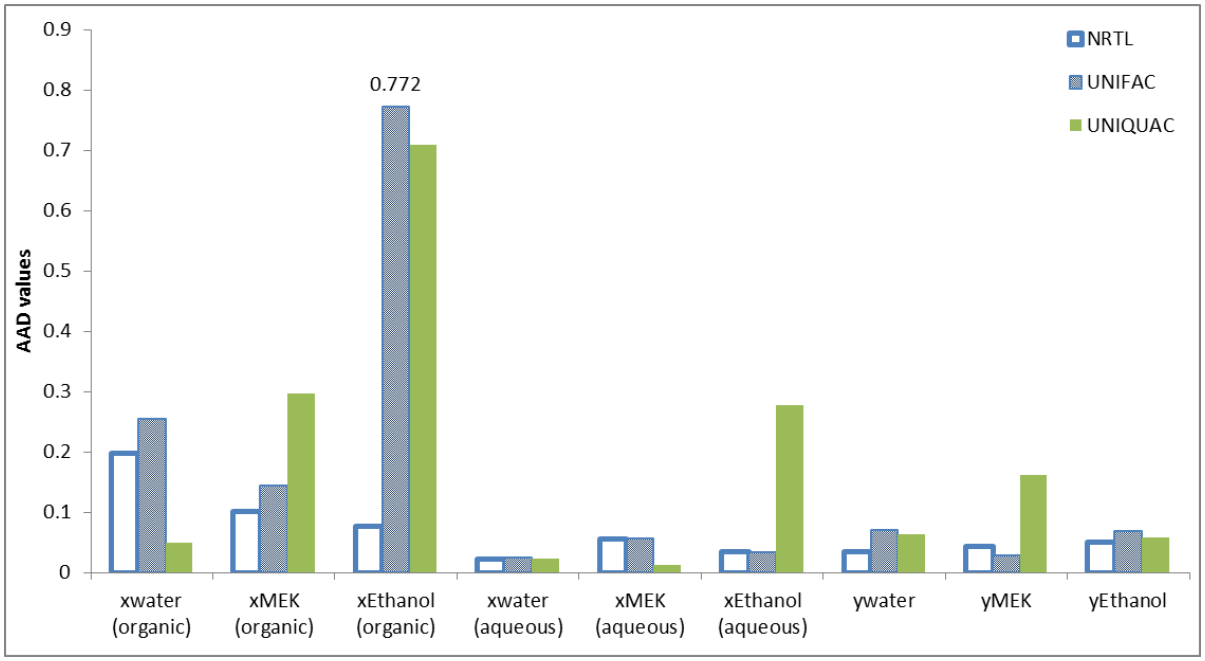

Figure 7-14: ***AAD values for ethanol/MEK/water system at 101.3 kPa when compared to NRTL, UNIFAC and UNIQUAC simulated data.***

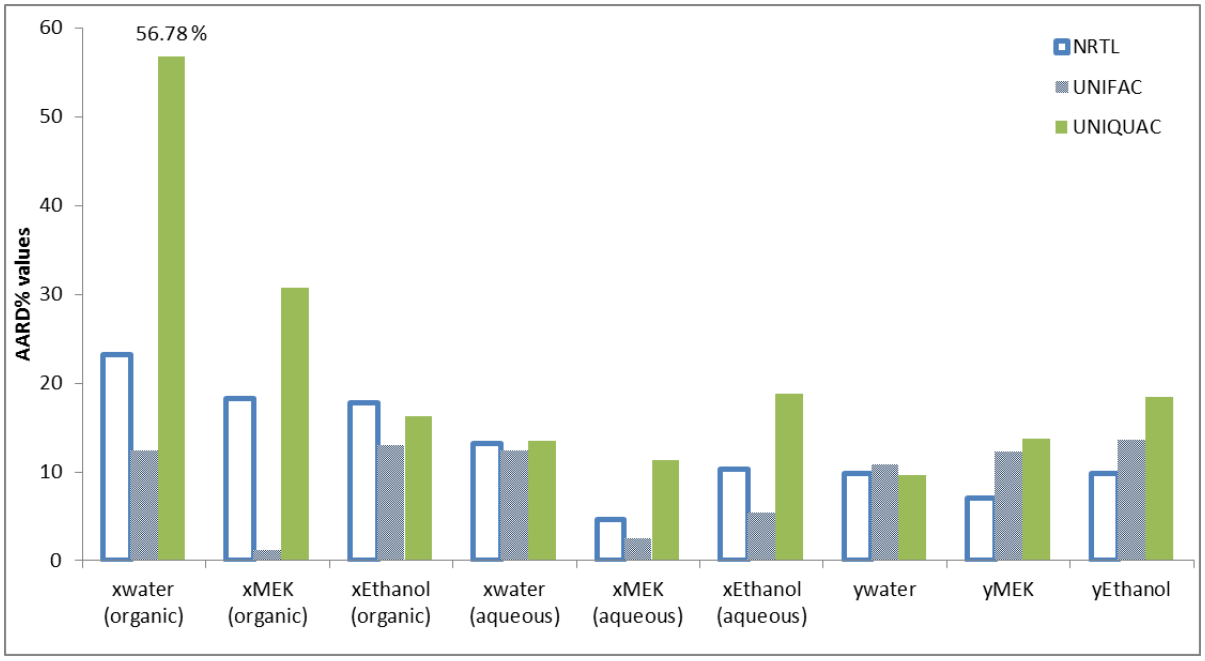

Figure 7-15: ***AARD% values for ethanol/MEK/water system at 101.3 kPa when compared to NRTL, UNIFAC and UNIQUAC simulated data.***

The error associated in the predictions shows the inability of the models to predict the binary MEK/water phase information. For this reason, the model will be refit to incorporate accurate binary MEK/water phase information.

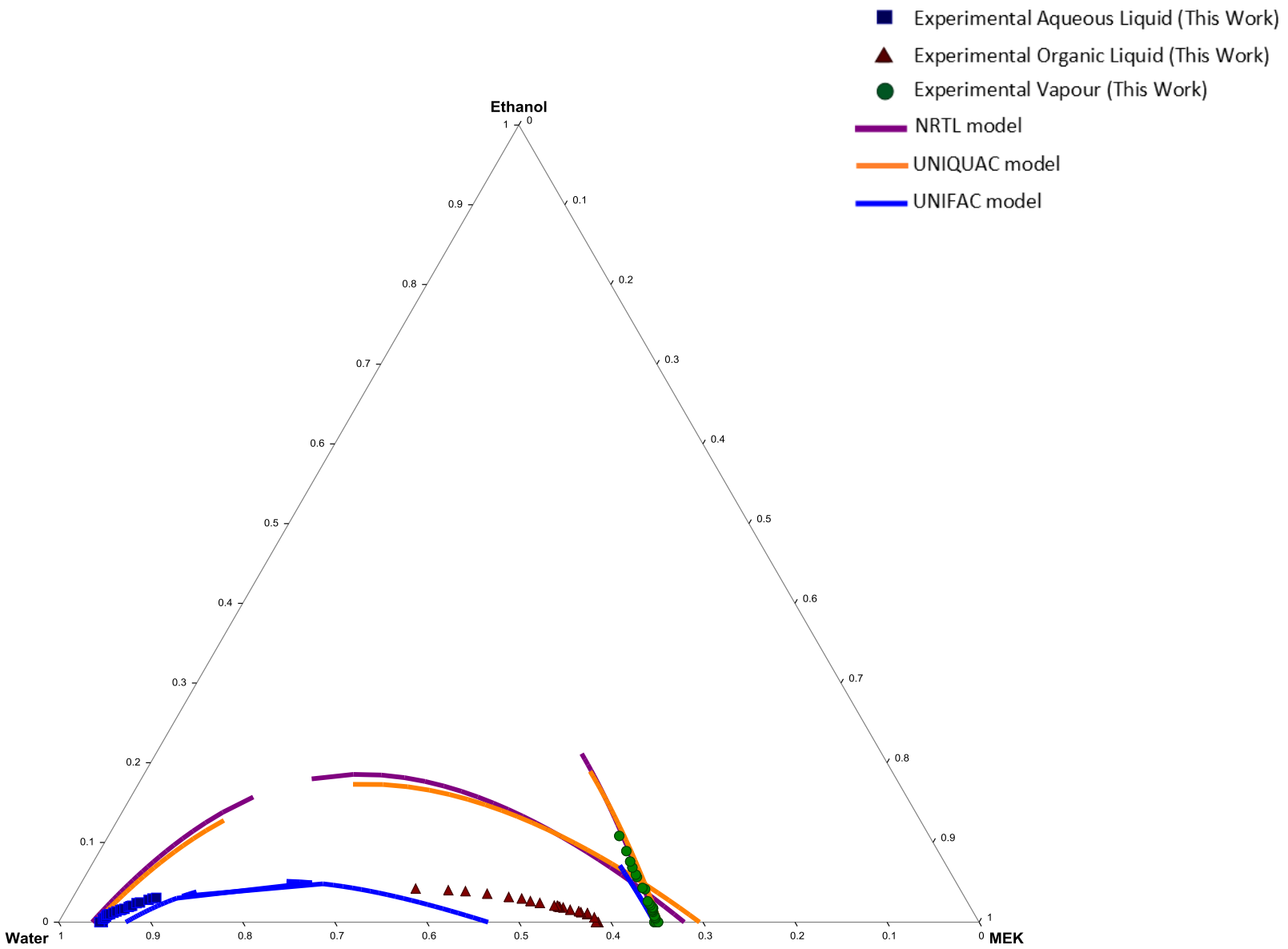

Figure 7-16: ***Ternary phase diagram for experimental ethanol/MEK/water results and thermodynamic model (NRTL, UNIFAC and UNIQUAC) predictions at 101.3 kPa.***

7.3.2 n-Propanol/MEK/Water

The ternary phase diagram comparing experimental data and simulated data can be seen in Figure 7-19. Owing to the fact that the water/MEK binary azeotrope was the only azeotrope measured experimentally for the n-propanol/MEK/water system, calculation of AAD and AARD% values will be limited to this single binary azeotrope (see Table 7-7). From this it could be seen that the UNIFAC model was the unable to accurately predict the composition of the water/MEK azeotrope (AARD value of 19.53%), where the NRTL and UNIQUAC models were able to model both the temperature and the composition of the binary azeotrope relatively well (with AARD% values of less than 6%).

Table 7-7: ***Comparison of experimental azeotropes with model predictions for the n-propanol/MEK/water system.***

Source	Temperature (°C)	AAD	AARD%	y_{Water}	y_{MEK}	$y_{n\text{-}Propanol}$	AAD	AARD%
This work	**73.60**			**0.3518**	**0.6482**	**-**		
This work	**73.62**			**0.3510**	**0.6490**	**-**		
This work	**73.59**			**0.3537**	**0.6463**	**-**		
NRTL	73.65	0.047	3.48	0.3644	0.6356	-	0.026	5.36
UNIFAC	73.64	0.037	12.65	0.3076	0.6924	-	0.089	19.53
UNIQUAC	73.47	0.133	3.62	0.3649	0.6351	-	0.025	5.58

Visually, there is no apparent correlation between the experimental equilibria phase's data and the data modelled using the thermodynamic models and built-in Aspen Plus® parameters (see Figure 7-19). Both the NRTL and UNIQUAC models fail to predict the liquid de-mixing that occurs at higher n-propanol concentrations. The UNIFAC model, on the other hand, is able to predict the shape of the liquid-liquid region. Due to the UNIFAC models' inability to model the binary water/MEK behaviour correctly, it is proposed that, if the binary data had to be refit, the UNIFAC model would be able to model the entire phase behaviour of the n-propanol/MEK/water system at 101.3 kPa. This is due to the fact that the UNIFAC model is also able to predict the vapour phase compositions determined experimentally.

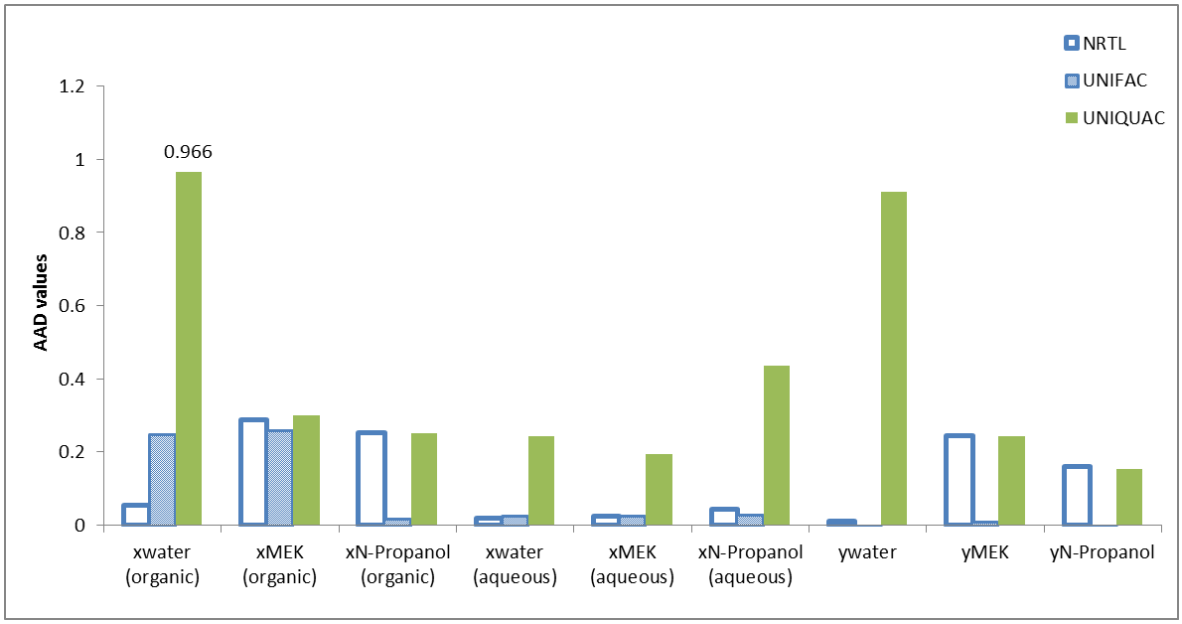

Figure 7-17: ***AAD values for n-propanol/MEK/water system at 101.3 kPa when compared to NRTL, UNIFAC and UNIQUAC simulated data.***

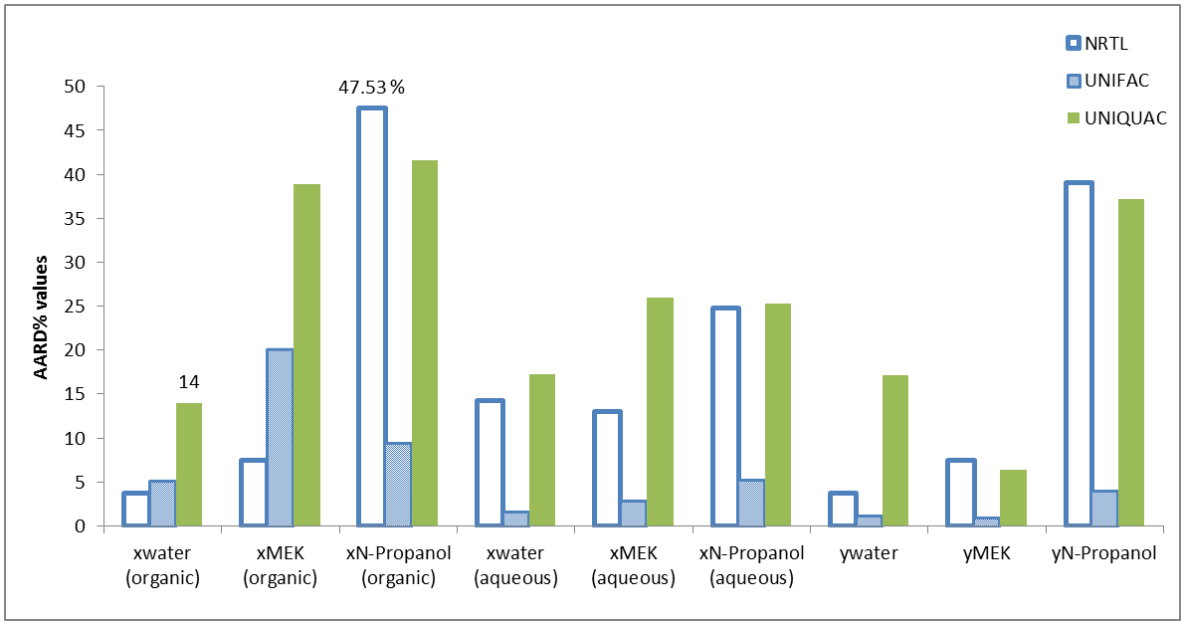

Figure 7-18: ***AARD% values for n-propanol/MEK/water system at 101.3 kPa when compared to NRTL, UNIFAC and UNIQUAC simulated data.***

These findings are reflected in the AAD and AARD% values calculated for the n-propanol/MEK/water system (Figure 7-17 and Figure 7-18, respectively). With the lowest overall AAD and AARD% found for the UNIFAC model, specifically for the UNIFAC vapour phase compositions, it can be said that the UNIFAC model best predicts the overall phase behaviour of the n-propanol/MEK/water system.

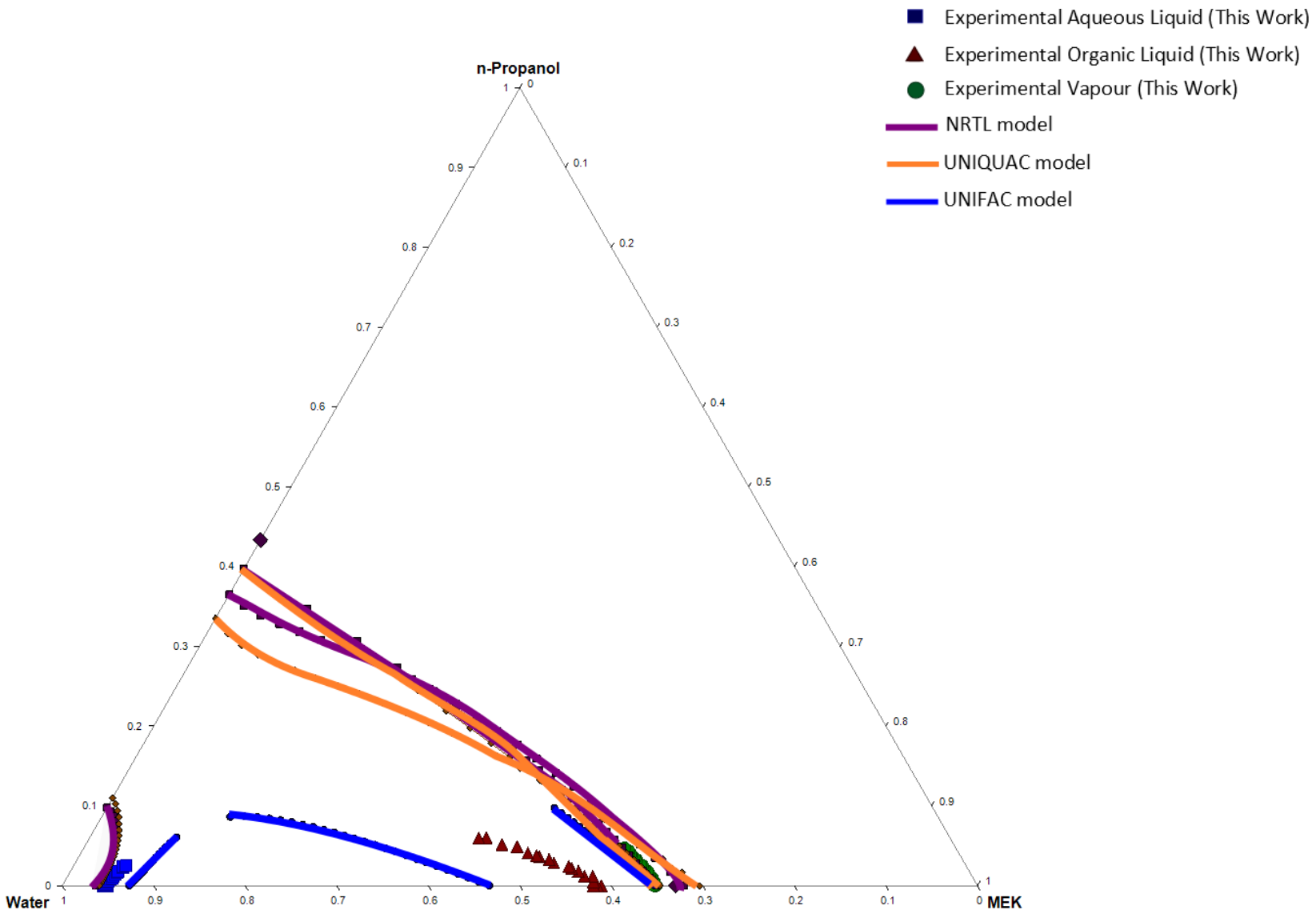

Figure 7-19: ***Ternary phase diagram for experimental n-propanol/MEK/water results and thermodynamic model (NRTL, UNIFAC and UNIQUAC) predictions at 101.3 kPa.***

7.3.3 IPA/MEK/Water

It was shown that the NRTL, UNIFAC and UNIQUAC models all predict the presence of a ternary azeotrope. The NRTL and UNIFAC model predicts that a ternary homogeneous azeotrope exists for the IPA/MEK/water system, where as the UNIQUAC model predict the presence of a ternary heterogeneous azeotrope exists at 101.3 kPa at 73.37°C. This is, however, not the case as proven by the experimental results generated for this work. The inability of UNIQUAC to accurately predict phase equilibrium data for this system is further proven when comparing the experimental data to the simulated data through visual analysis (Figure 7-22) and statistical analysis (Figure 7-20 and Figure 7-21). From the AAD and AARD% values it can be seen that the UNIQUAC model gives the worst prediction for the water/MEK azeotrope (with the highest AARD% value of 50.01%).

Table 7-8: ***Comparison of experimental azeotropes with model predictions for the IPA/MEK/water system.***

Source	Temperature (°C)	AAD	AARD%	y_{Water}	y_{MEK}	y_{IPA}	AAD	AARD%
This work	**73.53**			**0.3524**	**0.6476**	**-**		
This work	**73.60**			**0.3539**	**0.6461**	**-**		
This work	**73.55**			**0.3531**	**0.6469**	**-**		
NRTL	73.64	0.0800	12.893	0.3076	0.6924	-	0.0911	19.933
UNIFAC	73.65	0.0900	3.1908	0.3644	0.6356	-	0.0225	4.9324
UNIQUAC	73.47	0.0900	1.8498	0.3466	0.6534	-	0.0130	2.8598

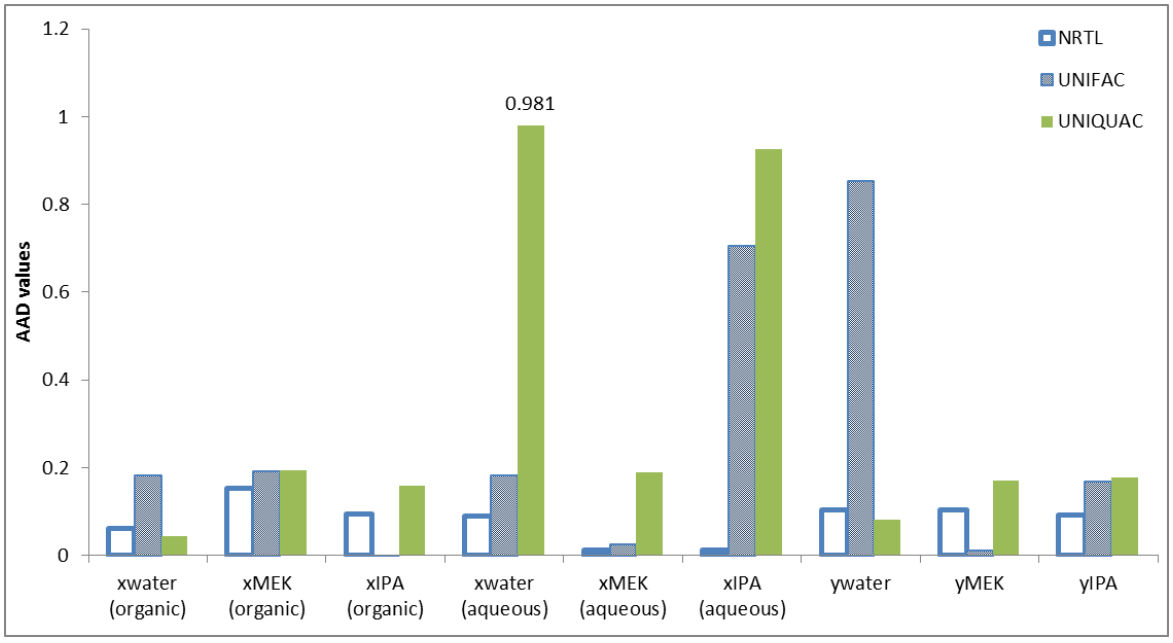

Figure 7-20: ***AAD values for IPA/MEK/water system at 101.3 kPa when compared to NRTL, UNIFAC and UNIQUAC simulated data.***

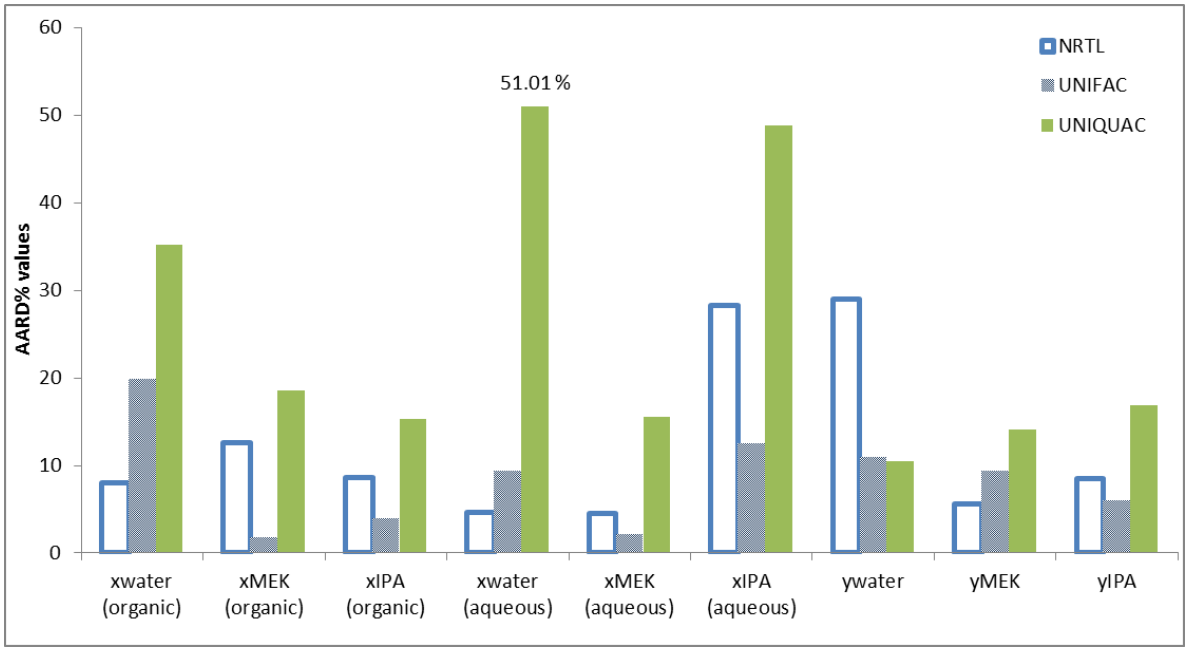

Figure 7-21: ***AARD% values for IPA/MEK/water system at 101.3 kPa when compared to NRTL, UNIFAC and UNIQUAC simulated data.***

The NRTL model fails to predict the vapour phase compositions but is able to best predict the liquid-liquid behaviour of the IPA/MEK/water system. This is reflected in the relatively low AAD and AARD% values calculated for the organic- and aqueous-liquid phase compositions.

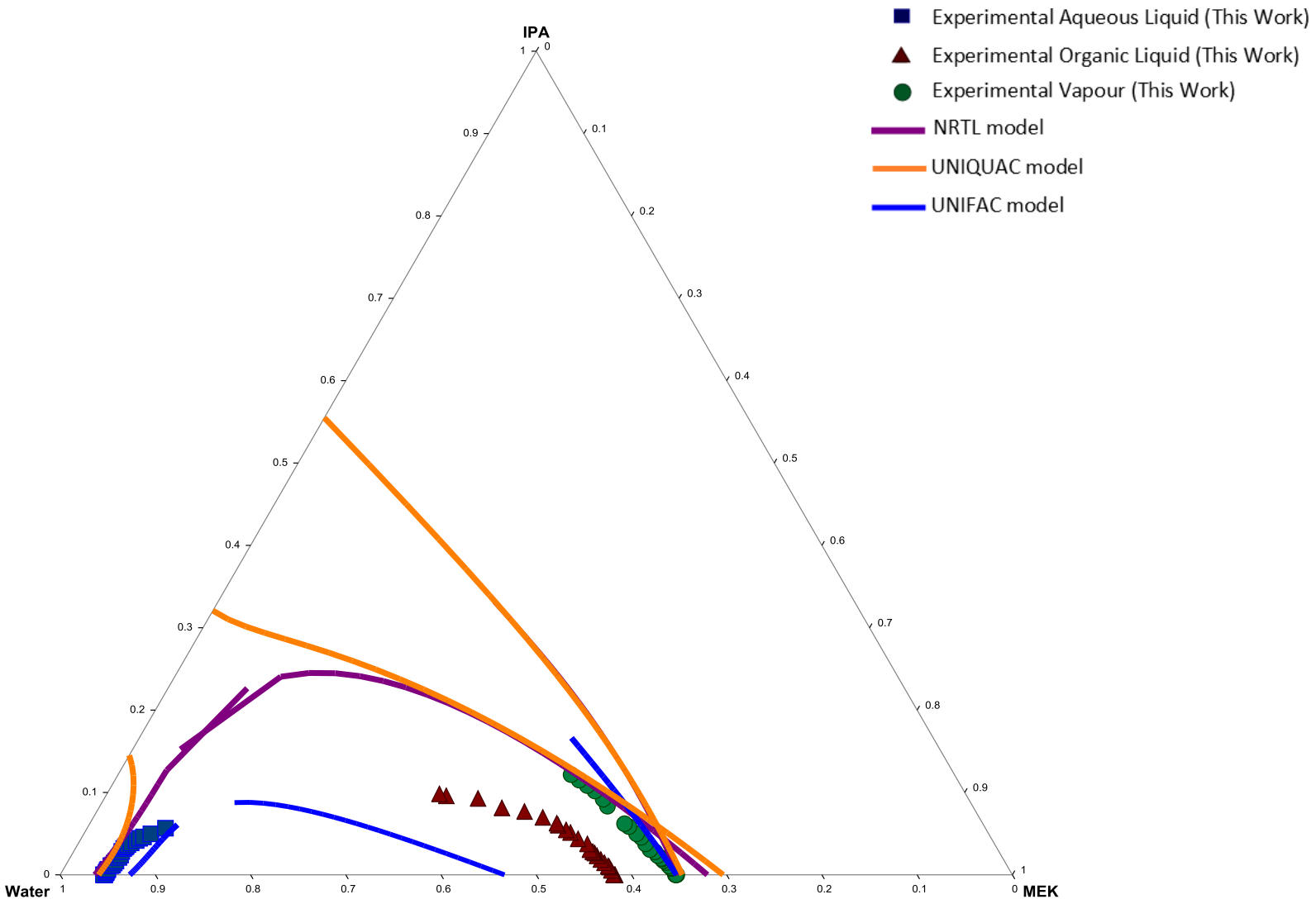

Figure 7-22: ***Ternary phase diagram for experimental IPA/MEK/water results and thermodynamic model (NRTL, UNIFAC and UNIQUAC) predictions at 101.3 kPa.***

7.4 Using Regressed Parameters for Comparison

As discussed in section 7.4, the models do not seem to accurately predict the binary phase behaviour of water/MEK. Using the Aspen Plus® Data Regression System (DRS) to regress new binary parameters the models were refit. The parameters were taken from those calculated by Pienaar et al. (2013), who used weighted data obtained from literature. The weights were varied to obtain parameters that would improve the fit of the model predictions on the data. These obtained parameters can be found listed in Appendix H. The results can be seen in Figure 7-17 to 7-20. To try and explain the liquid-liquid demixing present for the n-propanol/MEK/water and IPA/MEK/water systems, regressed parameters for the n-propanol/water and IPA/water systems published by this research group was used.

7.4.1 Ethanol/MEK/water

Through data regression, it can be seen that the liquid-liquid region is now modelled quiet well by all three thermodynamic models. It can be noticed, graphically (Figure 7-29) and from the calculated AAD and AARD% values (Figure 7-23 and Figure 7-24 respectively), that the aqueous liquid phase correlates well with that modelled by the by the UNIFAC model with regressed water/MEK parameters.

The highest AAD and AARD% value has gone from 0.772 to 0.409 and 56.78% to 30.78%, respectively.

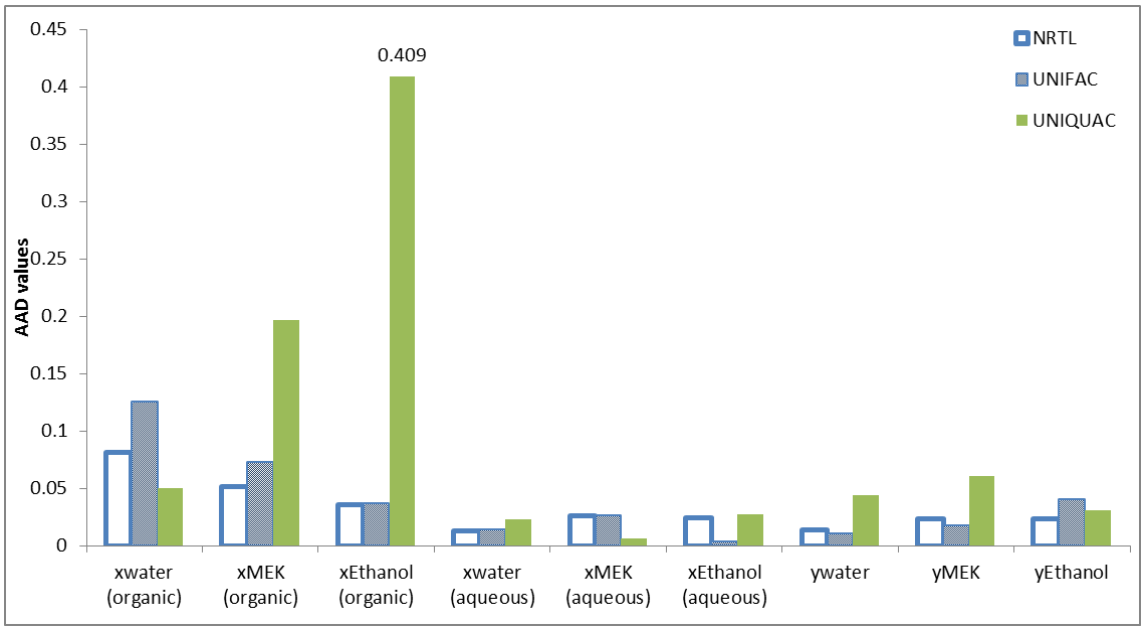

Figure 7-23: ***AAD values for ethanol/MEK/water system at 101.3 kPa when compared to NRTL, UNIFAC and UNIQUAC simulated data using regressed parameters.***

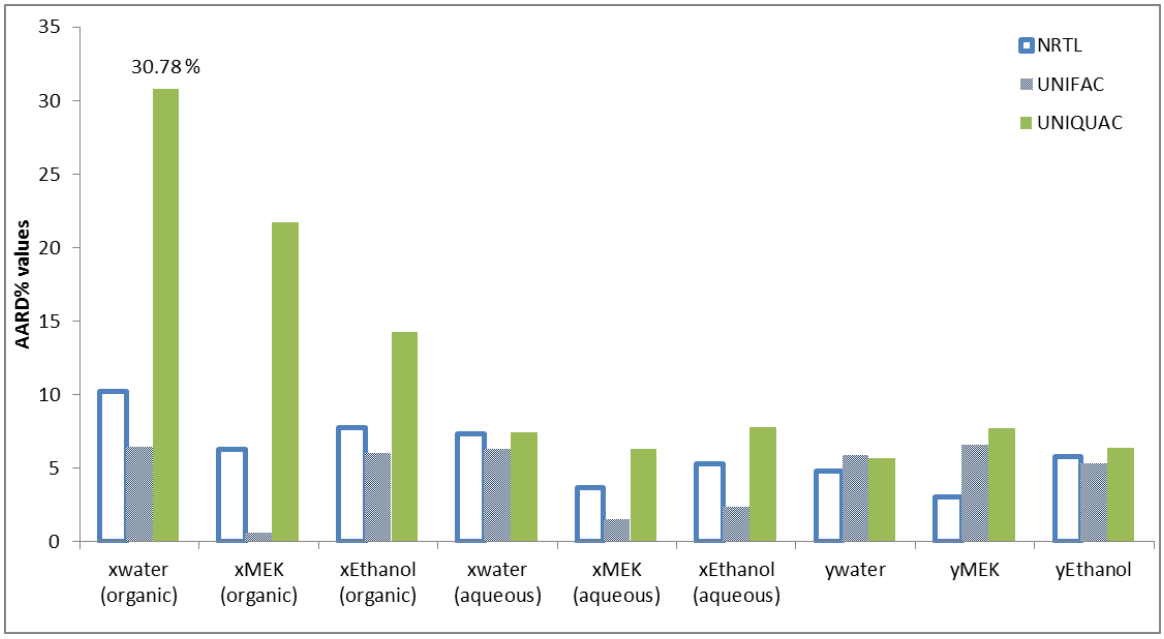

Figure 7-24: ***AARD% values for ethanol/MEK/water system at 101.3 kPa when compared to NRTL, UNIFAC and UNIQUAC simulated data using regressed parameters.***

7.4.2 n-Propanol/MEK/water

By refitting the n-propanol/water and water/MEK binary parameters for all three models, has drastically changed the way they model the ternary phase behaviour. The NRTL model is now able to accurately model the liquid-liquid demixing (see Figure 7-30). However the UNIQUAC model still fails to accurately predict the liquid-liquid region as well as the vapour phase compositions.

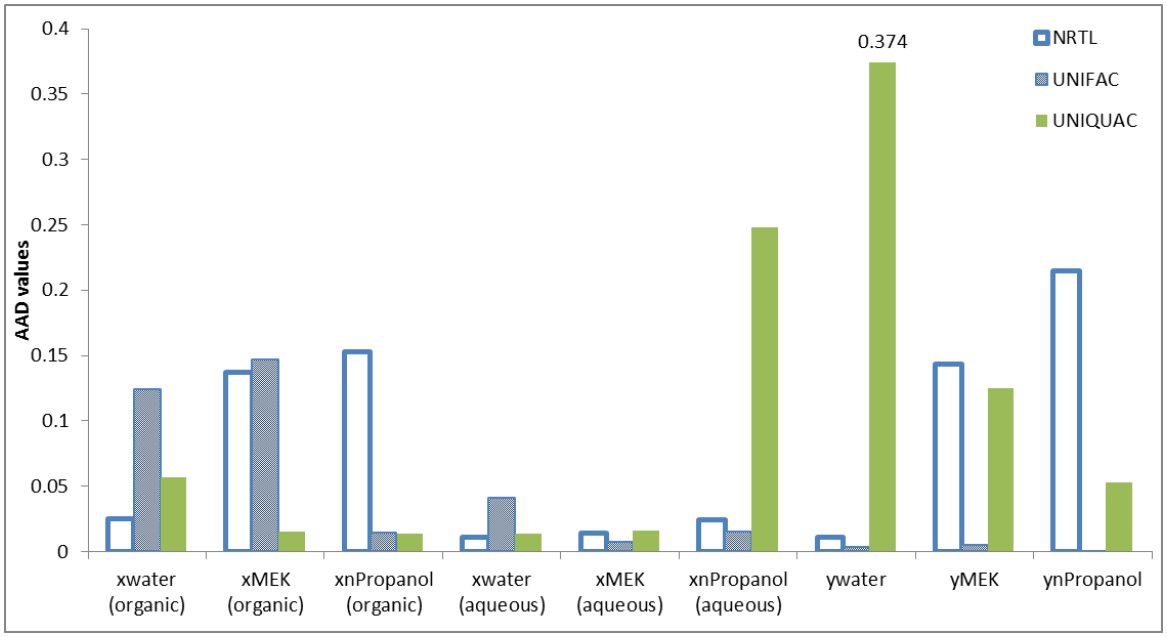

Figure 7-25: ***AAD values for n-propanol/MEK/water system at 101.3 kPa when compared to NRTL, UNIFAC and UNIQUAC simulated data using regressed parameters.***

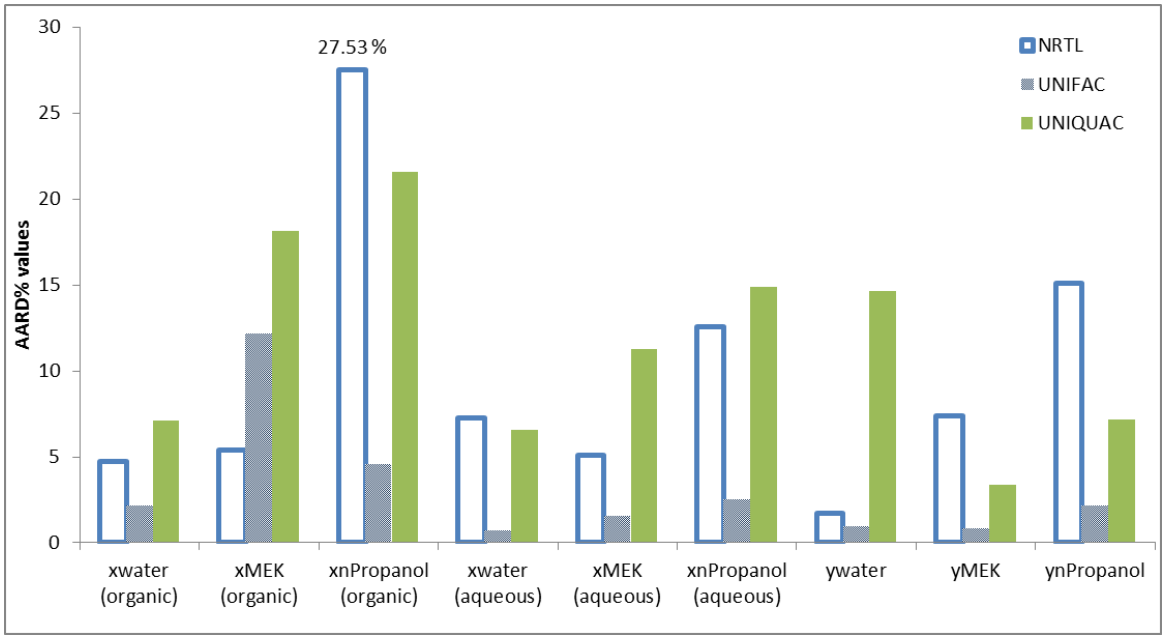

Figure 7-26: ***AARD% values for n-propanol/MEK/water system at 101.3 kPa when compared to NRTL, UNIFAC and UNIQUAC simulated data using regressed parameters.***

7.4.3 IPA/MEK/water

Like with the n-propanol/MEK/water system, refitting the binary parameters for IPA/MEK and water/MEK has increased the ability of the three models to predict the ternary IPA/MEK/water phase behaviour (Figure 7-19). Still, the UNIQUAC model is unable to accurately predict the liquid-liquid demixing that occurs in the real system.

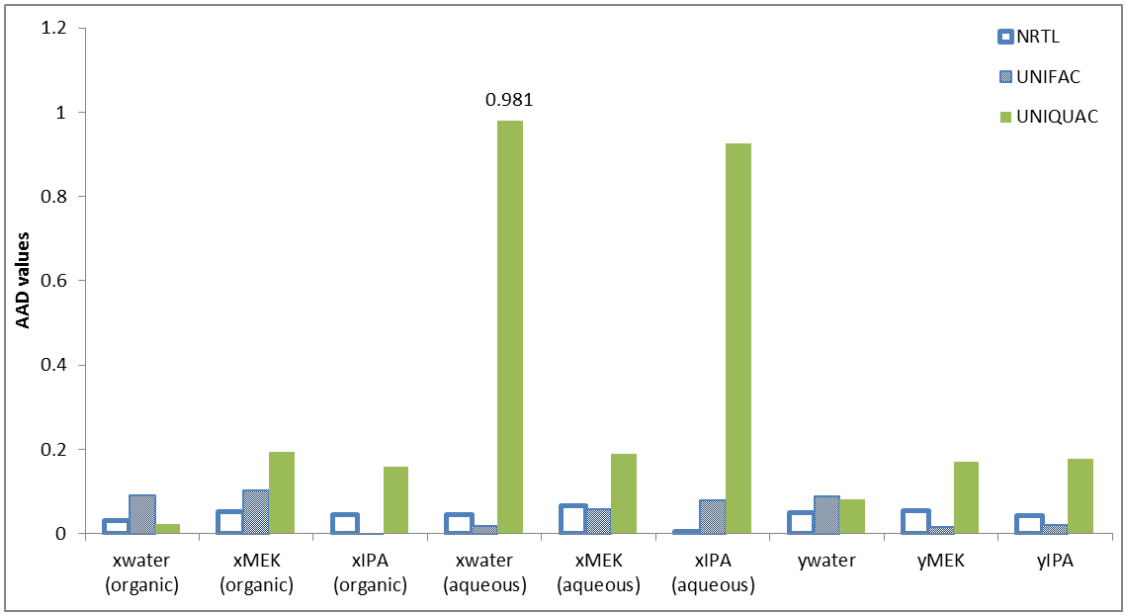

Figure 7-27: ***AAD values for IPA/MEK/water system at 101.3 kPa when compared to NRTL, UNIFAC and UNIQUAC simulated data using regressed parameters.***

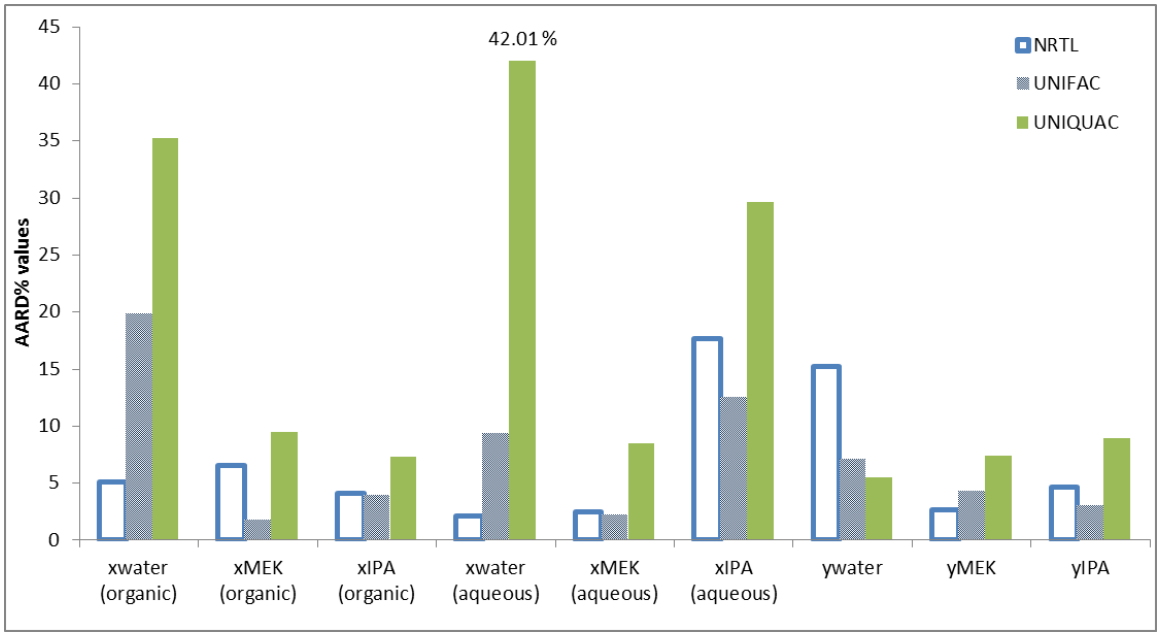

Figure 7-28: ***AARD% values for IPA/MEK/water system at 101.3 kPa when compared to NRTL, UNIFAC and UNIQUAC simulated data using regressed parameters.***

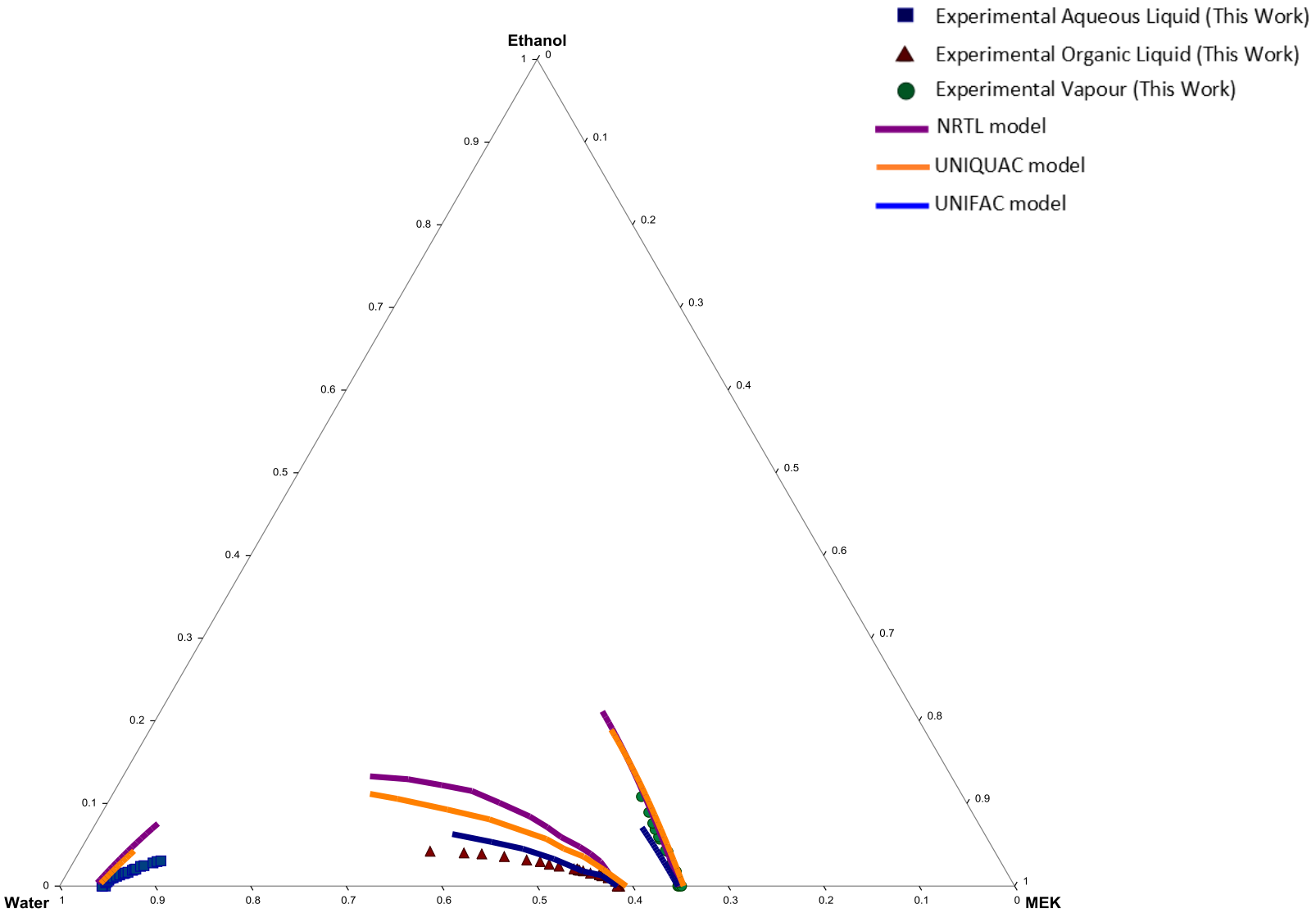

Figure 7-29: ***Ternary phase diagram for experimental ethanol/MEK/water results and thermodynamic model (NRTL, UNIFAC and UNIQUAC) predictions using regressed parameters at 101.3 kPa.***

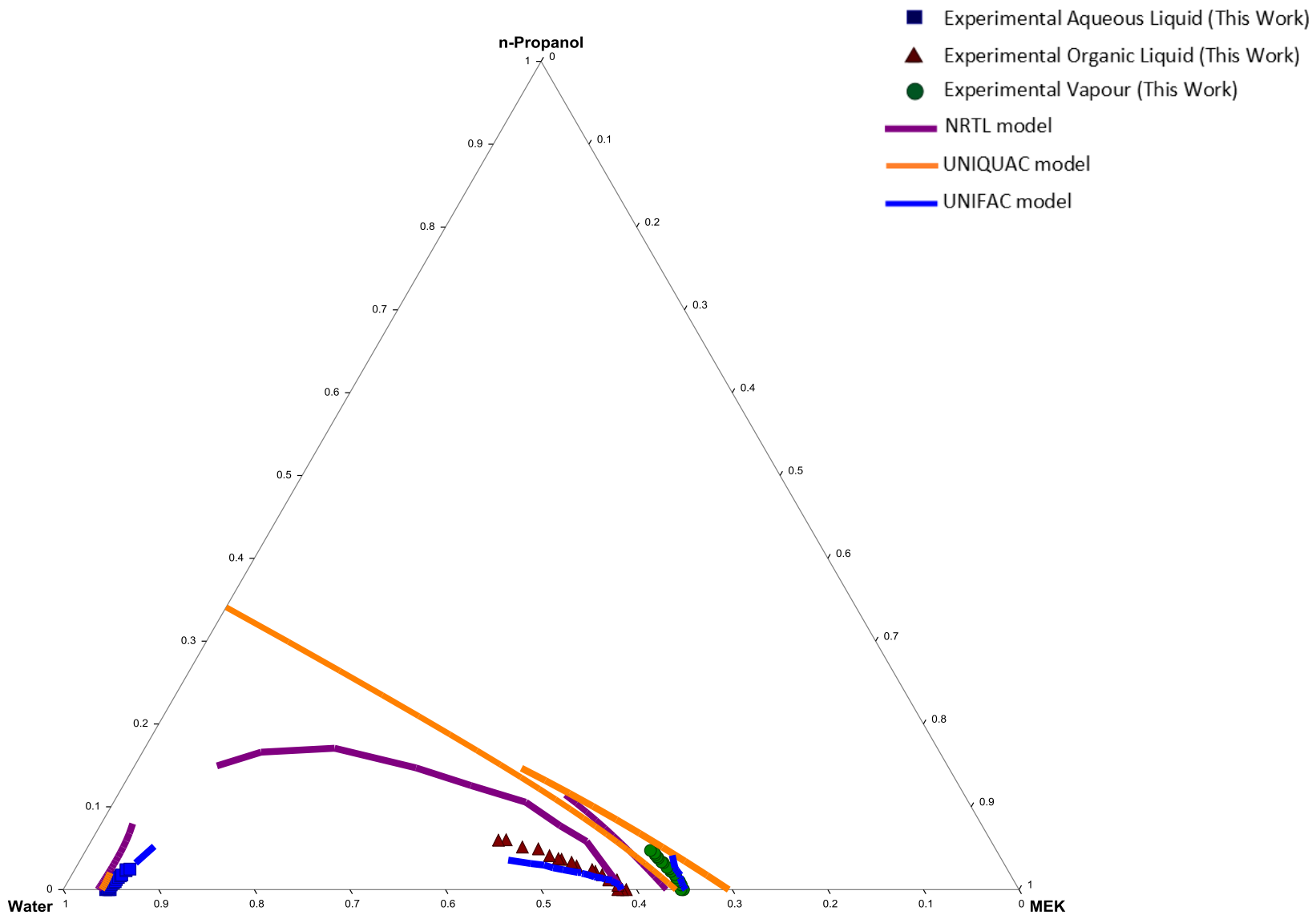

Figure 7-30: ***Ternary phase diagram for experimental n-propanol/MEK/water results and thermodynamic model (NRTL, UNIFAC and UNIQUAC) predictions at 101.3 kPa.***

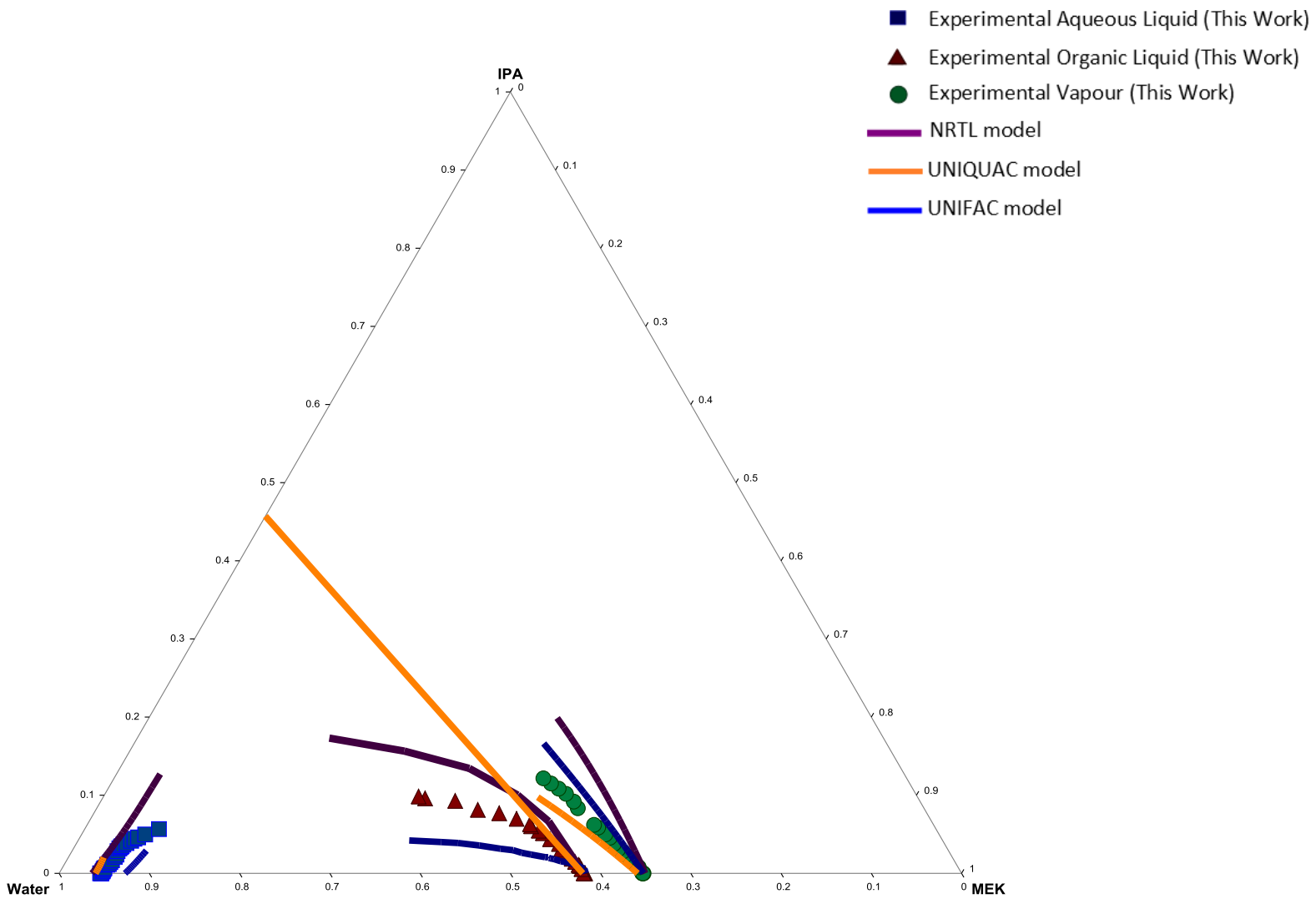

Figure 7-31: ***Ternary phase diagram for experimental IPA/MEK/water results and thermodynamic model (NRTL, UNIFAC and UNIQUAC) predictions at 101.3 kPa.***

7.5 Chapter Summary

After thorough verification of the experimental set-up and procedure (by measuring two binary and one ternary system), all new experimental VLLE data was deemed accurate and repeatable. New experimental VLLE data was determined for three systems: ethanol/MEK/water, n-propanol/MEK/water and IPA/MEK/water. All data was measured at 101.3 kPa with pressure fluctuations of ±0.2 kPa observed. All deviations from published data were accounted for by including the compositional error associated with this work (±0.014 mole fraction).

The thermodynamic consistency of all generated data, both verification and novel, was tested using the L/W Consistency Test and the McDermott-Ellis Consistency Test. Details and results of these consistency tests are listed in Appendix F. Othmer-Tobias Correlations were studied and found to be adequate (Appendix G).

By comparing the generated data to modelled data generated using the NRTL, UNIFAC and UNIQUAC models, it was seen that the models failed to predict the ternary phase behaviour of the alcohol/MEK/water systems listed above. Through data regression the models were refit and it was found that their overall ability to model ternary phase behaviour had improved.

Although no ternary heterogeneous azeotropes were found/modelled, the possibility of a ternary homogeneous azeotrope was noted for the ethanol/MEK/water and IPA/MEK/water systems. This was not confirmed experimentally, due to the scope of this research project, but it may perhaps mean that, although MEK could not be used as an entrainer for the dehydration of ethanol, n-propanol and IPA using heterogeneous azeotropic distillation, it could be a possible entrainer to dehydrated ethanol and IPA using homogeneous azeotropic distillation.

Due to the inability of the models to account for the binary behaviour of MEK/water, n-propanol/water and IPA/water parameters were regressed for the MEK/water and regressed parameters published in literature (by this research group) were used to obtain a better fit.

Even though these changes to the models' parameters allowed for superior correlation between the experimental and modelled data, both visually and mathematically (AAD and AARD% values), the importance of experimental, accurate VLLE data was emphasised: important aspects of equilibria, azeotropic composition and liquid-liquid demixing, are not explained by any of these models (NRTL, UNIFAC and UNIQUAC).

8 CONCLUSIONS AND RECOMMENDATIONS

The aim of this research project was the measurement and evaluation of accurate, repeatable isobaric VLE and VLLE data for three alcohol/entrainer/water systems at 101.3 kPa: 1) ethanol/entrainer/water; 2) n-propanol/entrainer/water; and 3) IPA/entrainer/water. This required the initial design, assessment and verification of the chosen experimental methodology. All generated data sets (VLLE data for ethanol/MEK/water, n-propanol/MEK/water and IPA/MEK/water systems) were subsequently deemed sufficiently accurate and repeatable.

By comparing the new generated data to literature data, using appropriate phase diagrams, the performance of selected entrainers for the dehydration of low-molecular weight alcohols using heterogeneous azeotropic distillation were methodically assessed. Although it was proven that, in the absence of a ternary heterogeneous azeotrope in all three studied systems, MEK is not a suitable entrainer for the dehydration of ethanol, n-propanol and IPA with heterogeneous azeotropic distillation; the research project had achieved its original aim.

The project's objectives, and how they were ultimately attained, are discussed to evaluate the overall success of this research project:

- Objective 1: Literature study

An extensive literature study was completed, focussing on azeotropes, heterogeneous azeotropic distillation of low-molecular weight alcohol/water azeotropes and entrainer selection methodology. The economic and environmental importance of the dehydration of ethanol, n-propanol and iso-propanol using heterogeneous azeotropic distillation techniques was outlined.

- Objective 2: Entrainer Selection

Through careful consideration, MEK was chosen as the entrainer to be studied by this research project. When compared to benzene, which has been used as an entrainer in the past, MEK is inexpensive (8, 053 ZAR/tonne for MEK and 15, 451 ZAR/tonne for benzene) and does not have the associated health risks that is associated with exposure to benzene. There is also a lack of comprehensive binary and/or ternary VLE and VLLE data where MEK is a featured component. From table 4-1 it can be seen that VLLE data on two MEK systems has been published at 101.3 kPa: acetone/MEK/water and 2-butanone/MEK/water.

- Objective 3: Experimental Verification

In order to confidently authenticate the accuracy and repeatability of all new data generated by the equipment and experimental procedure, verification experiments were completed. To this end, isobaric VLE and VLLE data was measured for the binary ethanol/isooctane, ternary ethanol/n-butanol/water and ternary n-propanol/isooctane/water systems. The compositional error reported, and used in thermodynamic testing, was ±0.014 mole fraction. All generated experimental data were found to be thermodynamically consistent by passing both the L/W and McDermott-Ellis consistency tests.

- Objective 4: VLLE data generation

Isobaric experimental data were generated for three ternary alcohol/entrainer/water systems:

  - ethanol/MEK/water
  - n-propanol/MEK/water
  - IPA/MEK/water.

All data sets were tested using both the L/W and McDermott-Ellis test and found to be thermodynamically consistent. The Othmer-Tobias correlation was used to show the measured LLE data followed a steady trend.

- Objective 5: Entrainer Comparison:

Suitable entrainers were compared for the dehydration of ethanol, n-propanol and iso-propanol using heterogeneous azeotropic distillation. This was done by visual inspection of the ternary phase equilibrium diagrams generated with experimental and literature data. The vapour phase compositions, for each of the three systems, were outside the liquid-liquid phase envelope and the absence of heterogeneous azeotropes was established. The possibility of a ternary homogeneous azeotrope was noted for the ethanol/MEK/water and IPA/MEK/water system and the prospect of ethanol and IPA dehydration using MEK as entrainer for homogeneous azeotropic distillation was pointed out.

- Objective 6: Thermodynamic modelling:

The ability of thermodynamic models (NRTL, UNIFAC and UNIQUAC) to predict experimentally determined VLLE data was assessed. It was found that, although each model manages to calculate some aspects of phase equilibria (azeotropic composition, boiling temperatures and phase envelope shape), all of the models failed to accurately predict isobaric VLLE data.

The models were also unable to accurately predict binary VLE for MEK/water, n-propanol/water and IPA/water systems. For this reason, new parameters were regressed for MEK/water and parameters n-propanol/water and IPA/WATER were obtained from literature. The thermodynamic models were refit in Aspen Plus® and compared visually and mathematically (with AAD and AARD% values) with the experimentally determined VLLE data. Although, the refit data did compare better to the experimental data, in comparison to the data modelled using built-in Aspen Plus® parameters, none of the thermodynamic models were able to accurately predict the experimental phase data.

In light of the results and findings of this work, the following recommendations are made for future work:

Accuracy and repeatability can be increased by fitting the equilibrium still with an online GC machine. This has been proven to be a superior method of GC analysis due to the elimination of human error as well as reducing the time between sampling to analysis. This limits the amount of demixing that occurs within the sample as well as loss of due to the relative volatilities of the components being studied. This would require the still to be modified to allow online sampling; this can be expensive and time consuming.

The flame ionization detector (FID) would have to be replaced, due to its inability to quantify water content. The GC analytical machine could be fitted with thermal conductivity detector (TCD). TCD's are universal detectors.

Online gas chromatography also opens up the opportunity to combine GC with mass spectroscopy (GC/MS) which is an extremely powerful, sensitive analytical set-up.

Another recommendation for future work would be the screening of several entrainers, before experimentation, using ASPEN PLUS® in order to select candidate entrainers. As discussed, RCM technology has been used in the past to select entrainers regardless of the inability of thermodynamic models to predict experimental data.

For future work, MEK could be studied as a suitable entrainer for the dehydration of ethanol and IPA using homogeneous azeotropic distillation.

REFERENCES

ABELLEIRA, J., SÁNCHEZ-ONETO, J., PORTELA, J.R. and MARTÍNEZ DE LA OSSA, E.J., 2013. Kinetics of supercritical water oxidation of isopropanol as an auxiliary fuel and co-fuel. *Fuel,* **111**, 574-583.

ADAIR, C. and WILSON, J.T., 2009. Prospects for anaerobic biodegradation of biofuels (ethanol and biodiesel) and proposed biofuels (n-propanol, iso-propanol, n-butanol, and 2, 5-dimethylfuran) in aquifer sediments, *In Situ and On-Site Bioremediation-2009: Proceedings of the 10th International In Situ and On-Site Bioremediation Symposium*.

AICHER, T., BAMBERGER, T. and SCHLUNDER, E.U., 1995. Liquid-Liquid and Vapor-Liquid Phase Equilibria for 1-Butanol + Water + 2-Propanol at Ambient Presure. *J. Chem. Eng. Data*, **40**, pp. 696- 698.

AMICK, E.H., WEISS, M.A. and KIRSHENBAUM, M.S., 1951. System Methyl Ethyl Ketone-sec-Butyl Alcohol. Vapor-Liquid Equilibria, *Industrial and Engineering Chemical Research*, **43**, pp. 969.

ASENSI, J.C. MOLTO, J., DEL MAR OLAYA, M., RUIZ, F. and GOMIS, V. 2002, Isobaric vapour-liquid-liquid equilibria data for the binary system 1-propanol+1-pentanol and isobaric vapour-liquid-liquid equilibria data for the ternary system water+1-propanol+1-Pentanol at 101.3 kPa. *Fluid Phase Equilibria,* **200** (2), pp. 287-293.

AYOTTE-SAUVÉ, E. and SORIN, M., 2010. Energy requirements of distillation: Exergy, pinch points, and the reversible column. *Industrial and Engineering Chemistry Research,* **49** (11), pp. 5439-5449.

BARBAUDY, J., 1926. Système alcool éthylique-benzène-eau. I étude de la surface de trouble. *Recueil des Travaux Chimeques des Pays-Bas,* **45** (3), pp. 207-213.

BARNICKI, S.D., HOYME, C.A. and SIIROLA, J.J., 2000. Separations Process Synthesis. *Kirk-Othmer Encyclopedia of Chemical Technology.* John Wiley & Sons, Inc.

BATCHELDER, H.R., 1970. Chemicals from coal. *Industrial and Engineering Chemistry Product Research and Development,* **9** (3), pp. 341-343.

BENEDICT, M., and RUBIN, L.C., 1945. Extractive and Azeotropic Distillation, Theoretical Aspects 1. *Trans. AIChe,* **41**, pp. 353.

BERCKMULLER, M., TAIT, N.P and GREENHALGH, D.A., 1997. The Influence of Local Fuel Concentration on Cyclic Variability of a Lean Burn Stratified Engine, *SAE Technical Paper* 970826.

BLACKFORD, D and YORK, R., 1965, Vapor-Liquid Equilibira of the System Acrylonitrile-Acetonitrile-Water. *Journal of Chemical and Engineering Data,* **10** (4), pp. 313-318.

Biofuels: The fuel of the future, 2010. Available from: <biofuel.org.uk/bioalcohols.html>. [12 September 2014].

BINOUS, H., 2007. Residue curve map for homogeneous reactive quaternary mixtures. *Computer Applications in Engineering Education,* **15** (1), pp. 73-77.

BRIGNOLE, E.A., BOTTINI, S. and GIANI, R., 1990. A strategy for the design and selection of solvents for separation processes. *Fluid Phase Equilibria,* **29**, pp. 125-132.

CAIRNS, B.P. and FURZER, I.A., 1990. Multicomponent three-phase azeotropic distillation. 1. Extensive experimental data and simulation results. *Industrial and Engineering Chemistry Research®,* **29** (7), pp. 1349-1363.

CAIRNS, B.P. and FURZER, I.A., 1990. Multicomponent Three-phase azeotropic distillation. 3. Modern thermodynamic models and multiple solutions. *Industrial and Engineering Chemistry Research®,* **29** (7), pp. 1383-1395.

CARNITI, P., CORI, L. and RAGAINI, V., 1978. A critical analysis of the hand and Othmer-Tobias correlations. *Fluid Phase Equilibria,* **2** (1), pp. 39-47.

Centres for decease control and prevention. (1969, October 13). Retrieved from http://www.cdc.gov/ [8th Feb 2013].

CHALLIS, A.A.L., 1954, *Azeotropic distillation of propyl amines,* US Patent 2, 691,624.

CHAMORRO, C.R., SEGOVIA, J.J., MARTÍN, M.C. and VILLAMAÑÁN, M.A., 2001. Thermodynamics of octane-enhancing additives in gasolines: Vapor-liquid equilibrium of binary and ternary mixtures containing di-isopropyl ether or heptane and 1-hexene + cyclohexane at 313.15 K. *Journal of Chemical and Engineering Data,* **46** (6), pp. 1574-1579.

CONNEMANN, M., GAUBE, J., KARRER, L., PFENNIG, A. and REUTER, U., 1990. Measurement and representation of ternary vapour-liquid-liquid equilibria. *Fluid Phase Equilibria,* **60** (1-2), pp. 99-118.

COTELLE, E.A., 1861, Improved mode of manufacturing alcohol from olefiant gas. U.S. Pat. 41,685.

DAVENPORT, B., GUBLER, R. and YONEYAMA, M., 2002. Ethyl Alcohol. *Chemical Economics Handbook*, SRI International, California.

DE VILLIERS, W.E., FRENCH, R.N. and KOPLOS, G.J., 2002. Navigate phase equilibria via residue curve maps. *Chemical Engineering Progress,* **98** (11), pp. 66-71.

DOHERTY, M.F. and PERKINS, J.D., 1978. On the dynamics of distillation processes-I. The simple distillation of multicomponent non-reacting, homogeneous liquid mixtures. *Chemical Engineering Science,* **33** (3), pp. 281-301.

DOHERTY, M.F. and KNAPP, J.P., 2000. Distillation, Azeotropic, and Extractive. *Kirk-Othmer Encyclopedia of Chemical Technology.* John Wiley & Sons, Inc.

DOHRN, R., PEPER, S. and FONSECA, J.M.S., 2010. High-pressure fluid-phase equilibria: Experimental methods and systems investigated (2000–2004). *Fluid Phase Equilibria.* **288** (2), pp. 1–54.

DOW, C.C., 1962. *Azeotropic data-II.* Washington, D.C.: Washington, D.C.: American Chemical Society.

FAN, Z., ZHANG, X., CAI, W. and WANG, F., 2013. Design and Control of Extraction Distillation for Dehydration of Tetrahydrofuran. *Chemical Engineering and Technology,* **36** (5), pp. 829-839.

FERNANDEZ, L. and KELLER, A.A., 2000. Cost-benefit analysis of methyl tert-butyl ether and alternative gasoline formulations. *Environmental Science and Policy,* **3** (4), pp. 173-188.

FILSER, J.G., CSANÁDY, G.A., DIETZ, W., KESSLER, W., KREUZER, P.E., RICHTER, M. and STÖRMER A., 1996. Comparative estimation of the neurotoxic risks of n-hexane and n-heptane in rats and

humans based on the formation of the metabolites 2,5-hexanedione and 2,5-heptanedione. *Advanced Experimental and Medical Biology,* **387**, pp. 411–427.

FONT, A., ASENSI, J.C., RUIZ, F. and GOMIS, V., 2004. Isobaric vapor-liquid and vapor-liquid-liquid equilibria data for the system water + isopropanol + isooctane. *Journal of Chemical and Engineering Data,* **49** (4), pp. 765-767.

FONT, A., ASENSI, J.C., RUIZ, F. and GOMIS, V., 2003. Application of isooctane to the dehydration of ethanol. Design of a column sequence to obtain absolute ethanol by heterogeneous azeotropic distillation. *Industrial and Engineering Chemistry Research,* **42** (1), pp. 140-144.

FOUCHER, E.R., DOHERTY, M.F. and MALONE, M.F., 1991. Automatic screening of entrainers for homogeneous azeotropic distillation. *Industrial amp; Engineering Chemistry Research®,* **30** (4), pp. 760-772.

FREDENSLUND, A., 1989. UNIFAC and related group-contribution models for phase-equilibria. *Fluid Phase Equilibria;* **52**, pp. 135-150.

FURTER, W.F., 1993. Production of fuel-grade ethanol by extractive distillation employing the salt effect. *Separation and Purification Methods,* **22** (1), pp. 1-21.

GAUBE, J., KRENZER, L., OLF, G. and WENDEL, R., 1987. Vapour-liquid equilibria measurements for some binary mixtures showing partial miscibility. *Fluid Phase Equilibria,* **35**(1-3), pp. 279-289.

GMEHLING, J., 1994. Phase equilibrium models in the synthesis and design of separation processes. *Chemie-Ingenieur-Technik*, **66** (6), pp. 792-808.

GMEHLING, J., KOLBE, B., KLEIBER, M. and RAREY, J., 2012. *Chemical thermodynamics: for process simulation.* Weinheim: Weinheim: Wiley-VCH.

GMEHLING, J. and MÖLLMANN, C., 1998. Synthesis of distillation processes using thermodynamic models and the Dortmund data bank. *Industrial and Engineering Chemistry Research,* **37** (8), pp. 3112-3123.

GOMIS, V., FONT, A. and SAQUETE, M.D., 2006. Vapour-liquid-liquid and vapour-liquid equilibrium of the system water + ethanol + heptane at 101.3 kPa. *Fluid Phase Equilibria*, **248** (2), pp. 206-210.

GOMIS, V., FONT, A., PEDRAZA, R. and SAQUETE, M.D., 2007. Isobaric vapor-liquid and vapor-liquid-liquid equilibrium data for the water-ethanol-hexane system. *Fluid Phase Equilibria,* **259** (1 SPEC. ISS.), pp. 66-70.

GOMIS, V., FONT, A., PEDRAZA, R. and SAQUETE, M.D., 2005. Isobaric vapor-liquid and vapor-liquid-liquid equilibrium data for the system water + ethanol + cyclohexane. *Fluid Phase Equilibria,* **235**(1), pp. 7-10.GOMIS, V., PEDRAZA, R., FRANCÉS, O., FONT, A. and ASENSI, J.C., 2007. Dehydration of ethanol using azeotropic distillation with isooctane. *Industrial and Engineering Chemistry Research,* **46** (13), pp. 4572-4576.

GOMIS, V., PEQUENÍN, A. and ASENSI, J.C., 2010. A review of the isobaric (vapor + liquid + liquid) equilibria of multicomponent systems and the experimental methods used in their investigation. *Journal of Chemical Thermodynamics,* **42** (7), pp. 823-828.

GOMIS, V., RUIZ, F. and ASENSI, J.C., 2000. The application of ultrasound in the determination of isobaric vapour-liquid-liquid equilibrium data. *Fluid Phase Equilibria,* **172** (2), pp. 245-259.

GOMIS, V., FONT, A., SAQUETE, M.D. and GARCÍA-CANO, J., 2014. Isothermal (liquid + liquid) equilibrium data at T = 313.15 K and isobaric (vapor + liquid + liquid) equilibrium data at

101.3 kPa for the ternary system (water + 1-butanol + p-xylene). *The Journal of Chemical Thermodynamics,* **79**, pp. 242-247.

GRAHAM, E., 1927. Detonation specifications for automotive fuels. *SAE Technical Papers.*

GRANA, R., FRASSOLDATI, A., FARAVELLI, T., NIEMANN, U., RANZI, E., SEISER, R., CATTOLICA, R. and SESHADRI, K., 2010. An experimental and kinetic modeling study of combustion of isomers of butanol. *Combustion and Flame,* **157** (11), pp. 2137-2154.

GREEN, D. and PERRY, R., 2000. *Perry's chemical engineers' handbook*. New York: New York: McGraw-Hill.

GUNAWAN and CHIEN, I., 2008. Design of ethanol dehydration process: Heterogeneous azeotropic distillation vs. extractive distillation, *AIChE 100 - 2008 AIChE Annual Meeting, Conference Proceedings.*

GUO, Z., CHIN, J. and LEE, J.W., 2004. Feasibility of continuous reactive distillation with azeotropic mixtures. *Industrial and Engineering Chemistry Research,* **43** (14), pp. 3758-3769.

HAELSSIG, J.B., TREMBLAY, A.Y. and THIBAULT, J., 2012. A new hybrid membrane separation process for enhanced ethanol recovery: Process description and numerical studies. *Chemical Engineering Science,* **68** (1), pp. 492-505.

HALA, E., PICK, J., FRIED, V. and VILIM, O., 1967. *Vapour-Liquid Equilibrium*. AIChE Journal, **14** (3), pp. 521–523.

HAND, D.B., 1930. Dineric distribution. *Journal of Physical Chemistry,* **34** (9), pp. 1961-2000.

HANDS, C.H.G. and NORMAN, W.S., 1945. The dehydration of allyl alcohol by azeotropic distillation vapour-liquid and liquid-liquid equilibrium data for the systems allyl alcohol-water-trichloroethylene and allyl alcohol-water-carbon tetrachloride. *Trans.Instn.Chem.Eng.,* **23**, pp. 76-88.

HENLEY, E.J., 2011. *Separation process principles.* Hoboken, NJ: Hoboken, NJ: Wiley.

HENLEY, M., LETINSKI, D.J., CARR, J., CARO, M.L., DAUGHTREY, W. and WHITE, R., 2014. Health assessment of gasoline and fuel oxygenate vapors: Generation and characterization of test materials. *Regulatory Toxicology and Pharmacology*.

HERINGTON, E.F.G., 1947. A thermodynamic test for the internal consistency of experimental data on volatility ratios. *Nature,* **160** (4070), pp. 610-611.

HIAKI, T., TAKAHASHI, K., TOMOYA, H.M. and KOJIMA, K., 1994. Vapor-liquid equilibria of ethanol with 2,2,4-trimethylpentane or octane at 101.3 kPa. *Journal of Chemical and Engineering Data*, **39** (4), pp. 720-722.

HILLERT, M., 1998. *Phase equilibria, phase diagrams and phase transformations: their thermodynamic basis.* Cambridge University Press, Cambridge, England.

HO, W.S.W., and SIRKAR, K.K., 1992. *Membrane Handbook.* Van Nostrand Reinhold, New York.

HOFFMAN, E.J., 1964. *Azeotropic and extractive distillation.* New York, N.Y. : Wiley-Interscience.

HORSLEY, L.H., 1973. *Azeotropic data - III.* Washington, D.C. : American Chemical Society.

IARC, 1987. Overall evaluations of carcinogenicity: an updating of IARC Monographs volumes 1 to 42. *IARC Monogr Eval Carcinog Risks Hum Suppl*, **7**, pp. 1–440.

IARC, 2009. Some industrial chemicals and dyestuffs. *IARC Monogr Eval Carcinog Risk Chem Hum*, **29**, pp. 1–398.

IWAKABE, K. and KOSUGE, H., 2001. Isobaric vapour-liquid-liquid equilibria with a newly developed still. *Fluid Phase Equilibria,* **192** (1-2), pp. 171-186.

JULKA, V., CHIPLUNKAR, M. and O'YOUNG, L., 2009. Selecting entrainers for azeotropic distillation. *Chemical Engineering Progress,* **105** (3), pp. 47-53.

JUNKER, B., 2000. Fermentation. *Kirk-Othmer Encyclopedia of Chemical Technology.* John Wiley & Sons, Inc.

KAMIHAMA, N., MATSUDA, H., KURIHARA, K., TOCHIGI, K. and OBA, S., 2012. Isobaric vapor-liquid equilibria for ethanol + water + ethylene glycol and its constituent three binary systems. *Journal of Chemical and Engineering Data,* **57** (2), pp. 339-344.

KNAPP, J.P. and DOHERTY, M.F., 1992. A new pressure-swing-distillation process for separating homogeneous azeotropic mixtures. *Industrial & Engineering Chemistry Research,* **31** (1), pp. 346-357.

KOJIMA, K. and TOCHIGI, K., 1979. Prediction of vapor-liquid equilibria by the ASOG method, Elsevier, Kodansha, Tokyo.

KU, H.-C., TU, C.-H., 2005. Isobaric vapor-liquid equilibria for mixtures of acetone, ethanol, and 2,2,4-trimethylpentane at 101.3 kPa. *Fluid Phase Equilibria*, **231** (1), pp. 99-108.

KUMAR, S., SINGH, N. and PRASAD, R., 2010. Anhydrous ethanol: A renewable source of energy. *Renewable and Sustainable Energy Reviews,* **14** (7), pp. 1830-1844.

KURIHARA, K., NAKAMICHI, M. and KOJIMA, K., 1993. Isobaric vapor-liquid equilibria for methanol + ethanol + water and the three constituent binary systems. *Journal Of Chemical And Engineering Data,* **38** (3), pp. 446-449.

LECAT, M., 1947. Azéotropes binaires orthobares. *Annali de Chemica* (Paris), **2**, pp. 158-202.

LAI, H., LIN, Y. and TU, C., 2014. Isobaric (vapor + liquid) equilibria for the ternary system of (ethanol + water + 1,3-propanediol) and three constituent binary systems at P = 101.3 kPa. *Journal of Chemical Thermodynamics,* **68**, pp. 13-19.

LAROCHE, L., BEKIARIS, N., ANDERSEN, H.W., and MORARI, M., 1992. The Curious Behavior of Homogeneous Azeotropic Distillation - Implications for Entrainer Selection. AIChE J., **38** (9), pp. 1309–1328.

LEE, L. and SHEN, H., 2003. Azeotropic Behavior of a Water + n-Propanol + Cyclohexane Mixture Using Cyclohexane as an Entrainer for Separating the Water + n-Proponal Mixture at 760 mmHg. *Industrial and Engineering Chemistry Research,* **42** (23), pp. 5905-5914.

LEE, M., TSAI, L., HONG, G. and LIN, H., 2004. Multiphase equilibria for binary and ternary mixtures containing propionic acid, n-butanol, butyl propionate, and water. *Fluid Phase Equilibria,* **216** (2), pp. 219-228.

LEI, Z., LI, C. and CHEN, B., 2003. Extractive distillation: A review. *Separation and Purification Reviews,* **32** (2), pp. 121-213.

LI, C., ZHANG, X., HE, X. and ZHANG, S., 2007. Design of separation process of azeotropic mixtures based on the green chemical principles. *Journal of Cleaner Production,* **15** (7), pp. 690-698.

LLADOSA, E., MONTÓN, J.B., BURGUET, M. and DE LA TORRE, J., 2008. Isobaric (vapour + liquid + liquid) equilibrium data for (di-n-propyl ether + n-propyl alcohol + water) and (diisopropyl ether + isopropyl alcohol + water) systems at 100 kPa. *Journal of Chemical Thermodynamics,* **40** (5), pp. 867-873.

LOGSDON, J.E., 2000. Ethanol. *Kirk-Othmer Encyclopedia of Chemical Technology.* John Wiley & Sons, Inc.

LOGSDON, J.E. and LOKE, R.A., 2000. Isopropyl Alcohol. *Kirk-Othmer Encyclopedia of Chemical Technology.* John Wiley & Sons, Inc.

LUTUGINA, N.V., and SOBOLEVA, I.N., 1970. Study of Liquid-Liquid-Vapor Equilibrium in The System Nitrocyclohexane- Cyclohexanone Oxime- Water. *Journal of Applied Chemistry.* **43**, pp. 112-117.

LUYBEN, W.L., 2012. Economic optimum design of the heterogeneous azeotropic dehydration of ethanol. *Industrial and Engineering Chemistry Research,* **51** (50), pp. 16427-16432.

LUYBEN, W.L., 2006. Control of a multiunit heterogeneous azeotropic distillation process. *AIChE Journal,* **52** (2), pp. 623-637.

LUYBEN, W.L., 2010. *Design and control of distillation systems for separating azeotropes.* Hoboken, N.J.: Wiley.

Luyben, W.L. and Chien, I.L., 2010, *Design and Control of Distillation Systems for Separating Azeotropes,* Wiley, New Jersey.

MACHADO, G.B., BARROS, J.E.M., BRAGA, S.L. and BRAGA, C.V.M., 2013. Influence of toluene and iso-octane on combustion and performance parameters of spark ignition engines. *SAE Technical Papers,* **13**.

MARIANO, A.P., DIAS, M.O.S., JUNQUEIRA, T.L., CUNHA, M.P., BONOMI, A. and FILHO, R.M., 2013. Butanol production in a first-generation Brazilian sugarcane biorefinery: Technical aspects and economics of greenfield projects. *Bioresource technology,* **135**, pp. 316-323.

MARTIN, G.Q., 1984. MULTI-PHASE MIXING PROBLEMS IN A PLANT SCALE REACTING SYSTEM. *American Institute of Chemical Engineers, National Meeting* 1984.

MARTÍNEZ, N.F., LLADOSA, E., BURGUET, M. and MONTÓN, J.B., 2008. Isobaric vapour-liquid equilibria for binary systems of 2-butanone with ethanol, 1-propanol, and 2-propanol at 20 and 101.3 kPa. *Fluid Phase Equilibria,* **270** (1-2), pp. 62-68.

MASCAL, M., 2012. Chemicals from biobutanol: Technologies and markets. *Biofuels, Bioproducts and Biorefining,* **6** (4), pp. 483-493.

MCDERMOTT, C. and ELLIS, S.R.M., 1965. A multicomponent consistency test. *Chemical Engineering Science,* **20** (4), pp. 293-296.

MCMURRY, J., 1996. *Organic chemistry.* Pacific Grove, California. Brooks-Cole.

MILLER, K.J. and HUANG, H., 1972. Vapor-liquid equilibrium for binary systems 2-butanone with 2-butanol, 1-pentanol, and isoamyl alcohol. *Journal of Chemical and Engineering Data,* **17** (1), pp. 77-78.

MOUSSA, A.S. and JIMÉNEZ, L., 2006. Entrainer selection and systematic design of heterogeneous azeotropic distillation flowsheets. *Industrial and Engineering Chemistry Research,* **45** (12), pp. 4304-4315.

MULLER, W.C. and MILLER, F.D., 1957. (To National Petroleum Chemicals Corp.), U.S. Pat. 2,792,432.

MUROGOVA, R.A., TUDOROVSKAYA, G.I., PLESKACH, N.I., SAFONOVA, N.A., GRIDIN, I.D., and SERAFIMOV, L.A., 1973. Liquid-Vapor Equilibrium in The System Water-Acetic Acid- P-Xilene at 760. *Journal of Applied Chemistry,* **46**, pp. 2615-2617.

NAGATA,I.,OHTA,T., and NAKAGAWA,S., 1976. Excess Gibss free energies and heats of mixing for binary alcoholic liquid mixtures. *Journal of Chemical and Engineering Data,* **9**, pp. 276-281.

NEIER, W. and STREHLKE, G., 2002. 2-Butanone: *Ullmann's Encyclopedia of Industrial Chemistry*, Wiley-VCH, Weinheim.

NEWSHAM, D.M.T. and VAHDAT, N., 1977. Prediction of vapour-liquid-liquid equilibria from liquid-liquid equilibria - 1. Experimental results for the systems methanol-water-n-butanol, ethanol-water-n-butanol and n-propanol-water - n-butanol. *Chemical Engineering Journal and the Biochemical Engineering Journal,* **13** (1), pp. 27-31.

OGNISTY, T.P., 1995. Analyze distillation columns with thermodynamics. *Chemical Engineering Progress,* **91** (2), pp. 40-46.

OHTA, T., KOYABU, J. and NAGATA, I., 1981. Vapor-liquid equilibria for the ternary Ethanol-2-butanone-benzene system at 298.15 K. *Fluid Phase Equilibria,* **7** (1), pp. 65-73.

ORCHILLÉS, A.V., MIGUEL, P.J., VERCHER, E. and MARTÍNEZ-ANDREU, A., 2010. Using 1-ethyl-3-methylimidazolium trifluoromethanesulfonate as an entrainer for the extractive distillation of ethanol + water mixtures. *Journal of Chemical and Engineering Data,* **55** (4), pp. 1669-1674.

OTHMER, D.F., 1948. Composition of vapors from boiling solutions: Improved equilibrium still. *Analytical Chemistry,* **20** (8), pp. 763-766.

OZBEK, M.E., DE LA GARZA, J.M. and TRIANTIS, K., 2012. Efficiency measurement of the maintenance of paved lanes using data envelopment analysis.*Construction Management and Economics,* **30** (11), pp. 995-1009.

PEQUENÍN, A., ASENSI, J.C. and GOMIS, V., 2010. Isobaric Vapor-liquid-liquid equilibrium and vapor-liquid equilibrium for the quaternary system water-ethanol-cyclohexane-isooctane at 101.3 kPa. *Journal of Chemical and Engineering Data,* **55** (3), pp. 1227-1231.

PETERS, M., 2011. Renewable fuels and chemicals derived from isobutanol, *ACS National Meeting Book of Abstracts* 2011.

PIENAAR, C., SCHWARZ, C.E., KNOETZE, J.H. and BURGER, A.J., 2013. Vapor-liquid-liquid equilibria measurements for the dehydration of ethanol, isopropanol, and n-propanol via azeotropic distillation using DIPE and isooctane as entrainers. *Journal of Chemical and Engineering Data,* **58** (3), pp. 537-550.

PLA-FRANCO, J., LLADOSA, E., LORAS, S. and MONTÓN, J.B., 2013. Phase equilibria for the ternary systems ethanol, water+ethylene glycol or + glycerol at 101.3kPa. *Fluid Phase Equilibria,* **341**, pp. 54-60.

PRAUSNITZ, J.M., 1999. *Molecular thermodynamics of fluid-phase equilibria.* Upper Saddle River, N.J.: Prentice Hall.

RAAL, J.D. and Mühlbauer, A.L. 1998, *Phase equilibria: measurement and computation,* Taylor and Francis, Washington D.C.

RAWAT, B.S., GOSWAMI, A.N., and KRISHNA S., 1980. Isobaric Vapour-Liquid Equilibria of the Ternary System Hexane-Benzane-Sulpholane. *J. Chem. Tech. Biotechnol*, **30**, pp. 557 -562.

On the Thermodynamics of Solutions. IV. The Determination of Liquid--Vapor Equilibria by Measuring the Total Pressure

REDLICH, O. and KISTER, A.T., 1949. On the Thermodynamics of Solutions. IV. The Determination of Liquid--Vapor Equilibria by Measuring the Total Pressure. *J. Am. Chem. Soc*, **71** (2), pp. 505–507.

REINDERS, W. and DEMINJER, C.M., 1947. Vapour-liquid equilibria in ternary systems. VI. The system water-acetone-chloroform. *Recueil des Travauz Chimiques de Pays-Bas,* **66** (9), pp. 573-604.

ROUSSEAU, R. W. and FAIR, J. R., 1987. *Handbook of separation process technology.* Wiley-IEEE. pp. 261–262.

RYAN, P.J. and DOHERTY, M.F., 1989. Design/optimization of ternary heterogeneous azeotropic distillation sequences. *AIChE Journal,* **35** (10), pp. 1592-1601.

SANDER, U. and SOUKUP, P., 1988. Design and operation of a pervaporation plant for ethanol dehydration. *Journal of Membrane Science,* **36** (C), pp. 463-475.

SANDLER, S.I., 1989. *Chemical and engineering thermodynamics.* New York, N.Y.: Wiley.

SCENNA, N.J., BENZ, S.J., RODRÍGUEZ, N.H. and KLARIC, J.I., 2005. Startup of homogeneous azeotropic distillation sequences with multiple steady states. *Industrial and Engineering Chemistry Research,* **44** (24), pp. 9208-9220.

SEADER, J.D., 1998. *Separation process principles.* New York, N.Y: Wiley.

SEADER, J. D. and HENLEY, E.J. 2006. *Separation process principles.* New York, N.Y: Wiley.

SERINYEL, Z., BLACK, G., CURRAN, H.J. and SIMMIE, J.M., 2010. A shock tube and chemical kinetic modeling study of methy ethyl ketone oxidation.*Combustion Science and Technology,* **182** (7), pp. 574-587.

SHULGIN, I., FISCHER, K., NOLL, O. and GMEHLING, J., 2001. Classification of homogeneous binary azeotropes. *Industrial and Engineering Chemistry Research,* **40** (12), pp. 2742-2747.

SIMMROCK, K.H., FRIED, A. and WELKER, R., 1993. Expert system for the design of separation sequences for close-boiling and azeotropic mixtures.*International Chemical Engineering,* **33** (4), pp. 577-590.

SINGH, N. and PRASAD, R., 2011. Fuel grade ethanol by diffusion distillation: An experimental study. *Journal of Chemical Technology and Biotechnology,***86** (5), pp. 724-730.

SMITH, J.M.(., 2001. *Introduction to chemical engineering thermodynamics.* Boston: McGraw-Hill.

SOLOMONS, T.W.G., 2002. *Organic chemistry.* New York: J. Wiley.

SORIANO, T., MENÉNDEZ, M., SANZ, P. and REPETTO, M., 1996. Method for the simultaneous quantification of n-hexane metabolites: Application to n-hexane metabolism determination. *Human and Experimental Toxicology,* **15** (6), pp. 497-503.

SUM, A.K., and SANDIER, S.I., A Novel approach to phase equilibria predictions using ab initio methods. *Industrial and Engineering Chemistry Research,* **38** (7), pp. 2849-2855.

TANAKA, H., MURAMATSU, T. and KATO, M., 1992. Isobaric vapor-liquid equilibria for three binary systems of 2-butanone with 3-methyl-1-butanol, 1-butanol, or 2-butanol. *Journal of Chemical and Engineering Data,* **37** (2), pp. 164-166.

TANAKA, T., 1985. Attempting the Predicition of an Azeotrope and Its x-y Curve on the Basis of the Molecular Parameters. *Fluid Phase Equilibria*, **24**, pp. 187-198.

TOCHIGI, K., INOUE, H. and KOJIMA, K., 1985. Determination of azeotropes in binary systems at reduced pressures. *Fluid Phase Equilibria,* **22** (3), pp. 343-352.

TREYBAL, R.E.E., 1915-, 1963. *Liquid extraction.* New York, N.Y.: McGraw-Hill.

TURNER, C.F. and MCCREERY, J.W., 1981. *The Chemistry of Fire and Hazardous Materials*. Boston, Massachusetts: Allyn and Bacon, Inc. p. 118.

UNRUH, J.D. and PEARSON, 2000. *N-Propyl alcohol. Kirk-Othmer Encyclopedia of Chemical Technology. John Wiley & Sons, Inc.*

URDANETA, R.Y., BAUSA, J., BRÜGGEMANN, S. and MARQUARDT, W., 2002. Analysis and conceptual design of ternary heterogeneous azeotropic distillation processes. *Industrial and Engineering Chemistry Research,* **41** (16), pp. 3849-3866.

U.S. Environmental Protection Agency, 1994. Carcinogenic effects of benzene: an update. Prepared by the National Center for Environmental Health, Office of Research and Development. Washington, DC.

U.S. Environmental Protection Agency, 1999. Integrated Risk Information System (IRIS) on n-Hexane. National Center for Environmental Assessment, Office of Research and Development, Washington, DC.

VANE, L.M., 2008. Separation technologies for the recovery and dehydration of alcohols from fermentation broths. *Biofuels, Bioproducts and Biorefining,* **2** (6), pp. 553-588.

VANE, L.M., 2005. A review of pervaporation for product recovery from biomass fermentation processes. *Journal of Chemical Technology and Biotechnology,* **80** (6), pp. 603-629.

F. VAN ZANDIJCKE, F. and VERHOEYE, L., 1974. 9The vapour-liquid equilibrium of ternary systems with limited miscibility at atmospheric pressure. *Journal of Chemical Technology and Biotechnology,* **24** (12), pp. 709–729.

VASCONCELOS, C.J.G., XAVIER, P.F., BROGLIO, M.I. and WOLF-MACIEL, M.R., 2001. Optimization and control of heterogeneous azeotropic batch distillation. *Chemie-Ingenieur-Technik,* **73** (6), pp. 714.

VELOO, P.S. and EGOLFOPOULOS, F.N., 2011. Studies of n-propanol, iso-propanol, and propane flames. *Combustion and Flame,* **158** (3), pp. 501-510.

VERHOEYE, L.A.J., 1968. The system cyclohexane-2-propanol-water. Journal of Chemical and Engineering Data, **13** (4), pp. 462-467.

VERHOEYE, L.A.J., 1970. The system 2-isopropoxypropane-2-propanol-water. *Journal of Chemical and Engineering Data,* **15** (2), pp. 222-226.

VOLPICELLI, G., 1968. Vapor-liquid and liquid-liquid equilibria of the system acrylonitrile-acetonitrile-water. *Journal of Chemical and Engineering Data,***13** (2), pp. 150-154.

WADROP, K., 2010. Biobutanol - A future fuel? *Chemical Engineer,* **825**, pp. 36-39.

WAHNSCHAFFT, O.M. and WESTERBERG, A.W., 1993. The product composition regions of azeotropic distillation-columns .2. Separability in 2-feed columns and entrainer selection. *Industrial & Engineering Chemistry Research,* **32** (6), pp. 1108-1120.

WANG, H., CUI, X., LI, C. and FANG, J., 2013. Separation of Ethyl Acetate-Dichloromethane-Ethanol by Extractive Distillation: Simulation and Optimization. *Chemical Engineering and Technology,* **36** (4), pp. 627-634.

WEN, C. and TU, C., 2007. Vapor-liquid equilibria for binary and ternary mixtures of ethanol, 2-butanone, and 2,2,4-trimethylpentane at 101.3 kPa.*Fluid Phase Equilibria,* **258**(2), pp. 131-139.

WESTERBERG, A.W., WAHNSCHAFFT, O., 1996. Synthesis of Distillation-Based Separation Systems. *Advances in Chemical Engineering,* **23** (C), pp. 63-170.

WILSON, S.R., PATEL, R.B., ABBOTT, M.M. and VAN NESS, H.C., 1979. Excess thermodynamic functions for ternary systems. 4. Total-pressure data and GE for acetonitrile-ethanol-water at 50°C. *Journal of Chemical and Engineering Data,* **24** (2), pp. 130-132.

WINNICK, J., 1997. *Chemical engineering thermodynamics : an introduction to thermodynamics for undergraduate engineering students.* New York, N.Y. : Wiley.

WISNIAK, J., 1994. The Herington test for thermodynamic consistency. *Industrial & Engineering Chemistry Research,* **33** (1), pp. 177-180.

WISNIAK, J., 1993. A new test for the thermodynamic consistency of vapor-liquid equilibrium. *Industrial and Engineering Chemistry Research,* **32** (7), pp. 1531-1533.

WISNIAK, J., APELBLAT, A. and SEGURA, H., 1997. An assessment of thermodynamic consistency tests for vapor-liquid equilibrium data. *Physics and Chemistry of Liquids,* **35** (1), pp. 1-58.

WISNIAK, J. and TAMIR, A., 1977. Vapor-liquid equilibria in the ternary systems water-formic acid-acetic acid and water-acetic acid-propionic acid.*Journal of Chemical and Engineering Data,* **22** (3), pp. 253-260.

World Health Organisation, 1978. Cancer statistics: report of a WHO/IARC expert committee. *WHO technical report series,* **632,** pp. 47.

World Health Organisation, 2000. Benzene. In: Air quality guidelines for Europe, *Copenhagen, World Health Organization Regional Office for Europe*, 2nd edition.

World Health Organisation, 2007. Guidelines for drinking-water quality, 3rd edition incorporating 1st and 2nd addenda. *Recommendations. Geneva, World Health Organization*, **1**, pp. 312–313.

WU, H.S., HAGEWIESCHE, D. and SANDLER, S.I., 1988. Vapor-liquid equilibria of 2-propanol + water + N,N-dimethyl formamide. *Fluid Phase Equilibria,***43** (1), pp. 77-89.

WU, Y., LEE, H., TSAI, C., HUANG, H. and CHIEN, I., 2013. Design and control of a reactive-distillation process for esterification of an alcohol mixture containing ethanol and n-butanol. *Computers and Chemical Engineering,* **57**, pp. 63-77.

WU, Y., PAN, D., ZHU, J., CHEN, K., WU, B. and SHEN, Y., 2015. Isobaric Vapor-Liquid-Liquid Equilibria for 1-Butanol + Water + 2,3-Butanediol at 101.3 kPa. *Chemical Engineering Communications,* **202** (2), pp. 175-180.

WYCZESANY, A., 2014. Calculation of vapor-liquid-liquid equilibria at atmospheric and high pressures. *Industrial and Engineering Chemistry Research,***53** (6), pp. 2509-2519.

YOUNG, S., and FORTEY, E.C., 1902. The Properties of Mixtures of the Lower Alcohols with Water. *Journal of Chemical Engineering Society*, **81**, pp. 717-739.

YOUNIS, O.A.D., PRITCHARD, D.W. and ANWAR, M.M., 2007. Experimental isobaric vapour–liquid–liquid equilibrium data for the quaternary systems water (1)–ethanol (2)–acetone (3)–n-butyl acetate (4) and water (1)–ethanol (2)–acetone (3)–methyl ethyl ketone (4) and their partially miscible-constituent ternaries. *Fluid Phase Equilibria,* **251** (2), pp. 149-160.

ZEMP, R.J. and FRANCESCONI, A.Z., 1992. Salt effect on phase equilibria by a recirculating still. *Journal of Chemical and Engineering Data,* **37** (3), pp. 313-316.

ZONG, Z.L., YANG, X.H. and ZHENG, X.Y., 1983. Determination and correlation of vapor-liquid-equilibria of alcohol solutions, *Journal of Chemical Engineering* (Japan), **16**, pp. 1-6.

ZIELKIEWICZ, J. and KONITZ, A., 1991. (Vapour + liquid) equilibria of (N,N-dimethylformamide + water + propan-1-ol) at the temperature 313.15 K.*The Journal of Chemical Thermodynamics,* **23** (1), pp. 59-65.

APPENDIX A - MSDS FORMS

All Material Safety Data Sheet (MSDS) information was obtained from ScienceLab.com (2014).

Table A- 1: ***Benzene MSDS.***

Benzene

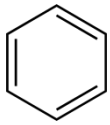

Physical and Chemical Properties:	
Physical State:	Liquid
Odour:	Aromatic, Gasoline-like
Molecular Formula:	C_6H_6
Molecular Weight (g/mol):	78.11
Colour:	Colourless
Boiling Point (°C):	80.1
Melting Point (°C):	5.5
Specific Gratify (water = 1):	0.8787
Vapour Pressure (kPa):	10
Vapour Density (air = 1):	2.8
Hazards Identification:	
Potential Acute Health Effects:	Very hazardous in case of eye contact (irritant), of inhalation. Hazardous in case of skin contact (irritant, permeator), of ingestion. Inflammation of the eye is characterized by redness, watering, and itching.
Potential Chronic Health Effects:	The substance is toxic to blood, bone marrow, central nervous system (CNS). The substance may be toxic to liver, Urinary System. Repeated or prolonged exposure to the substance can produce target organs damage.
Carcinogenic Effects:	Classified A1
Mutagenic Effects:	Classified POSSIBLE for human
Fire and Explosion Data:	
Flammability:	Flammable
Auto-Ignition Temperature (°C):	497.78
Flask Point (°C):	-11.1
Products of Combustion:	Carbon Oxides

Table A- 2 : *Cyclohexane MSDS.*

Cyclohexane

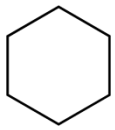

Physical and Chemical Properties:	
Physical State:	Liquid
Odour:	Chloroform-like odour
Molecular Formula:	C_6H_{12}
Molecular Weight (g/mol):	84.16
Colour:	Colourless
Boiling Point (°C):	80.7
Melting Point (°C):	6.47
Specific Gratify (water = 1):	0.7781
Vapour Pressure (kPa):	19.2
Vapour Density (air = 1):	2.98
Hazards Identification:	
Potential Acute Health Effects:	Slightly hazardous in case of skin contact (irritant, permeator), of eye contact (irritant), of ingestion, of inhalation.
Potential Chronic Health Effects:	The substance may be toxic to kidneys, liver, cardiovascular system, central nervous system (CNS). Repeated or prolonged exposure to the substance can produce target organs damage.
Carcinogenic Effects:	Not Available
Mutagenic Effects:	Not Available
Fire and Explosion Data:	
Flammability:	Flammable
Auto-Ignition Temperature (°C):	245
Flask Point (°C):	-18
Products of Combustion:	Carbon Oxides

Table A- 3 : *Hexane MSDS.*

Hexane

Physical and Chemical Properties:	
Physical State:	Liquid
Odour:	Gasoline-like or Petroleum like (slight)
Molecular Formula:	C_6H_{14}
Molecular Weight (g/mol):	86.18
Colour:	Colourless
Boiling Point (°C):	68
Melting Point (°C):	-95
Specific Gratify (water = 1):	0.66
Vapour Pressure (kPa):	17.3
Vapour Density (air = 1):	2.97
Hazards Identification:	
Potential Acute Health Effects:	Hazardous in case of skin contact (permeator), of ingestion, of inhalation. Slightly hazardous in case of skin contact (irritant), of eye contact (irritant).
Potential Chronic Health Effects:	The substance may be toxic to peripheral nervous system, skin, central nervous system (CNS). Repeated or prolonged exposure to the substance can produce target organs damage.
Carcinogenic Effects:	Not Available
Mutagenic Effects:	Mutagenic for Bacteria and/or yeast.
Fire and Explosion Data:	
Flammability:	Flammable
Auto-Ignition Temperature (°C):	225
Flask Point (°C):	-22.5
Products of Combustion:	Carbon Oxides

Table A- 4: ***n-Heptane MSDS.***

n-Heptane

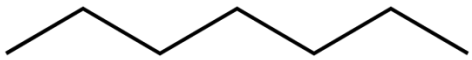

Physical and Chemical Properties:	
Physical State:	Liquid
Odour:	Gasoline-like
Molecular Formula:	C_7H_{16}
Molecular Weight (g/mol):	100.21
Colour:	Colourless
Boiling Point (°C):	98.4
Melting Point (°C):	-90.7
Specific Gratify (water = 1):	0.6838
Vapour Pressure (kPa):	5.3
Vapour Density (air = 1):	3.5
Hazards Identification:	
Potential Acute Health Effects:	Slightly hazardous in case of skin contact (irritant), of eye contact (irritant), of ingestion, of inhalation.
Potential Chronic Health Effects:	The substance may be toxic to lungs, peripheral nervous system, upper respiratory tract, skin, central nervous system (CNS). Repeated or prolonged exposure to the substance can produce target organs damage.
Fire and Explosion Data:	
Flammability:	Flammable
Auto-Ignition Temperature (°C):	203.89
Flask Point (°C):	-4
Products of Combustion:	Carbon Oxides

Table A- 5: ***Isooctane MSDS.***

Isooctane (2,2,4-trimethylpentane)

Physical and Chemical Properties:	
Physical State:	Liquid
Odour:	Gasoline-like
Molecular Formula:	C_8H_{18}
Molecular Weight (g/mol):	114.23
Colour:	Colourless
Boiling Point (°C):	99.238
Melting Point (°C):	-107.45
Specific Gratify (water = 1):	0.69194
Vapour Pressure (kPa):	5.4
Vapour Density (air = 1):	3.93
Hazards Identification:	
Potential Acute Health Effects:	Hazardous in case of eye contact (irritant), of ingestion, of inhalation. Slightly hazardous in case of skin contact (irritant, permeator).
Potential Chronic Health Effects:	The substance is toxic to eyes. The substance may be toxic to kidneys, lungs, liver, skin, central nervous system (CNS).
Fire and Explosion Data:	
Flammability:	Flammable
Auto-Ignition Temperature (°C):	418
Flask Point (°C):	-12
Products of Combustion:	Carbon Oxides

Table A- 6: ***DIPE MSDS.***

Diisopropyl ether (DIPE)

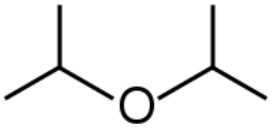

Physical and Chemical Properties:	
Physical State:	Liquid
Odour:	Ethereal
Molecular Formula:	$C_6H_{12}O$
Molecular Weight (g/mol):	102.18
Colour:	Colourless
Boiling Point (°C):	68.5
Melting Point (°C):	-86
Specific Gratify (water = 1):	0.7257
Vapour Pressure (kPa):	15.87
Vapour Density (air = 1):	3.52
Hazards Identification:	
Potential Acute Health Effects:	Very hazardous in case of eye contact (irritant), of ingestion, of inhalation. Hazardous in case of skin contact (irritant, permeator). Inflammation of the eye is characterized by redness, watering, and itching.
Potential Chronic Health Effects:	The substance is toxic to lungs, the nervous system, mucous membranes. Repeated or prolonged exposure to the substance can produce target organs damage.
Fire and Explosion Data:	
Flammability:	Flammable
Auto-Ignition Temperature (°C):	443
Flask Point (°C):	-28
Products of Combustion:	Carbon Oxides

Table A- 7: *2-Butanone MSDS*

Methyl Ethyl Ketone (MEK, 2-Butanone)

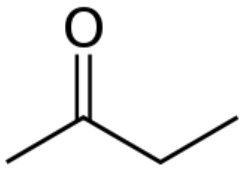

Physical and Chemical Properties:	
Physical State:	Liquid
Odour:	Acetone-like, Sweetish
Molecular Formula:	C_4H_8O
Molecular Weight (g/mol):	72.12
Colour:	Colourless
Boiling Point (°C):	79.6
Melting Point (°C):	-86
Specific Gratify (water = 1):	0.805
Vapour Pressure (kPa):	10.3
Vapour Density (air = 1):	2.41
Hazards Identification:	
Potential Acute Health Effects:	Hazardous in case of skin contact (irritant, permeator), of eye contact (irritant), of ingestion, of inhalation (lung irritant).
Potential Chronic Health Effects:	Repeated or prolonged exposure to the stubstance can produce target organs damage.
Fire and Explosion Data:	
Flammability:	Flammable
Auto-Ignition Temperature (°C):	404
Flask Point (°C):	-9
Products of Combustion:	Carbon Oxides

APPENDIX B - CALIBRATION CERTIFICATES

Unique Metrology
Eskom Research & Innovation Centre
Lower Germiston Road • Rosherville
P O Box 145296 • Bracken Gardens • 1452
Tel: 011 626 3808 • Cell: 083 254 3635 • Fax: 086 610 4196
Web: www.unimet.co.za

sanas Calibration Laboratory
306 205

SANAS ACCREDITED CALIBRATION LABORATORY No 306

TEMPERATURE METROLOGY

CERTIFICATE OF CALIBRATION

Date of issue : 26/11/2012

Certificate No : 1211T4452-1

Technical Signatory

M Mathieson.

Page 1 of 2 pages.

The results of all measurements are traceable to the national measuring standards.

The values in this certificate are correct at the time of calibration. Subsequently the accuracy will depend on such factors as the care executed in handling and use of the device, and the frequency of use. Recalibration should be performed after the period so chosen to ensure that the instrument's accuracy remains within the desired limits.

This certificate is issued in accordance with the conditions of the accreditation granted by the South African National Accreditation System (SANAS). It is a correct record of the measurements made. This certificate may not be reproduced other than in full except with prior written approval of the issuing laboratory. Legal liability shall be limited to the cost of recalibration and or certification, but the applicant indemnifies Unique Metrology (Pty) Ltd against any consequential or other loss.

The South African National Accreditation System (SANAS) is a member of the International Laboratory Accreditation Cooperation (ILAC) Mutual Recognition Arrangement (MRA). This arrangement allows for the mutual recognition of technical test and calibration data by the member accreditation bodies worldwide. For more information on the Arrangement please contact www.ilac.org.

Unique Metrology
Eskom Research & Innovation Centre
Lower Germiston Road • Rosherville
P O Box 145296 • Bracken Gardens • 1452
Tel: 011 626 3808 • Cell: 083 254 3635 • Fax: 086 610 4196
Web: www.unimet.co.za

sanas Calibration Laboratory 306 205

CERTIFICATE OF CALIBRATION

Certificate Number	: 1211T4452-1		
Calibration of a	: PT100 Resistance Thermometer		
Manufacturer & Type	: Wika 4 wire		
Serial Number	: TE-7855		
Calibrated for	: University of Stellenbosch, Process Engineering, Stellenbosch.		
Procedure Number	: 53-166-03		
Date of Calibration	: 23/11/2012		
Date of Issue	: 26/11/2012		
Laboratory Environment	: 21.4°C.		
Reference Standards	: 306-S-21	Fluke 9144 Block Calibrator	S/N B26027
	306-S-07	Hewlett Packard Multimeter	S/N 1206L5
	306-S-05	Time Electronics Current Sourse	S/N 3146A70688

Reference Temperature °C	Indicated Reading Ohms	Equivalent Temperature °C	Correction °C
40	115.565	40.1	-0.1
80	130.950	80.2	-0.1
140	153.622	140.1	-0.1
200	175.952	200.3	-0.3

The uncertainty of measurement is ± 0.3°C
The reported uncertainty is based on a standard uncertainty multiplied by a coverage factor of k=2, which unless specifically stated otherwise, provides a confidence level of 95%, in accordance with the Guide to the Uncertainty in Measurement, first edition, 1993.

Comments: The correction should be added to the indicated temperature to obtain the actual temperature.
The PT100 was submerged to a constant depth of 150mm in the block calibrator during the calibration.

Calibrated by : AJ Mathieson

Technical Signatory

ALEXANDER WIEGAND SE & Co. KG

WIKA

zertifiziert nach DIN ISO 9001
certified by DIN ISO 9001
DQS Reg. Nr. 1830-01

UniTrans

Messwertprotokoll für Drucktransmitter

Test certificate for Pressure Transmitter

Gerätedaten:
Instrument Data:

Kopf-Nr. Head No.	Messbereichsanfang Start of Range	Messbereichsende End of Range	Druckeinheit Unit of Pressure	Genauigkeit [%] Accuracy [%]
SZ65	0	1,6	bar / abs.	0,1

Ausgang bei 20°C:
Output at 20°C:

Nullpunkt Zero		Endwert Full Scale	
3,99	mA	20,00	mA

Kennlinienwerte:
Characteristics:

Referenzdruck Ref Pressure		Linearitätsabweichung [%] Deviation of linearity [%]	
[%]	[bar]	bei / at 10°C	bei / at 40°C
0	0,000	0,000	0,000
10	0,160	0,020	0,001
20	0,320	0,021	0,002
30	0,480	0,021	0,013
40	0,640	0,024	0,005
50	0,800	0,016	-0,005
60	0,960	0,014	0,014
70	1,120	0,003	0,009
80	1,280	0,028	0,010
90	1,440	0,022	0,009
100	1,600	0,000	0,000

Linearitätsabweichung [%]:

Deviation of linearity [%]:

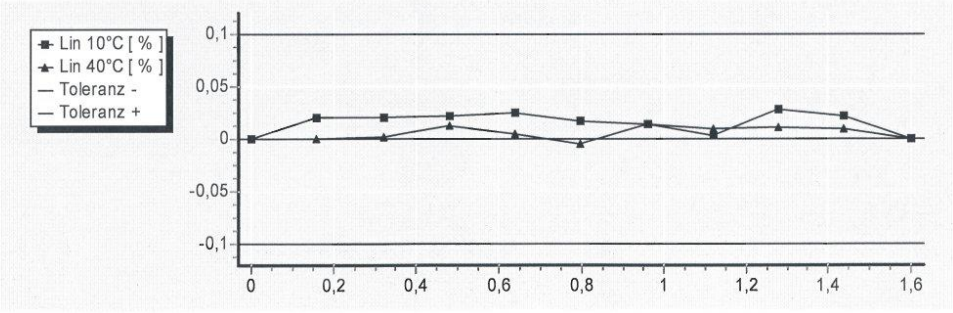

Referenzdruck [bar]
Ref ressure [bar]

Datum: 10.09.2012
Date:

geprüft von : 012
testet by:

Die Produktionsabteilung für Druckmessgeräte wird unterstützt und überwacht von dem WIKA DKD-Kalibrationslabor für Druck DKD-K-03701

The pressure department is supported and monitored by the WIKA pressure DKD-Calibration-Laboratory-DKD-K-03701

Druck + Temperatur

WIKA Alexander Wiegand SE & Co. KG
Alexander-Wiegand-Straße 30
63911 Klingenberg
Germany

Tel. +49 9372 132-0
Fax +49 9372 132-406
E-Mail info@wika.de
www.wika.de

Kommanditgesellschaft: Sitz Klingenberg - Amtsgericht Aschaffenburg HRA 1819
Komplementärin: WIKA Verwaltungs SE & Co. KG - Sitz Klingenberg - Amtsgericht Aschaffenburg HRA 4685

Komplementärin:
WIKA International SE - Sitz Klingenberg - Amtsgericht Aschaffenburg HRB 10505
Vorstand: Alexander Wiegand
Vorsitzender des Aufsichtsrats: Dr. Max Egli

TC Ltd, Units 1-6, Brimington Rd North, Chesterfield, S41 9BE, United Kingdom
Email: callab@tc.co.uk - Web: www.tc.co.uk
Tel: 01895 252222 - Fax: 01895 273540

KALIBRIERSCHEIN

Datum der Messung:	23 Dezember 2010
Auftraggeber:	Pilodist GmbH
Anschrift Auftraggeber:	Auf Der KaiserFuhr 43 53127 Bonn
Bestell-Nr. Auftraggeber:	Fax Vom 14.12.2010
Auftrag-Nr. TC GmbH:	AU23339
Auftragsdatum:	14 Dezember 2010
Kalibriergegenstand:	Pt100 6.0mm x 200mm
Serien Nr.	AU23339/1B
Typenbezeichnung:	16-1-6.0-4-200-CE1A-R100-1/10-2Mtrs RT47/NO BRAID/SMALL Platin-Widerstandsthermometer
Umgebungstemperatur:	20°C +/- 2°C

Zugelassener Unterzeichner:
L R Walker
K M Donaldson

KDonaldson

Kalibrierschein-Nr:
10034-1B

Kalibrierverfahren: Das Thermometer wurde durch Vergleich mit zwei Referenz-Widerstandsthermometern kalibriert. Die Kalibrierung erfolgte in einem gerührtem Wasserbad der Firma Grant und einem Hart Trockenblock-Kalibrator. Alle Messungen können auf nationale Normale zurückgeführt werden. Die Widerstände wurden mit Präzisions-Digitalmultimetern gemessen. Alle Messungen wurden unter kontrollierten Umgebungsbedingungen unter Verwendung von Geräten mit bekannten und zurückverfolgbaren Werten durchgeführt. Die Temperaturmessungen lassen sich auf die Internationale Temperaturskala ITS-90 zurückführen. Die Umrechnung der Widerstandswerte des Thermometers erfolgte gemäß IEC60751:2008.

Referenz-Temperatur (°C)	Widerstand Prüfling (Ω)	Temperatur kalkuliert gem. IEC (°C)	Fehler (°C)
49.88	119.369	49.93	0.05
199.83	175.832	199.93	0.10

Die Eintauchtiefe des geprüften Thermometers betrug 150mm

Kalibriert von: T Heath

Datum der Kalibrierung: 23 Dezember 2010

Die angegebenen signifikanten Stellen erleichtern dem Anwender des Kalibrierscheins die Interpolation, sie entsprechen nicht der tatsächlichen Messunsicherheit. Die Angaben zur Messgröße erfolgen ohne Berücksichtigung der Messunsicherheit.

Bemerkung: Es liegt in der Verantwortung des Anwenders die Langzeitdrift sowie die Messunsicherheit unter den Bedingungen der Nutzung zu bestimmen.

Issue 02/01

APPENDIX C - GC CALIBRATION CURVES & ERROR ANALYSIS RESULTS

C.1 Pressure effect error analysis

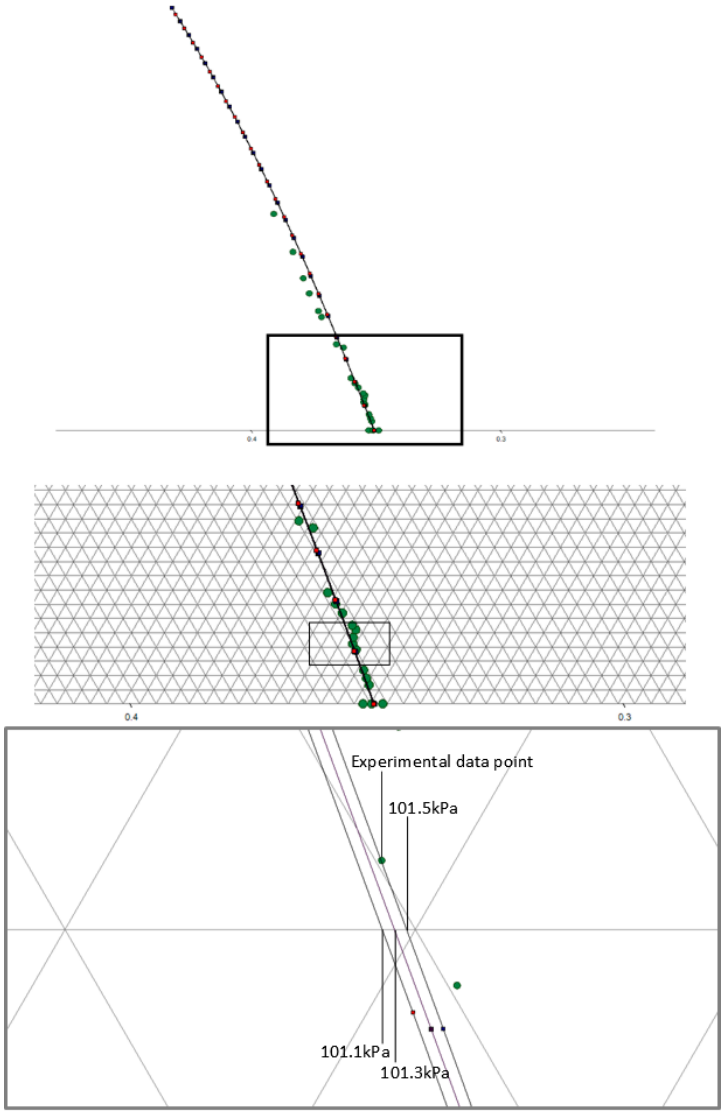

Figure C- 1: ***Error effects of pressure deviations on associated equilibrium composition measurements of the ethanol/MEK/water system at 101.1 kPa, 101.3 kPa and 101.5 kPa.***

Table C- 1: *Tabulated results for the analysis of the effect of pressure deviation on equilibrium compositions.*

Pressure (kPa)	Water (mol fraction)	MEK (mol fraction)	Ethanol (mol fraction)
101.1	0.347907	0.6387173	0.0133757
101.3	0.348029	0.6385953	0.0133757
101.5	0.348146	0.6384783	0.0133757
Deviation (101.3-101.1)	0.000122		
Deviation (101.3-101.5)	0.000117		
Maximum absolute deviation:	**0.000122**		

C.2 GC Calibration Curves

Ethanol/Isooctane System

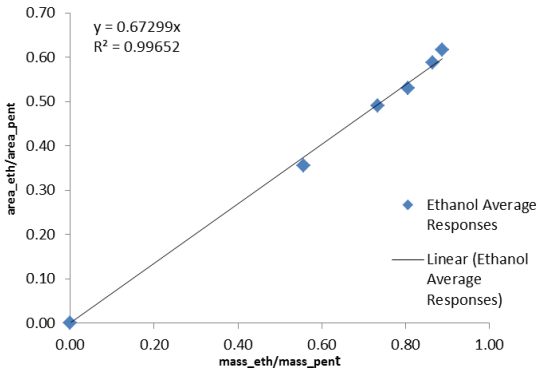

Figure C- 2: ***Ethanol calibration curve for GC analysis in ethanol/isooctane system.***

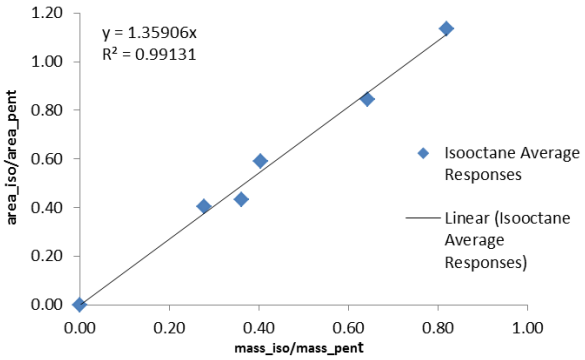

Figure C- 3: ***Isooctane calibration curve for GC analysis in ethanol/isooctane system.***

Table C- 2: ***Data used in calibration curve generation for ethanol/isooctane system.***

Sample	Component	Mass (g)	Run A		Run B		Run C		Average RF
			Area	*RF*	*Area*	*RF*	*Area*	*RF*	
	Ethanol	0.0453	993503	0.6138	993500	0.6176	1001503	0.618748	0.6167
S1	Isooctane	0.0184	700258	0.4326	690258	0.4291	710258	0.438811	0.4335
	2-Pentanol	0.0510	1618597	1.0000	1608597	1.0000	1618597	1	1.0000
	Ethanol	0.0245	594838	0.4899	589838	0.4898	594838	0.489878	0.4899
S2	Isooctane	0.0093	485225	0.3996	490025	0.4069	485225	0.399607	0.4020
	2-Pentanol	0.0334	1214257	1.0000	1204257	1.0000	1214257	1	1.0000
	Ethanol	0.0187	541749	0.3558	541751	0.3559	541750	0.355759	0.3558
S3	Isooctane	0.0216	1284558	0.8436	1284618	0.8440	1284566	0.843555	0.8437
	2-Pentanol	0.0336	1522797	1.0000	1522097	1.0000	1522800	1	1.0000
	Ethanol	0.0183	421232	0.5309	420232	0.5297	421241	0.530945	0.5305
S4	Isooctane	0.0186	900361	1.1348	900433	1.1349	900357	1.134837	1.1349
	2-Pentanol	0.0227	793384	1.0000	793390	1.0000	793380	1	1.0000
	Ethanol	0.0344	943730	0.5882	943727	0.5882	943740	0.589704	0.5887
S5	Isooctane	0.0161	943741	0.5882	943749	0.5882	943744	0.589706	0.5887
	2-Pentanol	0.0398	1604363	1.0000	1604359	1.0000	1600363	1	1.0000

Ethanol/1-Butanol/Water System

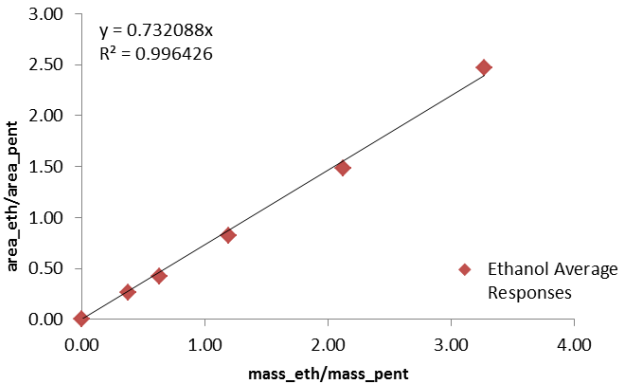

Figure C- 4: ***Ethanol calibration curve for GC analysis in ethanol/1-butanol/water system.***

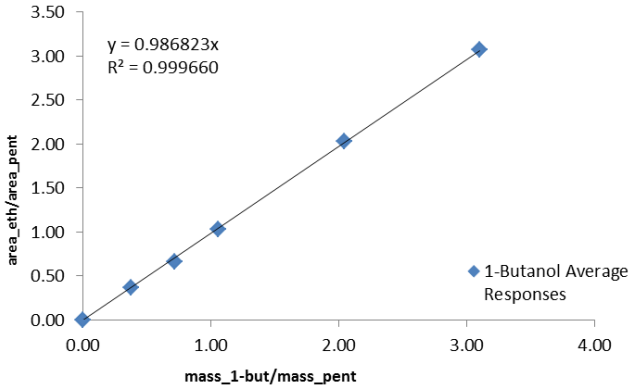

Figure C- 5: ***1-Butanol calibration curve for GC analysis in ethanol/1-butanol/water system.***

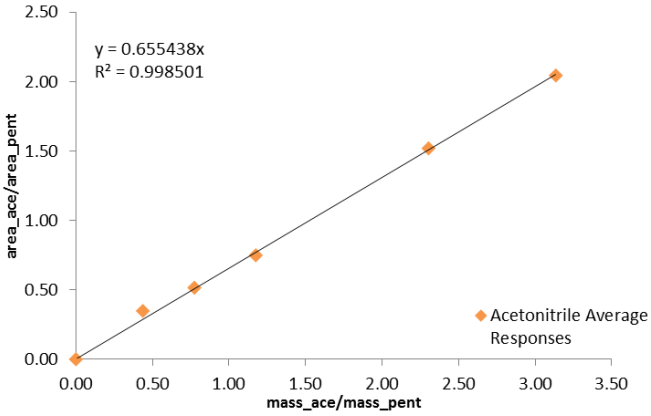

Figure C- 6: ***Acetonitrile calibration curve for GC analysis in ethanol/1-butanol/water system.***

Table C- 3: ***Data used in calibration curve generation for ethanol/1-butanol/water system.***

Sample	Component	Mass (g)	Run A		Run B		Run C		Average RF
			Area	*RF*	*Area*	*RF*	*Area*	*RF*	
	Acetonitrile	0.0500	1734873	0.4527	1644100	0.4482	1490697	0.43648203	0.4458
S1	Ethanol	0.0267	1013618	0.2645	954202	0.2601	898696	0.26314178	0.2626
	1-Butanol	0.0264	1453528	0.3793	1357816	0.3702	1241574	0.36353782	0.3710
	2-Pentanol	0.0705	3831931	1.0000	3667956	1.0000	3415254	1	1.0000
	Acetonitrile	0.0455	1639060	0.5592	1517000	0.5524	1411049	0.55170307	0.5544
S2	Ethanol	0.0315	1224814	0.4179	1155658	0.4208	1086424	0.42477862	0.4212
	1-Butanol	0.0358	1945378	0.6637	1822463	0.6636	1706574	0.66724976	0.6649
	2-Pentanol	0.0501	2931074	1.0000	2746247	1.0000	2557624	1	1.0000
	Acetonitrile	0.0334	1204463	0.5756	1137920	0.5750	1069718	0.55455427	0.5684
S3	Ethanol	0.0457	1721229	0.8226	1624783	0.8211	1580766	0.81948751	0.8211
	1-Butanol	0.0407	2147448	1.0263	2033750	1.0277	1981100	1.02702532	1.0270
	2-Pentanol	0.0384	2092380	1.0000	1978906	1.0000	1928969	1	1.0000
	Acetonitrile	0.0281	951240	0.8339	882131	0.8299	879079	0.78774543	0.8172
S4	Ethanol	0.0497	1681886	1.4744	1597894	1.5033	1638017	1.46783214	1.4819
	1-Butanol	0.0479	2351626	2.0615	2135084	2.0087	2273029	2.03686837	2.0357
	2-Pentanol	0.0234	1140743	1.0000	1062893	1.0000	1115943	1	1.0000
	Acetonitrile	0.0173	511393	0.850669949	464394	0.8397	494485	0.65854152	0.7830
	Ethanol	0.0661	1483213	2.467231126	1403569	2.5379	1806827	2.4062825	2.4705
S5	1-Butanol	0.0627	1833104	3.049252701	1691642	3.0588	2325284	3.09674928	3.0683
	2-Pentanol	0.0202	601165	1	553033	1	750879	1	1.0000

Ethanol/2-Butanone/Water System

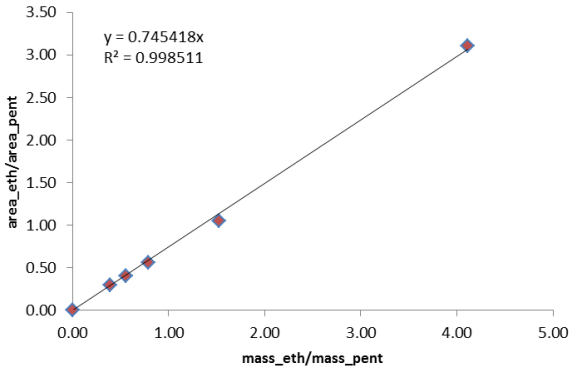

Figure C- 7: ***Ethanol calibration curve for GC analysis in ethanol/2-butanone/water system.***

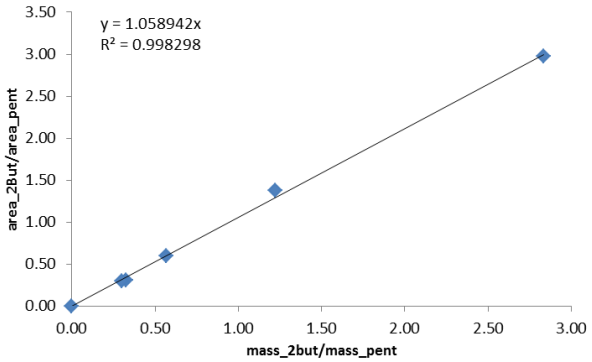

Figure C- 8: ***2-Butanone calibration curve for GC analysis in ethanol/2-butanone/water system.***

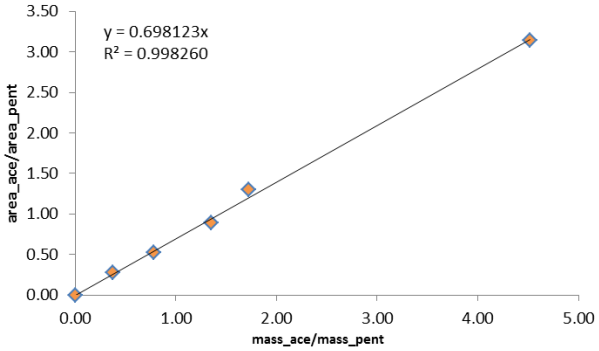

Figure C- 9: ***Acetonitrile calibration curve for GC analysis in ethanol/2-butanone/water system.***

Table C- 4: ***Data used in calibration curve generation for ethanol/2-butanone/water system.***

Sample	Component	Mass (g)	Run A		Run B		Run C		Average RF
			Area	*RF*	*Area*	*RF*	*Area*	*RF*	
B1	2-Butanone	0.0240	836288	0.317354	769905	0.29709	743098	0.30593	0.30679
	Pentanol	0.0735	2635187	1	2591474	1	2428922	1	
B2	2-Butanone	0.0211	575411	0.307463	494762	0.29059	461096	0.29028	0.29611
	Pentanol	0.0696	1871476	1	1702593	1	158845	1	
B3	2-Butanone	0.0325	417916	0.575241	344803	0.57779	327294	0.63090	0.59464
	Pentanol	0.0570	726505	1	596754	1	518769	1	
B4	2-Butanone	0.0485	726649	1.299030	627558	1.34415	595126	1.49640	1.37986
	Pentanol	0.0397	559378	1	466881	1	397703	1	
B5	2-Butanone	0.0609	1858313	3.053934	2026841	2.92811	190590	2.93196	2.97134
	Pentanol	0.0215	608498	1	692199	1	650043	1	0
A1	Acetonitrile	0.0226	368815	0.259422	321948	0.26631	290572	0.28981	0.27185
	Pentanol	0.0611	1421678	1	1208894	1	100262	1	
A2	Acetonitrile	0.0377	797142	0.519060	782939	0.52497	724316	0.53272	0.52558
	Pentanol	0.0485	1535739	1	1491371	1	135964	1	
A3	Acetonitrile	0.0393	778493	0.880477	744812	0.88925	675033	0.91611	0.89528
	Pentanol	0.0291	884171	1	837567	1	736846	1	
A4	Acetonitrile	0.0549	545338	1.219079	630272	1.26599	525204	1.40057	1.29521
	Pentanol	0.0318	447336	1	497846	1	374991	1	
A5	Acetonitrile	0.0809	1112280	3.003313	1020786	3.26115	104239	3.14612	3.13686
	Pentanol	0.0179	370351	1	313014	1	331326	1	
E1	Ethanol	0.0311	396603	0.311957	436216	0.31408	350321	0.27342	0.29982
	Pentanol	0.0796	1271337	1	1388855	1	128122	1	
E2	Ethanol	0.0327	1132738	0.406672	1048966	0.40161	102032	0.40480	0.40436
	Pentanol	0.0592	2785384	1	2611854	1	252051	1	
E3	Ethanol	0.0400	1384256	0.560081	1369368	0.56446	137681	0.56225	0.56226
	Pentanol	0.0509	2471524	1	2425947	1	244873	1	
E4	Ethanol	0.0609	1608700	1.033046	1394723	1.0088	160875	1.10305	1.0483
	Pentanol	0.0400	1557239	1	1382557	1	145845	1	
E5	Ethanol	0.0917	1459352	3.171938	1385016	3.03183	142218	3.10213	3.10197
	Pentanol	0.0223	460082	1	456824	1	458453	1	

n-Propanol/2-Butanone/Water System

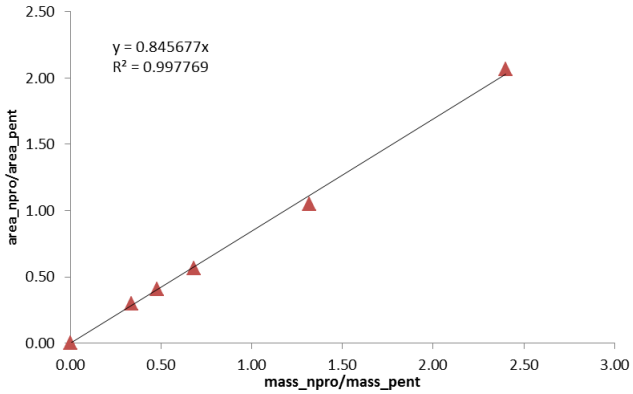

Figure C- 10: ***n-Propanol calibration curve for GC analysis in n-propanol/2-butanone/water system.***

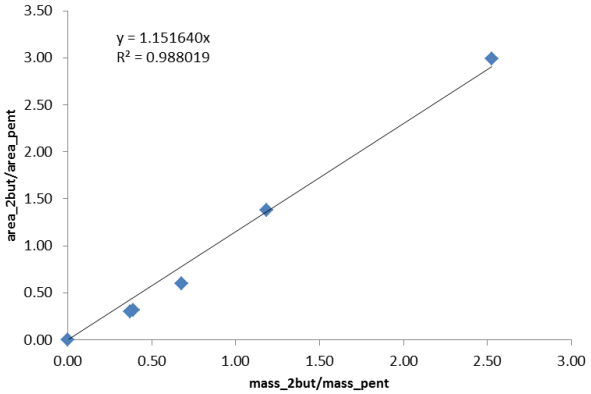

Figure C- 11: ***2-Butanone calibration curve for GC analysis in n-propanol/2-butanone/water system.***

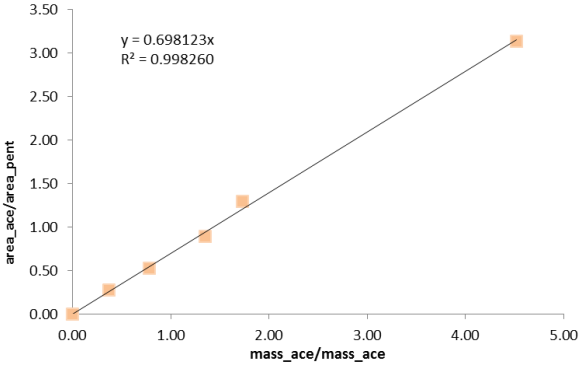

Figure C- 12: ***Acetonitrile calibration curve for GC analysis in n-propanol/2-butanone/water system.***

Table C- 5: ***Data used in calibration curve generation for n-propanol/2-butanone/water system.***

Sample	Component	Mass (g)	Run A		Run B		Run C		Average RF
			Area	*RF*	*Area*	*RF*	*Area*	*RF*	
B1	2-Butanone	0.0300	836466	0.31741	770083	0.29714	803274.5	0.33069	0.31508
	Pentanol	0.0773	2635287	1	2591574	1	2429022	1	
B2	2-Butanone	0.0271	575546	0.307505	494897	0.29064	461231	0.29033	0.29615
	Pentanol	0.0734	1871663	1	1702780	1	1588640	1	
B3	2-Butanone	0.0385	418261	0.575443	345148	0.57804	327639	0.63115	0.59487
	Pentanol	0.0570	726850	1	597099	1	519114	1	
B4	2-Butanone	0.0515	727502	1.298575	628411	1.34352	595979	1.49534	1.37914
	Pentanol	0.0435	560231	1	467734	1	398556	1	
B5	2-Butanone	0.0639	1858370	3.053637	2026898	2.92782	1942634	2.98668	2.98938
	Pentanol	0.0253	608576	1	692288	1	650432	1	
A1	Acetonitrile	0.0236	0.0226	368815	0.259422	321948	0.26631	290572	0.28981
	Pentanol	0.0649	0.0611	1421678	1	1208894	1	1002621	
A2	Acetonitrile	0.0387	0.0377	797142	0.519061	782939	0.52497	724316	0.53272
	Pentanol	0.0523	0.0485	1535739	1	1491371	1	1359642	
A3	Acetonitrile	0.0403	0.0393	778493	0.880478	744812	0.88925	675033	0.91611
	Pentanol	0.0329	0.0291	884171	1	837567	1	736846	
A4	Acetonitrile	0.0559	0.0549	545338	1.219079	630272	1.26599	525204	1.40057
	Pentanol	0.0356	0.0318	447336	1	497846	1	374991	
A5	Acetonitrile	0.0819	0.0809	1112280	3.003313	1020786	3.26115	1042393	3.14612
	Pentanol	0.0217	0.0179	370351	1	313014	1	331326	
Sample	Component	Mass (g)	Run A		Run B		Run C		Average RF
			Area	*RF*	*Area*	*RF*	*Area*	*RF*	
E1	n-Propanol	0.0316	396603	0.311957	436216	0.31408	350321	0.27342	0.29982
	Pentanol	0.0834	1271337	1	1388855	1	1281226	1	
E2	n-Propanol	0.0332	1132738	0.406672	1048966	0.40161	1020322	0.40480	0.40436
	Pentanol	0.0630	2785384	1	2611854	1	2520517	1	
E3	n-Propanol	0.0405	1384256	0.560082	1369368	0.56446	1376812	0.56225	0.56226
	Pentanol	0.0509	2471524	1	2425947	1	2448736	1	
E4	n-Propanol	0.0547	1608700	1.033046	1394723	1.0088	1608751	1.10305	1.0483
	Pentanol	0.0438	1557239	1	1382557	1	1458451	1	
E5	n-Propanol	0.0922	1459352	2.129083	1385016	2.00760	1422184	2.06814	2.06827
	Pentanol	0.0261	685437	1	689886	1	687661.5	1	

iso-Propanol/2-Butanone/Water System

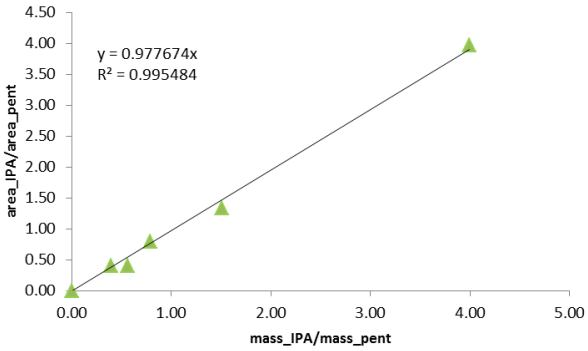

Figure C- 13: ***iso-Propanol calibration curve for GC analysis in IPA/2-butanone/water system.***

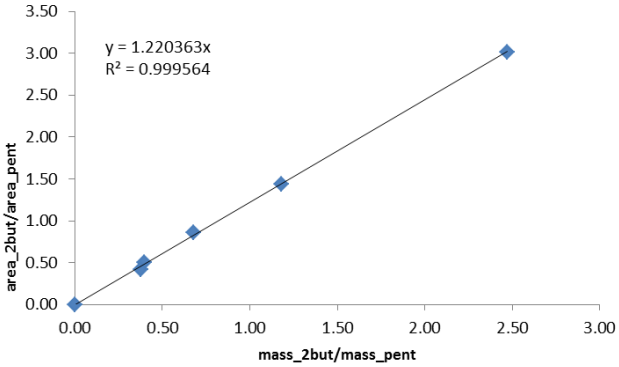

Figure C- 14: ***2-Butanone calibration curve for GC analysis in IPA/2-butanone/water system.***

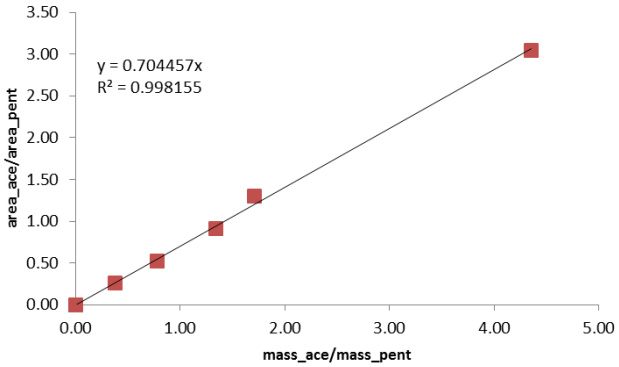

Figure C- 15: ***Acetonitrile calibration curve for GC analysis in IPA/2-butanone/water system.***

Table C- 6: ***Data used in calibration curve generation for IPA/2-butanone/water system.***

Sample	Component	Mass (g)	Run A		Run B		Run C		Average RF
			Area	*RF*	*Area*	*RF*	*Area*	*RF*	
B1	2-Butanone	0.0300	836466	0.31741	770083	0.29714	803274	0.33069	0.31508
	Pentanol	0.0773	2635287	1	2591574	1	2429022	1	
B2	2-Butanone	0.0271	575546	0.307505	494897	0.29064	461231	0.29033	0.29615
	Pentanol	0.0734	1871663	1	1702780	1	1588640	1	
B3	2-Butanone	0.0385	418261	0.575443	345148	0.57804	327639	0.63115	0.59487
	Pentanol	0.0570	726850	1	597099	1	519114	1	
B4	2-Butanone	0.0515	727502	1.298575	628411	1.34352	595979	1.49534	1.37914
	Pentanol	0.0435	560231	1	467734	1	398556	1	
B5	2-Butanone	0.0639	1858370	3.053637	2026898	2.92782	1942634	2.98668	2.98938
	Pentanol	0.0253	608576	1	692288	1	650432	1	
A1	Acetonitrile	0.0226	368815	0.259422	321948	0.26631	290572	0.28981	0.27185
	Pentanol	0.0611	1421678	1	1208894	1	1002621	1	
A2	Acetonitrile	0.0377	797142	0.519061	782939	0.52497	724316	0.53272	0.52558
	Pentanol	0.0485	1535739	1	1491371	1	1359642	1	
A3	Acetonitrile	0.0393	778493	0.880478	744812	0.88925	675033	0.91611	0.89528
	Pentanol	0.0291	884171	1	837567	1	736846	1	
A4	Acetonitrile	0.0549	545338	1.219079	630272	1.26599	525204	1.40057	1.29521
	Pentanol	0.0318	447336	1	497846	1	374991	1	
A5	Acetonitrile	0.0809	1112280	3.003313	1020786	3.26115	1042393	3.14612	3.13686
	Pentanol	0.0179	370351	1	313014	1	331326	1	
Sample	Component	Mass (g)	Run A		Run B		Run C		Average RF
			Area	*RF*	*Area*	*RF*	*Area*	*RF*	
E1	IPA	0.0311	396603	0.311957	436216	0.31408	350321	0.27342	0.29982
	Pentanol	0.0796	1271337	1	1388855	1	1281226	1	
E2	IPA	0.0327	1132738	0.406672	1048966	0.40161	1020322	0.40480	0.40436
	Pentanol	0.0592	2785384	1	2611854	1	2520517	1	
E3	IPA	0.0400	1384256	0.560082	1369368	0.56446	1376812	0.56225	0.56226
	Pentanol	0.0509	2471524	1	2425947	1	2448736	1	
E4	IPA	0.0609	1608700	1.033046	1394723	1.0088	1608751	1.10305	1.0483
	Pentanol	0.0400	1557239	1	1382557	1	1458451	1	
E5	IPA	0.0917	1459352	2.129083	1385016	2.00760	1422184	2.06814	2.06827
	Pentanol	0.0223	685437	1	689886	1	687661	1	

C.3 GC Error Analysis

Ethanol/Isooctane System

Table C- 7: ***Repeatability results for GC error analysis in Ethanol/Isooctane system.***

Sample	Mass added (g)			Mole Fraction		Area			Predicted mass (g)		Mole Ethanol (mol)	Mole Isooctane (mol)	Mole Fraction		Absolute Error	Average Absolute Error
	Ethanol	Isooctane	2-Pentanol	Ethanol	Isooctane	Ethanol	Isooctane	Pentanol	Ethanol	Isooctane			Ethanol	Isooctane		
S1A	0.0455	0.0256	0.0339	0.815133	0.184867	1347924	1592210	1355951	0.050074	0.029289	0.0010870	0.0002565	0.809076	0.190924	0.00606	0.00292
S1B	0.0455	0.0256	0.0339	0.815133	0.184867	1285736	1441269	1241943	0.052149	0.028946	0.0011320	0.0002535	0.817034	0.182966	0.00190	
S1C	0.0455	0.0256	0.0339	0.815133	0.184867	1182488	1349467	1162091	0.051256	0.028965	0.0011126	0.0002537	0.814344	0.185656	0.00079	
S2A	0.0369	0.0243	0.0337	0.790233	0.209767	988980	1275680	1146979	0.043177	0.027578	0.0009372	0.0002415	0.795111	0.204889	0.00488	0.00923
S2B	0.0369	0.0243	0.0337	0.790233	0.209767	981457	1217792	1109983	0.044277	0.027204	0.0009611	0.0002382	0.801361	0.198639	0.01113	
S2C	0.0369	0.0243	0.0337	0.790233	0.209767	873645	1080130	1000068	0.043745	0.026781	0.0009496	0.0002345	0.801932	0.198068	0.01170	
S3A	0.0408	0.0334	0.0193	0.751891	0.248109	1209505	1978719	849671	0.040823	0.03307	0.0008861	0.0002896	0.75368	0.24632	0.00179	0.00326
S3B	0.0408	0.0334	0.0193	0.751891	0.248109	1201515	1947877	830227	0.041503	0.033317	0.0009009	0.0002918	0.755362	0.244638	0.00347	
S3C	0.0408	0.0334	0.0193	0.751891	0.248109	1124338	1812313	759952	0.042429	0.033865	0.0009210	0.0002966	0.756423	0.243577	0.00453	

Ethanol/1-Butanol/Water System

Table C- 8: ***Repeatability results for GC error analysis in Ethanol/1-butanol/water system.***

Sample	Mass added (g)				Mole Fraction			Predicted mass from GC (g)			Mole Fraction from GC			Absolute Error	Average Absolute Error
	Ethanol	Butanol	Acetonitrile	Pentanol	Ethanol	Butanol	Acetonitrile	Ethanol	Butanol	Acetonitrile	Ethanol	Butanol	Acetonitrile		
S3A	0.0408	0.0334	0.0287	0.0193	0.4351	0.2214	0.3435	0.0409	0.0342	0.0299	0.4274	0.2220	0.3506	0.00770	
S3B	0.0408	0.0334	0.0287	0.0193	0.4351	0.2214	0.3435	0.0409	0.0334	0.0287	0.4356	0.2209	0.3436	0.00044	0.00276
S3C	0.0408	0.0334	0.0287	0.0193	0.4351	0.2214	0.3435	0.0408	0.0315	0.0297	0.4353	0.2086	0.3562	0.00016	
S4A	0.0233	0.0205	0.0410	0.0250	0.2840	0.1553	0.5608	0.0255	0.0213	0.0456	0.2834	0.1470	0.5696	0.00051	
S4B	0.0233	0.0205	0.0410	0.0250	0.2840	0.1553	0.5608	0.0249	0.0204	0.0458	0.2797	0.1427	0.5777	0.00429	0.00217
S4C	0.0233	0.0205	0.0410	0.0250	0.2840	0.1553	0.5608	0.0239	0.0225	0.0416	0.2823	0.1658	0.5519	0.00171	
S5A	0.0182	0.0332	0.0352	0.0523	0.2323	0.2634	0.5043	0.0198	0.0341	0.0359	0.2440	0.2609	0.4951	0.01168	
S5B	0.0182	0.0332	0.0352	0.0523	0.2323	0.2634	0.5043	0.0188	0.0333	0.0360	0.2348	0.2594	0.5057	0.00252	0.00976
S5C	0.0182	0.0332	0.0352	0.0523	0.2323	0.2634	0.5043	0.0184	0.0369	0.0385	0.2172	0.2711	0.5117	0.01509	

Ethanol/MEK/Water System

Table C- 9: ***Repeatability results for GC error analysis in Ethanol/MEK/water system.***

Sample	Mass added (g)				Mole Fraction			Predicted mass from GC (g)			Mole Fraction from GC			Absolute Error	Average Absolute Error
	Ethanol	MEK	Acetonitrile	Pentanol	Ethanol	MEK	Acetonitrile	Ethanol	MEK	Acetonitrile	Ethanol	MEK	Acetonitrile		
S3A	0.0455	0.0209	0.0235	0.014	0.5339	0.1567	0.3094	0.0469	0.0216	0.0236	0.5377	0.1584	0.3039	0.003833	
S3B	0.0455	0.0209	0.0235	0.014	0.5339	0.1567	0.3094	0.0452	0.0208	0.0257	0.5173	0.1522	0.3304	0.016542	0.00849
S3C	0.0455	0.0209	0.0235	0.014	0.5339	0.1567	0.3094	0.0459	0.0200	0.0236	0.5390	0.1500	0.3110	0.005090	
S4A	0.0225	0.0530	0.0168	0.0304	0.2991	0.4502	0.2507	0.0226	0.0531	0.0167	0.3003	0.4507	0.2490	0.001123	
S4B	0.0225	0.0530	0.0168	0.0304	0.2991	0.4502	0.2507	0.0234	0.0533	0.0159	0.3108	0.4522	0.2370	0.011629	0.01010
S4C	0.0225	0.0530	0.0168	0.0304	0.2991	0.4502	0.2507	0.0203	0.0512	0.0170	0.2816	0.4537	0.2647	0.017548	
S5A	0.0599	0.0182	0.0329	0.0572	0.5523	0.1072	0.3405	0.0601	0.0184	0.0323	0.5560	0.1086	0.3354	0.003714	
S5B	0.0599	0.0182	0.0329	0.0572	0.5523	0.1072	0.3405	0.0601	0.0184	0.0330	0.5519	0.1080	0.3401	0.000395	0.00352
S5C	0.0599	0.0182	0.0329	0.0572	0.5523	0.1072	0.3405	0.0589	0.0182	0.0333	0.5459	0.1078	0.3464	0.006447	

n-Propanol/MEK/Water System

Table C- 10: ***Repeatability results for GC error analysis in n-Propanol/MEK/water system.***

Sample	Mass added (g)				Mole Fraction			Predicted mass from GC (g)			Mole Fraction from GC			Absolute Error	Average Absolute Error
	n-Prop	MEK	Acetonitrile	Pentanol	n-Prop	MEK	Acetonitrile	n-Prop	MEK	Acetonitrile	n-Prop	MEK	Acetonitrile		
S3A	0.0208	0.0767	0.0874	0.0881	0.09780	0.30056	0.60163	0.02489	0.07480	0.08840	0.1149	0.2877	0.5974	0.01709	
S3B	0.0208	0.0767	0.0874	0.0881	0.09780	0.30056	0.60163	0.02140	0.07670	0.08710	0.1005	0.3003	0.5991	0.00275	0.00664
S3C	0.0208	0.0767	0.0874	0.0881	0.09780	0.30056	0.60163	0.02090	0.07860	0.08680	0.0979	0.3068	0.5953	0.00010	
S4A	0.0252	0.0119	0.0121	0.0553	0.47699	0.18772	0.33529	0.02590	0.01210	0.01290	0.4720	0.1838	0.3442	0.00496	
S4B	0.0252	0.0119	0.0121	0.0553	0.47699	0.18772	0.33529	0.02670	0.01210	0.01400	0.4661	0.1760	0.3578	0.01085	0.01384
S4C	0.0252	0.0119	0.0121	0.0553	0.47699	0.18772	0.33529	0.02770	0.01180	0.01200	0.5027	0.1785	0.3188	0.02572	
S5A	0.0543	0.0447	0.0686	0.0725	0.28284	0.19404	0.52311	0.05970	0.04500	0.07000	0.2990	0.1878	0.5132	0.01614	
S5B	0.0543	0.0447	0.0686	0.0725	0.28284	0.19404	0.52311	0.05500	0.04510	0.06790	0.2865	0.1958	0.5178	0.00363	0.00682
S5C	0.0543	0.0447	0.0686	0.0725	0.28284	0.19404	0.52311	0.05420	0.04460	0.06880	0.2822	0.1935	0.5243	0.00068	

IPA/MEK/Water System

Table C- 11: ***Repeatability results for GC error analysis in IPA/MEK/water system.***

Sample	Mass added (g)				Mole Fraction			Predicted mass from GC (g)			Mole Fraction from GC			Absolute Error	Average Absolute Error
	IPA	MEK	Acetonitrile	Pentanol	IPA	MEK	Acetonitrile	IPA	MEK	Acetonitrile	IPA	MEK	Acetonitrile		
S3A	0.0258	0.0735	0.0387	0.0428	0.17953	0.42623	0.39423	0.0261	0.0731	0.039	0.18111	0.42272	0.39617	0.00158	
S3B	0.0258	0.0735	0.0387	0.0428	0.17953	0.42623	0.39423	0.0260	0.0736	0.0380	0.18186	0.42903	0.38911	0.00233	0.00197
S3C	0.0258	0.0735	0.0387	0.0428	0.17953	0.42623	0.39423	0.0262	0.0741	0.0385	0.18155	0.42791	0.39055	0.00202	
S4A	0.076	0.0603	0.064	0.0492	0.34554	0.22848	0.42598	0.0761	0.0605	0.0642	0.34512	0.22865	0.42623	0.00042	
S4B	0.076	0.0603	0.0640	0.0492	0.34554	0.22848	0.42598	0.0758	0.0610	0.0649	0.34199	0.22936	0.42866	0.00355	0.00200
S4C	0.076	0.0603	0.0640	0.0492	0.34554	0.22848	0.42598	0.0759	0.0603	0.0630	0.34756	0.23011	0.42233	0.00202	
S5A	0.0231	0.0193	0.0166	0.0764	0.36386	0.25335	0.38279	0.0245	0.0194	0.0169	0.37457	0.24718	0.37825	0.01071	
S5B	0.0231	0.0193	0.0166	0.0764	0.36386	0.25335	0.38279	0.0239	0.0196	0.0160	0.37545	0.25660	0.36796	0.01159	0.00819
S5C	0.0231	0.0193	0.0166	0.0764	0.36386	0.25335	0.38279	0.0231	0.0190	0.0165	0.36615	0.25098	0.38287	0.00229	

C.4 Karl Fischer Error Analysis

Table C- 12: *Repeatability and error analysis results for Karl Fisher Analysis.*

Sample	Water (g)	Methanol (g)	Total (g)	Water (wt%)	KF measured water (wt%)				
					Run A	Run B	Run C	Average	Absolute Error
1	0.00000	0.03000	0.03000	0	0.0000	0.0000	0.0000	0.0000	0.0000
2	0.00021	16.47816	16.47837	0.00130	0.0000	0.0000	0.0000	0.0000	0.0013
3	0.00061	23.59163	23.59224	0.00260	0.0000	0.0000	0.0000	0.0000	0.0026
4	0.00125	25.42999	25.43124	0.00490	0.0000	0.0000	0.0000	0.0000	0.0049
5	0.00232	26.93161	26.93393	0.00860	0.0087	0.0089	0.0119	0.0098	0.0012
6	0.00142	11.90914	11.91056	0.01190	0.0156	0.0103	0.0129	0.0129	0.0010
7	0.00602	19.19174	19.19776	0.03135	0.0326	0.0457	0.0460	0.0414	0.0101
8	0.02220	10.45760	10.47979	0.21181	0.2257	0.2675	0.2111	0.2348	0.0230
9	0.02226	0.91591	0.93818	2.37306	2.3657	2.3737	2.3985	2.3793	0.0062
10	0.02382	0.89869	0.92250	2.58165	2.5897	2.6587	2.5488	2.5990	0.0174
11	0.02462	0.16384	0.18846	13.06228	13.0257	13.0569	13.0634	13.0486	0.0136
12	0.03338	0.19192	0.22530	14.81504	14.8155	14.8652	14.8166	14.8324	0.0174
13	0.03424	0.14098	0.17522	19.54262	19.5446	19.5412	19.5429	19.5429	0.0003
14	0.03480	0.12777	0.16257	21.40394	21.4003	21.4055	21.4625	21.4228	0.0188
15	0.03751	0.12319	0.16070	23.33883	23.3431	23.3336	23.3362	23.3376	0.0012
16	0.04109	0.11083	0.15192	27.04605	27.0540	27.0384	27.0422	27.0449	0.0012
17	0.04147	0.10344	0.14491	28.61701	28.6177	28.6091	28.6130	28.6133	0.0037
18	0.04184	0.08542	0.12726	32.87682	32.8795	32.8696	32.8732	32.8741	0.0027
19	0.04225	0.07358	0.11583	36.47435	36.4752	36.4672	36.4708	36.4711	0.0033
20	0.04883	0.06943	0.11826	41.29335	41.2965	41.2864	41.2899	41.2910	0.0024
21	0.05114	0.05843	0.10957	46.67750	46.6794	46.6697	46.6736	46.6742	0.0033
22	0.05657	0.06169	0.11826	47.83805	47.8399	47.8327	47.8354	47.8360	0.0021
23	0.05673	0.04727	0.10400	54.55191	54.5547	54.5445	54.5482	54.5491	0.0028
24	0.05748	0.03875	0.09623	59.73057	59.7325	59.7298	59.7302	59.7308	0.0002
25	0.05966	0.03941	0.09907	60.22356	60.2314	60.2192	60.2214	60.2240	0.0004
26	0.05983	0.03692	0.09675	61.83785	61.8440	61.8307	61.8343	61.8363	0.0015
27	0.06268	0.03290	0.09558	65.58121	65.5828	65.5783	65.5797	65.5803	0.0009
28	0.06304	0.02825	0.09129	69.05909	69.0666	69.0568	69.0579	69.0605	0.0014
29	0.06973	0.02561	0.09534	73.13873	73.1475	73.1385	73.1386	73.1415	0.0028
30	0.07993	0.02824	0.10816	73.89350	73.8994	73.8924	73.8929	73.8949	0.0014
31	0.08266	0.02353	0.10618	77.84370	77.8469	77.8417	77.8427	77.8438	0.0001
32	0.08648	0.01708	0.10356	83.50871	83.5157	83.5014	83.5051	83.5074	0.0013
33	0.09018	0.01223	0.10240	88.05968	88.0645	88.0555	88.0576	88.0592	0.0005
34	0.09512	0.01124	0.10636	89.43278	89.4347	89.4318	89.4323	89.4329	0.0001
35	0.09516	0.00618	0.10134	93.89857	93.9066	93.8923	93.8955	93.8981	0.0005
36	0.09888	0.00000	0.09888	100	99.9998	100.0000	99.9980	99.9993	0.0007

APPENDIX D - SAMPLE CALCULATION

For each data set of a ternary system, consisting of a low-molecular weight alcohol (A), entrainer (E) and water (W), the following steps and calculations were performed. The following explanation the vapour sample taken from the equilibrium still as an example (see Figure D-1).

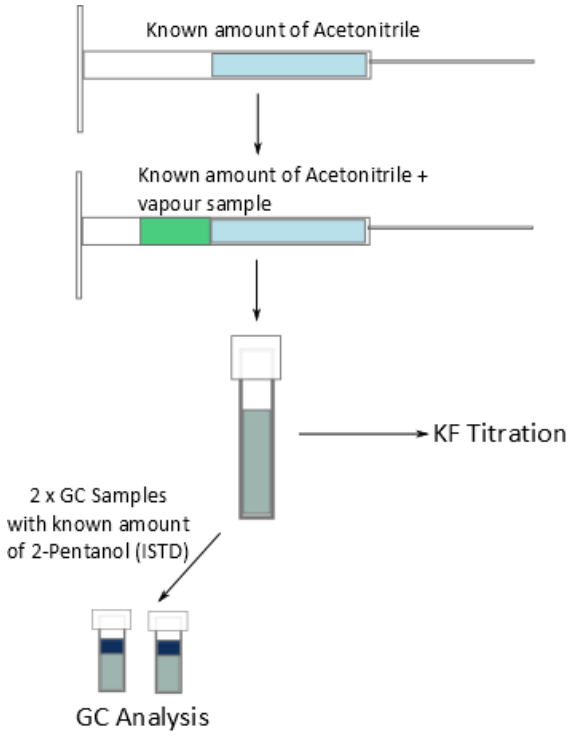

Figure D- 1: ***Schematic of vapour phase sampling and analysis sequence.***

For each component (A, E and Acetonitrile) a calibration curve is constructed through the addition of an internal standard (ISTD). For this research project, 5-pentanol was chosen as standard, due to its unique retention time.

From the GC calibration curve:

$$\frac{area_{comp}}{area_{ISTD}} = c\frac{mass_{comp}}{mass_{ISTD}} \qquad [D.1]$$

The constant *c* for each component is found. After analysing the two GC samples prepared, the mass of each of the components are known due to the fact that a known amount of ISTD has been added and the *c*-constant is known from the calibration curves:

$$mass_{comp} = \frac{mass_{ISTD} \times area_{comp}}{c \times area_{ISTD}} \qquad [D.2]$$

Assuming that a representative sample from the vial is used to make-up the GC samples:

$$\frac{mass_A^{GC}}{mass_{Acetonitrile}^{GC}} = \frac{mass_A^{Vial}}{mass_{Acetonitrile}^{Vial}} \quad [D.2]$$

The amount of each component in the original vial can be calculated (the amount of Acetonitrile in the GC samples has been measured and the amount of Acetonitrile in the original sample has been weighed).

The water content (w%) of the sample in the vial is determined by Karl Fischer titration:

$$mass_W^{Vial} = (w\%) \times 100 \times mass_{total}^{Vial} \quad [D.3]$$

From the known weights the molar amounts can be calculated:

$$n_{comp} = \frac{m_W^{Vial}}{Mw} \quad [D.4]$$

And the mole fraction of each component:

$$n_{component}^{fraction} = \frac{n_{component}}{n_{total}} \quad [D.5]$$

APPENDIX E - EXPERIMENTAL DATA

D.1 Verfication Data

Ethanol/Isooctane System

Table D- 1: ***Vapour – liquid equilibrium experimental results for ethanol/isooctane at 101.3 kPa.***

Temperature (K)	Liquid_eth (x)	Vapour_eth (y)
344.38	0.635846	0.622853
344.43	0.646647	0.622722
344.46	0.592445	0.654256
344.48	0.697447	0.654036
345.70	0.275197	0.629273
345.80	0.877350	0.739873
346.11	0.894667	0.760977
346.48	0.923058	0.741905
346.50	0.915952	0.758238
346.50	0.138478	0.560787
346.97	0.931675	0.789143
348.05	0.069746	0.524518
349.24	0.963520	0.885970
349.29	0.977733	0.896188
349.70	0.057588	0.518647
351.45	1.000000	1.000000
361.91	0.020052	0.279899
371.37	0.000000	0.000000

Ethanol/1-butanol/water System

Table D- 2: ***Vapour-liquid-liquid equilibrium experimental results for ethanol/1-butanol/water at 101.3 kPa.***

Temperature (K)	Organic			Aqueous			Vapor phase		
	x_{water}	$x_{butanol}$	$x_{ethanol}$	x_{water}	$x_{butanol}$	$x_{ethanol}$	y_{water}	$y_{butanol}$	$y_{ethanol}$
366.10	0.62740	0.37261	0.00000	0.98250	0.01750	0.00000	0.74700	0.25300	0.00000
366.36	0.63939	0.36061	0.00000	0.97801	0.02199	0.00000	0.75400	0.24600	0.00000
366.20	0.63656	0.35079	0.01265	0.97344	0.01748	0.00908	0.75474	0.22047	0.02479
365.81	0.64497	0.33205	0.02298	0.96378	0.02003	0.01619	0.73211	0.21316	0.05473
365.60	0.64991	0.32672	0.02336	0.96101	0.02103	0.01796	0.72829	0.21067	0.06104
365.11	0.66460	0.0133	0.03407	0.94458	0.03031	0.02511	0.71125	0.19827	0.09049
365.38	0.68510	0.27778	0.03713	0.90137	0.05673	0.04191	0.71619	0.20302	0.08079

Table D- 3: *Vapour-liquid-liquid equilibrium experimental results for ethanol/MEK/water at 101.3 kPa.*

Temperature (°C)	Vapour Phase			Aqueous Liquid Phase			Organic Liquid Phase		
	y_{Water}	y_{MEK}	y_{EthOH}	x_{Water}	x_{MEK}	x_{EthOH}	x_{Water}	x_{MEK}	x_{EthOH}
73.50	0.352734	0.647266	0	0.952	0.048	0	0.413608	0.586392	0
73.64	0.35100	0.64900	0	0.95500	0.04500	0	0.415037	0.584963	0
73.55	0.348739	0.651261	0	0.955666	0.044334	0	0.416303	0.583697	0
73.53	0.349253	0.646292	0.004455	0.949641	0.046237	0.004122	0.41504	0.578992	0.005968
73.52	0.349028	0.644948	0.006024	0.947443	0.047235	0.005322	0.420825	0.569171	0.010004
73.50	0.348618	0.64342	0.007962	0.944969	0.047957	0.007074	0.419767	0.568876	0.011357
73.48	0.347738	0.639503	0.012759	0.94279	0.048014	0.009196	0.426369	0.561212	0.012419
73.46	0.347765	0.638093	0.014142	0.941121	0.049222	0.009657	0.428072	0.558313	0.013615
73.44	0.346867	0.637514	0.015619	0.938893	0.050989	0.010119	0.436462	0.548064	0.015474
73.41	0.345465	0.637071	0.017464	0.934421	0.053708	0.011872	0.442671	0.538995	0.018334
73.39	0.345677	0.635844	0.018479	0.930361	0.056199	0.01344	0.446106	0.534754	0.01914
73.36	0.346244	0.632417	0.021339	0.925456	0.059444	0.015101	0.447481	0.53299	0.019529
73.33	0.346542	0.629998	0.02346	0.923409	0.060752	0.015839	0.44787	0.531538	0.020592
73.30	0.346802	0.627062	0.026136	0.919992	0.063247	0.016761	0.45114	0.528135	0.020725
73.27	0.342147	0.616495	0.041358	0.914284	0.066648	0.019068	0.465142	0.510808	0.02405
73.23	0.34419	0.612788	0.043022	0.911939	0.067973	0.020088	0.474266	0.499388	0.026346
73.20	0.343291	0.600046	0.056663	0.909825	0.069539	0.020636	0.482084	0.488319	0.029597
73.16	0.343095	0.597319	0.059586	0.903337	0.072798	0.023865	0.49521	0.47328	0.03151
73.11	0.342327	0.589187	0.068486	0.899246	0.076059	0.024696	0.516576	0.447756	0.035668
73.04	0.340956	0.582985	0.076059	0.888194	0.083803	0.028003	0.538567	0.422577	0.038856
72.97	0.338522	0.572267	0.089211	0.883129	0.087207	0.029664	0.556608	0.40334	0.040052
72.50	0.336732	0.55506	0.108208	0.87865	0.090833	0.030517	0.591044	0.366871	0.042085

Table D- 4: *Vapour-liquid-liquid equilibrium experimental results for n-propanol/MEK/water at 101.3 kPa.*

Temperature (°C)	Vapour Phase			Aqueous Liquid Phase			Organic Liquid Phase		
	y_{Water}	y_{MEK}	$Y_{n\text{-}Propanol}$	x_{Water}	x_{MEK}	$X_{n\text{-}Propanol}$	x_{Water}	x_{MEK}	$X_{n\text{-}Propanol}$
73.6	0.351849	0.648151	0	0.950793	0.049207	0	0.410903	0.589097	0
73.62	0.35100	0.649000	0	0.952458	0.047542	0	0.415012	0.584988	0
73.59	0.353672	0.646328	0	0.95555	0.04445	0	0.41973	0.58027	0
73.69	0.350488	0.643833	0.005679	0.954032	0.045421	0.000548	0.417113	0.577837	0.00505
74.24	0.350203	0.639867	0.00993	0.953499	0.045442	0.001059	0.414762	0.573576	0.011662
74.54	0.352022	0.636853	0.011125	0.951249	0.04641	0.002341	0.423589	0.564749	0.011662
75.48	0.351233	0.634453	0.014314	0.949116	0.046941	0.003943	0.427101	0.554901	0.017998
75.84	0.351147	0.630686	0.018167	0.946856	0.047343	0.005801	0.43233	0.545816	0.021854
76.06	0.353248	0.624733	0.022019	0.944587	0.047627	0.007787	0.434568	0.541374	0.024058
76.61	0.353101	0.621824	0.025075	0.94299	0.048582	0.008428	0.448587	0.522947	0.028466
77.04	0.354883	0.618315	0.026802	0.940717	0.049638	0.009645	0.451632	0.515495	0.032873
77.28	0.355939	0.611547	0.032514	0.938215	0.049578	0.012208	0.460338	0.503207	0.036455
77.46	0.357315	0.609241	0.033444	0.934881	0.050349	0.01477	0.463265	0.499454	0.037281
77.73	0.358617	0.603462	0.037921	0.931732	0.051639	0.016629	0.470779	0.488359	0.040862
78.55	0.358882	0.601426	0.039692	0.929856	0.052427	0.017718	0.478336	0.472537	0.049127
79.50	0.359597	0.598497	0.041906	0.922799	0.054358	0.022843	0.493934	0.454735	0.051331
79.50	0.359161	0.596719	0.04412	0.922135	0.053805	0.02406	0.506465	0.433389	0.060146
79.55	0.36187	0.5908	0.04733	0.917732	0.057503	0.024765	0.514852	0.425553	0.059595

Table D- 5: *Vapour-liquid-liquid equilibrium experimental results for IPA/MEK/water at 101.3 kPa.*

Temperature (°C)	Vapour Phase			Aqueous Liquid Phase			Organic Liquid Phase		
	y_{Water}	y_{MEK}	Y_{IPA}	x_{Water}	x_{MEK}	X_{IPA}	x_{Water}	x_{MEK}	X_{IPA}
73.53	0.352412	0.647588	0	0.953404	0.046596	0	0.417188	0.582812	0
73.60	0.353931	0.646069	0	0.953222	0.046778	0	0.417946	0.582054	0
73.55	0.353161	0.646839	0	0.95458	0.04542	0	0.41894	0.58106	0
73.55	0.353809	0.638494	0.007697	0.950824	0.046855	0.002321	0.418582	0.576024	0.005394
73.54	0.354313	0.636927	0.00876	0.949838	0.046827	0.003335	0.418561	0.572027	0.009412
73.54	0.355158	0.63409	0.010752	0.948024	0.046612	0.005365	0.419051	0.570198	0.010751
73.53	0.355908	0.629088	0.015004	0.946499	0.046845	0.006656	0.421114	0.564309	0.014577
73.52	0.357837	0.625034	0.017129	0.941169	0.047746	0.011085	0.422916	0.55849	0.018594
73.52	0.357447	0.623033	0.01952	0.938996	0.049089	0.011915	0.424668	0.552295	0.023037
73.52	0.358628	0.621413	0.019959	0.936073	0.049521	0.014406	0.425456	0.548107	0.026437
73.51	0.360816	0.615814	0.02337	0.933082	0.050206	0.016712	0.426678	0.545353	0.027969
73.50	0.361431	0.610679	0.02789	0.927752	0.051108	0.02114	0.428583	0.540962	0.030455
73.49	0.365213	0.604107	0.03068	0.924564	0.051435	0.024001	0.427529	0.534938	0.037533
73.49	0.366476	0.595936	0.037588	0.921072	0.0505	0.028429	0.434243	0.522102	0.043655
73.48	0.367093	0.587348	0.045559	0.917321	0.050744	0.031935	0.43837	0.510296	0.051334
73.48	0.369754	0.58044	0.049806	0.914831	0.051539	0.03363	0.441378	0.5041	0.054522
73.47	0.373469	0.567953	0.058578	0.913272	0.051899	0.03483	0.44692	0.492845	0.060235
73.46	0.376277	0.561667	0.062056	0.910497	0.052722	0.036781	0.447105	0.490268	0.062627
73.45	0.383598	0.533084	0.083318	0.906046	0.055143	0.038812	0.458303	0.471986	0.069711
73.45	0.383861	0.524281	0.091858	0.899343	0.058986	0.041671	0.473971	0.449177	0.076852
73.45	0.387491	0.510734	0.101775	0.89441	0.061243	0.044347	0.495494	0.423291	0.081215
73.44	0.392297	0.499317	0.108386	0.889505	0.064488	0.046007	0.514821	0.39246	0.092719

73.43	0.3974605	0.487542	0.114998	0.879807	0.070444	0.049749	0.546558	0.35755	0.095892
73.37	0.402624	0.475767	0.121609	0.86111	0.082266	0.056624	0.552582	0.349145	0.098273

APPENDIX F - THERMODYNAMIC CONSISTENCY TESTING RESULTS

The L/W Consistency Test was performed using *PRO-VLE 2.0* software, making use of the following component specific properties:

Table F-1: ***Component parameters used for thermodynamic consistency testing.***

	Water	Ethanol	n-Propanol	IPA	Isooctane	MEK
Antoine A*	8.108	7.557	7.744	4.57795	7.182	3.9894
Antoine B*	1750.28	-1261.78	1437.68	1221.423	1520.98	1150.207
Antoine C*	235	191.460	198.463	-87.474	253.59	-63.904
T_c (K)	647.13[b]	516.25[a]	536.78[b]	355.75	543.96	535.65[b]
P_C (atm)	217.68[b]	63.84	51.077[b]	48.3	25.68	42.25[a]
V_c ($cm^3.mol^{-1}$)	55.9[b]	166.9	219	222	468	267
T_b (K)	373.15[b]	351.44	370.35	508.7	372.39	352.79
ω	0.345	0.637	0.622	0.665	0.303	0.329
V^L ($cm^3.mol^{-1}$)	18.506	63.671	82.075[b]	24.46	180.124	156.65
ΔH_V ($cal.mol^{-1}$)	9751	9369	9954	10755	7537	7648.18
μ (Debye)	1.845	1.687	1.675[b]	1.66[b]	0[b]	2.76[b]

***Antoine Equation as $\log_{10}P(mmHg)=A-(B/(T(°C)+C))$**
All values taken from Perry's Chemical Engineering Handbook unless otherwise stated
[a]Correlations based on group contribution methods – Perry's Chemical Engineering Handbook
[b]DIPPR Database

Values for the activity coefficient were generated for each component at each data point within the PRO-VLE 2.0 software. These values, along with the observable temperature deviations (0.02 °C) and the maximum absolute deviation in reported concentration (0.014 mole fraction) were used to determine D and D_{max} for the McDermott-Ellis Consistency Test.

Table F-2: Thermodynamic consistency testing results for verification system: ethanol/isooctane.

			L/W Consistency Test				McDermott-Ellis Consistency Test		
T (K)	$x_{ethanol}$	$y_{ethanol}$	L_i	W_i	L_i/W_i	D	$\gamma_{ethanol}$	$\gamma_{isooctane}$	D_{max}
351.45	1.000	1.000							
344.38	0.636	0.623	8.673	8.933	0.971	1.472	1.001	0.799	0.960
344.43	0.647	0.623	9.808	10.334	0.949	2.613	1.096	0.851	0.953
344.46	0.592	0.654	1.939	2.033	0.954	2.350	1.004	0.769	0.945
344.48	0.697	0.654	2.504	2.752	0.910	4.708	1.094	0.368	0.892
345.70	0.275	0.629	8.938	9.074	0.985	0.753	1.020	0.994	0.875
345.80	0.877	0.740	8.886	9.587	0.927	3.793	1.015	0.935	0.835
346.11	0.895	0.761	6.937	7.667	0.905	4.998	1.023	0.924	0.801
346.48	0.923	0.742	6.020	6.597	0.913	4.570	1.063	0.026	0.678
346.50	0.916	0.758	9.142	9.204	0.993	0.339	1.001	0.474	0.678
346.50	0.138	0.561	6.258	6.605	0.947	2.700	1.006	0.603	0.581
346.97	0.932	0.789	1.204	1.209	0.996	0.219	1.008	0.725	0.565
348.05	0.070	0.525	1.555	1.563	0.995	0.257	1.097	0.976	0.547
349.24	0.964	0.886	2.658	2.868	0.927	3.798	1.053	0.676	0.502
349.29	0.978	0.896	9.256	9.984	0.927	3.782	1.040	0.420	0.493
349.70	0.058	0.519	6.388	6.454	0.990	0.511	1.028	0.760	0.427
361.91	0.020	0.280	1.629	1.776	0.917	4.328	1.002	0.993	0.417
371.37	0.000	0.000							

Table F-3: Thermodynamic consistency testing results for ethanol/MEK/water system.

			L/W Consistency Test				McDermott-Ellis Consistency Test
T (K)	$x_{ethanol}$	x_{MEK}	L_i	W_i	L_i/W_i	D	D_{max}
346.65	0.952	0.048	3.678	4.075	0.903	5.119	0.190
346.79	0.955	0.045	3.599	3.606	0.998	0.097	0.199
346.70	0.956	0.044	5.219	5.644	0.925	3.915	0.203
346.68	0.950	0.046	7.282	7.896	0.922	4.045	0.209
346.67	0.947	0.047	7.829	8.326	0.940	3.078	0.217
346.65	0.945	0.048	4.117	4.158	0.990	0.490	0.224
346.63	0.943	0.048	9.976	10.121	0.986	0.721	0.241
346.61	0.941	0.049	2.369	2.531	0.936	3.295	0.245
346.59	0.939	0.051	3.440	3.513	0.979	1.053	0.256
346.56	0.934	0.054	8.888	9.426	0.943	2.936	0.257
346.54	0.930	0.056	1.205	1.298	0.928	3.733	0.260
346.51	0.925	0.059	1.609	1.671	0.963	1.887	0.267

346.48	0.923	0.061	6.590	6.754	0.976	1.228	0.278
346.45	0.920	0.063	1.092	1.124	0.972	1.409	0.292
346.42	0.914	0.067	6.560	7.155	0.917	4.343	0.295
346.38	0.912	0.068	8.406	9.335	0.900	5.237	0.305
346.35	0.910	0.070	8.321	8.547	0.974	1.338	0.305
346.31	0.903	0.073	6.954	7.121	0.977	1.187	0.310

Table F-4: Thermodynamic consistency testing results for n-propanol/MEK/water system.

			L/W Consistency Test				**McDermott-Ellis Consistency Test**
T (K)	$x_{n\text{-propanol}}$	x_{MEK}	L_i	W_i	L_i/W_i	**D**	D_{max}
346.75	0.951	0.049	5.127	5.683	0.902	5.140	0.176
346.77	0.952	0.048	9.174	10.188	0.900	5.240	0.181
346.74	0.956	0.044	3.971	3.974	0.999	0.039	0.197
346.84	0.954	0.045	1.913	2.063	0.927	3.777	0.220
347.39	0.953	0.045	6.366	6.428	0.990	0.485	0.281
347.69	0.951	0.046	9.528	10.294	0.926	3.866	0.308
348.63	0.949	0.047	7.773	8.008	0.971	1.488	0.327
348.99	0.947	0.047	8.672	8.694	0.997	0.127	0.336
349.21	0.945	0.048	4.067	4.192	0.970	1.513	0.344
349.76	0.943	0.049	2.044	2.244	0.911	4.660	0.368
350.19	0.941	0.050	8.557	8.704	0.983	0.852	0.370
350.43	0.938	0.050	1.510	1.603	0.942	2.987	0.373
350.61	0.935	0.050	8.386	8.910	0.941	3.028	0.419
350.88	0.932	0.052	7.487	7.986	0.937	3.228	0.422
351.70	0.930	0.052	5.959	6.492	0.918	4.282	0.422
352.65	0.923	0.054	0.806	0.840	0.959	2.102	0.428
352.65	0.922	0.054	5.649	6.111	0.924	3.927	0.446
352.70	0.918	0.058	1.913	1.959	0.976	1.194	0.452

Table F-5: Thermodynamic consistency testing results for IPA/MEK/water system.

			L/W Consistency Test				McDermott-Ellis Consistency Test
T (K)	x_{IPA}	x_{MEK}	L_i	W_i	L_i/W_i	D	D_{max}
346.70	0.951	0.047	0.519	0.522	0.995	0.260	0.675
346.69	0.950	0.047	9.944	11.042	0.901	5.232	0.894
346.69	0.948	0.047	6.941	7.459	0.931	3.596	0.895
346.68	0.946	0.047	1.035	1.046	0.990	0.520	0.947
346.67	0.941	0.048	9.535	10.540	0.905	5.006	0.628
346.67	0.939	0.049	9.187	10.117	0.908	4.815	0.897
346.67	0.936	0.050	6.084	6.479	0.939	3.138	0.784
346.66	0.933	0.050	5.391	5.698	0.946	2.770	0.699
346.65	0.928	0.051	1.620	1.646	0.984	0.816	0.606
346.64	0.925	0.051	6.260	6.678	0.937	3.231	0.240
346.64	0.921	0.051	2.018	2.060	0.980	1.019	0.376
346.63	0.917	0.051	6.558	7.018	0.934	3.390	0.015
346.63	0.915	0.052	4.872	5.122	0.951	2.497	0.211
346.62	0.913	0.052	0.250	0.251	0.997	0.125	0.111
346.61	0.910	0.053	7.800	8.460	0.922	4.058	0.625
346.60	0.906	0.055	1.803	1.836	0.982	0.910	0.449
346.60	0.899	0.059	3.534	3.664	0.965	1.799	0.903
346.60	0.894	0.061	4.309	4.503	0.957	2.202	0.614
346.59	0.890	0.064	7.313	7.890	0.927	3.795	0.519
346.58	0.880	0.070	6.707	7.189	0.933	3.470	0.146
346.52	0.861	0.082	0.506	0.508	0.995	0.253	0.983

APPENDIX G - OTHMER-TOBIAS CORRELATIONS

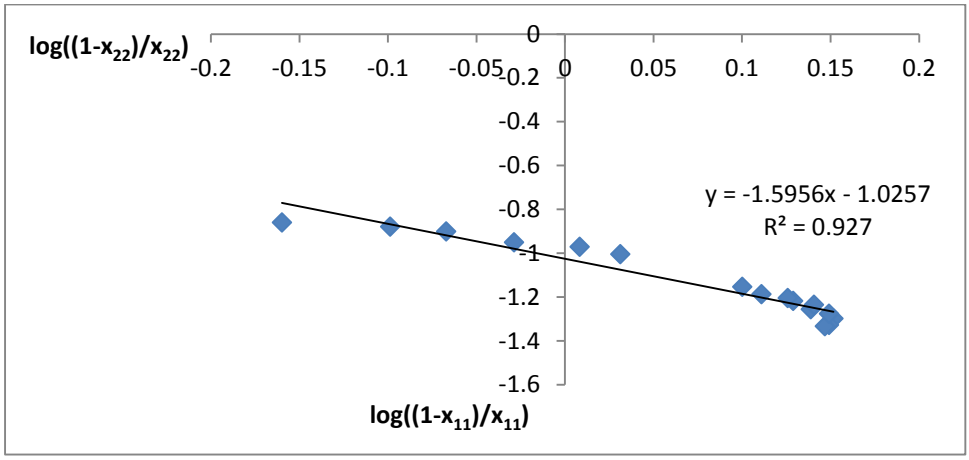

Figure G-1: Othmer-Tobias Correlation for the ethanol/MEK/water system's liquid phases at 101.3 kPa.

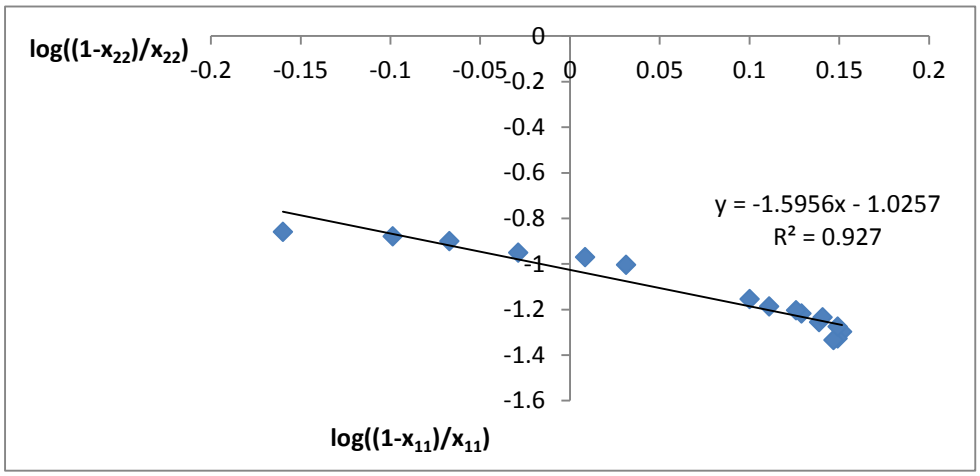

Figure G-2: Othmer-Tobias Correlation for the n-propanol/MEK/water system's liquid phases at 101.3 kPa.

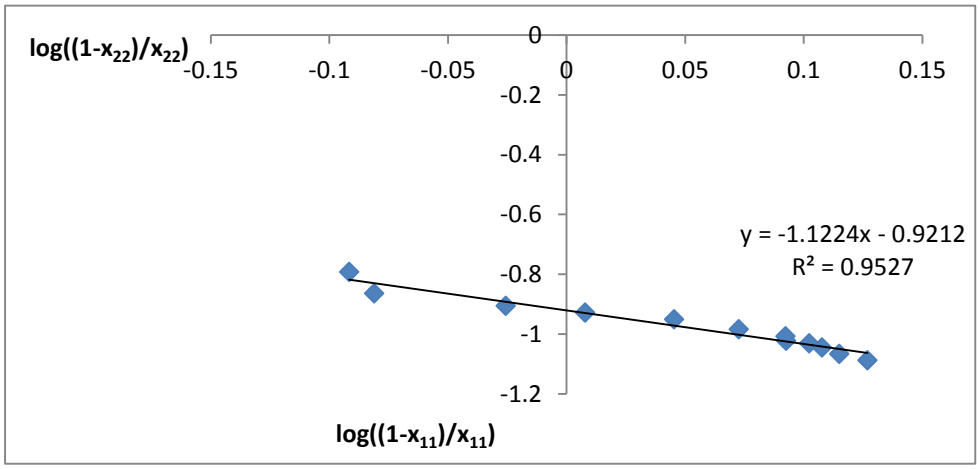

Figure G-3: Othmer-Tobias Correlation for the IPA/MEK/water system's liquid phases at 101.3 kPa.

APPENDIX H - BUILT IN ASPEN PLUS® PARAMETERS AND PARAMETERS OBTAINED FROM PIENAAR ET AL. (2013)

Table H- 1: *Built in Aspen Parameters for NRTL.*

Component *i*	**MEK**	**MEK**	**MEK**	**MEK**	**Water**	**Water**	**Water**	**Ethanol**	**Ethanol**	**1-Propanol**
Component *j*	Water	Ethanol	1-Propanol	IPA	Ethanol	1-Propanol	IPA	1-Propanol	IPA	ISOPR-01
Temperature units	C	C	C	C	C	C	C	C	C	C
Source	VLE-IG	VLE-IG	VLE-IG	VLE-IG	VLE-IG	VLE-IG	VLE-IG	VLE-IG	VLE-IG	VLE-IG
Property units										
A_{IJ}	0	0.7593	0	0	3.4578	5.4486	6.8284	8.2606	0.1352	0
A_{JI}	0	-1.5609	0	0	-0.8009	-1.7411	-1.3115	-9.721	0.7014	0
B_{IJ}	201.3011	-132.9897	-53.2457	212.173	-586.0809	-861.1792	-1483.4573	-2846.6829	-215.7354	556.3042
B_{JI}	1087.744	654.555	272.8955	11.2089	246.18	576.4458	426.3978	3409.6863	-58.384	-369.9008
C_{IJ}	0.3	0.3	0.3	0.3	0.3	0.3	0.3	0.3	0.3	0.3
D_{IJ}	0	0	0	0	0	0	0	0	0	0
E_{IJ}	0	0	0	0	0	0	0	0	0	0
E_{JI}	0	0	0	0	0	0	0	0	0	0
F_{IJ}	0	0	0	0	0	0	0	0	0	0
F_{JI}	0	0	0	0	0	0	0	0	0	0
TLOWER	73.3	25	79.9	55	24.99	25	25	40	40	82.5
TUPPER	100	78.3	94.8	80.7	100	100	100	97.16	82.39	97.15

Table H- 2: *Built in Aspen Plus® Parameters for UNIQUAC.*

Component *i*	**MEK**	**MEK**	**MEK**	**MEK**	**Water**	**Water**	**Water**	**Ethanol**	**Ethanol**	**1-Propanol**
Component *j*	Water	Ethanol	1-Propanol	IPA	Ethanol	1-Propanol	IPA	1-Propanol	IPA	ISOPR-01
Temperature units	C	C	C	C	C	C	C	C	C	C
Source	VLE-IG	VLE-IG	VLE-IG	VLE-IG	VLE-IG	VLE-IG	VLE-IG	VLE-IG	VLE-IG	VLE-IG
Property units										
A_{IJ}	0	-2.4936	-2.333	-3.3127	-0.833	0	0	-4.082	-0.026	0
A_{JI}	0	2.0046	1.7668	2.9234	0.8809	0	0	5.092	-0.3572	0
B_{IJ}	-71.0193	756.9477	600.4906	1045.5786	96.9968	13.4746	-138.5107	1433.9607	97.5813	-327.7583
B_{JI}	-311.2552	-728.9705	-651.2462	-1111.674	-248.2244	-90.7903	46.2032	-815.7489	22.4165	221.2834
C_{IJ}	0	0	0	0	0	0	0	0	0	0
D_{IJ}	0	0	0	0	0	0	0	0	0	0
E_{IJ}	0	0	0	0	0	0	0	0	0	0
E_{JI}	0	0	0	0	0	0	0	0	0	0
F_{IJ}	73.3	24.99	25	25	25	79.9	55	40	40	82.5
F_{JI}	100	100	100	100	78.3	94.8	80.7	97.16	82.39	97.15
TLOWER	0	0	0	0	0	0	0	0	0	0
TUPPER	0	-2.4936	-2.333	-3.3127	-0.833	0	0	-4.082	-0.026	0

Table H- 3: ***NRTL model parameters for the Water (1) + MEK (2) + Ethanol (3) system, regressed by Pienaar et al. (2013)***

i	j	A_{ij}	A_{ji}	B_{ji}	B_{ij}	C_{ij}
1	2	-2.49	2.01	756.95	-728.90	0.7
1	3	-0.83	0.88	97.00	-248.22	0.3
2	3	-2.76	-5.14	1549.35	2063.90	0.78

Table H- 4: ***NRTL model parameters for the Water (1) + MEK (2) + n-Propanol (3) system, regressed by Pienaar et al. (2013)***

i	j	A_{ij}	A_{ji}	B_{ji}	B_{ij}	C_{ij}
1	2	-2.49	2.01	756.95	-728.90	0.3
1	3	4.86	-1.13	726.32	737.43	0.490
2	3	-0.31	0	13.47	-90.79	0.3

Table H- 5: ***NRTL model parameters for the Water (1) + MEK (2) + IPA (3) system***

i	j	A_{ij}	A_{ji}	B_{ji}	B_{ij}	C_{ij}
1	2	-2.49	2.01	756.95	-728.90	0.3
1	3	-6.40	10.22	-5966.13	-1960.98	-0.071
2	3	0	0	-138.51	46.20	0.3

Table H- 6: UNIQUAC *model parameters for the Water (1) + MEK (2) + Ethanol (3) system, regressed by Pienaar et al. (2013)*

i	j	A_{ij}	A_{ji}	B_{ji}	B_{ij}
1	2	0	0	201.30	1087.74
1	3	3.46	-0.80	-586.08	246.18
2	3	-2.76	-5.14	1549.35	2063.90

Table H- 7: UNIQUAC *model parameters for the Water (1) + MEK (2) + n-Propanol (3) system, regressed by Pienaar et al. (2013)*

i	j	A_{ij}	A_{ji}	B_{ji}	B_{ij}
1	2	0	0	201.30	1087.74
1	3	0.09	-1.13	-297.36	403.12
2	3	-2.33	1.77	600.49	-651.24

Table H- 8: UNIQUAC *model parameters for the Water (1) + MEK (2) + IPA (3) system*

i	j	A_{ij}	A_{ji}	B_{ji}	B_{ij}
1	2	0	0	-71.02	-311.25
1	3	0	0	-138.51	46.20
2	3	-3.31	2.92	1045.58	-1111.67

APPENDIX I - DETAILED EXPERIMENTAL PROCEDURE

I.1 Experimental Procedure

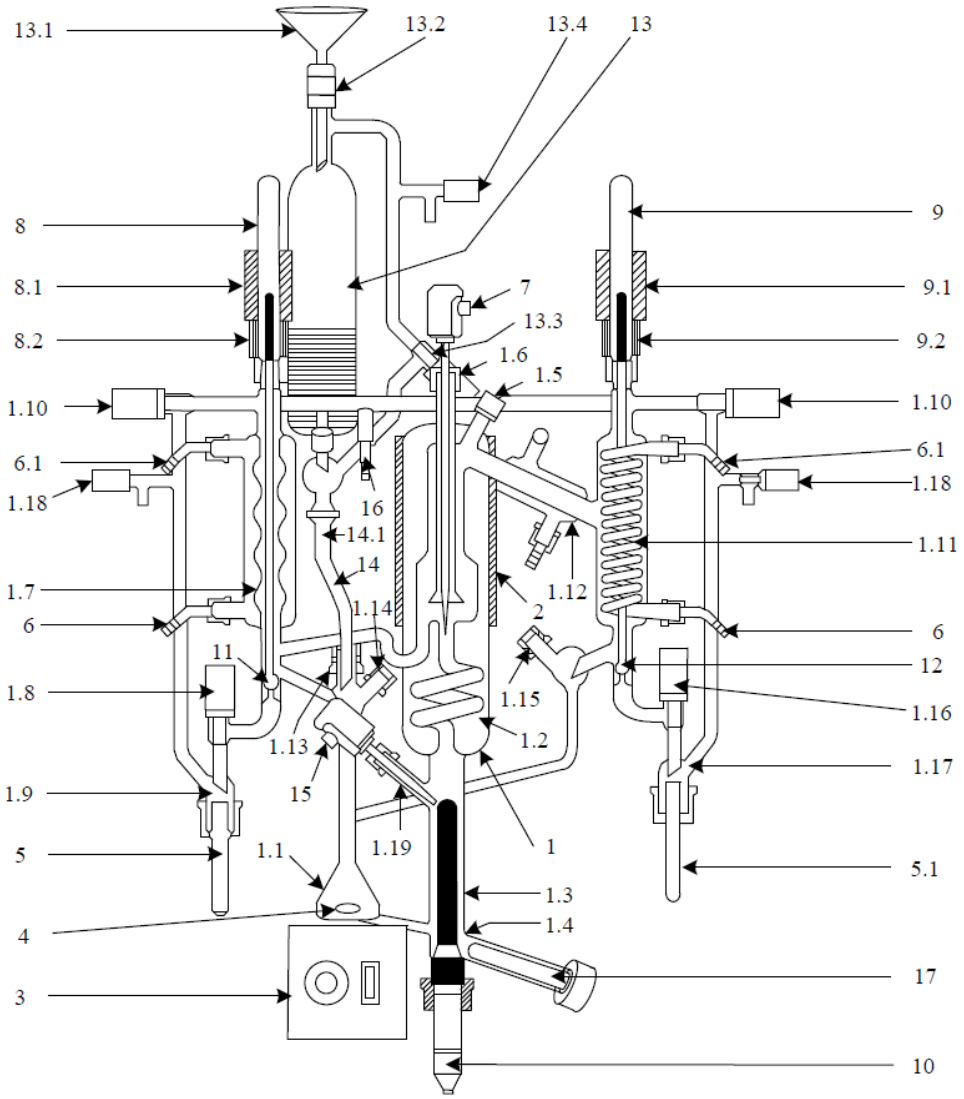

Figure H-0-1: ***Schematic representation of the Pilodist dynamic recirculating still used for VLE and VLLE measurements.***

I.1.1 Initial Procedure

The following preliminaries should be performed and checked at the beginning of each new day of experimentation:

- Washing with acetone, as discussed in the section DRAINING AND WASHING, should prevent contamination of the still with impurities. Compressed air may be passed through the entire all-glass still in order to ensure that the still is dry and free of was acetone as well as all previous chemical components used. The stop valves (1.10) and aeration valves (1.18) must be opened when flushing with compressed air.

- The tap to allow cooling water through condensers (1.11 & 1.12) and the liquid cooler (1.7) should be opened and checked for constant flow.
- The oil level in the pump, found at the back of the unit, should have appropriate clarity (a murky or bubbly appearance may warrant a complete replacement) and have a midrange level. If the level seems too low, oil should be added to maintain the desired level.
- When operating at overpressure, as opposed to vacuum conditions, check that the overpressure throttle valve on the hydraulic box is fully closed. The nitrogen canister can then be opened, ensuring that only a small flow is registered through the regulator.
- Under vacuum conditions, the maintenance of the vacuum pump should be confirmed.

The still can now be turned on using the green power switch on the hydraulic box and the control software opened on the computer next to the unit.

I.1.2 Still Preparation

Select operating pressure conditions (atmospheric, vacuum or overpressure) by switching the three-way valve on the hydraulic box to the desired pressure conditions and changing the settings within the software. In order to maintain standard atmospheric pressure (101.325 kPa), overpressure was selected for all my experimental work due to the lower pressure at atmospheric conditions. Fit and secure the homogeniser (17) to the still and close the discharge valve (1.4) and the precision control valve (13.5). Now, the burette can be filled to approximately 110ml with the starting mixture via the filler nozzle (13.1). Open the precision control valve (13.5) on the feed burette to allow liquid to flow into the mixing chamber (1.1). Close the precision control valve (13.5) when the desired volume has been transferred and switch on the magnetic stirrer (3). The amount required may vary depending on the volatilities of the mixture and the intended operation of the still; however, the volume must be sufficient to cover the immersion heater (10). Check that the glass receiver vials (5 & 5.1) are securely fitted; and ensure that the sampling nozzle caps (1.14 & 1.15) and aeration valves (1.18 & 13.4) are closed. The stop valves (1.10) must now be opened in order to ensure that the entire apparatus maintains equal pressure during the course of the experimental run.

The software must now be programmed to achieve suitable system temperatures and pressures to vaporise the starting mixture, causing vapour and liquid return. The heater power setting is dependent on both the feed liquid as well as the system pressure. It is important to choose a power setting high enough to vaporise the inventory while avoiding the exclusive production of vapour.

When working with systems where the vapour temperature exceeds 100°C, the mantle heater must be used to prevent the partial condensation of the vapour phase on the mantle walls. This can be achieved through the use of the software package. The set point should be approximately 15°C lower than the vapour temperature in order to compensate for the simple on-off control of the

heater. For isobaric experimental runs, with the pressure set at 101.3 kPa, pressure control is achieved by balancing the amount of nitrogen entering the system through the manual overpressure regulator on the hydraulic box with that leaving the stop valves (1.10). When operating at vacuum conditions (not dealt with in this work), manual pressure regulation is achieved by setting the pressure point in the software to 50 mbar lower than the intended pressure value and using the manual vacuum regulator valve on the hydraulic box.

I.1.3 Experimental Runs

The apparatus can be started by selecting *Start* within the software package interface.

In approximately 5 minutes, liquid return should begin. If liquid return does not occur, the power must be increased by 2% and monitored for a further 5 minutes before being re-adjusted. Under the appropriate power settings (depending on ambient temperature and boiling temperature of the starting mixture), vapour return should be evident in 20 minutes, with a sudden increase in the recorded bubble temperature. During this period of time, the pressure will fluctuate and will require monitoring and adjustment until a stable pressure of 101.3 kPa is reached. Once this has been achieved, the ultrasonic homogeniser can be switched on to ensure thorough mixing of the liquid and vapour phases. Owing to the concave nature of the sample wells (11 & 12), periodic flushing is required. This entails opening the stop valves (1.8 & 1.16) as well as the solenoid valves (9) by using the Pilodist remote control, allowing the congregated liquid to wash away into the receiver vials (5 & 5.1). This process ensures that the final vapour and liquid samples will not be contaminated. The collected liquid should be drained from the vials and the valves closed again. Equilibrium is achieved within in the still after approximately 60 minutes, indicated by a steady registered vapour temperature and a steady liquid return as well as a droplet return rate of approximately 30 drops per minute on the vapour side. Samples are now taken according to the procedure detailed in the following section, SAMPLING. The experimental run is concluded by selecting *Stop* within the software package. The magnetic stirrer (3) can now be switched off and the apparatus brought back to ambient temperature and pressure. When operating under vacuum conditions, the aeration valves (1.18 & 13.4) need to be opened slowly. In the case of overpressure, the overpressure throttling valve on the hydraulic box must be closed and the aeration valves (1.18 & 13.4) opened. Some of the liquid may be drained via the discharge valve (1.4) or added through the feeding burette to top-up and change the composition of the starting mixture. A new experimental run must be executed according to the procedure set out above.

I.1.4 Sampling

Before the final samples are taken, the sampling wells (11 & 12) need to be flushed according the procedure described in the above section and replaced with clean receiving vials (5 & 5.1). The

vapour temperature should be closely monitored during the sampling procedure. If the temperature does not stay constant during the sampling procedure, the samples must be disregarded and the still allowed to achieve a state of equilibrium once again.

I.1.4.1 Vapour phase

Using a gas-tight syringe, containing a known amount of standard, a sample is taken directly from the gaseous phase in the separation chamber at the sampling nozzle (1.5). The addition of the standard compound prevents phase separation effects that occur as a result of temperature change. For this experimental work, approximately 0.2 ml of Acetonitrile was used as standard, as it is completely miscible with water and the chemicals used. The resulting mixture is then placed in a 2 ml vial for further analysis.

I.1.4.2 Liquid phases

For the sampling of the aqueous and organic liquid phases, a sample is taken according to the flushing procedure discussed above. The liquid return can either flow back into the mixing chamber (1.1) or be deviated by using the solenoid valves (9). Approximately 4 ml of the dispersed liquid phases is obtained in the receiving vial (5). Fitted with a silicone rubber cover, the sampling vial is then placed in a water bath, with a temperature equal to the boiling point of the mixture, for two hours. After this period of time, using a gas-tight syringe (containing a known amount of Acetonitrile), a sample of each one of the distinctive liquid phases is taken and placed in 2 ml sample vials.

A sample of the overall liquid phase (global heterogeneous mixture) is also taken off using the same gas-tight syringe method through the sampling nozzle (1.14). When taking the overall liquid phase sample, approximately 0.4 ml of Acetonitrile is added to guarantee a homogeneous mixture.

I.1.5 Draining and Washing

When a satisfactory number of experimental runs have been executed for a particular binary or ternary mixture, the still must be drained and washed. This aids the removal of any non-volatile components from the still and avoids contamination of the feed mixture for the subsequent experimental run. The mixture, still and immersion heater should be given enough time to cool to ambient temperatures. The mixture can then be drained through the discharge valve (1.4) and the ultrasonic homogeniser (17) carefully detached to drain any residual liquid. The homogeniser can then be reattached and the feed burette charged with approximately 110 ml acetone. Following the experimental procedure as detailed above, the apparatus should be allowed to run for 30 min, the wash acetone drained and the process repeated. The apparatus can now be stopped, allowed to

cool and drained as before. The apparatus can be switched off by the green power switch found on the hydraulic box, the software closed and the control unit powered down; ensuring that the nitrogen cylinder and cooling water tap are closed and all the valves are opened to allow the still to dry.

I.1.6 Analysis

Sample analysis was performed using both capillary gas chromatography and Karl Fischer titration, owing to the fact that the column-detector combination used could not quantify the amount of water within the samples. A complete explanation and sample calculation can be seen in Appendix D.

I.1.6.1 Gas Chromatography

The organic compositions of the samples were quantified through capillary gas chromatography using a Varian CP-3380 GC equipped with an auto sampler and a flame ionization detector (FID). The column chosen, a ZB Wax chromatographic column with dimensions 30m x 0.32mm x 1µm, was run at a temperature of 170 °C. The split ratio was 20 and the flow rate of carrier gas was approximately 5.0 mL/min. The injection temperature was set to 250 °C and sample volume was 0.1 mL from a 2 mL vial. The lowest method detection limit was 9.5 mg/L and the average recovery rate was 99.1%. Sample preparation was achieved as follows:

- Sample vials were loaded with ±1.5 mL of 2-ethyl-1-hexanol
- Approximately 35 mg of 2-(±)-Pentanol was added to the vial as internal standard
- Approximately 40 mg of experimentally obtained vapour/liquid sample was added to the vial

Each analytical sample was run three times to obtain the average composition of the sample with quantification made possible through calibration curves. Calibration curves were obtained by making up five standard samples containing a known mass of 2-(±)-Pentanol and chemical component in varying concentration ratios. Each standard was run three times to obtain an average. Details of the response factors and calibration curves obtained for each chemical compound used can be found in Appendix C.

I.1.6.2 Water analysis

Karl Fischer titration was used to quantitatively determine the water content in each of the experimentally obtained vapour/liquid samples. A 701 Volumetric Titrino and 703 Titrino stand, manufactured by Metrohm, were used.

I.1.6.2.1 Background

Unlike conventional drying methods of moisture determination, where the loss on drying as opposed to the water content is determined, Karl Fischer titration solely determines the water content of a sample. This method of water analysis works over a wide range of water concentration (from ppm to 100% water).

The sulphur dioxide in the Karl Fischer reagent, HYDRANAL®-Composite 5, reacts with the HYDRANAL®-Methanol dry to form a monomethyl sulfite ion:

$$2CH_3OH + SO_2 \leftrightarrow CH_3OH_2{}^+ + SO_3CH_3{}^-$$

The base in the Karl Fischer reagent, Imadazole (1,3-diazacyclopenta-2,4-diene), acts as a buffer reagent and can therefore be replaced by any other suitable base (RN):

$$CH_3OH + SO_2 + RN \rightarrow [RNH]^+SO_3CH_3{}^-$$

The revised Karl Fisher reaction, in a methanolic solution, can be formulated as follows:

$$H_2O + I_2 + [RNH]^+SO_3CH_3{}^- + 2\,RN \rightarrow [RNH]^+SO_4CH_3{}^- + 2[RNH]^+I^-$$

I.1.6.2.2 Sample analysis

The size of sample required for analysis increases with increasing heterogeneous water distribution. Approximately 2 ml of sample is required for an accurate, repeatable analysis. This generally means that the entire vapour/liquid sample taken from the still, minus the ±40 mg sample required for GC analysis, is necessary. For samples with a high water content (>40%), such as the aqueous liquid phase, an inert dry solvent may be used for dilution before titration. Methanol was the chosen solvent for this experimental work. The 701 Titrino needs to be calibrated each day, the best average titer value chosen and the sample directly injected into the analysis chamber. The introduction of atmospheric humidity constitutes the constant re-calibration to ensure accurate results. The Titrino automatically includes the blank drift into the final calculation of water concentration.

APPENDIX J - EXAMPLE AAD AND AARD% CALCULATIONS

Equations used in the calculation of AAD and AARD:

$$AAD = \frac{1}{N_T}\sum_{i=1}^{N_T}\left|x_{i,calculated} - x_{i,measured}\right| \quad [J.1]$$

$$AARD\% = \frac{100}{N_T}\sum_{i=1}^{N_T}\left|\frac{x_{i,calculated} - x_{i,measured}}{x_{i,measured}}\right| \quad [J.2]$$

As an example, take the vapour phase compositions measured for the IPA/MEK/water system, and that calculated by the NRTL model:

Table J-1: Results for the measured and modelled vapour composition of the IPA/MEK/water system at 101.3 kPa.

Vapour Phase (Experimental)			Vapour phase (NRTL model)		
y_{Water}	y_{MEK}	Y_{IPA}	y_{Water}	y_{MEK}	Y_{IPA}
0.352412	0.647588	0	0.3489843	0.6363286	0.0146871
0.353931	0.646069	0	0.3476635	0.6235151	0.0288214
0.353161	0.646839	0	0.3465399	0.6110016	0.0424585
0.353809	0.638494	0.007697	0.3456054	0.5987431	0.0556514
0.354313	0.636927	0.00876	0.3448537	0.5866946	0.0684516
0.355158	0.63409	0.010752	0.3442798	0.5748106	0.0809095
0.355908	0.629088	0.015004	0.3438807	0.563044	0.0930753
0.357837	0.625034	0.017129	0.3436548	0.5513455	0.1049996
0.357447	0.623033	0.01952	0.3436028	0.5396625	0.1167347
0.358628	0.621413	0.019959	0.3437272	0.5279376	0.1283352
0.360816	0.615814	0.02337	0.3440333	0.5161074	0.1398593
0.361431	0.610679	0.02789	0.3445294	0.5041003	0.1513703
0.365213	0.604107	0.03068	0.3452275	0.4918343	0.1629382
0.366476	0.595936	0.037588	0.3461439	0.4792142	0.1746419
0.367093	0.587348	0.045559	0.3473008	0.4661274	0.1865718
0.369754	0.58044	0.049806	0.3487275	0.452439	0.1988334
0.373469	0.567953	0.058578	0.3504626	0.4379857	0.2115518
0.376277	0.561667	0.062056	0.3525564	0.4225665	0.2248771
0.383598	0.533084	0.083318	0.3550749	0.4059322	0.2389929
0.383861	0.524281	0.091858	0.3581047	0.3877699	0.2541254
0.392297	0.499317	0.108386	0.3489843	0.6363286	0.0146871

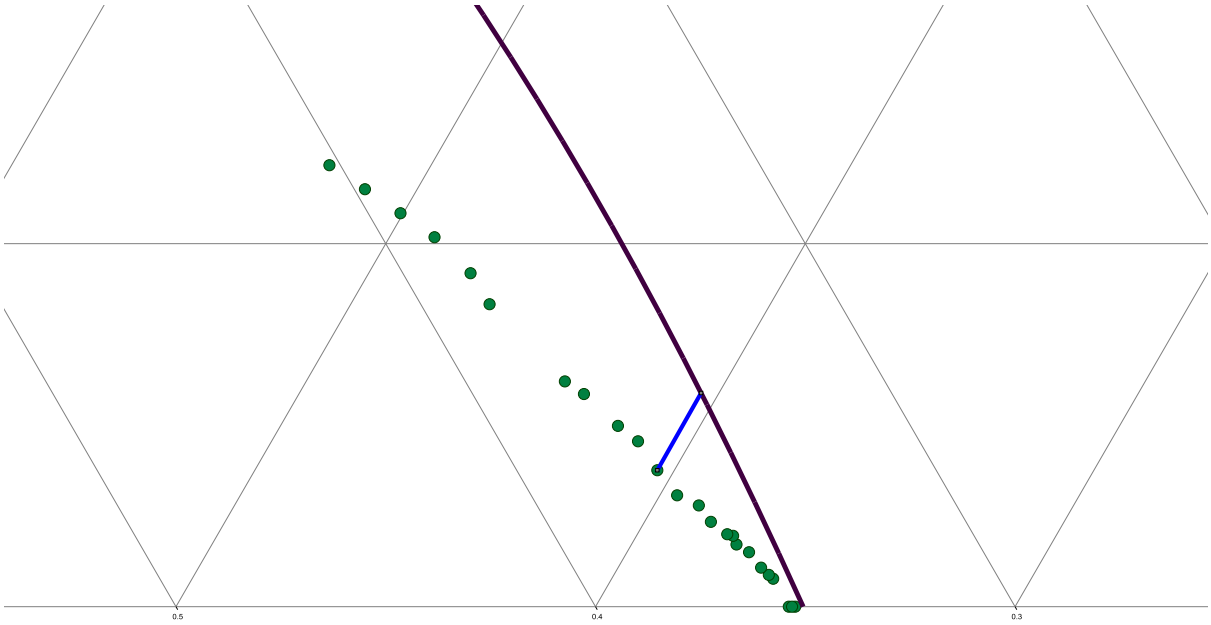

Figure J- 1: Section of a ternary phase diagram for the IPA/MEK/water system, showing the experimental results (•) and results calculated using the NRTL model (—).

Assume the water-component in the vapour phase is x, the MEK-component is y and the Ethanol-component is z. The absolute value of the difference between the measured value of x and the modelled/calculated value of x is calculated for each data point measured; this means where either the value of y or z is the same for both the measured and modelled data sets.

APPENDIX K - AAD AND AARD% RESULTS

Table K-1: ***AAD and AARD% values for ethanol/MEK/water system at 101.3 kPa when compared to NRTL, UNIFAC and UNIQUAC simulated data.***

	organic			aqueous			vapour		
	x_{water}	x_{MEK}	x_{EthOH}	x_{water}	x_{MEK}	x_{EthOH}	y_{water}	y_{MEK}	y_{EthOH}
NRTL									
AAD	0.198	0.101	0.077	0.023	0.056	0.034	0.034	0.043	0.050
AARD%	23.24	18.30	17.74	13.20	4.66	10.31	9.79	7.05	9.82
UNIFAC									
AAD	0.255	0.143	0.772	0.024	0.056	0.033	0.070	0.027	0.069
AARD%	12.44	1.24	13.06	12.42	2.50	5.36	10.88	12.32	13.62
UNIQUAC									
AAD	0.050	0.297	0.709	0.023	0.013	0.278	0.064	0.161	0.059
AARD%	56.78	30.71	16.280	13.47	11.30	18.82	9.69	13.71	18.41

Table K-2: ***AAD and AARD% values for n-propanol/MEK/water system at 101.3 kPa when compared to NRTL, UNIFAC and UNIQUAC simulated data.***

	organic			aqueous			vapour		
	x_{water}	x_{MEK}	$x_{N\text{-}Propanol}$	x_{water}	x_{MEK}	$x_{N\text{-}Propanol}$	y_{water}	y_{MEK}	$y_{N\text{-}Propanol}$
NRTL									
AAD	0.055	0.287	0.253	0.020	0.023	0.042	0.011	0.243	0.159
AARD%	3.74	7.41	47.53	14.28	13.02	24.73	3.74	7.41	39.00
UNIFAC									
AAD	0.251	0.260	0.020	0.027	0.027	0.031	0.006	0.010	0.002
AARD%	5.19	20.14	9.58	1.72	3.01	5.30	1.22	1.08	4.07
UNIQUAC									
AAD	0.966	0.299	0.250	0.242	0.194	0.436	0.911	0.244	0.152
AARD%	14.00	38.93	41.56	17.22	25.98	25.30	17.10	6.39	37.18

Table K-3: ***AAD and AARD% values for IPA/MEK/water system at 101.3 kPa when compared to NRTL, UNIFAC and UNIQUAC simulated data.***

	organic			aqueous			vapour		
	x_{water}	x_{MEK}	x_{IPA}	x_{water}	x_{MEK}	x_{IPA}	y_{water}	y_{MEK}	y_{IPA}
NRTL									
AAD	0.0620	0.153	0.095	0.090	0.012	0.012	0.104	0.104	0.093
AARD%	7.97	12.63	8.66	4.68	4.49	28.23	29.02	5.55	8.53
UNIFAC									
AAD	0.182	0.192	0.003	0.182	0.025	0.704	0.853	0.011	0.167
AARD%	19.84	1.82	3.98	9.42	2.22	12.58	11.00	9.36	6.07
UNIQUAC									
AAD	0.043	0.195	0.160	0.981	0.189	0.927	0.082	0.170	0.178
AARD%	35.24	18.51	15.33	51.01	15.50	48.77	10.49	14.04	16.89

Table K-4: ***AAD and AARD% values for ethanol/MEK/water system at 101.3 kPa when compared to NRTL, UNIFAC and UNIQUAC simulated data using regressed parameters.***

	organic			aqueous			vapour		
	x_{water}	x_{MEK}	x_{EthOH}	x_{water}	x_{MEK}	x_{EthOH}	y_{water}	y_{MEK}	y_{EthOH}
NRTL									
AAD	0.081	0.051	0.036	0.013	0.026	0.024	0.014	0.023	0.023
AARD%	10.24	6.30	7.74	7.31	3.66	5.31	4.79	3.05	5.82
UNIFAC									
AAD	0.125	0.073	0.037	0.014	0.026	0.003	0.010	0.017	0.040
AARD%	6.44	0.64	6.05	6.32	1.54	2.36	5.88	6.62	5.32
UNIQUAC									
AAD	0.050	0.197	0.409	0.023	0.006	0.027	0.044	0.061	0.031
AARD%	30.78	21.71	14.280	7.47	6.30	7.82	5.69	7.71	6.41

Table K-5: ***AAD and AARD% values for n-propanol/MEK/water system at 101.3 kPa when compared to NRTL, UNIFAC and UNIQUAC simulated data using regressed parameters.***

	organic			aqueous			vapour		
	x_{water}	x_{MEK}	$x_{N\text{-}Propanol}$	x_{water}	x_{MEK}	$x_{N\text{-}Propanol}$	y_{water}	y_{MEK}	$y_{N\text{-}Propanol}$
NRTL									
AAD	0.025	0.137	0.153	0.011	0.014	0.024	0.011	0.143	0.215
AARD%	4.74	5.41	27.53	7.28	5.12	12.57	1.74	7.41	15.12
UNIFAC									
AAD	0.124	0.147	0.014	0.041	0.007	0.015	0.003	0.005	0.002
AARD%	2.19	12.14	4.59	0.72	1.57	2.54	0.98	0.87	2.14
UNIQUAC									
AAD	0.057	0.015	0.014	0.014	0.016	0.248	0.874	0.125	0.053
AARD%	7.12	18.12	21.57	6.57	11.25	14.87	14.65	3.39	7.18

Table K-6: ***AAD and AARD% values for IPA/MEK/water system at 101.3 kPa when compared to NRTL, UNIFAC and UNIQUAC simulated data using regressed parameters.***

	organic			aqueous			vapour		
	x_{water}	x_{MEK}	x_{IPA}	x_{water}	x_{MEK}	x_{IPA}	y_{water}	y_{MEK}	y_{IPA}
NRTL									
AAD	0.0320	0.053	0.045	0.045	0.067	0.005	0.051	0.054	0.043
AARD%	5.14	6.57	4.15	2.15	2.47	17.65	15.24	2.68	4.65
UNIFAC									
AAD	0.091	0.102	0.002	0.0182	0.057	0.079	0.088	0.015	0.020
AARD%	19.84	1.82	3.98	9.42	2.22	12.58	7.12	4.36	3.07
UNIQUAC									
AAD	0.023	0.195	0.160	0.981	0.189	0.927	0.082	0.170	0.178
AARD%	35.24	9.51	7.33	42.01	8.50	29.68	5.49	7.44	8.98

APPENDIX L - NIST UNCERTAINTY CALCULATIONS

The uncertainty of the result of a measurement generally consists of several components which, in the International Committee for Weights and Measures (CIPM) approach, may be grouped into two categories according to the method used to estimate their numerical values:

A. those which are evaluated by statistical methods

B. those which are evaluated by other means

Type A evaluation of standard uncertainty may be based on any valid statistical method for treating data. Examples are calculating the standard deviation of the mean of a series of independent observations; using the method of least squares to fit a curve to data in order to estimate the parameters of the curve and their standard deviations; and carrying out an analysis of variance (ANOVA) in order to identify and quantify random effects in certain kinds of measurements. Type A evaluations of uncertainty based on limited data are not necessarily more reliable than soundly based Type B evaluations.

Type B evaluation of standard uncertainty is usually based on scientific judgment using all the relevant information available, which may include: measurement data, general knowledge of, the behavior and property of relevant materials and instruments, manufacturer's specifications and data provided in calibration and other reports. Type B evaluation of standard uncertainty was used for this research project: measurement data, general knowledge and data provided in calibration reports were used to obtain the uncertainty associated with the experimental measurements.

APPENDIX M – PROBLEMS ENCOUNTERED AND HOW THEY WERE RECTIFIED

- It was found that the mixture in the boiling flask did not want to start boiling until the glass was slightly tapped to "seed" the boiling.
- A new gas-tight syringe was bought to sample from the vapour phase, and only the vapour phase to limit contamination and accurate measurements.
- The gas-tight syringe used for vapour sampling was kept in the freezer overnight, in a sealed bag, before sampling. This was done due to the fact that the Acetonitrile is extremely volatile and limits the loss of the internal standard during sampling.
- The vapour phase samples were analysed immediately after sampling and it was found that this improved results.